European Cells and Materials Vol. 4. Suppl. 2, 2002 (page 96) ISSN 1473-2262

MICROFABRICATION OF EXTRACELLULAR MATRIX

R. Keatch[1], K. Armoogum[1], S. Schor[2], M. Pridham[1]
[1] *Microengineering & Biomaterials Group,* [2] *Cell & Molecular Biology Unit*
Dundee University Tissue Engineering Centre, University of Dundee, Scotland, UK

INTRODUCTION: In the engineering of tissue growth, the extracellular matrix, on which the cells grow, plays a pivotal role in cell seeding, proliferation and the formation of new tissue [1].

The fundamental role of this scaffold has led to research using microengineering techniques to create regular, 3-dimensional geometric (layered) microstructures. This micropatterned substrate is then subsequently used to facilitate fibroblast adhesion and proliferation (figure 1). The microengineered structure may also be used as a 'master' over which a liquid prepolymer is cast to form an elastomeric stamp which is a key component in soft lithography [2]. This in turn leads to the formation of micropatterned adhesive islands containing proteins which may be used to tether the cell to a specific location.

METHODS: The microengineered substrates are fabricated using techniques adapted from the microelectronics sector combined with subsequent thin film coating processes. This produces biocompatible microstructures, which in turn are used as scaffolds for microcellular growth. Since cell dimensions (>10µm) are much larger than typical sizes encountered in microelectronic devices, novel processes have been utilised to generate high aspect ratio microstructures (HARMS) using photosensitive resins (figure 2) and multi-layering techniques [3,4].

Microengineered structures used for fundamental studies on tissue repair are required to be highly contoured and 3-dimensional to replace the natural occurring extracellular matrix present at the site of tissue growth. This engineered surface should promote a more in-vivo like tissue reconstruction. To complement this, materials such as biodegradable polymers (PLA and PGA) are of particular interest as scaffold material. The porous nature of these materials enables blood capillaries to penetrate and vascularise the growing tissue (angiogenesis) thus increasing the chance of tissue survival.

RESULTS: Current research is focused on generating native and denatured thin films on the microengineered substrate. Studies into cell migration and the eliciting of specific cytokines under different environmental factors have been initiated. This should lead to a much better understanding of cell signal transduction in wound healing [5].

Other areas of research are focused on the fabrication of multi-layered, complex 3D scaffolds using various techniques. These structures will be used to promote cell infiltration and enhance angiogenesis into the extracellular matrix.

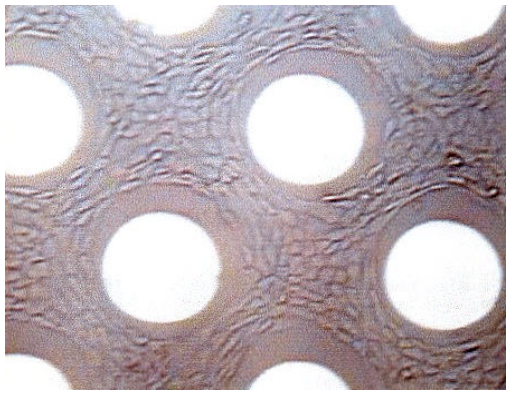

Figure 1: Endothelial Cells on Microstructures.

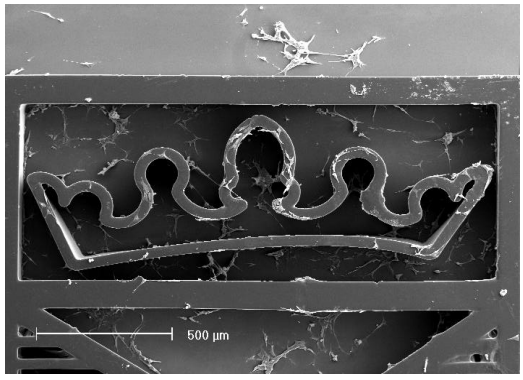

Figure. 2: SU8 fabricated HARMS (200mm tall) inocculated with 3T3 fibroblasts

REFERENCES: [1] Curtis A, et al (1997) Topographical control of cells. *Biomaterials*. 18: 1573-1583. **[2]** Kane RS, et al. (1999) Patterning proteins and cells using soft lithography. *Biomaterials*. 20: 2363-2376. **[3]** Keatch RP, et al (2000) The production of high-aspect-ratio microstructures (HARMs). *J Fusion Technol*. 38: 139-142. **[4]** Keatch RP, et al (2000) Novel three-dimensional microengineering techniques. *J Fusion Technol*. 38: 119-122. **[5]** Schor SL, et al. (1996) Substratum-dependent stimulation of fibroblast migration by the gelatin-binding domain of fibronectin. *J Cell Sci*. 109: 2581-2590

European Cells and Materials Vol. 4. Suppl. 2, 2002 (page 41) ISSN 1473-2262

THE EFFECT OF ITACONIC ACID ON BIOCOMPATIBILITY OF HEMA

R. Sariri, Ph.D., CChem, FRSC, & V Jafarian

Department of Biochemistry, Faculty of Science, Gilan University, Rasht, Iran

Hydrogels are hydrophilic polymer molecules, which are cross-linked by water. The use of hydrogels as synthetic articular cartilage has met with little clinical or commercial success to date. The reason is their poor mechanical properties. However, by the use of composite structure of natural cartilage as a model, a new family of hydrogels based on interpenetrating polymer network (IPN) technology has been introduced. The polymer networks produced in this way possess high mechanical property, but a medium biocompatibility. The aim of this research was to improve the biocompatibility of hyroxyethyl methacrylate by copolymerisation with a more hydrophilic monomer to be used in the structure of a synthetic cartilage. Itaconic acid is a relatively week dicarboxylic acid which can be obtained by dry distillation of citric acid and subsequent treatment of the anhydride with water. It is also obtained commercially from beetroot and cane wastes and aerobic fermentation of *aspergillus terreus*. The product obtained in this last way is very hydrophilic and is expected to show high biocompatibility because of its natural source.

A group of copolymers were synthesized using HEMA as the major monomer and a range of itaconic acid with varying concentrations. The cross-linking agent was 2% ethylene glycol dimethacrylate (EGDM). The equilibrium water content (EWC) of the resulting copolymer was 35-40%. To investigate the biocompatibility of the copolymer, their resistance against albumin adsorption was measured spectrophotometrically. The UV absorption of a solution with known concentration of albumin was measured at 280 nm before and after the insertion of a 1-cm2 disk made of the copolymer. The difference in the UV absorption was related to the protein adsorbed on the polymer surface, i.e. the extent of its biocompatibility. The results showed that copolymers with higher ITC content adsorbed less albumin. Albumin is a large compact protein which is negatively charged, therefore is less adsorbed to surfaces with higher ITC content, recall that ITC has some negative charges due to the presence of two carboxylic acid groups.

PROOPIOMELANOCORTIN ANTI-INFLAMMATORY PEPTIDE SIGNALLING IN HUMAN SKIN KERATINOCYTE CELLS

[1]R.J.Elliott, [1]M.Szabo, [2]M.J.Wagner, [1,2]S.MacNeil, [1]R.D.Short and [1]J.W.Haycock.

[1]Department of Engineering Materials, University of Sheffield, Sheffield, U.K.

[2]Section of Medicine, University of Sheffield, Sheffield, U.K.

INTRODUCTION: Wound bed inflammation following skin burn injury is associated with the prevention of successful graft replacement, leading to failure/rejection. The use of steroids as antiinflammatory compounds are associated with side effects including the inhibition of wound healing. We have previously reported that MSH/ACTH peptides are potent anti-inflammatory molecules in keratinocytes [1,2]. However, they also have pigmentation potential. α-MSH signals by binding to the melanocortin-1 receptor (MC-1R) generating a cyclic AMP or calcium signal. The carboxyl terminal tripeptides (KPV/KP-$_D$-V) are the smallest minimal sequences that prevent inflammation, however no data is available on pigmentation potential. The aim of this study was to identify the potency and specificity of α-MSH, ACTH, ACTH 1-17, KPV and KP-$_D$-V peptides for the MC-1 receptor using intracellular calcium signalling in normal and continuous human keratinocytes. We also investigated dopa oxidase pigmentation activity of the above peptides in a murine melanoma cell line.

METHODS: Intracellular calcium levels were measured by loading normal human and HaCaT keratinocytes with Fura-2AM. λex=340nm and λem=490nm were detected in real-time by a Kontron SFM25 fluorimeter, and by a Leica DM-IRB fluorescence microscope. After loading, cells were incubated with peptides: α-MSH, KPV, KP-$_D$-V, ACTH 1-17 and ACTH (10^{-15}M to 10^{-6}M) ± PIA (10^{-5}M, an adenosine agonist that unmasks calcium signals). Dopa oxidase activity in B16-F10C1 cells was determined by specific oxidation of L-Dopa to dopaquinone, with optical measurement at 490nm. Cells were incubated with the above peptides for 24 hours. Dopa oxidase activity was calculated by change in absorbance (at 490nm) per minute.

RESULTS: Positive intracellular calcium responses were observed in HaCaT and normal human keratinocytes in response to α-MSH (10^{-12}M to 10^{-7}M), KPV (10^{-13}M to 10^{-7}M) and KP-$_D$-V (10^{-15}M to 10^{-7}M) in the presence of PIA (at 10^{-5}M). Normal keratinocytes responded to all the above peptides but in addition responded to ACTH (10^{-12}M to 10^{-7}M), and ACTH 1-17 (10^{-12}M to 10^{-7}M), This was in contrast to the HaCaT keratinocytes.

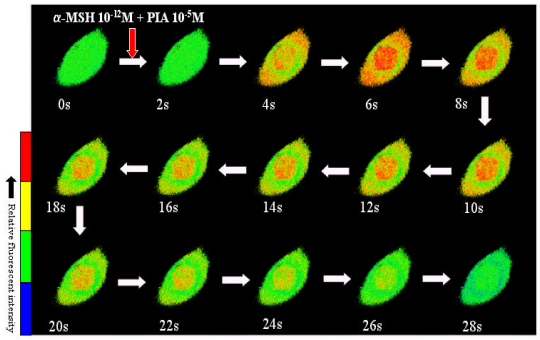

Fig.1: Acute intracellular calcium release in a HaCaT keratinocyte in response to α-MSH (10^{-12}M) + PIA (10^{-5}M).

Incubation of B16-F10C1 cells with α-MSH, ACTH and ACTH 1-17 (10^{-9} M to 10^{-6} M) alone caused larger increases in dopa oxidase activity, in comparison to KPV or KP-$_D$-V (10^{-9} M to 10^{-6} M).

DISCUSSION & CONCLUSIONS: The acute intracellular calcium responses in HaCaT cells to MSH but not ACTH peptides indicates specificity of the MSH peptides for the MC-1 receptor. Responses of MSH and ACTH peptides in normal keratinocytes correlates with reported MC-1 and MC-2R expression and further supports a broad action of the MSH / ACTH peptides in preventing inflammation. The reduced dopa oxidase response in pigmentary B16-F10C1 cells with KPV and KP-$_D$-V suggests that the MSH carboxyl terminal tripeptides do not have pigmentation potential, in contrast to α-MSH. Therefore the data reported provides a potential basis for the use of the KPV / KP-$_D$-V peptides as anti-inflammatory molecules in superficial skin burn injury to augment epithelial grafting or skin tissue engineering applications.

REFERENCES: [1]M. Moustafa, M. Szabo, G. Ghanem et al (2002) *J Invest Dermatol*.(In press). [2]J.W. Haycock, S.J.Rowe, S. Cartledge et al. (2000) *J Biol Chem* **275** (21), 15629-36.

ACKNOWLEDGEMENTS: EPSRC (UK) and NHS Trust (NGH, Sheffield, UK.)

European Cells and Materials Vol. 4. Suppl. 2, 2002 (pages 97-98) ISSN 1473-2262

GRAFTING COLLAGEN ON POLY(L-LACTIDE) BY GAMMA IRRADIATION

Y.Yang[1], M-C. Porté[2], P. Marmey[2], J. Amédée[2], C.Baquey[2], A.El Haj[1]

Centre for Science and Technology in Medicine, Keele University, England, UK

INSERM U-443, University Victor Segalen Bordeaux 2, Bordeaux, France

INTRODUCTION: A key element of tissue engineering is controlling the growth, differentiation and behaviour of cells on biodegradable scaffolds, facilitating their organisation into functional tissue. The initial attachment of a cell to a substrate is mediated by cell-surface adhesion factors. Cell-extracellular matrix (ECM) interactions participating directly in promoting cell adhesion, migration, growth and differentiation are well documented. In this study results of grafting ECM molecules onto poly(l-lactide) by gamma irradiation is reported. The aim of the project is to immobilize protein onto polymers covalently and increase stability of proteins on polymers. The effect of irradiation on the grafting efficiency, surface morphology and the ECM molecule activity were tested.

METHODS: Poly(l-lactide) (PLLA) films of about 500 μm thickness with a molecular weight of 360,000 were used. Gamma irradiation was carried out using a Cesium137 source (IBL 337 from Cis Bio International) and a dose-rate of 3 kGy h-1. Reaction mixtures containing PLLA, acrylic acid (AA), collagen type I were prepared in Schlenk tubes and were deoxygenated by three freeze-thaw cycles in vacuum. The mixtures were then exposed to gamma radiation at room temperature for different time periods ranging from 1 - 7 hours. After irradiation, the PLLA films were washed with distilled water for 30 hours with stirring, to remove un-reacted monomers, non-grafted products and other compounds from the reaction mixture, and were then dried in a vacuum desiccator. The grafted PLLA were characterised by grafting yield, XPS, immunostain (DAKO-HRP collagen ELISA kit).

RESULTS: The grafting yield (i.e. weight change after irradiation) *versus* irradiation dose is plotted in Figure1. With the exception of the lowest irradiation dose of 3 kGy (1 hour irradiation), the grafting yield increased with increasing irradiation dose. Table 1 shows the XPS results of the collagen type I-grafted PLLA films. Nitrogen was introduced onto the film as a result of the gamma irradiation. With increasing irradiation time (and therefore dose), the percentage of nitrogen increased, indicating that more proteins had grafted onto the PLLA film. The collagen-grafted PLLA films stained positive (brown) for collagen, as shown in Figure 2.

DISCUSSION & CONCLUSIONS: In our results, XPS confirmed the presence of proteins on the grafted PLLA. Localisation of collagen using immunostaining showed high levels of collagen on the grafted PLLA, confirming that the grafted collagen in the PLLA was still biologically active. The presence of collagen epitopes on the surface, i.e. having reactivity of the antibody against collagen on the surface of the grafted PLLA, demonstrated that irradiation may not alter

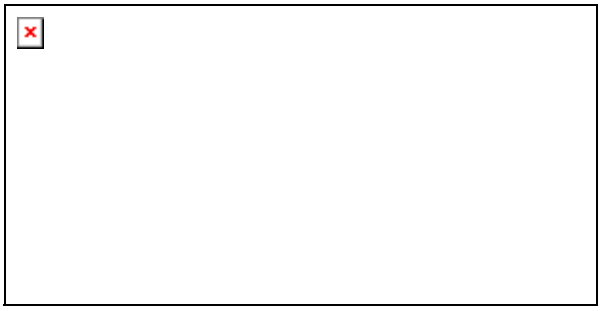

Figure 1 Effect of irradiation dose on the grafting Yield.

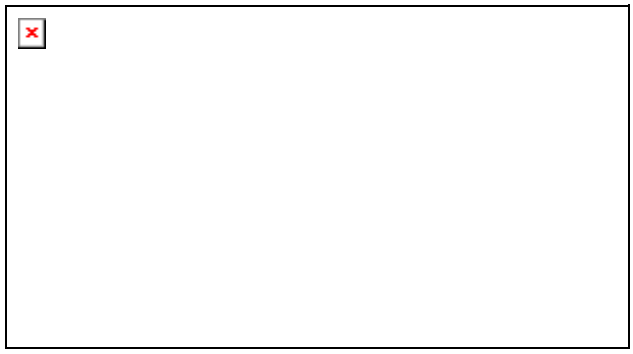

Figure 2 Immunostain of grafted PLLA films

Dose	C	O	N	Si
0kGy	74.3	21.3	0	4.4
3kGy	62.8	36.4	0.43	0.27
15kGy	61.8	34.1	1.7	2.3

Table 1 Elemental analysis of the PLLA films

availability of active binding sites. These results indicate that the single-step procedure of grafting by gamma irradiation could provide a simple but efficient technique to modify the biocompatibility alongside sterilisation of a scaffold for use in tissue engineering.

ACKNOWLEDGEMENTS: this project is financially supported by European Commission Vth framework programme, BITES.

European Cells and Materials Vol. 4. Suppl. 2, 2002 (pages 47-49) ISSN 1473-2262

POLYMER DEMIXED NANO - TOPOGRAPHY: RANDOM ISLANDS GIVE AN ORDERED RESPONSE FROM HUMAN FIBROBLASTS.

M.Dalby[1], M.Riehle[1], S.J. Yarwood[1], H.J.H Johnstone[2], S. Affrossman[2] & A.S.G. Curtis[1]

[1] *Centre for Cell Engineering, IBLS, University of Glasgow, Glasgow, UK*

[2] *Department of Pure and Applied Chemistry, University of Strathclyde, Glasgow, UK*

INTRODUCTION: Topography has been shown to be of importance when considering cell response to materials. Further to this, cells have been shown to react to nanometric surface features (bellow 300 nm dimensions). Nanotopography has successfully been fabricated by methods such as photolithography, which can give vertical resolution of around 200 nm and electron beam lithography, giving a lateral and vertical resolution of about 5 nm. These procedures, whilst giving reproducible and organised topography, are costly and time consuming. Thus, there is incentive to find simple methods of nanotopography fabrication that elicit cellular reactions. One of several methods under investigation is polymer demixing, blends of polystyrene and poly(4-bromostyrene) spontaneously undergo phase separation during spin casting onto glass coverslips. By controlling the solvent (toluene) concentration and proportions of the polymers, different topographies can be produced; these can be pits, bumps, or ribbons of varying height. XPS and SIMS have shown the surface of the blends to be composed of just polystyrene. In this study, morphological examination of the cells and their cytoskeletons have been observed in response to polymer demixed topographies. Microarrays have also been used to investigate cell signalling events.

METHODS: Demixing polystyrene (PS) and polybromostyrene (PBrS) produced island heights of 13, 35 and 95 nm (fig 1). Flat PS was used as a control. H-Tert BJ1 human fibroblasts were used as a cell model. Image analysis was used to quantify cell morphology, SEM and fluorescence microscopy were used to observed morphology and cytoskeleton in response to the islands. 1718 gene microarrays were then used to measure gene regulations in response to the 13 nm islands. Genes of interest were selected from four categories; proliferation, cytoskeleton, signalling and extracellular matrix. The selection was further thresholded by only selecting genes that had changed by more than 25% from control.

RESULTS: *Morphology:* Image analysis showed cells to be more spread on the 13 nm islands, no difference between the 35 nm islands, and less well spread on the 95 nm islands compared to control. SEM confirmed these results, and also showed distinct interactions between cell filopodia and the islands. These interactions increased with island size, where the cells were ultimately seen to form large 'amoeboid-like' pseudopodia, and appeared to be using the island tops as 'stepping-stones'. *Cytoskeleton:* The 13 nm islands and flat controls supported fibroblasts with well defined actin and tubulin cytoskeletons. The 35 nm islands supported cells with less distinct cytoskeleton, and the cytoskeleton for cells on the 95 nm islands was poorly organised. *Microarray*: Due to the 13 nm islands stimulating cell spreading and cytoskeletal organisation, they were selected for gene array. A large number of interesting gene up-regulations were observed.

Fig. 1: AFM images of polymer demixed islands. 13 nm islands (a), 35 nm islands (b) and 95 nm islands (c).

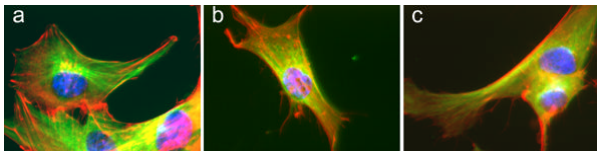

Fig. 2: SEM images of fibroblast interactions with (A) 13 nm islands, (B) 35 nm islands and (C) 95 nm islands.

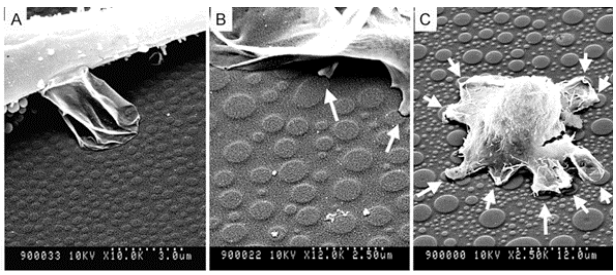

Fig 3: Fluorescence images of actin (red) and tubulin (green) cytoskeleton - nucleus is blue. 13 nm (a), 35 nm (b) and 95 nm (c).

DISCUSSION & CONCLUSIONS: In order to proliferate, fibroblasts need to spread on the material surface. The increased spreading of

fibroblasts on the 13 nm islands coupled to the increase in transcription factors observed by microarray, and previous observation of increase BrdU incorporation[1] shows that the cells on the 13 nm islands are more proliferative than on the control.

Up-Regulated Genes
Cytoskeleton
Tubulin Beta-3 Chain
Myosin Heavy Chain, Nonmuscle Type A
Keratin, Type I Cytoskeletal 18
Cofilin, Non-Muscle Isoform.
Keratin, Type I Cytoskeletal 10
Lamin A
Tropomyosin, Fibroblast Non-Muscle Type
Villin
Extracellular Matrix
Procollagen Alpha 1(II) Chain Precursor
Stromelysin-3 Precursor (MMP-11)
Laminin Alpha-4 Chain Precursor
Collagen Alpha 5(IV) Chain Precursor
Laminin Alpha-3 Chain Precursor
Fibrinogen Beta Chain Precursor
Collagenase 3 Precursor (MMP-13)
Procollagen Alpha 1(V) Chain Precursor
Replication
Transcription Initiation Factor TFIID 20/15 Kd Subunits
Zinc Finger Protein 76
Fos-Related Antigen 2
Transcription Initiation Factor IIe, Beta Subunit
Transcription Factor Ap-2
CCAAT-Binding Transcription Factor Subunit A
Transcriptional Enhancer Factor Tef-1
Transcription Factor 11
Nuclear Factor NF-Kappa-B P100 Subunit
Transcription Factor Jun-B
Zinc Finger X-Chromosomal Protein
Transcription Initiation Factor TFIID
Zinc Finger Protein 139 (Fragment)
DNA-Directed RNA Polymerase II
Zinc Finger Protein GlI3
Possible Global Transcription Activator
Possible Global Transcription Activator SNF2l2
ETS-Domain Transcription Factor ERF
Zinc Finger Protein 135
Zinc Finger Protein 7
C-Jun N-Terminal Kinase 2
Transcription Factor ITF-2 (Fragment)
Transcription Factor RelB
Signalling
G Protein-Coupled Receptor Kinase Grk6
Tyrosine-Protein Kinase Ryk Precursor
Transforming Protein RhoB
Protein-Tyrosine Phosphatase Pcp-2 Precursor
Ras-Related Protein R-Ras2
Early Growth Response Protein 1
Calcium-Activated Potassium Channel Beta Subunit
Protein-Tyrosine Phosphatase Delta Precursor
Fibroblast Growth Factor Receptor 2 Precursor
Integrin Alpha-6 Precursor
Chloride Intracellular Channel Protein 2
Tyrosine-Protein Kinase Receptor Tie-1 Precursor
Cadherin-11 Precursor
Protein-Tyrosine Phosphatase G1
Ras GTPase-Activating-Like Protein
Protein Kinase C, Zeta Type
Camp-Dependent Protein Kinase, Beta-Catalytic Subunit
Tyrosine-Protein Kinase Syk
Protein-Tyrosine Phosphatase Delta Precursor
Transforming Protein RhoA
Integrin Beta-5 Subunit Precursor
Ras-Related Protein Rab-9
Chloride Intracellular Channel Protein 2
Protein-Tyrosine Phosphatase LC-PTP
Intercellular Adhesion Molecule-3 Precursor (ICAM-3)
Protein-Tyrosine Phosphatase X Precursor
Ras-Related Protein Rab-1C
IL-1 Receptor
IL-1
Growth Hormone Receptor

Table 1. Selected Gene Up-Regulations.

SEM showed fibroblasts cultured on the 35 nm islands were using filopodia to interact with the features. Also of interest, was the observation that despite having the same average area as cells on the flat control, cells cultured on the islands had a less defined cystoskeleton.

In response to the 95 nm islands, the cells took on an unusual morphology, with rounded cell bodies and thick, pseudopodial, processes. The cytoskeleton was poorly formed in relation to the control[1], and results from previous studies show proliferation to be less on these structures than control. Time course studies with this material (Dalby *et al*, submitted), have shown that the cells initially adhere and spread better on the large island than the control, but by 24 hours of culture, the cells take on the 'amoeboid' morphology and proliferate very slowly.

Microarray for cells on the 13 nm islands, showed up-regulations for a number of G-proteins and their receptors. Also noted were tyrosine kinase up-regulations. These proteins are involved in cell signalling and have down-stream effects on cell movement, cytoskeleton and gene regulation. Signalling moelcules such as FGF, IL-1 and growth hormone receptors were also noted.

These results tie in with observations of increased adhesion and spreading on the 13 nm islands compared to control initiating signal transduction and protein production. Up-stream events are seen in the form of increased cytoskeletal organisation and microarray showing up-regulation of ECM constituents.

For further reading please see[2-4].

REFERENCES: [1] M.J. Dalby, M. Riehle, H.J.H. Johnstone, S. Affrossman, A.S.G. Curtis (In Press). *Tissue Engineering.* [2] M.J. Dalby. M. Riehle, H.J.H. Johnstone, S. Affrossman, A.S.G. Curtis (2002) *Biomaterials* **23**: 2945-2954. [3] M.J. Dalby, S.J. Yarwood, M. Riehle, H.J.H. Johnstone, S. Affrossman, A.S.G. Curtis. (2002)*Experimental Cell Research* **276***:* 1-9. [4] M. Riehle, M.J. Dalby, H. Johnstone, J. Gallagher, M.A. Wood, B. Casey, K. McGhee, S. Affrossman, C.D.W. Wilkinson, A.S.G. Curtis. (2002) Materials Research Society Proceedings **705**: Y5.1.1 - Y5.1.11.

ACKNOWLEDGEMENTS: This work was supported by the EU framework V grant QLK3-CT-2000-01500 (Nanomed). Thanks to the IBLS Molecular Biology Support Unit (MBSU) and Integrated Microscopy Facility.

European Cells and Materials Vol. 4. Suppl. 2, 2002 (pages 125-126) ISSN 1473-2262

PLATELET ADHESION TO NANOFABRICATED POLYCAPROLACTONE

G.E.Marshall [1], H. Agheli [2] & D.S. Sutherland [2]

[1] *Centre for Cell Engineering, IBLS, Glasgow University, Scotland, GB*

[2]*Department of Applied Physics, Chalmers University of Technology, Fysikgraend 3, 41296 Gothenburg, Sweden*

INTRODUCTION: We describe the effect of nanofabricated surfaces on the level of platelet adhesion to PCL. Plain ion etched PCL surfaces were compared to three structures: - nano-cylinders, nano-cones and nano-hemispheres.

METHODS: The experiment was conducted on quadriplicate samples of each nano-structure and repeated three times, with fresh blood from a different blood donor being used on each occasion. Samples were incubated with 0.5ml of the platelet suspension diluted in HEPES saline, at 37^0C for one hour, fixed in 4% formalin-PBS, immunohistochemically stained with a CD41 antibody followed with an antibody conjugated to alkaline phosphatase. Immunohistochemical labelling was visualized with Fast Red reactant. Nine images were grabbed at x10 magnification from each specimen, giving a total of five hundred and seventy six images in the study.
Image analysis was performed to gain information on two features: [1] the number of adherent platelets, [2] the percentage of the nano-fabricated surface that was covered by adherent platelets.
RESULTS: Nano-cylinders had the lowest platelet density and coverage of all the tested samples, including the flat ion etched controls. Both platelet numbers and platelet coverage were higher on nano-cones and nano-hemispheres when compared with either the nano-cylinders or the flat ion etched controls. All these differences were statistically significant. No difference was noted when comparing nano-cones with nano-hemispheres.

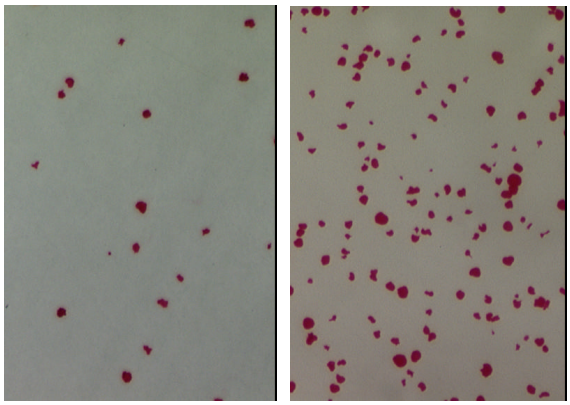

Fig 1: Fewer platelets adhere to nano-cylinders (left) than to nano-hemispheres (right).

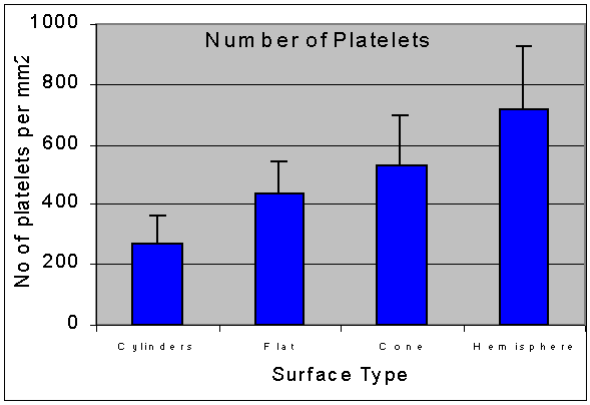

Fig 2: Numbers of platelets adhering to three patterned surfaces and flat control

DISCUSSION & CONCLUSIONS: Nano-fabricated nano-cylinders have the largest surface area. However, only a portion of their overall surface may be available for adhesion. Their walls, being vertical, may not be available for adhesion. Nano-cylinders may also obstruct cell contact immediately adjacent to their bases. Thus adhesion to the nano-fabricated cylinders is less than the plain surface controls. Most of the surfaces of the nano-cones and nano-hemispheres, being less acute than the vertical, may be available for cell adhesion. As their three-dimensional area is greater within the same field of view compared to flat controls, adhesion would be greater.

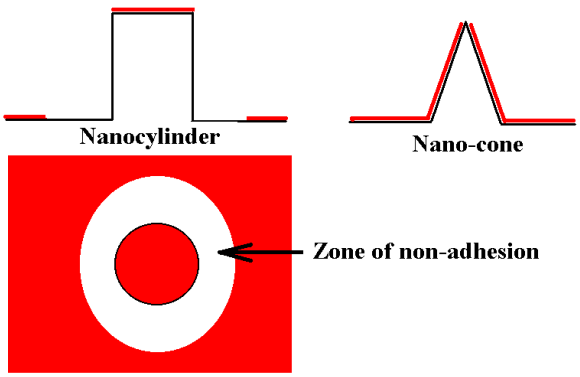

Fig 3: Surface available to adhesion is marked in red.

ACKNOWLEDGEMENTS: This work was supported by the EU framework V grant QLK3-CT-2000-01500 (Nanomed).

a-MELANOCYTE-STIMULATING HORMONE ANTI-INFLAMMATORY ACTION IN HUMAN DERMAL FIBROBLAST CELLS

R.P. Hill[1], S. Tao[1], M. Szabo[1], S. MacNeil[1,2] & J.W. Haycock[1]

[1] *Department of Engineering Materials, University of Sheffield, Sheffield, U.K.*

[2] *Section of Medicine, University of Sheffield, Sheffield, U.K.*

INTRODUCTION: Excessive inflammation resulting from a partial thickness or deep burn injury to skin tissue compromises autograft or allograft acceptance. The use of steroidal drugs as a means to alleviate inflammation is associated with a number of side effects including inhibition of wound healing. We have previously reported on the potency of several melanocyte stimulating hormone (MSH) peptides as anti-inflammatory molecules. The MSH peptides act on a number of different cell types via the melanocortin-1 (MC-1) receptor, generating a cyclic AMP signal. The anti inflammatory biology has previously been traced to the carboxyl terminal tripeptide (Lys-Pro-Val / Lys-Pro-D-Val)[1,2]. The aim of this investigation was to identify if human dermal fibroblasts express the MC-1 receptor and confirm if α-MSH and Lys-Pro-D-Val peptides are effective at inhibiting cytokine stimulated NF-κB activity (a transcription factor that controls expression of many proinflammatory genes) and cytokine stimulated intercellular adhesion molecule-1 (ICAM-1) upregulation.

METHODS: MC-1 receptor expression was determined by immunofluorescent microscopy on fibroblast cultures and on isolated membranes via SDS-PAGE and Western blotting using an anti MC-1 receptor antibody (Santa Cruz Inc., [N-19]). Human dermal fibroblasts grown in culture and whole skin were stimulated with TNF-α (10, 50, 200 and 1000 units/ml; 5 minutes to 24 hours). Nuclear verses cytoplasmic immunofluorescent labeling of NF-κB/p65 was used to determine the relative activation of NF-κB using anti-NF-κB/p65 antibody (Santa Cruz Inc. [sc-302]) with FITC detection (λex=495 nm, λem=515nm). MSH peptides (10^{-10} to 10^{-6}M) were then incubated with TNF-α to investigate potential inhibition of NF-κB. Expression of ICAM-1 was determined in control and TNF-α (200 units/ml; 4days) stimulated cells by SDS-PAGE/Western blotting using an anti-ICAM-1 antibody (Santa Cruz Inc, [H-108]) with 3,3'-diaminobenzidine detection.

RESULTS: Human dermal fibroblasts were positive for the MC-1 receptor by immunolabelling and Western blotting, identifying a predicted molecular weight product of 37 kDa.

TNF-á was observed to induce nuclear translocation of NF-êB as soon as 10 minutes. However, nuclear activation was maximal using a TNF-á dose of 200 units/ml for 60 minutes. In contrast, dermal fibroblasts contained within whole human skin tissue took 4 hours for maximum activation. The presence of α-MSH (10^{-10} to 10^{-6}M) + TNF-α or Lys-Pro-D-Val (10^{-10} to 10^{-6}M) + TNF-α decreased the degree of NF-κB nuclear translocation caused by TNF-α alone by approximately 50% for fibroblasts in culture.

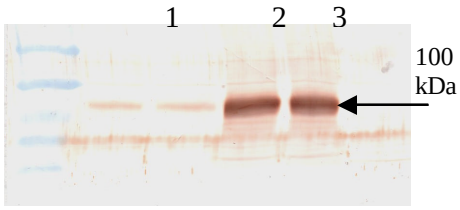

Figure 1: Upregulation of ICAM-1 in dermal fibroblasts in response to TNF-a (lanes 3 and 4). Control unstimulated cells (lanes 1 and 2).

TNF-α stimulation (200 units/ml) over 4 days caused upregulation of ICAM-1, identified as a 100kDa band by Western blotting.

DISCUSSION & CONCLUSIONS: MC-1 receptor presence was observed in human dermal fibroblasts by immunolabelling and Western blotting. This is fundamental for MSH peptide signaling in dermal fibroblast cells. TNF-α challenge lead to a rapid activation of NF-κB and considerable upregulation of ICAM-1. Use of MSH peptides was observed to inhibit TNF-α activation of NF-κB. The ability of MSH peptides to inhibit TNF-α stimulated ICAM-1 upregulation is currently underway. Preliminary data are consistent with MSH as an antiinflammatory peptide in fibroblast cells, supporting a potential use in augmenting therapy for dermal burns injury in grafting and engineered applications.

REFERENCES: [1]M. Moustafa, M. Szabo, G. Ghanem et al (2002) *J Invest Dermatol.* (In Press). [2]J.W. Haycock, S.J. Rowe, S. Cartledge et al (2000) *J Biol Chem* **275** (21), 15629-36

ACKNOWLEDGEMENTS: We thank EPSRC (UK) for funding.

European Cells and Materials Vol. 4. Suppl. 2, 2002 (pages 127-128) ISSN 1473-2262

ADDITION OF HUMAN MESENCHYMAL STEM CELLS & OSTEOGENIC PROTEIN–1 TO DEMINERALISED BONE MATRIX AND INSOLUBLE COLLAGENOUS MATRIX RESULTS IN *DE NOVO* BONE FORMATION

Z Ali[1], L Di Silvio[1], AE Goodship[1], E Tsiridis[1].

[1]*The Institute of Orthopaedics, Royal Free and University College London Medical School. Royal National Orthopaedic Hospital Trust, Stanmore, Middlesex, HA7 4LP., UK*

INTRODUCTION: Current bone grafts include allograft and autografts, both of which have limitations. Autograft, regarded as the gold standard, has limited availability, donor site morbidity, increased operative time, blood loss and additional cost. Tissue engineering biotechnology has shown considerable promise in improving grafts. An optimal bone graft material must allow the interaction of three essential elements; a suitable cell source, growth and differentiation stimulating factors, and a scaffold matrix to support the attachment, migration, and proliferation of these cells. This provides an osseconductive and osseoinductive bone graft allowing the regeneration of bone. The objective of this study was to improve to the osseoinductive capacity of human demineralised bone matrix (DBM) and human insoluble collagenous matrix (ICM), following incorporation of recombinant human osteogenic protein 1 (rhOP-1) and human mesenchymal stem cells (MSCs).

METHODS: Recombinant human osteogenic protein – 1 (400ng/0.25g of bone) was seeded onto DBM and ICM together with human MSCs (1 x 10^5). Cellular proliferation was quantitatively evaluated *in vitro* using Alamar Blue and 3H-TdR assays. Quantitative cellular differentiation was assessed using the alkaline phosphatase assay. Von Kossa staining, X-ray analysis, and PCR were used for qualitative evaluation of cellular differentiation. Qualitative analysis of proliferation and differentiation was assessed using scanning electron microscopy (SEM).

RESULTS: MSC proliferation and differentiation down the osteogenic lineage was observed on DBM and ICM in the presence of OP-1, and also on DBM alone. Alamar blue and ^{3}H-TdR assays confirmed that MSC proliferation occurred on both DBM and ICM, with the values being significantly greater with addition of OP-1 ($P \leq 0.05$). The ALP activity showed that MSCs differentiated into osteoblasts on DBM alone, and on DBM and ICM with OP-1. In all cases, OP-1 had a significant effect on MSCs ($P \leq 0.05$).

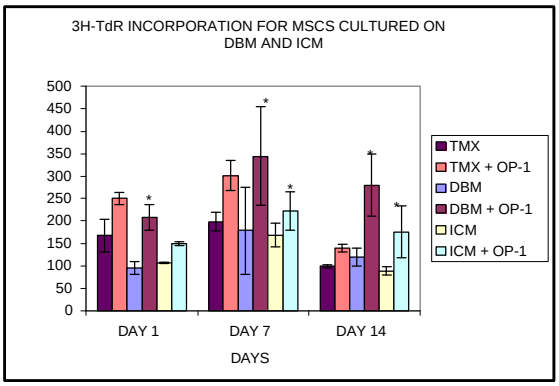

*Fig 1. Cell proliferation results from 3H-TdR assay showed a peak on day 7, with all values greater than their corresponding day 1 and 14 values. Statistically significant differences between materials with and without OP-1 (denoted by *, [$P<0.05$], n=8) were observed in DBM on day 1, and both DBM and ICM on day 7 and 14. TMX was used as a control.*

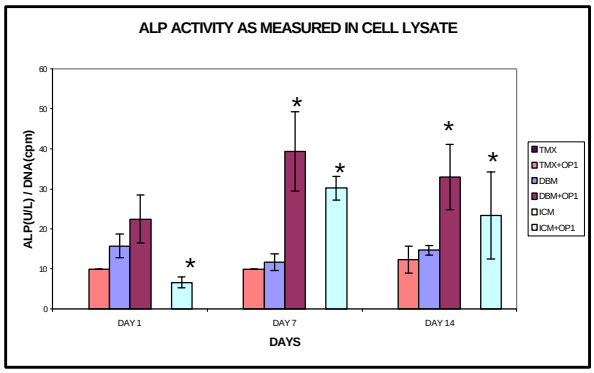

*Fig 2 shows that ICM with no OP-1 added did not register any values at any of the timepoints whereas DBM on its own did. The addition of OP-1 increases ALP activity, and results are statistically significant (denoted by *, [$P \leq 0.05$]n=8) for ICM on day 1, 7, and 14, and DBM on day 7, and 14. TMX was used as a control.*

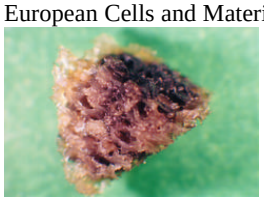

Fig 3A DBM

FIG 3B DBM + OP-1

Figure 3A shows that DBM without OP-1 has a mild degree of mineralization compared to DBM with OP-1 (fig 3B) which exhibits extensive calcium deposition.

Fig 4A ICM

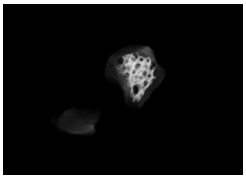

Fig 4B ICM + OP-1

Figures 4. ICM with no OP-1 (fig 4A) did not show any mineralization. Thus the mineralization seen in fig 4B with ICM + OP-1 is de novo mineralization as a result of the experimental procedure.

DISCUSSION: DBM with OP-1 proved to be the best graft in terms of *in vitro* bone formation. The results of this study also confirmed DBM's intrinsic osteoinductive capacity, as well as the pleiomorphic capabilities of OP-1.
DBM and ICM when seeded with MSCs and OP-1 provide an osteoconductive and osteoinductive graft material resulting in *de novo* bone formation. Hence both systems provide an improved osteoinductive graft.

REFERENCES:

[1] Bruder SP, Fox BS; Tissue Engineering of Bone: Cell Based Strategies; *Clin Orthop 367S; S68-S83,1998.* [2] Cook SD, Dalton JE, Tan EH et al; In vivo Evaluation of Recombinant Human Osteogenic Protein-1 (rhOP-1) Implants as a Bone Graft Substitute for Spinal Fusions; *Spine 19: 1655-63, 1994* [3] Geesink RGT, Hoefnagels NHM, Bulstra SK; Osteogenic Activity of OP-1 Bone Morphogentic Protein (BMP 7) in a Human Fibular Defect; *JBJS (Br); 81B:710-18, 1999* [4] Reddi AH; Bone Morphogenetic Proteins: From Basic Science To Clinical Applications; *JBJS (Am) 83A Suppl 1, Part 1, 2001*

ACKNOWLEDGEMENTS: Mr M Kayser, Dr P Sarathchandra, Dr N Gurav, Prof M Ferguson-Pell, Culyer Award (RNOHT)

European Cells and Materials Vol. 4. Suppl. 2, 2002 (page 129) ISSN 1473-2262

ENHANCING THE OSSEOINDUCTIVE PROPERTIES OF HYDROXYAPATITE BY THE ADDITION OF HUMAN MESENCHYMAL STEM CELLS, AND RECOMBINANT HUMAN OSTEOGENIC PROTEIN 1 (BMP-7).

A. Bhalla, E Tsiridis, AE Goodship, L Di. Silvio.

The Institute of Orthopaedics, Royal Free and University College London Medical School. Royal National Orthopaedic Hospital Trust, Stanmore, Middlesex, HA7 4LP.

INTRODUCTION: The traditional bone graft substitutes such as the autograft and allograft have known limitations. Tissue engineering of bone is thus an attractive alternative. The development of biomimetic biomaterials for use in bone tissue engineering is an important goal. Hydroxyapatite (HA) is such a suitable biomaterial as it mimics the inorganic phase of bone, as it is osseoconductive and minimally osseoinductive. Improving the osseoinductive property of HA by the incoporation of a growth stimulating factor or addition of human mesenchymal stem cells (MSC) may in the future expand clinical application and allow use in load bearing situations.

HYPOTHESIS: "The MSC's attach to the HA surface and given appropriate stimuli from human osteogenic protein 1 (BMP-7) will differentiate into osteogenic cells. Thus the HA/MSC/BMP-7 composite will display superior osseoinductive properties compared to HA alone"

METHODS: Porous hydroxyapatite (74.6% porosity, IRC) loaded with MSC's (2 x 105) were compared to samples loaded with rhBMP-7 (400 ng) of the same MSC concentration over a fourteen day period. Quantitative analysis (Cell proliferation, Cell differentiation, and DNA analysis) and qualitative using Scanning Electron Microscopy were performed. The Students T-test was performed to determine the significance of the results between the means.

RESULTS: Cell proliferation was significantly enhanced ($P<0.05$) in the BMP-7 loaded composite at all time points. ALP production and release was enhanced in loaded samples. ALP production per unit DNA was also enhanced in the loaded samples and was significant at day fourteen.

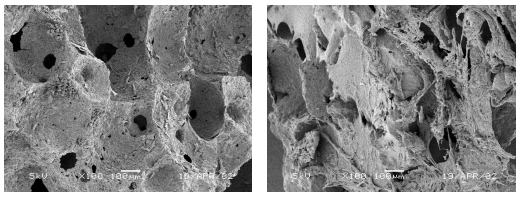

SEM analysis indicated loaded samples to have enhanced cellular attachment and proliferation at all time points. Figures 1A and 1B represent unloaded and loaded samples at day 7.

DISCUSSION: Results indicate that the loaded composites showed enhanced cell proliferation, and ALP production and release. SEM analysis also demonstrated enhanced cell attachment and an increase number of proliferative cells. Thus the HA/MSC/BMP-7 composite displayed superior osseoinductive properties in comparison to the HA/MSC composite.

CONCLUSION: The composite may enhance and advance the regeneration process; thus providing earlier mechanical support, and extending the clinical applications for example; non union fracture healing, spinal fusions, and use in revision arthroplasty in cases of excessive bone loss.

NEW BONES FOR OLD - MESENCHYMAL STEM CELLS AND BIOMIMETIC SCAFFOLDS

Richard OC Oreffo

University Orthopaedics, University of Southampton, Southampton, SO16 6YD, UK

OVERVIEW: The requirement for new bone to replace or restore the function of traumatised or degenerated bone, or for the replacement of lost mineralised tissue as a consequence of increasing age is a major clinical and socio-economic need. To date, bone formation stimulation regimes, although attractive, have yet to demonstrate clinical efficacy. Bone is unique with a vast potential for regeneration from cells with stem cell characteristics. Mesenchymal stem cells or human bone marrow stromal stem cells are defined as pluripotent progenitor cells with the ability to generate cartilage, bone, muscle, tendon, ligament and fat.

These primitive progenitors exist postnatally and exhibit stem cell characteristics, namely low incidence and extensive renewal potential. These properties in combination with their developmental plasticity has generated tremendous interest in the potential use of mesenchymal stem cells to replace damaged tissues. In essence mesenchymal stem cells could be cultured to expand their numbers then transplanted to the injured site or after seeding in/on shaped biomimetic scaffold to generate appropriate tissue constructs. Thus, an alternative approach for skeletal repair is the selection, expansion and modulation of osteoprogenitor cells in combination with a conductive or inductive scaffolds to support and guide regeneration together with judicious selection of osteotropic growth factors. Furthermore, these biomimetic structures, when coupled with appropriate osteoinductive factors, can provide positional and environmental information to drive osteogenesis. These approaches, often referred to as bone tissue engineering or regeneration may provide alternative solutions for skeletal tissue reconstruction.

Current concepts, approaches and challenges to be presented from work in our group include: i)

the use of isolated and selected human osteoprogenitor cell populations with selected osteotropic agents in an attempt to modulate the phenotype of the mesenchymal stem cell to generate mineralised bone tissue, ii) Manipulation of the developmental potential of these osteoprogenitors on modified PLA / PLGA polymer structures and biomimetic structures with bone morphogenetic factors, and iii) the potential to combine gene delivery with tissue engineering to generate bone *in vivo*. While our knowledge of the processes of bone cell differentiation has increased, the mechanisms involved in many of these processes and how the architecture of bone can be developed in these new model systems are still unclear.

Although clinical efficacy has yet to be achieved, development of protocols, new tools and above all multidisciplinary approaches for *de novo* bone formation that utilise mesenchymal stem cells with biomimetic scaffolds offer significant rewards for an increasing aged population both in terms of healthcare costs and, more importantly, improved quality of life.

ACKNOWLEDGEMENTS: Funding from the BBSRC, EPSRC, Royal Society, Nuffield Foundation and Wishbone Trust is gratefully acknowledged. The work presented and many useful discussions is derived from all at University Orthopaedics, Daniel Howard, Rahul Tare, Xuebin Yang, David Green, Kris Partridge, Trudy Roach and Nicholas Clarke as well as fruitful collaborations with Professors Shakesheff and Howdle (University of Nottingham), Professor Mann (University of Bristol) and Dr Julian Chaudhuri (University of Bath).

European Cells and Materials Vol. 4. Suppl. 2, 2002 (pages 28-29) ISSN 1473-2262

NANOSTRUCTURE INFLUENCES CELL ALIGNMENT AND MORPHOLOGY

D. S. Sutherland, J.Brink, P.Olsson, U.Lidberg and A-S.Andersson

Dept. of Applied Physics, Chalmers, Göteborg, Sweden

INTRODUCTION: The interaction of cells with surfaces has been a subject of interest over a number of years. The effect of topography has been widely studied and in particular the alignment of cells to micro and nanoscale steps and grooves is well known. Although there are a number of proposed mechanisms for this alignment no clear picture remains, especially for alignment to nanometer step edges. In this work we address the importance of the sharp edge of the step in the alignment process. Nano and microfabrication have been used to define a range of model surfaces which have step edges which are continuous or discontinuous.

METHODS: A combination of photolithography and colloidal lithography have been used to define a range of model substrates. Silicon wafer chips were coated with thin films of oxidized titanium to ensure that the surfaces had homogeneous surface chemistry. Grooved samples were fabricated using photolithography. The exposed wafers were coated with titanium before lift-off processing, the groove/ridge width was 15ìm, the groove depth was varied from 40 to 400nm. Nanostructured samples were fabricated by colloidal lithography [1], polystyrene particles were adsorbed to surfaces and subsequently coated in titanium films by electron beam induced evaporation. Some nanostructured samples were fabricated from flat substrates and some from grooved substrates. All samples were oxidized in a reactive ion etcher (O_2 0.5Torr 200w 120s) and treated with UV/ozone for 20 minutes before cell culture. The dimensions of the grooves were determined with a profilometer and scanning electron microscope (SEM). SEM images of the nanostructured surfaces were analysed with scion image software.

Mouse mammary gland epithelial cells (HC11) were cultured on the substrates in RPMI 1640 medium contyaing 10% FCS and 1% PEST for 10h and 24h at 37°C. At 10h and 24h the cells were fixed and stained for nuclei and actin (cytoskeleton). Images were taken using a fluorescence microscope at 40X mag. Digital image analysis was used to classify cells as `round´, `rectangular´ or `spool´ shaped. The classification was based on training groups including the parameters elongation, dispersion and form C. The alignment of the cells was also measured. Only single cells were analysed.

RESULTS: The morphology and alignment of cells was strongly affected by the surface topography presented to them. The effects were more visible after 10 hours of culture compared to 24 hours. The shape of the cells was systematically dependent on the size of nanoscale features (nanostructure size or groove depth). Alignment of cells correlated to shape and to nanometer surface structure. Alignment of cells to grooves with continuous edges was both higher and more persistent over time than for cells on grooves with discontinuous step edges.

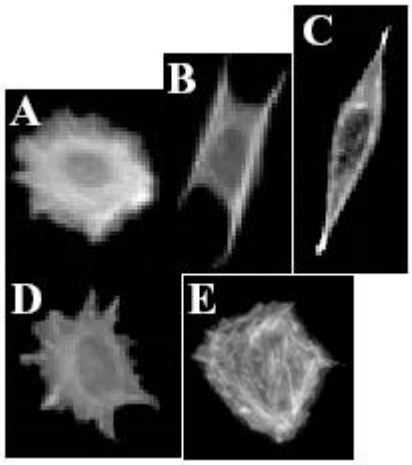

Fig. 1: The cells marked A,B,C are examples of cells classified as `round´, `rectangular´ and `spool´ respectively. The cells marked D and E are examples of cells which remain unclassified. Cell C is around 30 microns long

DISCUSSION & CONCLUSIONS: The alignment of cells to nanometer deep (40-400nm) grooves appears to depend on the presence of a `continuous´ step edge on the nanometer scale. The morphology of cells on `discontinuous´ topographically structured surfaces is different from cells on `continuous´ flat controls and is systematically effected by the scale of the topographic structure.

REFERENCES: [1] P.Hanarp, D.Sutherland, J. Gold and B. Kasemo (1999) *Nanostr. Mat.* **1-4:**429-432.

ACKNOWLEDGEMENTS: This work has been funded by the SSF foundation in Sweden under the biocompatible materials programme.

EFFECT OF EXTRACELLULAR MATRICES ON CULTURED HUMAN RENAL PROXIMAL AND DISTAL TUBULAR CELLS

Patrick C. Baer, & Helmut Geiger

Medical Clinic, Nephrology, J.W.Goethe University, Frankfurt/M; Germany

INTRODUCTION: Chronic renal failure is a basic problem which is currently far away from a satisfactory medical treatment. With the demonstration of experimental success with animal renal cells [1], the aim of this project is to develop functional human kidney equivalents for the replacement of tubular function during chronic renal failure. Therefore, the effects of extracellular matrices (ECM) on the attachment and proliferation of primary human renal cells were examined in order to use tubular cell monolayers cultured in precoated hollow fibers as bioartificial renal tubular devices.

METHODS: Human renal proximal and distal tubular epithelial cells (PTC / DTC) have been isolated immunomagnetically and cultured in medium 199 with 10% FCS [2-4]. 96-well-plates were precoated with gelatin (1%), matrigel (50µg/ml), collagen IV (50µg/ml), collagen IV+FCS, FCS, or PBS (as a control) for 1 hour. The liquids were removed and washed three times with PBS. 2000 cells were seeded and cultured for 96 hours. A rapid non-radioactive fluorescence assay (DAPI, 4,6-diamino-2-phenylindole) for the measurement of both cell number and proliferation was used [5]. Data are represented as relative fluorescence intensity (means ± SD, n=6). Alterations in per cent are calculated versus PBS-"precoated" wells.

RESULTS: The data from the DAPI-assay are summarized in Fig.1. The highest cell numbers were observed after matrigel-precoating (PTC +285%, DTC +167%). Gelatin- and collagen IV-precoating resulted in no significant higher cell numbers after 96 hours of culture, whereas a significant increase by precoating with collagenIV+FCS and FCS alone was observed (PTC: +198% / +137%, DTC: +109% / +76%, $p<0.01$ vs. PBS). This effect was significant higher in proximal cell cultures compared to distal cell cultures ($p<0.01$).

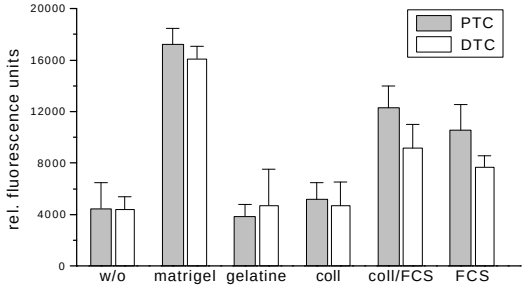

Fig 1: Effects of different matrices on total cell number of PTC and DTC. Data are represented as relative fluorescence intensity (means ± SD, n=6).

DISCUSSION & CONCLUSIONS: In the development of a bioartificial renal tubular device it is necessary to evaluate the optimal environment for cell attachment, spreading, proliferation and differentiation. Our data indicate the positive effects of precoating with matrigel or FCS. As in older studies with tubular cell lines (MDCK) no positive effects of collagen IV or gelatin alone could be demonstrated [6]. The described effects may be due to growth factors involved in matrigel / FCS. Further studies have to be perfomed to characterize the effects of growth factor and the influence of ECM-precoating on cell differentiation. Nevertheless, this study is the first step in the development of a bioartificial renal tubular device with seeded human tubular cells.

REFERENCES: [1] Humes HD, Buffington DA, MacKay S, et al (1999) *Nature Biotec* **17**:451-455. [2] Baer PC, Nockher WA, Haase W, et al (1997) *Kidney Int* **52**:1321-1331. [3] Baer PC, Tunn UW, Nunez G, et al (1999) *Exp Nephrol* **7**:306-313. [4] Baer PC, Scherberich JE, Bereiter-Hahn J, et al (2000) *Transplant* **69**(11): 2456-2462. [5] Blaheta RA, Franz M, Auth MKH, et al (1991) *J Immunol Meth* **142**:199-206. [6] Kanai N, Fujita Y, Kakuta T et al (1999) *Artif Org* **23**:114-118.

European Cells and Materials Vol. 4. Suppl. 2, 2002 (pages 52-54) ISSN 1473-2262

SPATIAL CONTROL OF CELL ATTACHMENT USING PLASMA MICROPATTERNED POLYMERS

Prize winning poster

S. A. Mitchell[1], N. Emmison[1]& A. G. Shard[2]

[1]*Advanced Materials Surfaces & Interfaces Research Group, Robert Gordon University, Scotland, GB*

[2]*Department of Engineering Materials, University of Sheffield, England, GB*

INTRODUCTION: In recent years, techniques have been developed to produce surfaces with well-defined chemical heterogeneity, which are suitable for promoting rapid cellular adhesion and spreading[1]. Spatial control of cells has been successfully demonstrated using such techniques as micro-contact printing[2], micro-fluidic channels, laminar flow patterning, self assembling peptides, and patterned self assembled monolayers (SAMs), typically using a photolithographic technique[3]. The spatial resolution of these techniques is sufficient to produce patterns of sub-cellular dimensions. It has been shown that high resolution patterns of this type can be employed to modify the size and shape of attached cells, influencing cell behavior[1]. Previous studies demonstrate the possibility of directing cell growth and behavior through the use of advanced surface engineering of physicochemical and topographical effects that influence the spatial organisation of cells[4]. This work demonstrates that plasma polymers may be patterned with sub-cellular dimensions and highlights some of the physicochemical factors that may be of importance in achieving high spatial resolution using this approach.

METHODS: The internal surfaces of 35mm Tissue Culture Polystyrene (TCPS) dishes were modified with a n-Hexane plasma polymer using an inductively coupled plasma chamber. A constant flow rate of ~9.5 Sccm and incident power of 10W were used in all experiments with a variety of deposition times (10-600s). The culture media used was Ham's F-12 with HEPES modification. The dishes were incubated at 37°C in a 5% CO_2 atmosphere. The surface chemical composition of unmasked dishes were characterised using a Kratos Axis Hsi 5 channel imaging XPS using monochromated Alk_α radiation (1486.6 eV). Topography was studied using a Digital Instruments Nanoscope IIIa SPM under ambient conditions. The masked mica was imaged in contact mode using a silicon nitride tip. The wettability of the n-Hexane plasma treated surfaces was assessed with a FTÅ125 Dynamic Contact Angle analyser.

RESULTS AND DISCUSSION: Exposure to a hexane plasma resulted in a reduction in the surface oxygen concentration from 10.5% to 1.8% after 600 seconds plasma treatment, figure 1. This is primarily due to a hydrocarbon plasma polymer being deposited on top of the TCPS surface, although reduction of the oxidised functionalities may also be occurring. The contact angle of water with the plasma modified TCPS demonstrates a marked increase in hydrophobicity with increasing treatment times, as shown in figure 2a. Figure 2b shows the wettability of a n-Hexane treated TCPS surface (wetted areas are untreated). Figure 3a shows the boundary between plasma treated and native (masked) TCPS on a masked dish. The cells attached to the masked TCPS show a flat morphology, indicating strong attachment and spreading, whereas the unmasked TCPS predominantly shows round cells that are only loosely attached to the surface. Figure 3b displays a similar surface, which has been rinsed with 2 × 5 ml of PBS to remove loosely adhered cells demonstrating that cells on the treated surface are easily removed. Figure 4 demonstrates that after an initial induction period of 16 to 19 hours there is an approximately linear increase in the number of spread cells on both the treated and masked areas of TCPS after 10 s of plasma treatment. Figure 5 shows the relative rate proliferation relative to TCPS is almost zero at low surface oxygen concentrations but rapidly increases once a threshold oxygen concentration is reached. The AFM image in figure 6 shows deposition depth is 5-10 nm and image resolution 5 ìm under these conditions. The growth of CHO cells on TCPS patterned using a variety of TEM grids and 300s n-Hexane plasma deposition are shown in figures 7 and 8. Scale bars = 100 µm.

CONCLUSIONS: Plasma polymerization can be used as a simple, rapid, and cost effective method for this purpose. The resulting surfaces have both a controllable chemical functionality and a pattern resolution comparable to other more widely used patterning techniques. This work demonstrates that chemical patterns with spatial resolution of less than 5 ìm can be achieved using patterned plasma polymerisation. Furthermore, these patterns can be deposited onto rough surfaces (such as TCPS) and be used to achieve spatial control, cellular attachment and proliferation of CHO cells. We suggest that deposition rate is a key factor in

determining the spatial definition of the chemical patterns. Topographic effects cannot be totally ruled out although the topography is very shallow, a few nanometres depth over a micrometre is a gradient of 1:1000.

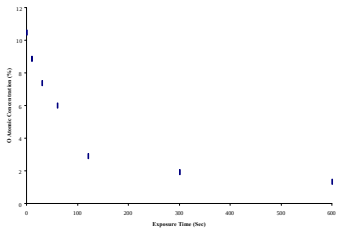

Fig 1. Oxygen concentration of the n-Hexane plasma treated surfaces

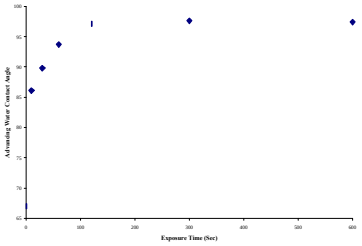

Fig 2a. Advancing water contact angle with n-Hexane plasma treated surfaces.

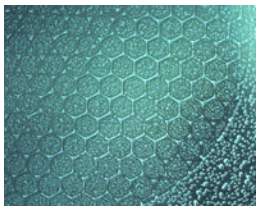

Fig 2b. n-Hexane patterned plasma hexagonal grid on TCPS

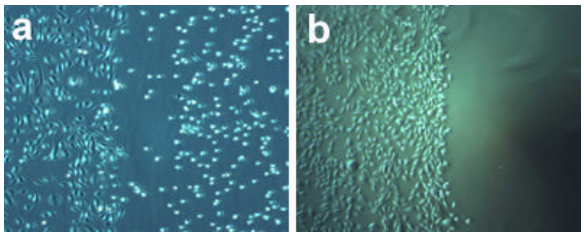

Fig 3a. Treated (RHS) and untreated (LHS) TCPS surface. 600s deposition, 24 hours incubation. Fig 3b. Treated (RHS) and untreated (LHS) TCPS surfaces following PBS wash. 300s deposition, 24 hours incubation.

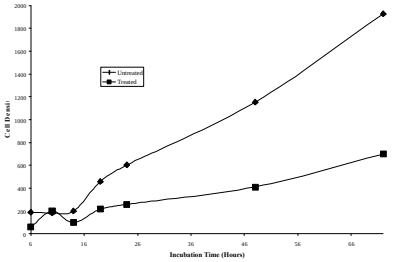

Fig 4. Density (No. of cells/mm^2) of spread cells attached to the treated and untreated surfaces.

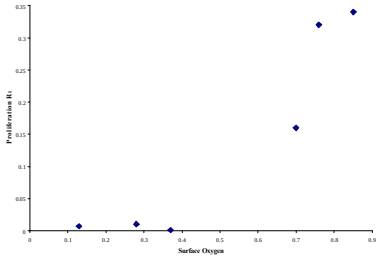

Fig 5. Rate of CHO proliferation on treated surfaces against surface oxygen concentration as determined by XPS.

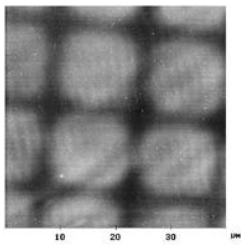

Fig 6. Patterned n-Hexane deposition on mica. 300s deposition, 1500 mesh grid.

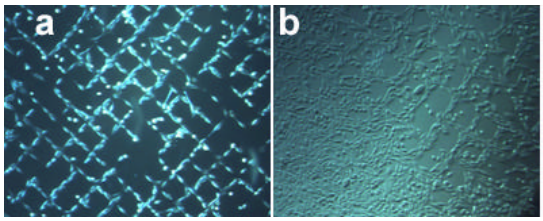

Fig 7a and b. 24 hours incubation, 200 (a) and 250 (b) mesh grid.

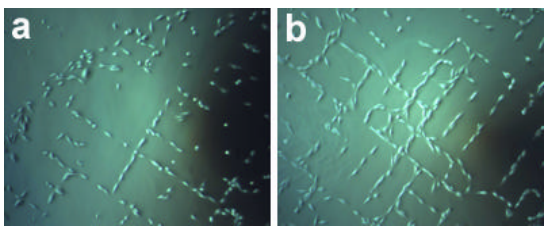

Fig 8a and b. 24 (a) and 48 (b) hours incubation, 1500 mesh grid.

REFERENCES: [1]C. S. Chen, M. Mrksich, S. Haung, G. M. Whitesides, D. E. Ingbar, *Science* 276, 1425-1428 (1997). [2]P. M. St. John, L. Kam,

S. W. Turner, H. G. Graighead, M. Issacson, J. N. Turner and W. Shain, *Journal of Neuroscience Methods*, 75, 171-177 (1997). [3]M. Mrksich and G. M. Whitesides, *Tibtech Reviews*, 13, 228-235 (1995). [4]D. R. Jung, R. Kapur, T. Adams, K. A. Giuliano, M. Mrksich, H. G. Craighead and D. L. Taylor, *Critical Reviews in Biotechnology* 21(2), 111-154 (2001).

ACKNOWLEDGEMENTS: Financial aid is acknowledged from the EPSRC grant number GR/M86996.

European Cells and Materials Vol. 4. Suppl. 2, 2002 (pages 9-10) ISSN 1473-2262

EFFECTS OF HIGH MOLECULAR WEIGHT HYALURONAN ON CHONDROCYTES CULTURED WITHIN SPONGOSTAN, A RESORBABLE GELATIN SPONGE.

+Goodstone, N; Gargiulo B; Cartwright, A; Ashton, B

The Arthritis Research Centre, The Robert Jones & Agnes Hunt Orthopaedic Hospital, University of Keele, Oswestry, Shropshire, SY10 7AG, UK

INTRODUCTION: Articular cartilage has a limited capacity for self-repair and is consequently vulnerable to injuries and disease that may lead to irreversible damage. Although there are many surgical techniques available to try to prevent or delay the need for joint replacement surgery, few techniques can repair extensive cartilage defects in the knee. This can be problematic in those patients considered too young for joint replacement surgery. Ideally, engineered cartilage could be used where native tissue has been lost or compromised by trauma or pathological disease. Engineering a fully mature cartilage construct and using it clinically is fraught with problems. Consequently, a partially formed building block comprising a biodegradable matrix scaffold loaded with a homogeneous cell population may be more attainable. Further, remodeling could then occur *in vivo* under physiological conditions of mechanical loading.

Biodegradable matrix scaffolds composed of gelatin have not been widely investigated as cell delivery systems. In this study we determined whether Spongostan, a resorbable gelatin sponge derived from porcine skin, has the potential to be used as a cell delivery system. In order to generate a partially formed building block, it is imperative to get an adequate number of cells of optimal phenotype. Small cartilage biopsies, particularly those from adults, do not produce sufficient numbers of chondrocytes without i*n vitro* expansion in monolayer culture. The disadvantage of this expansion is that chondrocytes dedifferentiate. Many naturally occurring extracellular matrix components, such as hyaluronan (HA), can influence chondrocyte proliferation, metabolism and matrix turnover. Herein, we also investigated if extrinsic high molecular weight HA could be used as a tool to not only expand freshly isolated chondrocyte numbers within a sponge but also prevent their dedifferentiation.

METHODS: Seeding sponges with chondrocytes: Freshly isolated bovine articular chondrocytes were seeded into Spongostan Standard (Johnson & Johnson) at 2.5 x 10^6 cells/0.5 x 1 x 1cm sponge). After 48 h in static culture, seeded sponges were tumbled in the presence of 0, 10 100μg/ml uncrosslinked, high molecular weight hyaluronan (Healon, Pharmacia) for a month. Media were replenished every other day. Cell loss was assessed in both static and tumble culture. Sponges were analysed after 1, 7, 14, 21 and 28 days.

Histology and Immunohistochemistry: Sponges were formalin-fixed, wax embedded, sectioned (5um) at <1mm and 5mm distances into the sponge, and stained with either Toluidine blue or H&E. Using a biotinylated HA-specific probe, immunohistochemistry was performed to confirm that extrinsic HA could access all pores within the sponge. Cell death was assessed by the TUNEL assay.

Biochemical Analysis: Sponges were analysed for glycosaminoglycan content using a DMMB assay and DNA content using a Picogreen fluorescent dye assay (Molecular Probes).

RT-PCR analysis of collagen types I, II and aggrecan mRNA expression: Total RNA was isolated using TriReagent (Sigma), reverse transcribed and amplified using bovine specific primers. PCR products were separated on 1.5% (w/v) agarose gels and visualised using ethidium bromide.

Statistics: All sponges were assayed in triplicate, and each experiment was repeated at least twice with chondrocytes from three different animals. Where appropriate results are expressed as the mean ± the standard error of the mean (S.E.M.).

RESULTS: Immunohistochemistry confirmed that extrinsic HA could access all pores within the sponge (data not shown). After initial seeding, the physical presence of extrinsic hyaluronan helped to retain more chondrocytes within the sponges (**Figure 1**). **Figure 2** demonstrates that Spongostan can be uniformly loaded and also supports chondrocyte proliferation and matrix production. **Figure 3** illustrates that extrinsic HA enhanced

chondrocyte proliferation 2-fold and also slightly enhanced matrix production. Expression of aggrecan and collagen type II mRNA, but not collagen type I, were detected in both control and HA-treated cells for all time points tested (data not shown). This data suggests that the freshly isolated chondrocytes did not dedifferentiate within the sponge. This will be confirmed by quantitative real-time PCR.

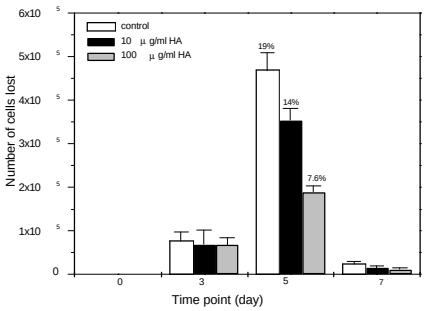

Figure 1: *Effects of high molecular weight HA on the reduction of cell loss from sponges. Cell loss as a percentage of total cells seeded are illustrated.*

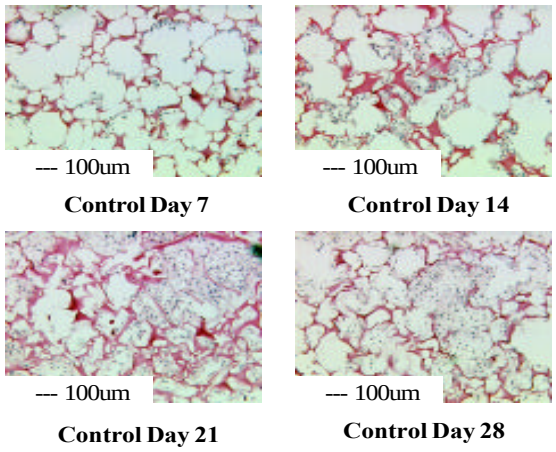

Figure 2: H&E stained sections (5um) cut from the middle of the sponges.

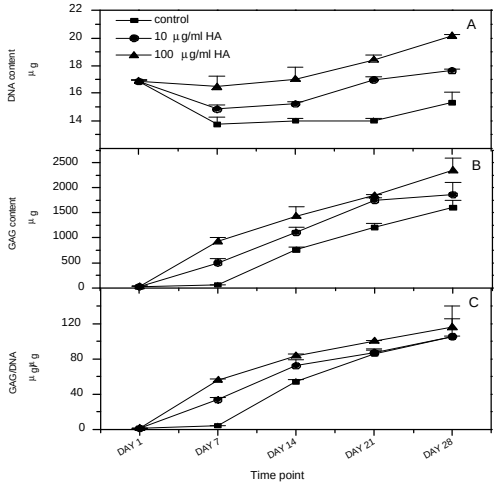

Figure 3*: Triplicate sponges were analysed for DNA (A) and GAG content (B). Data were expressed as GAG/DNA (C).*

DISCUSSION: This study shows that Spongostan has the potential to be used as a cell delivery system because it not only can be reproducibly seeded with chondrocytes but it can support their metabolism. In addition, these data indicate that extrinsic high molecular weight HA can influence chondrocyte proliferation and matrix production. This work suggests that extrinsic high molecular weight HA could be a useful tool for not only expanding initial low numbers of human chondrocytes loaded into a resorbable sponge but also preventing their dedifferentiation.

ACKNOWLEDGEMENTS:

We thank Dr Raija Tammi, Dept., of Anatomy, University of Kuipio and her technical support for the HA immunostaining. We thank our colleagues in the Dept., of Histology, The Robert Jones & Agnes Hunt Orthopaedic Hospital, for their help.

This work is funded by a European Commission grant entitled Biomechanical Interactions in Tissue Engineering and Surgical Repair.

European Cells and Materials Vol. 4. Suppl. 2, 2002 (pages 42-44) ISSN 1473-2262

THEORY AND APPLICATIONS OF A MAGNETIC FORCE BIOREACTOR

J. Dobson, A. Keramane and A.J. El Haj

Centre for Science & Technology in Medicine, Keele University, Thornburrow Drive, Hartshill, Stoke-on-Trent ST4 7QB United Kingdom

INTRODUCTION: The development and use of bioreactors are critical to progress in *ex vivo* tissue engineering. One of the developing areas in this field where there is a critical need for advances in bioreactor technology involves the production of autologous human bone and connective tissue for replacement surgery.

Evidence suggests that to achieve *ex vivo* production of functional bone, cells growing on scaffolds within the bioreactor must experience mechanical stimuli similar to those experienced *in vivo*[1]. These applied stresses are necessary to initiate biochemical reaction pathways (for example through the activation of mechanosensitive [MS] Ca^{++} ion channels) which allow human bone and cartilage to develop their characteristic mechanical properties. This requirement presents problems due to the fragile nature of the scaffold materials and the fact that any force-producing mechanism which invades the bioreactor introduces a pathway for infection.

Recently bioreactors have been developed which apply mechanical forces via piston systems, substrate bending, hydrodynamic compression, etc. Although these systems support cartilage and bone development, they face major problems – i.e. the profusion of cell nutrients may be interrupted, long term sterility is often a problem and, in the case of compression systems, gels must infiltrate the matrix in order to transmit the applied forces. In addition, with bioreactors presently in use, it is not possible to apply *three-dimensional,* spatially varying stresses in order to form complex tissue structures.

Here we present the theoretical principles of a novel system designed to apply stress to cells growing in bioreactors using forces on magnetic micro- and nanoparticles. In this system, biocompatible magnetic particles are attached to the cell membrane (e.g. via RGD, collagen or integrin receptors) or directly to the extracellular portion of an ion channel protein. These cells are seeded into the scaffold and introduced into a bioreactor. The application of time varying external magnetic fields applies either a translational force (for superparamagnetic nanoparticles) or a combination of translational force and torque (for larger, magnetically blocked nanoparticles and microparticles) which is transmitted directly to the cell membrane and can be varied in three dimensions within the scaffold.

This system offers several potential advantages over existing bioreactors: (i) continuous nutrient profusion during mechanical stimulation, (ii) no requirement for mechanically strong scaffold materials, (iii) the potential to iteratively investigate a wide range of force vectors (i) a closed system which reduces the chances of infection, (iv) a spatially scalable system.

METHODS: The initial version of the magnetic force bioreactor is based on the physical principles describing translational motion of magnetic particles, ferrofluids and materials in high magnetic field gradients. In this system, biocompatible magnetic nanoparticles – usually comprising a magnetic core with a polymer coating[2] - are functionalized and attached to the cell membrane prior to seeding onto polymer scaffolds in the bioreactor. Strong magnetic field gradients produced by an array of rare earth (generally NdFeB) magnets or electromagnetic coils generate a translational motion on the nanoparticles, producing compressive or tensile force on the cells in the scaffold as shown in Figure 1. This force will simulate mechanical loading without requiring direct access to the cells inside the bioreactor and without requiring the stress to be transmitted from the scaffold to the cells. Loads can be easily varied by changing the magnetic field strength and gradient or the magnetic properties of the nanoparticles compressing the tissue constructs.

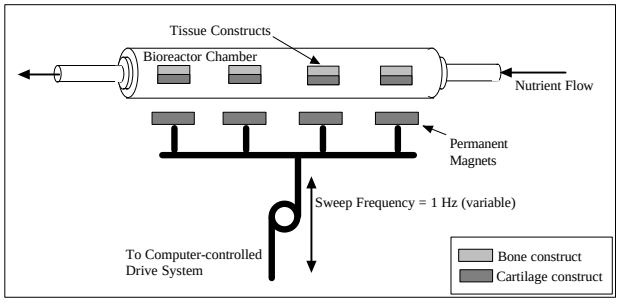

Figure 1: Magnetic bioreactor schematic.

The origin of the force for translational magnetic compression loading in a diamagnetic (tissue or culture) medium can be approximately derived by the expression:

$$F_{mag} = (c_2 - c_1)V\frac{1}{m_o}B(\nabla B) \quad (1)$$

Where χ_2 is the volume magnetic susceptibility of the magnetic particle attached to the cell, χ_1 is the volume magnetic susceptibility of the surrounding medium (i.e. tissue/bone), μ_o is the magnetic permeability of free space, **B** is the magnetic flux density in Tesla (T). Though this assumes spherical particles and no magnetic dipole interactions, it should give a good approximation of the field and gradient required for the system.

As the value of χ_1 for human tissue is very small and negative in comparison with the magnetic susceptibility of magnetite (the material which will be used in the ferrofluids, and nanoparticles), χ_1 is negligible for this calculation and the expression ($\chi_2 - \chi_1$) can be reduced to χ_2. Also, as we are interested in the translational motion of the magnetite particle/fluid/material in an applied field along the z-axis (vertical and close to the magnet) and, assuming a relative permeability of 1, the force expression can be reduced to:

$$F_{mag} = (c_2)VB\frac{dB}{dz} \quad (2)$$

It can be seen from these equations that the compressional force experienced by the tissue constructs in the presence of ferrofluids and magnetic particles is dependent on the strength of the field, the field gradient and the volumetric and magnetic properties of the particles. One of these parameters will have a strong spatial variation – the field strength/gradient product. This will enable the application of differential forces in three dimensions. In addition, by seeding different regions of the scaffold with particles, ferrofluids and magnetic materials of differing magnetic and volumetric properties, the three-dimensional variation in applied force can be enhanced. This should facilitate the growth of complex bone/cartilage tissue structures via the spatial variation of applied forces in later versions of the bioreactor.

In addition, theoretical analysis of the effects of applied magnetic fields on biogenic magnetite-bearing cells reveals that activation of MS transmembrane ion channels by applied fields is likely under certain conditions (i.e. rigid attachment of the particles to the cell membrane either directly or indirectly via cytoskeletal coupling)[3]. In this case, magnetically blocked particles experience a torque rather than a translational motion when the applied field is at an angle to the particle's magnetization vector according to the equation:

$$\tau = \mu \mathbf{B}\sin\theta \quad (3)$$

where τ is the torque, μ is the magnetic moment, **B** is the magnetic flux density and θ is the angle between the applied field and the particle's magnetization vector. This torque can also be used in the magnetic force bioreactor to activate MS ion channels.

RESULTS: Employing the theoretical principles described in the previous section, a prototype magnetic force bioreactor system has been produced which is designed for both 2D and 3D tissue culture applications. The system is controlled by custom software running on a Macintosh G4 computer. The magnetic system is housed, along with the bioreactor vessel, inside the incubator and is connected to the control electronics outside the incubator via a port as shown in Figure 2.

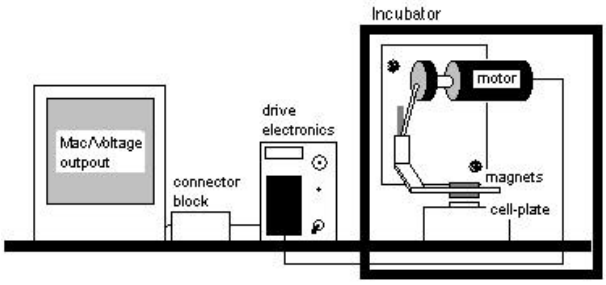

Figure 2: Magnetic drive and control system schematic.

DISCUSSION & CONCLUSIONS: The theoretical foundations for the design of a new type of stress-producing bioreactor have been presented. This system should provide many advantages over current systems such as the application of mechanical stress during continuous nutrient profusion, the use of mechanically weak scaffold materials, reduced infection potential, and unprecedented control of physical stress parameters. A prototype magnetic force bioreactor systems has been developed and built and the "proof-of-concept" testing of the device has begun, the initial results of which will be presented in another paper.

REFERENCES: [1] AJ El Haj et al. (1999) *Med. Biol. Eng. Comp.*, **37**: 403-409. [2] S Santra et al. (2001) *Langmuir* **17**: 2900-2906. [3] J Dobson and TG St. Pierre (1996) *Biochem. Biophys. Res. Commun.* **227**: 718-723.

ACKNOWLEDGEMENTS: This work is funded by EPSRC grant No. GR/R22247/01 and a Wellcome Trust Showcase Award.

European Cells and Materials Vol. 4. Suppl. 2, 2002 (pages 55-56) ISSN 1473-2262

CONTRACTILE BEHAVIOUR OF 3T3 MOUSE FIBROBLASTS IN ARTIFICIAL SKIN SUBSTITUTES: EFFECT OF DIFFERENT CELL-SEEDING METHODS

G. Ho[1], M.H. Grant[1] & J.C. Barbenel[2]

[1] *Bioengineering Unit, Wolfson Centre, Strathclyde University, Glasgow G4 0NW, UK*

[2] *Department of Electrical & Electronic Engineering, Strathclyde University, Glasgow, UK*

INTRODUCTION: With the rapid development of tissue engineering and gene therapy, collagen-based biomaterials are frequently used as cell transplant devices; an example is bio-artificial skin substitutes [1-3]. In this study, we determined the effects of two different cell-seeding methods, monolayer and suspension seeding, on the rate of contraction of free-floating collagen and collagen-glycosaminoglycan (GAG) gel matrices in vitro. 3T3 mouse fibroblasts were cultured in/on the matrices for up to 7 days.

METHODS: In monolayer cell seeding, 5ml of 0.3% (w/v) collagen gel matrices (24mm x 60mm) floating on 3ml of 10x complete Dulbecco's Modified Eagle's Medium (DMEM) in a hydrophobic cell chamber of 24mm x 60mm x 11mm were washed once in DMEM prior to seeding. To modify the gel matrices with GAG, chondroitin-6-sulphate (CH_6SO_4) was prepared at 3 mg/ml in 1x serum-free DMEM and incorporated into the collagen solution at 20%. 3T3 mouse fibroblasts in medium were then pipetted on the collagen and collagen-GAG gel matrices at a cell seeding density of 9×10^3 cells/cm^2. In suspension cell seeding, the 3T3 cells were seeded in suspension within the collagen gel matrices at a density of 1.3×10^5 cells/ml. The numbers of cells in both methods of seeding for both the collagen and collagen-GAG gel matrices were identical. Medium was changed daily. The area of contraction of the matrices was measured daily using a light-box over which the cell chambers were placed on a standard millimeter grid. Measurements were then calculated using digital planimetry and Scion imaging software (Scion Corporation, U.S.A.).

RESULTS: Fibroblasts seeded on the gel matrices as a monolayer culture induce significantly less contraction than fibroblasts seeded in suspension within the gel matrices (Fig. 1). It was shown that generally the extent of contraction was less in the GAG-treated collagen gel matrices. This difference was not significant.

CONCLUSIONS: These results showed that different cell-seeding methods do have an effect(s) on the contraction of collagen-based artificial skin substitutes.

REFERENCES: [1] S.T. Boyce, D.J. Christianson and J.F. Hansbrough (1988) Structure of a collagen-GAG dermal skin substitute optimized for cultured human epidermal keratinocytes, *J Biomed Mater Res* **22**(10):939-57. [2] S.T. Boyce, R.J. Kagan, N.A. Meyer, et al (1999) The 1999 clinical research award. Cultured skin substitutes combined with integra artificial skin to replace native skin autograft and allograft for the closure of excised full-thickness burns, *J Burn Care Rehabil* **20**(6):453-61. [3] W.H. Eaglstein, O.M. Alvarez, M. Auletta, et al (1999) Acute excisional wounds treated with a tissue-engineered skin (Apligraf), *Dermatol Surg* **25**(3):195-201.

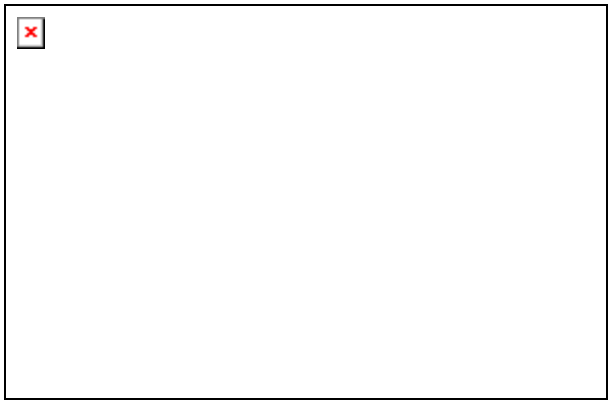

*Fig. 1: Effect(s) of different cell-seeding methods on the contraction of collagen-based artificial skin substitutes. Results are mean ± S.E.M., n=5. Using ANOVA, *p<0.05, compared with monolayer cell seeding on collagen gel matrices.*

European Cells and Materials Vol. 4. Suppl. 2, 2002 (pages 55-56) ISSN 1473-2262

European Cells and Materials Vol. 4. Suppl. 2, 2002 (page 35) ISSN 1473-2262

THE INFLUENCE OF ULTRAFINE SUBSTRATUM TOPOGRAPHY ON CYTOSKELETAL ORGANISATION IN EPITHELIAL CELLS.

Peter Clark

Division of Biomedical Sciences, *Imperial College, London, UK*

INTRODUCTION: Cell behaviour is strongly influenced by the shape of a cell's surroundings. Previously, it was found that the responses of MDCK epithelial cells to patterned substratum topography depended on cell-cell contact: single cells were highly sensitive, while cells in colonies were less affected [1, 2]. This investigation has attempted to determine how cells detect ultrafine features in their culture surfaces, by examining the cytoskeleton/focal adhesion organisation of single and colonial MDCK cells on planar and ultrafine grooved substrata (266 nm repeat).

METHODS: The ultrafine grooved surfaces were those used in previous studies[2-4]. They were defined in fused quartz microscope slides using laser interferometry and dry etching techniques, to give a grooved surface of approximately 266 nm period (i.e. groove width and groove separation half of this value) and 220 nm depth. MDCK epithelial cells (5×10^{-5}) were seeded onto grooved patterns in 6 cm culture dishes and cultured in 10% foetal bovine serum in Dulbecco's modified minimal essential medium for 24 or 48 hours before fixation. Cytoskeletal organization was determined using immuno-staining and both standard immuno-fluorescence and confocal microscopy.

RESULTS: On planar surfaces, isolated MDCK epithelial cells have polygonal outline radial arranged microtubules and strong circumferential F-actin staining. On ultrafine grooved surfaces, these cells are highly elongated and oriented to the grooves. Microtubules are generally aligned to the long axis of the cell, while F-actin is mainly found at the lateral edges. In dense culture, microtubules appear to have radial distribution on either surface. F-actin is found as polygonal outlines of regions of cell-cell contact on both substrata, however, stress fibre-like F-actin bundles are randomly oriented on palnar substrata but highly oriented on grooved substrata (Fig. 1). Optical sectioning by confocal microscopy showed that polygonal F-actin is in the apical region of the epithelial layer, while F-actin bundles are in the basal region, probably associated with cell-substratum contacts. Cell-substraum contacts at the leading edges of lamellopdial extensions were clustered in regularly spaced groups.

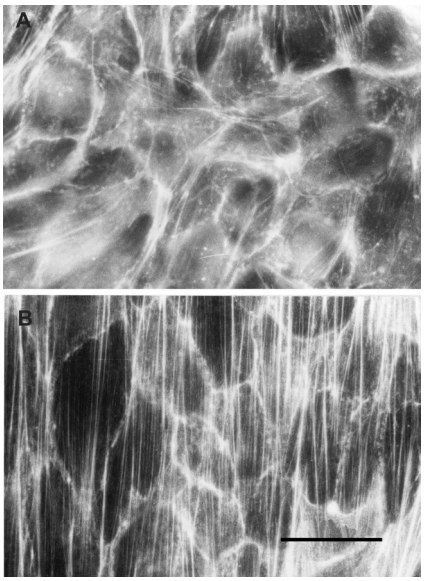

Fig. 1:Fluorescence micrograph of F-actin microfilaments in dense cultures of MDCK epithelial cells cultured on (a) unptaterned, planar surface or (b) 266 nm repeat grooved surface. (Bar = 32 μm)

DISCUSSION & CONCLUSIONS: Although epithelial cells appear to lose sensitivity to substratum alignment as the result of cell-cell contact and will form monolayers of poorly aligned, polygonal cells, the basal component of the actin cytoskeleton is profoundly affected by the underlying patterned substratum. Such an arrangement could have a strong influence of the mechanical properties and stability of cells in contact with micromachined devices.

REFERENCES: 1.Clark, P., et al., Topographical control o Cell Sci, 1995. 108(Pt 8): p. 2747-60. 4.Clark, P., et al., Alig

GROWTH AND VIABILITY OF OSTEOBLASTS ON HYDROXYAPATITE AND TRICALCIUM PHOSPHATE CERAMICS: EFFECT OF COLLAGEN COATING.

A.J. Ball[1], E.H. Rodgers[1], E. Goldie[1], G.Connel[1], R. Savage[2], J. Hamblin[2] & M.H. Grant1.

[1] *Bioengineering Unit, Strathclyde University, Wolfson Centre, Glasgow G4 0NW, UK.*

[2]Hi-Por Ceramics Ltd., Stubley Lane, Dronfield, Sheffield S18 1LS, UK.

INTRODUCTION: Hydroxyapatite (HA) and tricalcium phosphate (TCP) ceramics form the basis for bioartificial bone replacement materials. However, they lack mechanical strength and cannot at present be considered as replacements for load-bearing areas. We have investigated the characteristics of two ceramic materials, HA and a 60:40 composite of HA:TCP, which are being developed for facial bone reconstruction. The growth and viability of an immortalized cell line, FFC, derived from neonatal rat calvaria, was investigated when cultured on the materials for 7 days.

METHODS: Discs (12mm in diameter, 5mm in height) of the materials, synthesized by Hi-Por Ceramics, were sterilized by autoclaving, and placed in 24 well plates. FFC cells (2×10^4 cells in 0.2ml) were seeded and left to settle for 10 min, before 1ml of Dulbecco's Minimum Essential Medium containing 10% v/v foetal calf serum was added. Medium was changed at 3 and 5 days. After 7 days the discs were stained with 1mg/ml ethidium bromide (which penetrates the membranes of dead cells and stains their nuclei red) for 6 min, followed by 25µM carboxyfluorescein diacetate (CFDA) for 15 min at 4°C. In viable cells CFDA is de-acetylated to carboxyfluorescein which stains living cells bright green. Cells were examined immediately by confocal laser scanning microscopy (CLSM) using a x25 (N.A. 0.75) water immersion lens. In some experiments the HA and HA/TCP materials were coated with collagen type I isolated from rat tail tendons. The materials were coated by irrigating the discs with a solution of 7.8mg/ml collagen in 0.1% acetic acid followed by filtered air drying. The presence of the collagen coating was confirmed by staining the material with 0.1% w/v acriflavine (which stains collagen green) and examining it by CLSM.

RESULTS: After 7 days culture viable cells, stained green by CFDA, were evident growing on the surface of the uncoated HA material. In contrast, there were few intact cells observed on the HA/TCP material. On this material the cells were shrunken in appearance, and there were 'blebs' and cell fragments evident. They had retained the green CFDA-derived fluorescence, and had not allowed penetration of the ethidium bromide. This suggests that the cell membranes were intact in these structures. We propose that these are apoptotic bodies, and that the HA/TCP material had stimulated apoptosis in the osteoblasts. Acriflavine staining demonstrated that the collagen coating technique worked well for both materials. In the presence of collagen coating, growth of cells on both materials was improved. Viable cells grew around the rim of the pores, penetrated into the pores (to a depth of 45µm), and there was no indication of apoptotic cells on the collagen-coated HA/TCP. In fact, the cells were more numerous on this material than on the coated HA.

DISCUSSION & CONCLUSIONS: Collagen coating of ceramics may improve their integration into body tissues when used as bioartificial bone replacements by allowing cells to infiltrate into them more readily.

ACKNOWLEDGEMENTS: Alison Ball is a student sponsored by EPSRC. This project was supported by Hi-Por Ceramics Ltd.

European Cells and Materials Vol. 4. Suppl. 2, 2002 (page 99) ISSN 1473-2262

HIGHLY POROUS GEL-CAST CERAMICS IN MEDICAL APPLICATIONS

J. Hamblin[1], R. M. Sambrook[1]& N. J. Flowers, M. J. Hannon, M. R. Sambrook[2]

[1] Hi-Por Ceramics LTD, Stubley Lane, Dronfield, Sheffield, S18 1LS, England, GB

[2]Chemistry Department, The University of Warwick, Coventry, CV4 7AL, England, GB

INTRODUCTION: Ceramics with fully interconnected porous structures are prepared (by Hi-Por Ceramics LTD) using unique foaming methods. Porous hydroxyapatite (HA) (Fig. 1) prepared in this way is similar in chemical composition and porous structure to human cancellous bone. Synthetic HA acts as a biocompatible scaffold for the in-growth of healthy bone tissue. Synthetic HA/tri-calcium phosphate (TCP) composites allow more rapid resorption of the synthetic material as the healthy bone tissue grows to replace the implanted material. The preparation of drug/polymer/HA composites for the treatment of osteogenic sarcoma is currently under investigation. Removal of the diseased section of the bone is a common element in the treatment of osteogenic sarcoma resulting in the need for bone grafts to replace lost tissue.

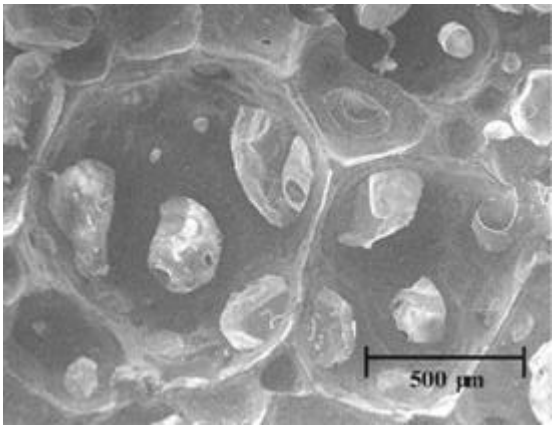

Fig. 1: SEM photograph of the porous HA foam

RESULTS: HA/Methotrexate composites were prepared and tested *in vitro*. The results demonstrated that the sustained release of the chemotherapeutic drug from the ceramic increased the effectiveness of the drug on osteosarcoma cell lines. The incorporation of biocompatible, biodegradable polymers into the ceramic/drug composites offers the potential for further control over drug release (Fig. 2). Results demonstrate that the rate of release of drugs from the ceramic is dependent on the biodegradation rate of the polymer and ceramic composition.

Figure 2: Graph demonstrates the increased control over drug release rate afforded by the biodegradable polymer

CONCLUSION: Drug/HA/polymer composites could act as a valuable form of local chemotherapy when used as strut grafts to repair bones after the removal of cancerous tissue. The incorporation of multiple drugs into implants could enable combination chemotherapy with drugs released at controlled time intervals.

European Cells and Materials Vol. 4. Suppl. 2, 2002 (pages 58-59) ISSN 1473-2262

A COMPARISON BETWEEN STATIC AND MICROGRAVITY (RCCS®) CULTURE ON THE GROWTH OF MCF-7 HUMAN BREAST CARCINOMA CELLS WITHIN A 3D ENVIRONMENT

Rose FRAJ[1], LJ Hodges[1], T Bradshaw[2], MFG Stevens[2], KM Shakesheff[1].

Tissue Engineering Group[1] and Drug Discovery and Cancer Chemotherapy[2], Institute of Pharmaceutical Sciences, University of Nottingham, University Park, Nottingham, England, GB.

INTRODUCTION: The need to develop novel tumour models that closely mimic the *in vivo* tumour environment is essential for drug validation and future advances in anti-carcinoma therapy[1]. Current methods employed in drug testing include monolayer culture, intra-peritoneal hollow fibre and xenograft *in vivo* models, all of which fall short of the ideal[2]. Applying tissue engineering strategies to the culture of cancer cells *in vitro* presents a real opportunity to develop a more accurate, ethical and cost effective model for anti-carcinoma drug screening. The aim of this study was to compare the effect of static and microgravity culture (Rotary Cell Culture System; RCCS®) on the growth of MCF-7 human breast carcinoma cells within a 3D environment.

METHODS: Poly(ethylene terephthalate) needled felt scaffolds (manufactured by Smith and Nephew, York, UK) were seeded by agitation with MCF-7 human breast carcinoma cells (p53), overnight at 37°C, 5% CO_2 in air. Following seeding, the seeded scaffolds were cultured either statically (in 6 well tissue culture plastic plates) or in a RCCS® Cellon, Luxembourg) for a period of 6 weeks. Constructs were sacrificed for image analysis at weeks 0 (post-seeding), 3 and 6. Image analysis included confocal microscopy, using a live/dead® stain (Molecular Probes, USA) to assess cell viability, and scanning electron microscopy (SEM) to demonstrate cell distribution within the scaffold.

RESULTS: Confocal microscopy revealed a mixed population of both viable and non-viable cells in both culture conditions at all time points. At week 6, a necrotic core was evident within the construct cultured in static conditions but not in the RCCS, which contained viable cells throughout. Cell proliferation in the RCCS was evident from SEM as an increase in cell mass, distributed throughout the construct, was observed throughout the experiment. In contrast, few cells were present throughout the statically cultured scaffold at weeks 3 and 6.

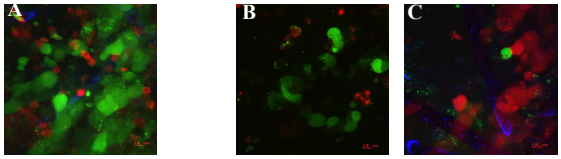

Fig. 1: Confocal microscopy demonstrating cell viability (green indicates viable cells; red indicates non-viable cells) and distribution of cells throughout scaffolds cultured in a RCCS (A) and static culture (B [scaffold surface] & C [scaffold centre]).

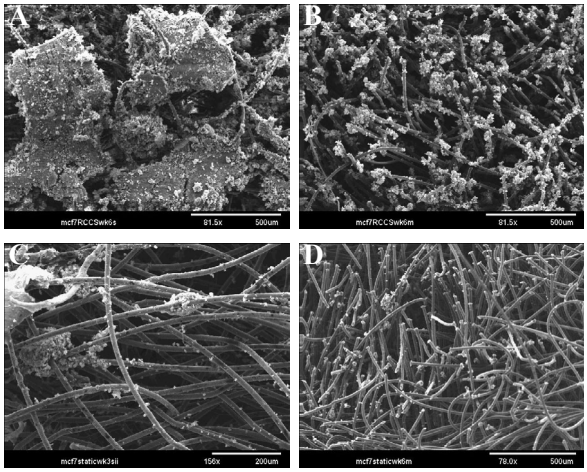

Fig. 2: SEM demonstrating cell distribution throughout scaffolds cultured in a RCCS (A [scaffold surface] & B [scaffold centre]) and static culture (C [scaffold surface] & D [scaffold centre]).

DISCUSSION & CONCLUSIONS: This study demonstrates that MCF-7 carcinoma cells can be cultured for up to 6 weeks in 3D culture conditions. Constructs cultured in static conditions resulted in a viable outer surface of cells but a necrotic inner core. In contrast, cells cultured in the RCCS proliferated to a greater extent and viable cells were observed throughout the construct. This phenomenon holds the potential for generating novel *in vitro* 3D models essential for early, accurate, high-throughput screening of new anti-carcinoma drug candidates.

REFERENCES: [1]Bhadriraju K, CS Chen. *Engineering cellular microenvironments to improve cell-based drug testing.* Drug Discovery Today 2002 7(11): 612-620. [2]Newell DR. *Flasks, fibres and flanks – pre-clinical tumour models for predicting clinical anti-tumour activity.* British Journal of Cancer 2001 84(10):1289-1290.

ACKNOWLEDGEMENTS: Confocal microscopy was carried out by Dr Susan Anderson, Department of Biomedical Sciences, University of Nottingham, Nottingham, GB.

European Cells and Materials Vol. 4. Suppl. 2, 2002 (pages 60-61) ISSN 1473-2262

CELL SURFACE MODIFICATION OF L6 MYOBLASTS *VIA* SODIUM PERIODATE TREATMENT

I. Wood[1], P. De Bank[1], B. Kellam[1], K. Shakesheff[1]& D. Kendall[2]

[1] *School of Pharmaceutical Sciences, University of Nottingham, England, UK*

[2]*School of Biomedical Sciences, QMC, University of Nottingham, England, UK*

INTRODUCTION: The site-specific innervation of engineered muscle tissue remains an elusive but potentially invaluable goal. Engineering of cell-cell interactions between the motorneuron and muscle cell would constitute a significant step forward along this path. We describe the remodeling of myoblast cell surfaces to form unnatural aldehyde groups on cell surface sialic acid via oxidation by periodate at room temperature (RT). These groups can subsequently be used to ligate moieties on to the cell surface using hydrazides.

METHODS: L6 myoblasts were treated with 1 mM sodium periodate for 5 minutes at room temperature and subsequently biotinylated by incubation with 5 mM biotin hydrazide for 90 minutes at room temperature. Cells were then double stained with 5 µg/ml FITC-avidin for 15 mins each at 4 °C in the dark and then fluorescence analyzed. These conditions were used to obtain confocal microscopy images of the FITC-avidin immobilization, and unless stated otherwise were the conditions used for other experiments. To determine optimum conditions, the length of treatment was varied from 1 to 5 minutes, and the concentration of periodate was varied from 5 µM to 1 mM in separate experiments. In both cases, fluorescence shift was compared to the control by flow cytometry analysis. To assess the effects of periodate on viability and total cell number, cells were treated with periodate and then cell counts were performed using trypan blue exclusion at various time intervals over 72 hours.

RESULTS: Immobilization of FITC-avidin (green) on the myoblast cell surface is shown in figure 1. (N.B. the nuclei are stained red with propidium iodide for reference.) It is apparent that there is no internal staining of the cells by FITC, and that staining is extensive on the cell surface including cellular processes. There is no visible immobilization of FITC on the control myoblasts.

The effect of length of treatment of periodate at RT is shown in figure 2. This demonstrates that cell surface oxidation is achieved rapidly under

these conditions even in times as short as one minute.

The effect of periodate concentration on fluorescence shift is shown in figure 3. A sigmoidal dose-response curve was fitted to the data and the EC_{50} was determined to be 377 µM (3SF) using Prism software.

The effect of periodate treatment on myoblast viability is shown in figures 4 and 5 respectively. Over the 72 hours following treatment, there is a small decrease in total cell number, and no significant difference in myoblast viability when compared to control myoblasts.

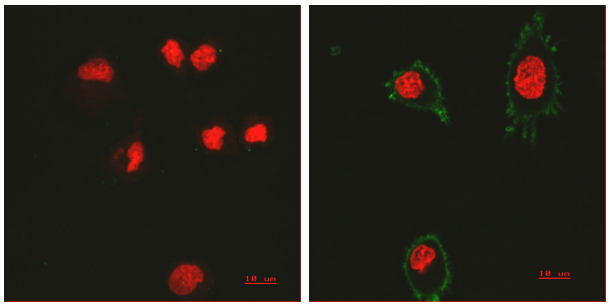

Fig. 1: Confocal microscope images of control myoblasts (left) and periodate-treated myoblast (right).

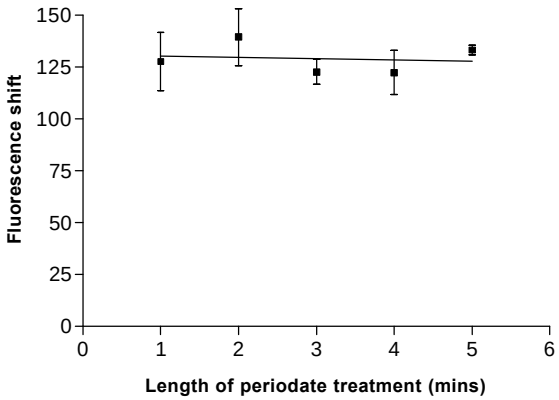

Fig. 2: Relationship between length of periodate treatment (1 mM, dark, RT) and fluorescence shift produced.

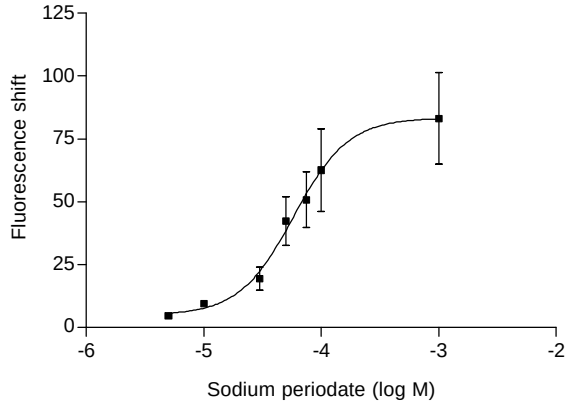

Fig. 3: Relationship between concentration of periodate (5 mins, dark, RT) used and fluorescence shift produced.

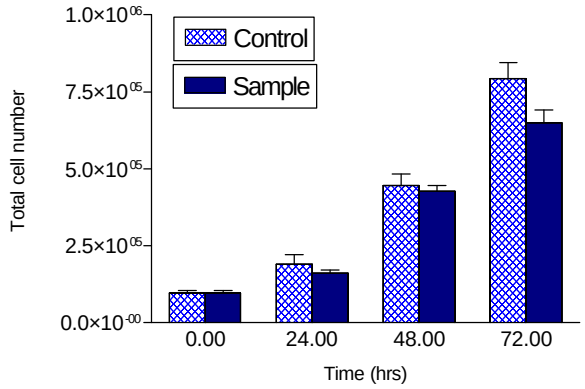

Fig. 4: Total cell number of periodate-treated and control myoblasts over 72 hours following periodate treatment (5 mins, 1 mM, dark at RT).

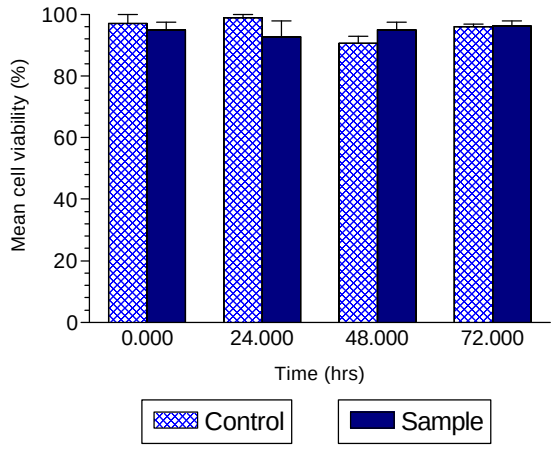

Fig. 5: Graph showing the viability of control and periodate-treated myoblasts over the 72 hrs following treatment with periodate (5 mins, 1 mM, dark, RT).

DISCUSSION & CONCLUSIONS We have demonstrated the ligation of biotin to cell surface aldehydes created by sodium periodate oxidation. This was detected by the immobilization of FITC-avidin and provides evidence for the successful engineering of the cell surfaces of L6 myoblasts. Furthermore, we have demonstrated that such cell surface oxidation can be achieved rapidly with one minute periodate treatment at RT. The rapid treatment time minimizes the time that the cells are out of their growth medium which, in turn, limits any potential harmful effects on the cell. The sigmoidal concentration-dependent effect curve (fig. 3) appears to plateau at around log [periodate] = -3 which suggests that 1 mM periodate is sufficient to cause maximal/near maximal cell surface oxidation at RT. We have also shown that sodium periodate treatment under these conditions does not significantly affect cell viability and only has a minor detrimental effect on total cell number. This difference could be attributed to a decrease in the rate of cell proliferation. Taken collectively, these results provide strong support for the use of 1 mM sodium periodate at room temperature for five minutes as a method of cell surface modification of L6 myoblasts**.**

ACKNOWLEDGEMENTS: We would like to thank Sue Anderson and Heather Judge for their help with confocal microscopy and flow cytometry, respectively.

SYNTHESIS AND CHARACTERISATION OF AN EXTENDED SERIES OF BIODEGRADABLE CYCLOALIPHATIC POLYESTERS

E. Barriau, P.A.G. Cormack, J.H. Daly, J.J. Liggat, and A. Quincy

Department of Pure and Applied Chemistry, University of Strathclyde, Glasgow G1 1XL, UK

INTRODUCTION: We report the synthesis and characterisation of an extended series of biodegradable cycloaliphatic polyesters for medical purposes. These polymers are based on cis- and trans-1,4-cyclohexanedicarboxylic acid, cis- and trans-1,4-cyclohexanediol and straight chain aliphatic diols and diacids with different chain lengths. The results demonstrate the possibility of controlling polymer morphology through the cis/trans composition of the 1,4-cyclohexane moiety. The trans isomer increases the regularity of the polymer chain and hence modifies the crystalline morphology, the most obvious indication of which is an increase in melting point.

METHODS: Cis and trans isomers of 1,4-cyclohexane-dicarboxylic acid or 1,4-cyclohexanediol were separated from commercially supplied mixtures by derivatisation and recrystallisation or solvent extraction. Diacids were converted with thionyl chloride into the more reactive acid chlorides. Polycondensations were then performed in the melt, and the polymers recovered and purified by dissolution and precipitation. Polymers were characterised by NMR, X-ray diffraction and thermal analysis.

RESULTS:

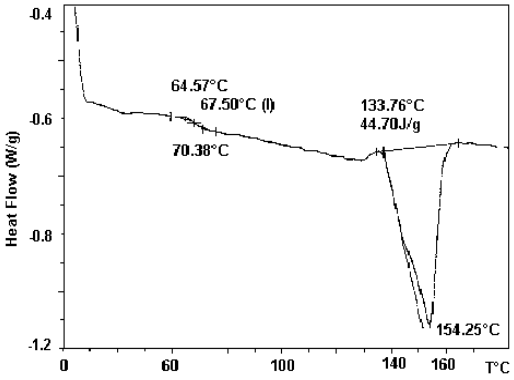

Fig. 1 Differential scanning calorimetry curve for poly(butyl-1,4-cyclohexanoate); 100% trans isomer, showing high melting point (154°C).

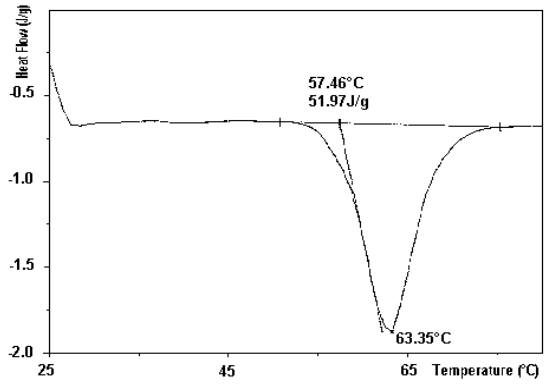

Fig. 2 Differential scanning calorimetry curve for poly(butyl-1,4-cyclohexanoate), 100% cis isomer, showing low melting point (63°C). Heat of fusion is essentially unchanged.

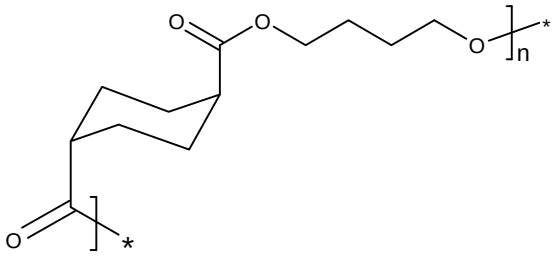

Fig. 3. Poly(butyl-1,4-cyclohexanoate), trans isomer.

DISCUSSION & CONCLUSIONS: The crystalline morphology of these polyesters is controlled by the cis/trans content of the cyclohexane moiety. Control of morphology offers the opportunity for the optimisation of mechanical properties and biodegradation lifetime.

ACKNOWLEDGEMENTS: This work was funded by the EC through programme number QLK3-CT-2000-01500 (NANOMED), and the Engineering and Physical Sciences Research Council through grant GR/R51193.

European Cells and Materials Vol. 4. Suppl. 2, 2002 (pages 36-37) ISSN 1473-2262

A PLASMA POLYMER SURFACE FOR THE CO-CULTURE OF HUMAN DERMAL FIBROBLASTS AND HUMAN EPIDERMAL KERATINOCYTES FOR WOUND HEALING.

Michael Higham [1], Robert Short [1], Marika Szabo [1], Rebecca Dawson[1], Sheila MacNeil [1]

[1] *Department of Engineering Materials, Sir Robert Hadfield Building, Mappin Street, University of Sheffield, S1 3JD.*

INTRODUCTION For wound cover, reconstructive surgery and for promoting healing in chronic non-healing wounds a number of approaches have been employed to expand skin cells in the laboratory and then transfer them to the patients wound bed. Several studies have employed animal derived products such as Collagen I for the culture of human epidermal keratinocytes and transfer of an integrated sheet to wound bed models. Against this background, this laboratory has recently developed a chemically defined surface for the culture and transfer of keratinocytes [1,2,3]. These are synthetic surfaces capable of influencing and controlling cell physiology either directly or through an adsorbed protein layer. These thin polymeric films, typically a few nm in thickness, are produced from continuous wave radio frequency induced plasmas of volatile organic compounds.

The objective of this study was to further develop the wound healing potential of keratinocytes cultured on this plasma polymer surface by including a growth arrested layer of fibroblasts to exploit the well documented interdependency of keratinocytes and fibroblasts. Accordingly we aim to determine a culture surface appropriate for coculture of fibroblasts and keratinocytes. Lethal gamma-irradiation allows fibroblasts to remain viable but unable to divide. This fibroblast feeder layer in turn secretes mitogens to promote keratinocyte colony formation. Potentially the inclusion of a fibroblast feeder layer will enhance the culture or "performance" of cultured keratinocytes in promoting wound healing.

MATERIALS AND METHODS: Surfaces containing 0, 1.5, 3.5 and 10% acid were prepared at a base pressure of $3x10^{-3}$ mbar. Surface chemistry was controlled by the incorporation of an octa-1,7-diene diluent into the monomer feed and by parameters such as power input, flow rate and deposition time. Plasma polymerised films were characterised using X-ray Photon Spectroscopy. Human dermal fibroblasts and epidermal keratinocytes were cultured with foetal calf serum on plasma polymer coated 24 well plates. Cell proliferation was assessed, with respect to positive and negative controls using MTT and DNA assays [1,2,3].

RESULTS Of the surfaces examined both keratinocytes and fibroblasts showed optimal attachment and proliferation over a 7 day period to a 100% acrylic acid surface (advancing contact angle 46°). This surface contained approximately 9.2% carboxylate groups. Fabricated at 10W it was stable to dissolution as assessed by advancing and receding contact angle measurements. The performance of cells on this surface was similar to their growth on Collagen I, a well-established substratum for the proliferation of keratinocytes. The 100% acrylic acid surface also supported the attachment of irradiated fibroblasts which did not increase in number. Keratinocytes formed good colonies and were able to expand more rapidly in the presence of a fibroblast feeder layer both on collagen I and on the 100% acrylic acid surface.

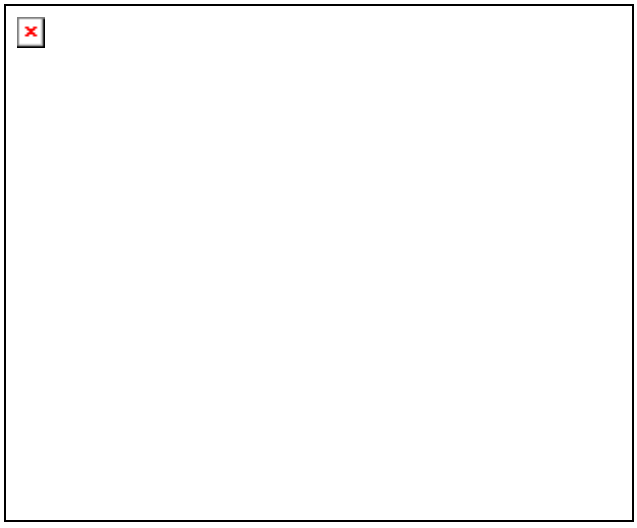

Figure 1*: DNA assay illustrating the effect of an irradiated dermal fibroblast feeder layer on the proliferation of keratinocytes cultured on a 100% acrylic surface and on collagen I after 7 days in culture.*

DISCUSSION Human keratinocytes and fibroblasts have been successfully cultured on plasma co-polymer surfaces containing carboxylate groups. Optimum proliferation of both cell types was observed on a pure acrylic acid surface, fabricated at 10W. The hydrocarbon dilutent, octa-1,7-diene, allowed control of the resulting functional group concentration by promoting cross-linking of the other monomer. Further work will now examine the potential of the keratinocytes to transfer to *in vitro* wound bed models and evaluate the contribution of the fibroblast to this culture system.

CONCLUSION The data reported shows that by using a plasma polymer surface as a synthetic substrate, it is possible to effectively co-culture human epidermal keratinocytes with a non-proliferative fibroblast feeder layer to achieve an increased rate of keratinocyte proliferation. This coculture system offers an attractive approach to the delivery of keratinocyte for clinical use.

REFERENCES [1]France RM *et al*. (1998), Chem Mater, **10**, 1176-1183. [2]Haddow D.B *et al*. (1999), Journal of Biomedical Materials, **47** (5), 379-387. [3]Haddow D.B et al (2002), Journal of Biomedical Materials (in press)

European Cells and Materials Vol. 4. Suppl. 2, 2002 (pages 7-8) ISSN 1473-2262

LIGHT-INDUCED CALCIUM SIGNALLING IN CHONDROCYTES

M.M. Knight, S.R. Roberts, D.A. Lee & D.L. Bader

IRC in Biomedical Materials, and Medical Engineering Division, Dept of Engineering, Queen Mary University of London, Mile End Rd, London, UK

INTRODUCTION: Reactive oxygen species (ROS) function as intracellular 2nd messengers in healthy tissue and are also involved in disease conditions including atherosclerosis, oseoarthritis and cancer [1]. Light stimulates the production of ROS either via damage to biological molecules or degradation of a fluorescent dye. Previous studies using clinical photodynamic agents, have reported light-induced release of ROS leading to activation of intracellular Ca^{2+} signalling and cell death [2,3]. This study tests the hypothesis that light-induced Ca^{2+} signalling and phototoxicity also occurs in chondrocytes due to the release of ROS from standard fluorescent probes used for microscopy

METHODS: Bovine articular chondrocytes were isolated by enzyme digestion and seeded in agarose constructs [4]. After 24 hrs in culture, cells were labelled with the calcium probe Fluo-4 AM, then bathed in EBSS and visualized over a 1 hour period using confocal microscopy (Perkin Elmer). Confocal laser power was set at either 15 or 30 μW termed low and high power respectively. Further group of specimens were incubated in 1mM ascorbate throughout the 1 hour imaging period. Control cells were either not labelled or not imaged. After imaging, cell-agarose constructs were returned to culture for 24 hours and then the same groups of cells assayed for viability using Calcein-AM and Ethidium homodimer (Sigma).

RESULTS: Chondrocytes visualised for 1 hour exhibited either 1 to 3 spontaneous Ca^{2+} transients, Ca^{2+} oscillations of 4 or more transients or a constant level of intracellular Ca^{2+} (Fig 1).

a)

b)

Fig. 1: Ca^{2+} traces from separate cells showing a single Ca^{2+} transient (a) and Ca^{2+} oscillations (b).

At high laser power 86% of cells exhibited at least one Ca^{2+} transient with 32% of these cells showing Ca^{2+} oscillations (Fig 2). At low laser power there was a significant reduction in the percentages of cells exhibiting single transients or oscillations. Treatment with the antioxidant, ascorbate, also reduced the Ca^{2+} response at both high and low power. 24 hours after exposure to the 1 hour imaging period, cell viability was maintaining at approximately 90% for control cells. By contrast, the viability of cells labelled with Fluo-4 AM and imaged for 1 hour at either high or low laser power was 20% and 57% respectively. Treatment with ascorbate increased cell viability to 65% for high laser power and 93% for low laser power.

Fig. 2: Percentages of cells showing 1-3 Ca^{2+} transients (□) or Ca^{2+} oscillations (□) in 1 hour.

DISCUSSION & CONCLUSIONS: Light-induced release of reactive oxygen species (ROS) initiates both Ca^{2+} signalling and cell death in chondrocytes labelled with Fluo-4 AM. Ca^{2+} signalling may trigger alterations in numerous cell processes and thereby represent an important and hitherto overlooked artifact in fluorescent microscopy of viable cells. Ca^{2+} oscillations were not always associated with cell death suggesting that the two events are not part of the same pathway. Sub-toxic light-activated Ca^{2+} signalling and associated changes in cell function, may therefore have applications in the development of therapeutic and tissue engineering technologies.

REFERENCES: [1]B.Halliwell (1994) *Lancet* **344**:721-4. [2]A.Hubmer *et al.*, (1996) *Photochem Photobiol* **64**:211-5. [3]Z.J.Cui & T.Kanno (1997) *J Physiol* **504**:47-55. [4]S.R.Roberts *et al.* (2001) *J Appl Physiol* **90**:1385-91.

ACKNOWLEDGEMENTS: MMK is funded as an EPSRC Advanced Research Fellow.

European Cells and Materials Vol. 4. Suppl. 2, 2002 (pages 62-63) ISSN 1473-2262

CELL ATTACHMENT AND PROLIFERATION ON NOVEL POLYCAPROLACTONE FIBRES HAVING APPLICATION IN SOFT TISSUE ENGINEERING.

Matthew R. Williamson, Eric F. Adams, Allan G. A. Coombes

Pharmaceutical Sciences Research Institute, Aston University, Birmingham, B4 7ET, U.K.

INTRODUCTION: Fibres produced from the synthetic poly(α-hydroxy acid) poly(L-lactide) (PLA) and poly (L lactide co-glycolide) [PLG] have been investigated extensively for applications in wound repair and tissue engineering (1). However in cases where tissue repair times are extended such as during bone regeneration, the use of fast resorbing (PLG) copolymers could relieve anchorage-dependant cells of a stable substrate for laying down extracellular matrix of optimal quality and orientation. PLA fibres while having resorption times in excess of one year suffer from low extensibility. The PLA starting material also shows a tendency to degrade during melt processing. PCL fibres present a promising alternative for production of 3-D matrices for use in tissue engineering. The higher compliance and extensibility of PCL relative to PLA, could present distinct advantages for regeneration of soft tissue.

METHODS: PCL fibres, 150ìm in diameter were produced using a wet spinning technique. The **surface morphology** of the as-spun and drawn fibres was examined using SEM. The **thermal characteristics** of as-spun fibres were investigated using differential scanning calorimetry at a heating rate of 10 C/min. **Fibre tensile properties** were measured using a Hounsfield tensometer at an extension rate of 15mm/min. The **proliferation rate** of Swiss 3T3 fibroblasts on PCL fibres was assessed using cell culture to provide a measure of colonisation efficiency. Tissue culture plastic (TCP) surfaces were used as controls. The number of cells attached to each substrate at various time intervals up to 8 days was measured using a haemocytometer following cell detachment by trypsin treatment. Cell numbers were also measured at time intervals up to 8 hours on gelatin coated fibres and TCP.

RESULTS:

Table 1. *Tensile properties of as-spun PCL fibres*

Yield stress MPa	5.0 ± 0.21
% extension at yield	11.5 ± 0.66
Failure stress MPa	9.3 ± 0.17
Failure % extension	651 ± 75.8
E-modulus GPa	0.07 ± 0.016

Table 2. *Tensile properties of drawn PCL fibres*

% extension	500
Yield stress MPa	31.7 ± 4.0
% extension at yield	14.2 ± 3.1
Failure stress MPa	42.7 ± 3.3
Failure % extension	140.5 ± 117
E-modulus GPa	0.31 ± 0.029

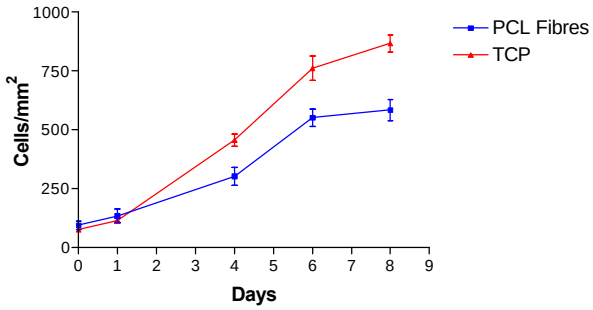

Fig 1. *Density of Swiss 3T3 fibroblasts on PCL fibres and TCP versus time.*

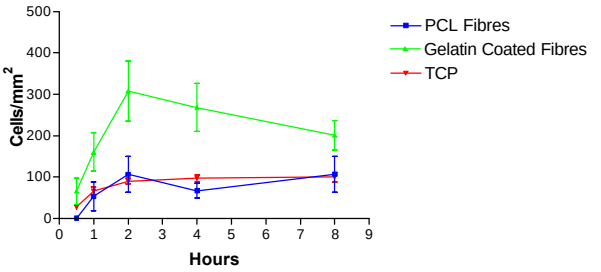

Fig 2. *Density of Swiss 3T3 fibroblasts on TCP, PCL fibres and gelatin coated fibres versus time.*

DISCUSSION & CONCLUSIONS: Highly drawn PCL fibres exhibited a Young's modulus of 0.3 GPa and tensile strength of around 40 MPa. The typical mechanical properties of hot drawn PLA fibres obtained by Leenslag et al are 9.5 GPa and 850 MPa respectively (2). The melting point (Tm 56 C) and percentage crystallinity (64%) of as-spun fibres were found to be similar to melt processed PCL pellets. The latter property was estimated using the reported heat of fusion of 139.5J/g for 100% crystalline polycaprolactone (4). The proliferation rate of fibroblasts on PCL fibres was lower than on TCP. However the number of fibroblasts reached confluence on PCL fibres in 6 days (584 cells/mm^2). The relatively high cell proliferation rates on PCL fibres indicate a favourable surface environment for adsorption and binding of cell adhesion glycoproteins such as fibronectin. This may be explained in part by the characteristic roughened and porous nature of wet-spun fibres. The attachment rate of fibroblasts on gelatin coated PCL fibres was 3 fold higher at 1 hour compared to TCP and uncoated PCL fibres, underlining the cell adhesion qualities of gelatin. The subsequent decrease in cell number on the gelatin-coated fibre can be explained by gradual loss of the coating.

The high growth rate of fibroblasts on PCL fibres (compared to TCP) combined with high fibre compliance indicate that PCL fibres could be advantageously applied for 3-D scaffold production in soft tissue engineering.

REFERENCES: [1] Hubbell, J.A (1995). *Biotechnology* 13;565-575, [2].Leenslag, J.W. et al (1984). *J. Applied Polymer Science*;24;2829 [3] Fanbri, L. et al (1994). *J. Mat. Sci. Materials in Medicine*;5;679-683 [4] Pitt, C.G. et al (1981). *J. Applied Polymer Science* 26;3779-3787

ACKNOWLEDGEMENTS: I would like to thank Dr. Coombes and Dr. Adams for their help and also the support of Aston University.

European Cells and Materials Vol. 4. Suppl. 2, 2002 (page 45) ISSN 1473-2262

GFP-LABELLED SCHWANN CELLS FOR THE STUDY OF BIO-ENGINEERED CELLULAR NERVE GRAFTS

M.P. Tohill[1], C. Mantovani[1], D. Mann[1], M. Wiberg[2] & G. Terenghi[1].

[1]*Blond McIndoe Centre, University Department of Surgery, Royal Free and University College Medical School, London, England*

[2]*Department of Hand and Plastic Surgery, University Hospital, Umeå, Sweden*

INTRODUCTION: To assess the survival and growth characteristics of cellular transplants *in-vivo* it is necessary to label donor cells to distinguish them from the host's own cells. The use of the *lac*Z nuclear marker [1] is sub-optimal because only the nucleus of the cell exhibits the marker, the intensity of staining can be weak and the staining process is chemical and therefore prevents the use of multi-staining immunofluorescence. The use of green fluorescent protein (GFP) is a superior method of labelling as the protein is expressed throughout the cytoplasm, cell cultures actively express GFP and therefore can be studied without fixation, and tissue sections containing GFP-labelled cells can be subjected to multi-staining immunofluorescent techniques [2]. Schwann cells were labelled with GFP to assess their integration in the process of nerve regeneration following transplantation and the suitability of GFP in histochemical analysis. The effect of transduction with this marker on the vitality and viability of cultured Schwann cells was also assessed.

METHODS: Schwann cells were harvested and expanded from neonatal rat sciatic nerves. A murine leukaemia retrovirus produced by a PT67 cell line was used to transduce the cells with the GFP gene. Transduction efficiency was measured along with cell viability and vitality assays in comparison with non-transduced controls. Conduits were made from a polyhydroxybutyrate (PHB) biopolymer. The conduit was seeded with GFP-labelled cells suspended in an alginate hydrogel matrix. Conduits containing transduced cells were implanted and harvested 2 weeks later. Subsequent immunohistochemical analysis was performed for S100, a marker of myelination, PGP, a marker for axonal regeneration and PCNA, a marker of cell proliferation.

RESULTS: Transduction efficiency was found to be approximately 40%. Schwann cells transduced with the GFP gene displayed the same growth characteristics as non-transduced cells. On histochemical analysis of conduits GFP was found to be a sensitive marker for transplanted Schwann cells. Transplanted cells also displayed PCNA indicating they were actively proliferating and were found to be related to axonal regeneration in the proximal ends of the conduits.

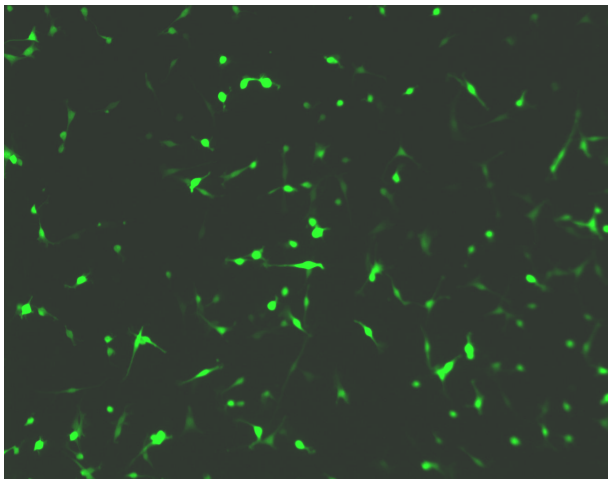

Fig. 1. Schwann cells transduced with GFP in culture.

DISCUSSION & CONCLUSIONS: These results show that transduction of Schwann cells with GFP does not alter their growth characteristics. Following transplantation of these cells in a nerve conduit GFP is an effective means of assessing their cellular integration. This highlights the potential application of this marker to other bio-engineered systems.

REFERENCES: [1] Mosahebi A., Woodward B., Wiberg M., Martin R., Terenghi G. (2001) Retroviral labelling of Schwann cells: In vitro characterisation and in vivo transplantation to improve peripheral nerve regeneration *GLIA* **34**:8-17. [2] Tsien R.Y. (1998) The Green Fluorescent Protein *Annu. Review. Biochem.* **67**:509-44.

European Cells and Materials Vol. 4. Suppl. 2, 2002 (pages 64-65) ISSN 1473-2262

DETECTION OF CELL FORCES BY MEASURING DEFORMATION OF POLYMER FILMS USING INTERFERENCE REFLECTION MICROSCOPY

L.Csaderova, M. Riehle & A.Curtis

Centre for Cell Engineering, IBLS, Glasgow University, Scotland, GB

INTRODUCTION: The basic idea of using The basic idea of using an elastic substrate for studying forces produced by single cells was originally conceived by Harris and co-workers [1]. As a result of compression and stretching wrinkles appeared in a thin silicone rubber substrate. Non-wrinkling polymer films were used for obtaining traction images by fluorescent observation of displacements of small beads embedded in the substrate plane. Silicone and prestressed silicone films, or recently polyacrylamide substrata of adjustable stiffness, were used for this purpose [2]. These methods concentrate on the measurement of forces which cells exert parallely with the substrate. The aim of the proposed method is to measure a cell force component perpendicular to the substrate.

METHODS: Interference reflection microscopy: The basic principle of IRM is that an incident beam is split in a reflected and transmitted beam at every optical interface according to Fresnel optical laws. All beams reflected back interfere and the resulting intensity can be observed by an oil immersion objective. Samples were observed under monochromatic epi-illumination (filter 546nm).

Measurement system: The system consists of a Caro's acid cleaned glass cover slip with evaporated gold layer followed by a polymer layer with evaporated gold layer on top. Polymer is Sylgard (Dow Corning), 50/1 elastomer/curing agent ratio. Cells move on top gold layer in medium.

Cells: Rat epitenon fibroblasts were grown from laboratory stock [3]. Cells were cultured on a measurement system overnight prior to measurement, seeding density was $1.5x10^5$ cells per 5 ml.

RESULTS: In our setup, interference reflection microscopy is used for measuring changes in the resulting interference image of the measuring system. Reflectance of the system can be calculated as the ratio of reflected and incoming intensities. Every optical interface of the system is characterised by Fresnel reflection r_{ij} and transmission t_{ij} coefficients and each layer is described by a phase shift β_{ij}. Total reflected intensity of a multilayer system, accounting for multiple reflections, can be calculated according to (1) when total reflectivity Rs,p can be derived from matrix formalism [4] and W is the weight function which accounts for the cylindrical symmetry of the illumination cone and different intensity contributions from different angular segments.

$$I_{tot}^{s,p} = \frac{I_0}{2}\sum_{n=0}^{a/dJ} W^2(n.dJ)(R^{s,p}(ndJ) * R^{s,p}(n.dJ))^{)} \quad (1)$$

The dependence of reflectance of the whole system on a polymer thickness is influenced by various thicknesses of evaporated metal layers as well as values of numerical aperture and should be tab centered, with the number in parentheses on the right.

Cells move on a top gold layer of the measurement system and exert forces leading to a deformation of the polymer underneath.

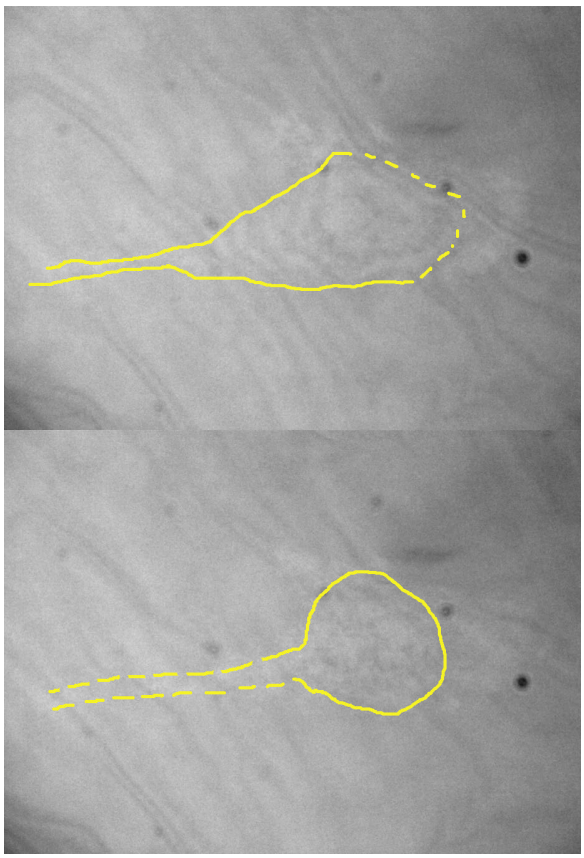

Fig. 1 Interference light images of the same cell taken two hours apart. Yellow lines show the shape

of the cell in the moment when picture was captured.

Deformation of a polymer and change of its thickness results in a change of the measured intensity of the light reflected from the whole system. Then the detected intensity can be compared with the calculated reflectance after the calibration according to measured values of the system of known reflected intensities. The important parameters of the setup are properties of the polymer layer – its elasticity modulus which must be sufficiently low to allow detectable deformation, its refractive index and thickness.

The interference reflection images of a moving cell show changes of measured reflected intensity in the area where a cell's shape was changed (Fig.1). Contours of the cell shape were drawn on a basis of a mixed light image which is a superposition of interference reflection microscopy and a transmitted light image.

DISCUSSION & CONCLUSIONS: At present, results are only qualitative. For the purpose of being able to estimate the actual cell force component, several experimental problems must be solved. It is particularly an accurate determination of Young's elasticity modulus of Sylgard, obtaining of sufficiently thin polymer films as well as precise calibration of incoming intensity. After optimasing the experimental setup, this method could give a possibility to calculate a normal force component using an analogy with the indentation method, modified for a film with a finite thickness bounded to a solid substrate.

REFERENCES: [1] A.K. Harris, P. Wild and D. Stopak (1980) *Science* **208**:177-179. [2] K. Beningo, Y.L. Wang (2002) *Trends Cell. Biol*. **12**:79-84. [3] B. Wojciak, J. Crossan, A. Curtis and C. Wilkinson (1995) *J. Mater. Sci.: Mater. Med*. **6**:266-271. [4] G. Wiegand, T. Javorek, G. Wegner and E. Sackmann (1997) *J. Coll. Sci.* **196**: 299-312.

ACKNOWLEDGEMENTS: This work was supported by the BITES project.

OSTEOBLAST-STIMULATING FACTOR-1 ENHANCES OSTEOGENIC DIFFERENTIATION OF BONE MARROW STROMAL CELLS, BUT IS NOT OSTEOINDUCTIVE

R. S. Tare, K. A. Partridge, X. B. Yang, N. M. P. Clarke, R. O. C. Oreffo, H. I. Roach

University Orthopaedics, University of Southampton, Southampton SO16 6YD, UK

INTRODUCTION: Osteoblast-stimulating factor-1 (OSF-1), also referred to as pleiotrophin and heparin-binding growth-associated molecule, is a secreted, extracellular matrix-associated, 136-amino acid polypeptide. Although o*sf-1* is expressed widely during fetal development, post natal expression is more restricted, the bone and brain being two sites with significantly high concentrations of OSF-1. The protein is synthesized by osteoblasts during early stages of osteogenic differentiation and deposited in the bone matrix [1]. The *osf-1* gene is expressed by primed osteoprogenitors from bone marrow. OSF-1 also functions as a chemoattractant for osteoprogenitors from human bone marrow [2]. The study examined i) whether OSF-1 influenced osteogenic differentiation of bone marrow-derived cells, ii) whether OSF-1 possessed the osteoinductive potential of Bone Morphogenetic Proteins (BMPs) and iii) the manner in which OSF-1 interacted with BMPs.

METHODS: Bone marrow-derived cells from BDF-1 mice (20-30-week-old) were cultured for 12 days in basal and osteogenic media, to which rhOSF-1 was added in concentrations ranging from ng/ml to pg/ml. Cultures to which 50 ng/ml rhBMP-2 was added served as a positive control. C2C12 cells (murine pluripotent premyoblastic cells) were cultured for 2-6 days with rhOSF-1 and rhBMP-2. At the end of the culture periods, osteogenic differentiation was determined by staining the cultures for alkaline phosphatase (ALP) and assaying for ALP activity, which was expressed per cell (ALP specific activity). Cell proliferation was determined by measuring the DNA content of cultures.

RESULTS: In cultures of mouse bone marrow cells, OSF-1 stimulated specific ALP activity at appreciably low (pg/ml) concentrations, while concentrations in the ng/ml range were ineffective in stimulating ALP. Although stimulation of ALP activity by BMP-2 was greater in comparison to that achieved by OSF-1, the stimulatory effect was observed in presence of ng/ml concentration of BMP-2 compared to the pg/ml concentration of OSF-1. A modest, but significant, mitogenic effect of OSF-1 was observed at pg/ml concentrations. With respect to pluripotent C2C12 cells, OSF-1 was not osteoinductive as it failed to initiate osteogenic differentiation unlike BMP-2, which initiated osteogenic differentiation evident by the appearance of numerous ALP +ve cells. OSF-1 inhibited BMP-mediated osteoinduction at concentrations as low as 0.05 pg/ml, when present with BMP-2 during the initial osteoinductive phase of culture. However, when OSF-1 was added after initiation of osteogenic differentiation by BMP-2, osteogenic differentiation of BMP-primed cell populations was further enhanced in presence of pg/ml concentrations of OSF-1.

DISCUSSION & CONCLUSIONS: Thus, the effect of OSF-1 on osteogenic differentiation depended on the concentration and the timing at which it was added. The protein was not osteoinductive, it inhibited BMP-mediated osteoinduction during the initial osteoinductive phase, but stimulated osteogenic differentiation of BMP-primed cell populations/ late-stage osteoprogenitors from bone marrow, provided it was present at low concentrations.

REFERENCES: [1] R.S. Tare, R.O.C. Oreffo, N. M. P. Clarke, H. I. Roach (2002) *Bone* 30 (3): 13S. [2] X.B. Yang, H.I. Roach, N.M.P. Clarke, S.M. Howdle, K.M. Shakesheff, R.O.C. Oreffo (2001) *Journal of Bone and Mineral Research* 16 (6): 1179.

ACKNOWLEDGEMENTS: The work was funded by the Wishbone Trust (British Orthopaedic Association) and Wessex Medical Trust (Southampton).

European Cells and Materials Vol. 4. Suppl. 2, 2002 (pages 101-102) ISSN 1473-2262

SURFACE MODIFICATION OF SUPERPARAMAGNETIC IRON OXIDE NANOPARTICLES AND THEIR INTRACELLULAR UPTAKE

Ajay K. Gupta and A. Curtis

Centre for Cell Engineering, IBLS, University of Glasgow, Glasgow, UK.

INTRODUCTION: The use of superparamagnetic nanoparticles can contribute to a precise delivery of drugs to an exact target site by application of external magnetic fields. Magnetic nanoparticles having specific shape and size with suitable surface chemistry can be used in numerous in vivo applications such as drug delivery, cell engineering, tissue repair or in diagnostics [1,2]. For these applications, the internalization of nanoparticles into specific cells is the critical step and severely limited by three factors: (a) a short blood half-life of the particles, (b) non-specific targeting and (c) low efficiency of internalization of endocytosed ligands grafted on the nanoparticles. Rapid elimination of the nanoparticles from the blood stream after administration is due to their recognition by macrophages of the mononuclear phagocyte system (MPS). When the nanoparticles are covered with adsorbed plasma proteins, they are quickly cleared by macrophages before they can reach target cells. One possible approach to increasing the blood circulation time of nanoparticles is to modify the surface of the nanoparticles by hydrophilic polymers such as poly(ethylene glycol) (PEG). Nanoparticle surface covered with PEG is biocompatible, i.e. non-immunogenic, non-antigenic and protein resistant [3].

Iron can be transported in plasma complexed with lactoferrin, a milk glycoprotein (Mw~90kDa), having very high affinity for iron. The uptake of iron by cells is mediated by cell surface receptors and since, various cells have these type of receptors at their surface, the utilization of lactoferrin-nanoparticle complex seems to be a promising pathway for the delivery of the drug/ genetic material to different tissues of an organism.

In this study, PEG was coated on the surface of the magnetic nanoparticles, to disperse particles, increase blood circulation times and improve their cell internalization. The particles were characterized by various physicochemical means. PEG coated nanoparticles were derivatized with lactoferrin to study their effect on cell adhesion.

METHODS: Highly monodispersed iron oxide nanoparticles were synthesised by coprecipitation of Fe^{3+} and Fe^{2+} salts (2:1 molar ratio) with sodium hydroxide by using the aqueous core of Aerosol-OT (AOT)/n-Hexane reverse micelles (w/o microemulsions) in N_2 atmosphere. The nanoparticles were coated with PEG and were characterized by various physico-chemical means.

Lactoferrin was attached at the nanoparticle surface by coupling the amine group of lactoferrin to the carboxyl group of MA-PEG coated particles using 1-Ethyl-3-(3-dimethylaminopropyl)-carbodi-imide (EDCI). The effect of nanoparticles on cell adhesion was determined with cell suspension incubated with/without nanoparticles. Infinity telomerase immortalized primary human fibroblasts (h-TERT BJ1) cells were seeded with nanoparticles for 24 hours onto 13mm coverslips. The cells were washed with PBS and stained for 2 minutes in coommassie blue at room temperature. The cell populations were counted in three separate light microscope fields with average normalized to control cell population.

RESULTS AND DISCUSSION: Magnetic nanoparticle were synthesized in w/o micro-emulsions by using the inner aqueous core of the reverse micelles. The size and size distribution of the particle was deter-mined by transmission electron microscopy (TEM) studies (fig.1). The picture shows that these particles have very small size (<10nm) with narrow size distribution.

The IR spectra of iron oxide is highly consistent with magnetite (Fe_3O_4) (bands at 408.9, 560.0 and 585 cm^{-1}). The spectra of PEG coated nanoparticles shows the small shift in the positions of the main peaks as compared to uncoated particles. This is due to the change in environment of the particles after PEG coating. The size of the particles after coating is around 40-50nm as was deter-mined by TEM and AFM studies. The core shell structure of the nanoparticles can be seen from AFM picture (fig.2).

Fig-3 shows the effect of magnetite and PEG coated nanoparticles on the number of adhered cells after 24 hour incubation. It is evident from the figure that PEG coated magnetic nanoparticles did not appear to influence cell adhesion as compared to control cell population. However cells exposed to magnetite showed a reduction in adhesion to glass of approximately 60%. This is because PEG has uncharged hydrophilic residues and very high surface mobility leading to high steric exclusion [4]. In addition it has been demonstrated that

particles with PEG-modified surface crosses cell membrane in non-specific cellular uptake.

Lactoferrin is an iron binding protein, which has major role in body's defence mechanism through its immune modulatory actions. It also has growth regulatory functions in normal cells, coagulation and cellular adhesion modulation. Figure-4 shows the effect of lactoferrin binding at the surface of uncoated particles on the number of adhered cells as compared to control cell population.

CONCLUSIONS: Magnetic nanoparticles were successfully prepared and modified with PEG and characterized by FTIR and TEM studies. The polyethylene glycol coated nanoparticles did not appear to influence cell adhesion as compared to control cell population. However the magnetic particles showed a great decrease in cell adhesion to glass.

REFERENCES: (1) P.K. Gupta, C.T. Hung, *Life Sci*.(1989), **44**:175-186; (2) Gruttner C et al, editors, Scientific and clinical applications of magnetic carriers. New York: Plenum Press, 1997, p53.; (3) S. Zalipsky, *Bioconjugate Chem*. (1995), **6**:150-165. (4) M. Zhang et al, Biomaterials (1998) **19**:953-960.

ACKNOWLEDGEMENTS: This work was supported by EC contract GRD5-CT2000-00375 project acronym: MAGNANOMED.

European Cells and Materials Vol. 4. Suppl. 2, 2002 (pages 1-2) ISSN 1473-2262

MONITORING NEO-CARTILAGE FORMATION IN CELL SEEDED ALGINATE CONSTRUCTS OF CLINICALLY RELEVANT DIMENSIONS

H.K Heywood[1,2], D.A. Lee[1]& D.L. Bader [1,2]

[1] *Medical Engineering Division, Dept of Engineering, Queen Mary University of London, UK.*

[2]*IRC in Biomedical Materials, Queen Mary University of London, UK.*

INTRODUCTION: Constraints to the physiological repair process have motivated the development of tissue engineered biological tissue replacements. The requirement for 3D cellular constructs with significant thickness demands optimal culture conditions to maintain viability and controlled matrix organisation throughout the final tissue. Such a process of optimization, in turn, requires the utilisation of techniques for monitoring tissue development in space and time. This study details the optimisation of culture conditions for 3D alginate-chondrocyte constructs, and introduces the application of Fluorescence Recovery After Photobleaching (FRAP) for the non-invasive examination of neo-cartilaginous tissue.

METHODS: Viability profiles. Chondrocytes were isolated from bovine articular cartilage by sequential enzyme digestion and incorporated into 1.5 % and 3 % low viscosity alginate constructs (LV Keltone, ISP alginates UK) at cell densities ranging from 5-40 $x10^6$ /ml. The constructs were gelled by dialysis against 150 ml of 100 mM calcium chloride and cultured in 20 ml 16% FCS DMEM under static culture conditions for up to 8 days. At regular time intervals the spatial viability distribution within each construct was assessed by a live-dead staining technique, utilizing calcien AM and ethidium homodimer-1, in conjunction with a systematic sampling procedure. The temporal rate of viability loss was determined from the time-points of the spatial viability profiles by one-way ANOVA ($\alpha = 0.05$).

Medium Volume. In a separate experiment constructs with 40 $x10^6$ cells /ml were cultured in doubling medium volumes from 0.4 to 6.4 ml per million cells for 14 days. The matrix and cell distributions within final constructs were assessed from 5 μm Safranin O and haemotoxylin stained histological sections. The distribution of cells and matrix within the bulk of the construct was compared to that in a 0.5 mm thick peripheral region.

FRAP experiments. Fluorescein isothiocyanate labeled Bovine serum albumin (FITC-BSA) or 500 kDa dextran (FITC –dextran) fluorescent probes were incorporated into cell free 3% alginate constructs at < 0.01 mg /ml prior to gelling. FRAP experiments were used to derive the diffusion coefficient of the incorporated fluorescent probes in the gelled constructs. The rate of fluorescence recovery within a 40 μm photobleached area of the alginate specimen was analysed from a time sequence of images by Spatial Fourier Analysis. An Olympus AX60 microscope fitted with x20 objective, mercury lamp and laser was used for imaging. In a separate experiment FITC-BSA was introduced into cellular ($10x10^6$ cells /ml) 3% alginate constructs prior to analysis, by equilibration in 1 ml DMEM culture medium containing < 0.01 mg /ml fluorescent probe. FRAP experiments were performed at 3, 6 and 12 days of culture. At the same time-points constructs were collected for biochemical (DMB assay for GAG in alginate[1]) and histological analysis of GAG content.

RESULTS: Viability was maintained throughout the constructs after gelling and at day 1 of culture. With subsequent culture, viability became significantly reduced at the construct centre. The time at which viability was reduced was inversely related to initial cell seeding density (Table 1). However, this parameter was insensitive to alginate concentration.

Table 1. Rate of viability loss with increasing construct cell density or alginate scaffold concentration (permeability).

Cell density ($x10^6$ /ml)	Culture (days) preceding significant central viability loss	
	1.5 % alginate	3 % alginate
5	8	8
10	6	6
20	6	6
40	-	3

Histological sections indicated distinct non-homogeneity of cell and matrix distributions between the centre and periphery of the constructs. Increasing the medium volume on a per cell basis

reduced this non-homogeneity by extending the intense staining periphery towards the center. Thus at the highest volume used, (6.4 ml medium per million cells), there was no significant difference in cell density between the centre and periphery (figure 1).

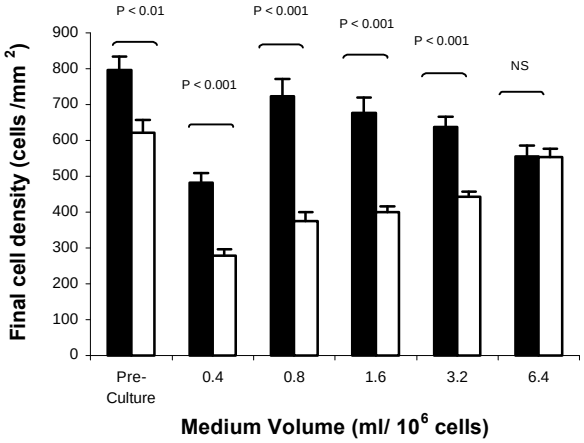

Fig. 1: Final cell distribution within 3% alginate constructs cultured for 14 days with 0.4 to 6.4 ml medium /x10^6 cells. Mean +/- SE of 20 samples. Significant differences between peripheral (solid bars) and central (open bars) regions of the construct were determined by ANOVA and post hoc Student T-test ($a = 0.05$).

FRAP studies within cell free alginate constructs indicated that the diffusion of a solute within alginate is sensitive to its molecular weight (figure 2), with a much lower diffusion coefficient of 500 kDa dextran compared to BSA. The diffusion rate of BSA within cellular constructs did not change with space or time in culture up to 12 days, despite GAG accumulation of 744 +/- 63 μg /ml (data not shown).

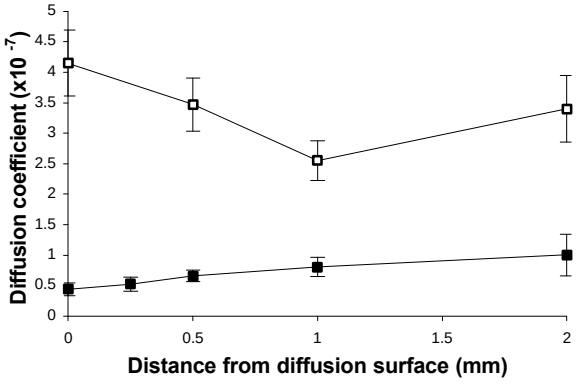

Fig. 2: The spatial distribution of BSA (open squares) and 500 kDa dextran (filled squares) diffusivity throughout 4 mm thick 3% alginate constructs. Mean +/- SD of three records.

DISCUSSION & CONCLUSIONS: The loss of viability within tissue engineered cartilaginous constructs of clinically relevant dimensions was examined. It was found to be insensitive to enhanced permeability achieved by reducing the density of the alginate constructs. In contrast, viability was inversely related to the initial seeding density of the constructs. Non-homogeneity of matrix and cell distributions within 3D constructs can be overcome by enhancing the bulk supply of medium on a per cell basis. Thus it can be concluded that the non- homogeneity of matrix and cell distributions occurs by a mechanism of cellular utilization under conditions of sub-optimal nutrient supply. Since the balance of nutrient supply and demand within 3D constructs is complex over an extended culture period, non-invasive techniques for observing tissue development are essential tools for monitoring bioreactor and culture regime performance. The basis of utilizing FRAP to monitor tissue formation is the measurement of a reduction in construct permeability due to the accumulation of new matrix. Diffusion within the alginate scaffold has been shown to be dependent on solute molecular weight, consistent with reports on the agarose hydrogel system[2]. Preliminary results with cellular constructs indicate that over a 12-day culture period no reduction in the diffusion coefficient of BSA could be detected by FRAP throughout the thickness of the alginate construct. Therefore, as a system for the detection of matrix development, FRAP appears to be applicable only for specific probe molecular weights, conditional to the substrate. Despite these limitations, this system has potential for the non-invasive examination of tissue development.

REFERENCES: [1] B.O Enobakhare et al. (1996) *Anal. Biochem* **243**:189-191. [2] A. Pluen et al (1999) *Biophys. J.* **77**(1):542-52.

ACKNOWLEDGEMENTS: This work was funded by the EPSRC. The FRAP studies were carried out as part of a collaboration with Prof. P. Netti, and Ms E. De Rosa of the Biomaterial laboratory, Department of Materials and Production Engineering, University *Federico II* of Naples, Italy.

European Cells and Materials Vol. 4. Suppl. 2, 2002 (pages 67-68) ISSN 1473-2262

THE INFLUENCE OF UNCOATED AND COATED MAGNETIC NANOPARTICLES ON HUMAN FIBROBLASTS IN CULTURE.

Berry CC[1], Wells S[2], Charles S[2] & Curtis ASG[1].

[1] *Centre for Cell Engineering, IBLS, Glasgow University, Scotland, UK*

[2] *Liquids Research Ltd., Mentec, Deiniol Road, Bangor, North Wales*

INTRODUCTION: Magnetic nanoparticles have been used for bio-medical purposes including drug delivery, cell destruction and as MRI contrast agents (1). A wide variety of iron oxide nanoparticles have been synthesised. They differ in type of coating material used (eg. dextran, starch, albumin and silicones), and size, resulting in hydrodynamic particle size varying between 10 and 3500 nm (2). However, prior to use *in vivo*, the particles must initially be characterised *in vitro*. To this end, magnetic nanoparticles (8-15 nm diameter) were synthesised and derivatised with various coatings by Liquids Research Ltd., producing stable fluids of neutral pH. The influence *in vitro*, including possible endocytosis, was subsequently assessed.

METHODS: Human dermal fibroblasts were cultured on glass coverslips for 24 hours and challenged nanoparticles (0.1 mg.ml^{-1}) for up to 72 hours (table 1). Cell morphology (coomassie staining, SEM), cytoskeleton (actin, tubulin, vinculin) and possible particle internalisation (clathrin, TEM).

Table 1: Nanoparticles used in studies.

Type of Particle
Plain uncoated
Transferrin coated
Albumin coated
RGD coated
Dextran coated

RESULTS: Cells exposed to the uncoated nanoparticles resulted in vesicle formation (Fig 1) as did several other types of coatings. In contrast, cells incubated in protein-coated particles such as transferrin, ensued good cell morphology and cytoskeleton, with an increase in cell proliferation. SEM results suggested particle uptake albumin coated particles, but adherence to the cell membrane with the transferrin particles as indicated in Figure 2.

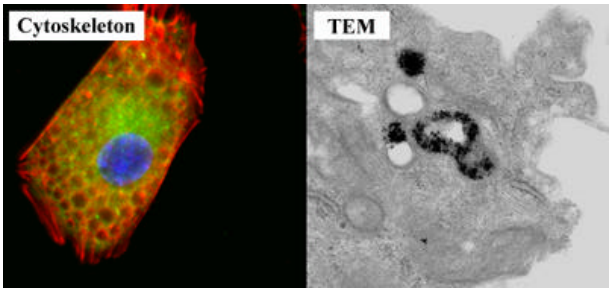

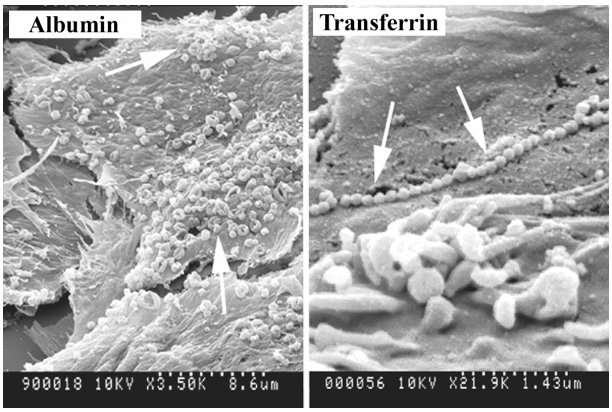

Figure 1*. Actin/vinculin cytoskeleton and TEM images of cells incubated with uncoated nanoparticles.*

Figure 2. Fibroblasts interacting with uncoated and albumin derivatised nanoparticles.

DISCUSSION & CONCLUSONS: The derivatisation of iron oxide nanoparticles with several proteins, such as transferrin or the RGD motif resulted in favourable changes in cell behaviour *in vitro*, with cells interacting with the particles in a positive manner as opposed to behaviour in response to the uncoated particles or particles coated with dextran or albumin. Such results are promising in terms of targeted particle drug delivery routes, whereby permitting targeted delivery of drugs, without complete drug internalisation by cells.

REFERENCES: [1] Curtis and Wilkinson (2001) Trends in Biotechnology, 19(3), 97-101. [2] Van Beers *et al* (1995) J. Radiol., 76, 991.

ACKNOWLEDGEMENTS:. Dr. Matt Dalby, Mr. Eoin Robertson, Dr. Mathis Riehle.

European Cells and Materials Vol. 4. Suppl. 2, 2002 (pages 130-131) ISSN 1473-2262

MECHANICAL CONDITIONING OF BONE CELLS *IN VITRO* USING MAGNETIC MICROPARTICLE TECHNOLOGY

S.H.Cartmell, J.Dobson, S.Verschueren, S.Hughes & A.J.El Haj

Centre for Science and Technology in Medicine, Keele University, England, UK

INTRODUCTION: Application of mechanical strains directly to cells has been performed using magnetic fields applied to magnetic particles that have been coated in a variety of proteins such as collagen type1[1], RGD[2], fibronectin[3], bovine serum albumin[4] and poly-l-lysine[5]. Translational stretches and torques have been applied to individual cells in this manner and an upregulation of Ca2+ influx into cells and significant alterations in the cytoskeletal network such as actin filament stiffening has been reported as a result of such strains. However, application of mechanical strain to cells has been predominantly focused on short-term single cell interactions. In this report we go further to investigate the use of magnetic microparticle technology on multiple cells grown in culture long-term. We have studied the effects of applying a cyclical mechanical strain directly to primary human osteoblasts for a 21-day period using magnetic particle technology.

METHODS: Ferromagnetic (CrO_2) particles (diameter ~4.5 microns, Spherotech) were coated with RGD (50mg/ml PBS) and adhered to primary human osteoblasts at a concentration of approximately two particles per cell. Approximately 100,000 cells (plus adhered particles) were placed into wells of a 6 well plate and cultured in the presence of culture medium (alpha-MEM), antibiotics, 10% fetal calf serum and osteogenic supplements (dexamethasone, â-glycerophosphate ascorbic acid) for 21 days. A 1 Hz/60 milliTesla, (max.) magnetic field generated by an oscillating NdFeB magnet array was applied to the cells plus adhered particles each day for 30 minutes (fig.1).

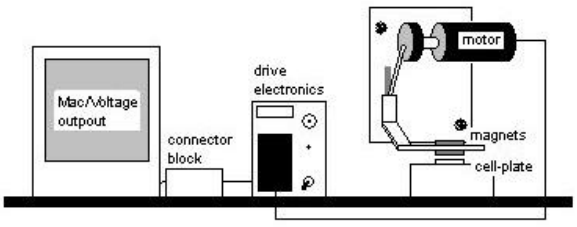

Fig.1: *Sketch of set-up used to apply cyclical magnetic field to cell/magnetic particle samples.*

Six sample groups were analysed (table 1). At 21 days, live/dead fluorescent staining (propridium iodide/syto9, Molecular Probes) and SEM analysis were performed to evaluate cell viability and morphology. Also at 21 days, a von kossa stain for phosphate deposits (mineralized bone matrix) was performed on all six samples. At this same time point, real-time RT-PCR was performed to quantify bone-related gene production of type I collagen, osteocalcin and osteocalcin normalised to GAPDH. Prostaglandin E_2 present at day three and osteocalcin present at day 21 in the culture media were quantified by ELISA. Laser scanning confocal microscopy (LSCM) was performed at week 1 on sample group (3) to visualize actin filaments and cytoskeletal arrangement.

Table 1. Sample groups and description.

(1)	Cells plus particles, with applied magnetic field, with 30 minutes at room temperature (as magnet was applied at room temperature for 30 minutes).
(2)	Cells with no particles, with applied magnetic field, with 30 minutes at room temperature.
(3)	Cells with particles, with 30 minutes at room temperature, with no magnetic field applied.
(4)	Cells with no particles, with 30 minutes at room temperature, with no magnetic field applied.
(5)	Cells with no particles, maintained in a CO2 incubator with no magnetic field applied.
(6)	No Cells, no magnetic field, maintained in a CO2 incubator.

RESULTS: Flourescent imaging showed for sample groups (1) – (5) a viable, confluent monolayer of cells covering the surface of the wells in the tissue culture plates. SEM imaging showed confluent cells in monolayer spread out and attached to the surface of the tissue culture well in samples (1) - (5). Von Kossa staining of the wells in sample groups (2) – (6) showed no phosphate deposition. However, sample group (1) (the experimental group) showed a small amount of mineralization. Real-time RT-PCR showed an upregulation of osteopontin in sample group (1) (the experimental group) in comparison to the control sample group (3) (sample group consisting

of cells with particles but no magnetic field) (figure 3).

Fig. 2: Flourescent microscope image of phalloidin stained actin filaments of 3 week primary human osteoblasts with internalised microparticles (left image) DAPI stain of nucleus (light microscope) of same cell (right image)

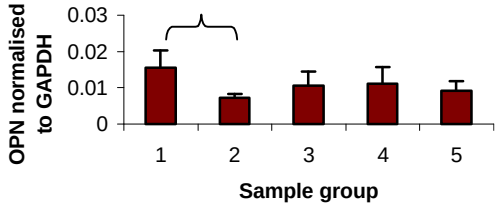

Fig. 3: Real-time RT-PCR data showing osteopontin (OPN) levels normalised to GAPDH. $p<0.05$.

There was no significant difference in the mRNA levels of osteopontin expressed between the other sample control groups. There was also no significant difference in the amount of osteocalcin or type 1 collagen mRNA produced at 21 days between sample groups (1) – (5).

The ELISA's performed showed a statistically significant ($p<0.05$) upregulation of prostaglandin E_2 from group (1) (the experimental group) in comparison to groups (2), (4), (5) and (6) (fig. 4). There was no significant difference in prostaglandin E_2 production between group (1) and group (3). The osteocalcin ELISA performed showed no significant difference between the sample groups at day 21.

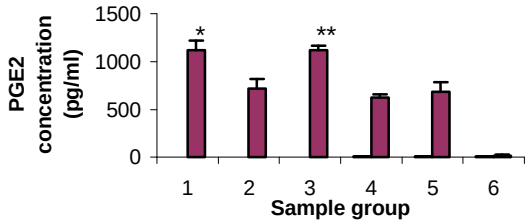

Fig. 4: *Prostaglandin E_2 ELISA data from three day culture media. * Group (1) is significantly different from groups (2), (4) – (6) ($p<0.05$). ** Group (3) is statistically significantly different from groups (2), (4) – (6) ($p<0.05$).*

The LSCM performed showed no significant alteration in the actin filament structure in the osteoblasts. It was clear that the majority of the particles had been internalized by the cells and that many of these particles appeared to be located close to the nucleus (figure 2).

DISCUSSION & CONCLUSIONS: The live/dead stain performed showed that the presence of the magnetic particles was not causing cell necrosis and particles were still present at 21 days. The small amount of mineralisation (as seen by the von kossa stain) in the sample group that had adhered particles plus magnetic field applied may be due to an upregulation in bone matrix production by the cells in response to mechanical stimulation from the particles in the applied magnetic field. Also, real-time RT-PCR results show an upregulation of osteopontin in experimental sample group (1) in comparison to group (2) which may also correlate to the same mechanical stimulation response. The increase in prostaglandin production in groups (1) and (3) in comparison to the other groups may be due to the internalization of the particles, which may also result in prostaglandin release. A comparison of the relationship between internalization effects and mechanical stimulation is currently being investigated which includes understanding how these particles are internalized.

Initial results indicate that adherence of RGD-coated, 4.5 ìm ferromagnetic particles to primary human osteoblasts does not initiate cell necrosis up to 21 days *in vitro*. Also, though these results are preliminary, mechanical stimulation of primary human osteoblasts by magnetic particle technology appears to have an influence on osteoblastic activity.

REFERENCES: [1] M. Glogauer J. Ferrier, and C. A. McCulloch (1995) *Am J Physiol* **269**:C1093-104. [2] J. Chen, B. Fabry, E. L. Schiffrin, and N. Wang (2001) *Am J Physiol Cell Physiol*, **280**:C1475-84. [3] A. R. Bausch, U. Hellerer, M. Essler, M. Aepfelbacher, and E. Sackmann, (2001) *Biophys J* **80:**2649-57. [4] M. Glogauer, P. Arora, G. Yao, I. Sokholov, J. Ferrier, and C. A. McCulloch (1997) *J Cell Sci*, **110(Pt 1)**:11-21. [5] M. D'Addario, P. D. Arora, J. Fan, B. Ganss, R. P. Ellen, and C. A. McCulloch (2001) *J Biol Chem* **276**: 31969-77.

ACKNOWLEDGEMENTS: The authors would like to thank Leanne Cioni and Julia Magnay for their technical expertise. Acknowledgements also go to EPSRC grant number GR/R22247/01 and BITES Vth framework European grant for financial support.

European Cells and Materials Vol. 4. Suppl. 2, 2002 (page 132) ISSN 1473-2262

STIMULATION OF BONE FORMATION IN VIVO USING HUMAN OSTEOPROGENITORS AND OSTEOBLAST STIMULATING FACTOR-1 ADSORBED SCAFFOLD CONSTRUCTS

Xuebin Yang[1], Helmtrud I. Roach[1], Nicholas MP Clarke[1], Steven M Howdle[2], Kevin M Shakesheff[3], and Richard OC Oreffo[1]

[1] *University Orthopaedics, University of Southampton, Southampton, SO16 6YD, UK*
[2] *School of Chemistry, University of Nottingham, Nottingham NG7 2RD, UK*
[3] *School of Pharmaceutical Sciences, University of Nottingham, Nottingham NG7 2RD, UK*

INTRODUCTION: The ability to augment bone formation remains a key clinical need. The process of bone growth, regeneration and remodelling is mediated, in part, by the immediate cell-matrix environment. Osteoblast stimulating factor-1 (OSF-1), also known as pleiotrophin or HB-GAM, is an extracellular matrix-associated protein, which is present in those matrices that act as targets for the deposition of new bone. Previously we have shown OSF-1 will induce human osteoprogenitor adhesion, chemotaxis, proliferation, differentiation and CFU-F formation in vitro. The aims of this study were to examine the potential of porous Poly (lactic acid) (PLA) and Poly (DL-lactic acid-co-glycolic acid) (PLGA) constructs adsorbed with OSF-1 to induce osteogenesis by primed human osteoprogenitors in vivo using the diffusion chamber and subcutaneous implant models.

METHODS: PLGA scaffolds of defined porosity (50-200um) were generated using a unique supercritical fluid mixing method. Primary human bone marrow cells derived from 5 patients (59-78 years of age) were grown in osteogenic media (ascorbate/dexamethasone for 21 days) impregnated onto PLA and PLGA (75:25) porous scaffolds adsorbed with or without recombinant human OSF-1(50ng/ml) in osteogenic conditions. Cell/growth factor constructs were subcutaneously implanted or placed within diffusion chambers before intraperitoneal implantation into athymic mice. After 6-12 weeks, samples were examined by X-ray analysis and processed for histology.

RESULTS: In diffusion chambers, no bone formation was observed in human bone marrow/scaffold constructs alone. OSF-1 adsorbed constructs showed morphologic evidence of new bone matrix and cartilage formation within diffusion chambers as evidenced by X-ray analysis, metachromatic staining with toluidine blue, sirius red and alcian blue staining as well as type I collagen and von Kossa histochemistry in 4 of 9 chambers. Evidence of organised new woven bone was confirmed by birefringence of collagen within spicules of new bone. Furthermore, cartilage formation was observed within PLA and PLGA scaffolds confirming penetration of human osteoprogenitors through the scaffold constructs. In addition, after 4-6 weeks, evidence of new bone formation was observed in subcutaneous implants as detected morphologically by Sirius red staining.

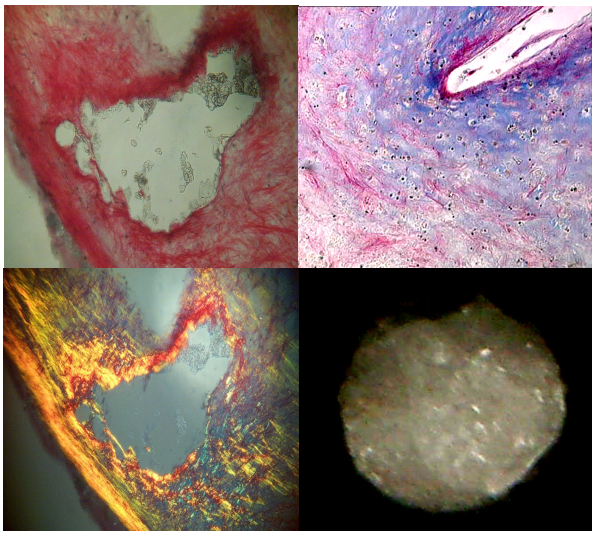

Fig. 1: Bone & cartilage tissue formation on/in OSF-1 adsorbed PLA and PLGA scaffold within diffusion chambers. Alcian blue and Sirius red stain (A.B). Birefringence(C). X-ray (D).

DISCUSSION & CONCLUSIONS: These results demonstrate that OSF-1 in combination with primed human osteoprogenitor populations promotes cartilage and bone formation within unique biodegradable porous PLA and PLGA scaffolds. The successful generation of osteogenic tissue within 3-D biomimetic structures incorporating OSF-1 indicates the potential of such approaches for the development of protocols for de novo bone formation for skeletal repair.

ACKNOWLEDGEMENTS: This work was supported by grants from DePuy International, BBSRC, Royal Society and The Nuffield Foundation.

COLLAGEN-DERIVED MATRICES FOR TISSUE ENGINEERING

M, Jarman-Smith[1], P. McFetridge[2] & J.B. Chaudhuri[1]

[1]*Department of Chemical Engineering, University of Bath, Bath, UK*

[2]*Department of Chemical Engineering and Materials Science, University of Oklahoma, USA*

INTRODUCTION: In vivo, tissue architecture consists of cells attached to and encapsulated within an extracellular matrix (ECM) network. Tissue engineering approaches to making replacement human tissues use either natural ECM polymers such as collagen, or synthetic polymers designed to mimic the ECM, eg poly(lactic-co-glycolic) acid. There are many advantages in using the natural material, which include an exact matching of chemical, biological and mechanical properties. However, advantages include problems with obtaining consistent source material, processing of the matrix and potential immunogenic reactions to the matrix. In this paper we will discuss some of our experiences on using porcine-derived collagen as a potential matrix for use in dermal replacements and small diameter vascular grafts.

METHODS: Two matrix types were investigated. Chemically crosslinked porcine dermal collagen sheets (Permacol, Tissue Science Laboratories plc, Aldershot) were used for the culture of human fibroblasts and smooth muscle cells. For the vascular graft studies, porcine carotid arteries, harvested from 6-8 month old Great White pigs, were processed and chemically crosslinked to generate a matrix consisting of mostly collagen and elastin, whilst retaining components of the internal elastic laminar and basement membrane. Human umbilical endothelial cells and human vascular smooth muscle cells were cultured on this matrix. Studies were carried out in both static culture and dynamic bioreactor cultures.

RESULTS: In both of the cases we studied, it was important to preserve the natural architecture of the collagen so that the 3D matrix was suitable for the desired application. Thus, matrix processing was aimed at removing the nonstructural components of the native scaffold to reduce the potentially immunogenic bioburden, without compromising structural stability.

Processing entailed solvent extraction of lipids, followed by proteolytic digestion. The choice of solvent and the time of treatment were found to be critical parameters in maintaining the matrix structure. The collagen matrix was then stabilized

against enzymatic degradation (which further reduces the potential for immune rejection) by cross-linking matrix proteins using either hexamethylene di-isocyanate or a photo-oxidative reaction using methylene green. The resulting materials were found to have approximately 3 times more resistance to enzymatic digestion than unprocessed tissue.

Both dermal- and carotid- derived matrices were found to be biocompatible with the requisite cell types. Improved cell attachment was achieved on conditioning the matrix with growth media prior to cell seeding.

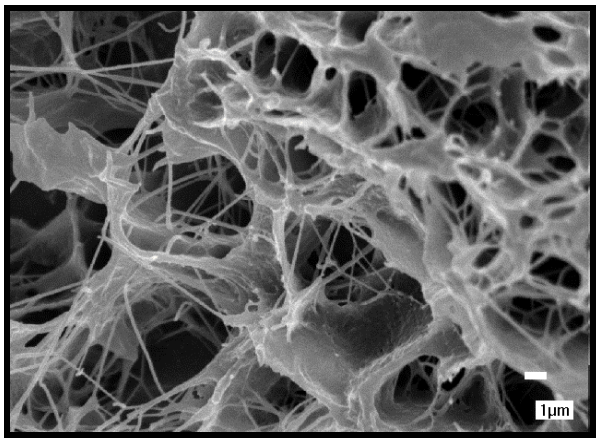

Fig. 1: LT-SEM detailing the fibrous structure of the porcine dermis-derived collagen matrix.

Both dermal- and carotid- derived matrices were found to be biocompatible with the requisite cell types. Improved cell attachment was achieved on conditioning the matrix with growth media prior to cell seeding. However, cell penetration was generally poor, with cells limited to surface attachment.

CONCLUSIONS: Collagen-derived matrices have structural advantages for their use in tissue engineering. The processing of the tissue may be extensive in order to make the material biocompatible. The degree of matrix cross-linking strongly affects cell migration of the scaffold.

ACKNOWLEDGEMENTS: We gratefully acknowledge the finanical support of Tissue Science Laboratories plc and the EPSRC.

European Cells and Materials Vol. 4. Suppl. 2, 2002 (page 109) ISSN 1473-2262

ADHESION OF CELLS AND MICROSPHERES IN A PARALLEL-PLATE FLOW CHAMBER

Elena Martines[1]

[1] *Centre for Cell Engineering, IBLS, Glasgow University, Scotland, GB*

INTRODUCTION: Cell adhesion under flow conditions has been extensively studied because of its important role e.g. in the immune and developmental system.

Since topographic cues have been shown to influence cell adhesion onto surfaces, our aim is to elucidate the mechanisms for the changes in adhesion onto nanometrically engineered surfaces. In particular, nanopillared surfaces have shown to be highly nonadhesive to living cells.

We will focus on the investigation of the interfacial forces of the nanopillared surface, by studying the interaction of charged microspheres and cells when flowing over the aforementioned substrate.

METHODS: A parallel plate flow chamber was built by melting a thermoplastic gasket (Sika Werke GmbH, thickness=150μm), between a glass slide and a solid PMMA sheet (Goodfellow Cambridge Ltd, thickness=250μm), the latter being the observed substrate.

The chamber is designed to create a laminar flow over the substrate: the flow is generated by a syringe pump, the syringe containing a suspension of cells or microspheres.

Phase contrast images were captured at 20X and 100X magnification, then digitized and analyzed.

The engineered PMMA is made by embossing a pillared pattern on the solid sheet. The pattern is written by electron beam lithography on a SiO_2 master, a nickel shim is then electroplated after the master, and used to emboss the polymer.

Carboxylated latex beads (ϕ=2μm) were purchesed from Molecular Probes, Leiden, The Netherlands; and suspended in different NaCl solutions (approx. 10^6 beads/ml).

Epitenon cells were suspended in ECT media, and the flow was kept for approximately 2 hours.

RESULTS: A parallel plate flow chamber was built, and its characteristics are shown fig.1

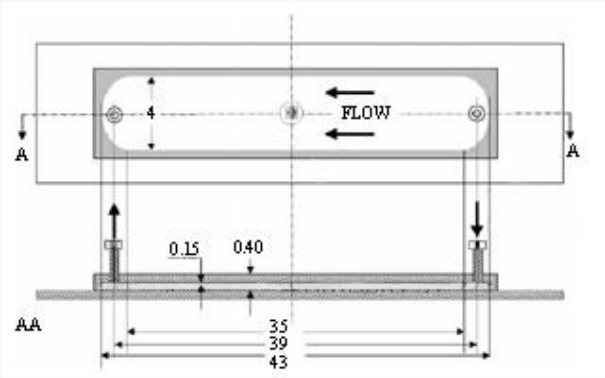

Fig.:. Parallel-plate flow chamber (from Pierres et al., 1996)

X100 magnified images allowed to draw the trajectory and calculate the velocity of a single sphere near the surface, while X20 magnified images were used to count the average number of beads adhering onto a 60mm^2 area after 18 mins from the start of the flow .

DISCUSSION & CONCLUSIONS: This flow chamber has a certain number of advantages and drawbacks: its height is only 150μm, which helps having a creeping flow, it is very transparent and easy to assemble. Nevertheless, it can hardly be used more than once, the hot-melting sealing technique restricts the choice of materials, and it is hand-made, so the flow conditions are not exactly reproducible.

The variation of trajectory and velocity of the charged beads near the substrate is expected to give us some information on the interfacial forces acting on the beads; similarly, the variation of trajectory, adhesion and spreading of the cells could help us understand better the influence of nanopillared surfaces on cell binding.

REFERENCES: Curtis *et al*. (2001). Biophys Chemi **94**: 275-283. Doroszewski *et al*. (1988). J Cell Sci **90**: 335-340. Pierres *et al*. (1996). J Immunol Meth **196**: 105-120.

ACKNOWLEDGEMENTS: I would like to thank Mathis Riehle, Adam Curtis and Chris Wilkinson for their help and support.

European Cells and Materials Vol. 4. Suppl. 2, 2002 (pages 133-134) ISSN 1473-2262

HUMAN OSTEOPROGENITOR ATTACHMENT, GROWTH AND DIFFERENTIATION ON MARINE INVERTEBRATE SKELETONS

D.W.Green, D. Howard, X. Yang, K.Partridge & R.O.C. Oreffo

University Orthopaedics, University of Southampton, UK.

INTRODUCTION: Natural inorganic skeletons from sea sponges, sea urchins, corals and molluscs are, in principle, ideal scaffolds for tissue engineering optimised by natural selection to provide structural environments analogous to bone as well as the architecture required for vascularisation, bone cell invasion and angiogenesis.[1] Coral has been successfully used in reconstructive surgery as passive biodegradable frameworks for bone regeneration and the osteogenic potential of nacre combined with its structural properties indicate a role as an orthopaedic filler.[2,3] The aim of these studies was to evaluate the osteoinductive potential of coral, sea sponge, and nacre and the capacity of these materials to support human osteoprogenitor cell attachment, migration, growth and differentiation.

METHODS: Primary human bone mesenchymal stem cells were isolated and expanded in culture and seeded onto collagen sea sponge, calcium carbonate sea urchin spines and nacre chips and basic bone histology and alkaline phosphatase specific activity measured at 4, 7, 14 and 28 days to determine osteoconductive potential and modulation of the osteoblast phenotype. The osteoinductive potential of these natural materials was examined using the C2C12 promyoblast cell line. In addition, primary human osteoprogenitors transfected with green fluorescence protein (GFP) or AxCAOBMP-2, a vector carrying the human BMP-2 gene to examine the potential to form mineralised structures on these scaffolds.

RESULTS: *Collagen sea sponge* provided a conductive framework for attachment and growth with osteoprogenitor growth aligned along the collagen struts and to span across large spaces (500-1250μm) between the collagen struts to form membranous sheets. Osteoprogenitor populations expressing BMP-2 rapidly developed into dense aggregates of tissue and expressed high levels of alkaline phosphatase within 7 days. Expression of alkaline phosphatase in the C2C12 promyoblast cell line following culture for 14 days confirmed the osteoinductive potential of nacre. Human osteoprogenitor cells were also observed to align preferentially on nacre as determined by fluorescence microscopy using GFP expressing cells and to express significantly increased alkaline phosphatase activity compared to control cultures. Poor osteoprogenitor growth was observed on sea urchin spines but despite this alkaline phosphatase expression was commensurate with controls at 7 days.

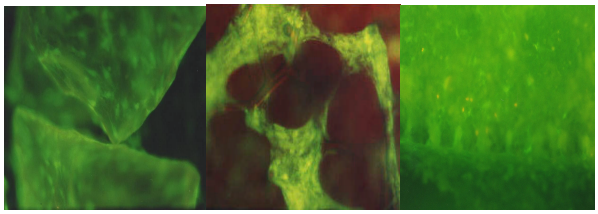

Fig. 1: Fluorescent labeled human osteoprogenitor cells cultured on nacre chips (left), sea sponge skeleton (middle) and sea urchin spine(right) after 7 days in basic media (x10).

(SD)*	**Nacre**	**Sea urchin**	**Sea sponge**
	7487 (2694)	473 (214)	925 (45)
Control	645 (25)	410 (160)	517 (160)

Table 1. Osteoprogenitor Alkaline phosphatase specific activity on nacre and sea urchin spines at 7 days and sea sponge at 14 days in basic media. (Figures = nMol PNPP/ hr/ mg DNA)

DISCUSSION & CONCLUSIONS: These studies demonstrate the osteoinductive property of nacre at the cellular level and the ability of selected natural materials to modulate human osteoprogenitor activity. The abundance and diversity of these natural materials and their potential application for tissue engineering as macro-porous scaffolds and or delivery vehicles offers great promise for tissue repair.

REFERENCES: [1] Green, D., Walsh, D., Mann, S., Oreffo, R.O.C. Oreffo, The potential of biomimesis in bone tissue engineering: leassons from the design and synthesis of invertebrate skeletons. *Bone* Vol. 30, (6): 810-815; 2002. [2]Petite, H., Viateau, V., Bensaid, W., Meunier, A., de Pollak, C., Bourguignon, M., Oudina, K., Sedel, L., Guillemin, G. Tissue engineered bone regeneration. *Nature Biotechnology*. Vol. 18: 959-963; 2000. Lamghari, M., Almeida, M.J., Berland, S., Huet, H., Laurent, A., Milet, C., Lopez, E.

Stimulation of bone marrow cells and bone formation by nacre in vivo and in vitro studies. **Bone.** 25 (2 Suppl): 91S-94S.

ACKNOWLEDGEMENTS: The authors thank Michelle Kelly Shanks of NIWA, N.Z. This work was supported by EPSRC & BBSRC.

European Cells and Materials Vol. 4. Suppl. 2, 2002 (pages 11-12) ISSN 1473-2262

ENGINEERING A GRAFT FOR CORONARY BYPASS SURGERY: ROLE OF CHEMICAL COATINGS TO ENHANCE ATTACHMENT OF SMOOTH MUSCLE CELLS TO COMPLIANT POLY(CARBONATE-UREA)URETHANE MATRICES

S. T. Rashid, H. Salacinski, B. Fuller, G. Hamilton, A. Seifalian

Tissue Engineering Centre, University Department of Surgery, The Royal Free Hospital and Royal Free & University College Medical School, University College London, London, UK

INTRODUCTION: Obstructive atherosclerotic vascular disease in the form of cardiovascular and cerebrovascular disease is the largest cause of mortality in the USA and Europe[1]. When angioplasty or stenting of the occluded vessels is not possible or unsuccessful then the surgical remedy for coronary artery ischaemia requires the use of bypass grafts. Normally this uses the patient's own blood vessels: principally the Internal Mammary Artery and the Long Saphenous Vein. However, in a third of patient's there is insufficient blood vessel available. The use of synthetic materials has largely been abandoned due to their poor patency and higher infection rates. Endothelial cell seeding of synthetic materials like expanded polytetrafluoroethylene (ePTFE) have shown higher patency rates in clinical trials.

To further improve this our group has been working on the development of a biological 4mm graft with both endothelial and smooth muscle cells incorporating an elastin and collagen matrix. The engineering of functional smooth muscle cells is critical in the development of such an engineered conduit. This study reports on the effects chemical coatings have in enhancing attachment and subsequent proliferation on matrices made of compliant poly(carbonate-urea)urethane (Myolink).

METHODS: Myolink was coated with: RGD - ARG-GLY-ASP – (633mcg/ml); Superfibronectin (42mcg/ml); Fibronectin (118mcg/ml); Fibronectin-Like Engineered Polymer Protein (118mcg/ml); Fibronectin-Like Engineered Polymer Protein Plus (133mcg/ml); Type 1 collagen (1mg/ml) or Native (no coating) overnight.

Small bioreactors were developed into which the coated Myolink was inserted, onto which was seeded smooth muscle cells (SMC) at a density of 2.27×10^5 SMCs/ml, radiolabelled with ^{111}In-Oxine as per our previous protocol[2].

After around 48 hours seeding, the solution was aspirated off and the Myolink sections were then washed with sterile PBS. The initial aspirate and then the washings were collected in separate tubes. The Myolink, aspirate and washings were then counted in a gamma counter to give the percentage attachment of SMCs to the Myolink. The radioactivity reflected the number of SMCs.

RESULTS: FEPP+ was significantly better than the native Myolink in terms of attachment of the SMCs, with a mean of 31.45% cell attachment compared to 20.71% for the Native graft ($p<0.01$) – see Figure 1 below.

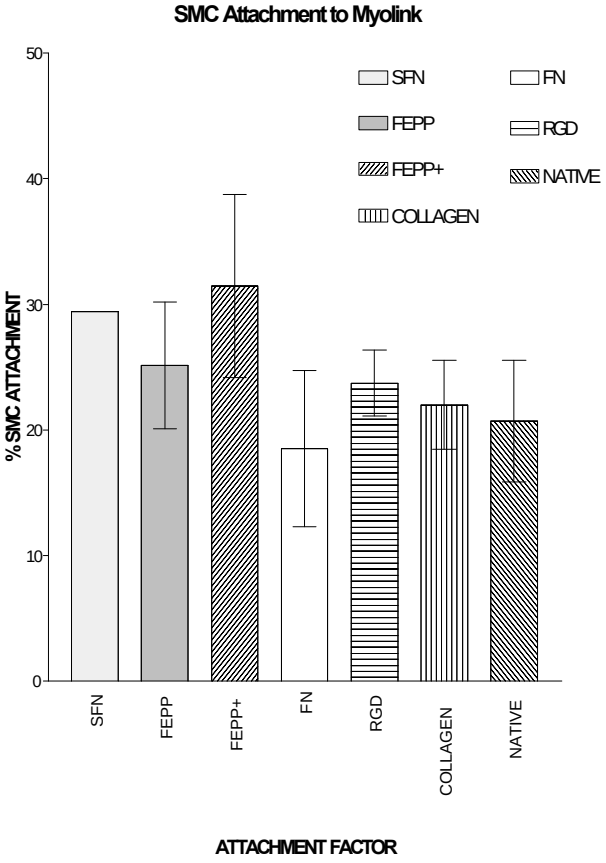

Figure 1: % SMC Attachment to Myolink using different Attachment Factors.

CONCLUSION: We report a new radiolabelling method for assessing attachment of SMCs to graft material. It has been validated by assessing the attachment of SMCs with different extra-cellular matrix materials. FEPP+ was found to have the most significant effect because it is positively

charged and thus attracts the negatively charged cells and has repeating sequences of RGD. This tissue-engineered material may find a clinical application and provide a tool to study molecular mechanisms in coronary graft development.

REFERENCES [1]World Health Organization. World Health Organization: The World Health Report 1999. 1-1-1999. Ref Type: Report. [2]Giudiceandrea A, Seifalian AM, Krijgsman B, Hamilton G. Effect of prolonged pulsatile shear stres

ACKNOWLEDGEMENTS: We thank Credant Vascular Technologies Ltd. for supplying 4mm graft and for financially supporting HS.

HOW DO LARVAE OF *LUCILIA SERICATA* INITIATE HUMAN WOUND HEALING?

A. J. Horobin[1], D. I. Pritchard[1] & K. M. Shakesheff[1]

[1] *School of Pharmaceutical Sciences, University of Nottingham, England, GB*

INTRODUCTION: The healing of recalcitrant wounds remains a major and unmet challenge of health care. Tissue engineering could play a role in providing new treatments, as demonstrated by recent developments including the use of growth factor delivery systems and skin replacement technology.

A potential avenue of new wound healing treatments may be found in the ancient practice of applying *Lucilia sericata* or greenbottle fly larvae to chronic wounds[1]. Observations have indicated the larvae to debride necrotic tissue, remove bacteria, including antibiotic-resistant strains such as MRSA (Methicillin-resistant *Staphylococcus aureus*)[2] and enhance the promotion of granulation tissue formation[1], thus behaving as accomplished tissue engineers. However, little research has been conducted into the molecular mechanisms responsible.

With the aim of identifying the promoters of granulation tissue formation, we investigated the effect of proteases within *L. sericata* larval secretions upon the behaviour of human dermal fibroblasts.

METHODS: Larval excretion/secretion (ES) collection: One-day-old sterile *L. sericata* larvae were bathed in phosphate buffered saline (PBS). ES/PBS mix was extracted and 0.2μM filtered. Protein concentration and protease activity was estimated using Bio-Rad's protein assay or fluoroscein isothiocyanate (FITC)-Casein assay respectively. Heat-treated ES was heated at 100°C for 30 min, yielding insignificant protease activity.

Cell adhesion assays: Human, dermal, neonatal fibroblasts were plated into wells pre-coated with fibronectin or collagen and either ES blank or 10μg ES protein/ml added. Following incubation and aspiration to leave adhered cells for assaying, ATP or nucleic acid concentrations were estimated using Packard's ATPLite™-M or Molecular Probes' CyQUANT® assay kits respectively.

Cell spreading: Cells were seeded into fibronectin or collagen pre-coated wells. After four hours incubation, images were taken using Leica DMIRB inverted microscope and analysed with QUIPS software.

RESULTS: Native ES reduced fibroblast cell adhesion upon both fibronectin and collagen substrates. This was confirmed by measuring both ATP and nucleic acid levels. Heat-treatment significantly decreased the inhibitory activity of ES, indicating a role for ES proteases.

ES also altered fibroblast cell morphology, reducing cell surface area and increasing roundness. Thus, fibroblast spreading was inhibited. This was particularly noticeable when fibronectin substrate was present. Again, heat-treatment reduced the activity of ES.

In some cases, cells were shielded from exposure to ES. Adhesion inhibition still occurred when these unexposed cells were seeded upon substrates that had been pre-exposed to ES. This indicated that ES inhibited adhesion by altering the substrate surface.

DISCUSSION & CONCLUSIONS: Interactions between fibroblasts and extracellular matrix (ECM) substrate surfaces were shown to be modified by *L. sericata* ES and in particular, the proteases present within the ES. As cell adhesion and spreading was reduced, ES may enhance fibroblast mobility. This may have implications in cell migration, with ES inducing fibroblast migration into the wound space, thus increasing granulation tissue formation. The apparent alteration of the ECM substrates by ES is also of interest. This is particularly so with fibronectin, whose proteolytic degradation products are capable of binding to fibroblasts to elicit different responses[3].

The link between the effects demonstrated and the potential to promote skin regeneration is being explored in 3D *in vitro* models of skin.

REFERENCES: [1] R.A. Sherman, M.J.R. Hall and S. Thomas (2000) *Annu. Re. Entomol.* **45**:55-81. [2] D. Bonn (2000) *Lancet* **356**:1174. [3] P. Huhtala, M.J. Humphries, J.B. McCarthy et al (1995) *J. Cell. Biol.* **129** (3): 867-879.

ACKNOWLEDGEMENTS: To Dr S. Woodrow for advising on ES collection, Dr R. Pearson for

microscopy assistance, Dr S. Dexter for assay advice and the EPSRC for funding.

European Cells and Materials Vol. 4. Suppl. 2, 2002 (pages 70-71) ISSN 1473-2262

BONE CELL RESPONSE TO NOVEL ION-IMPLANTED TITANIUM

S.Nayab[1,2], F.H.Jones[2] & I.Olsen[1]

[1]Departments of Periodontology and [2]Biomaterials, Eastman Dental Institute for Oral Health Care Sciences, University College London, 256 Grays Inn Road, London WC1X 8LD, UK

INTRODUCTION: Titanium (Ti) has been used extensively for bone and periodontal tissue reconstruction. However, despite its generally successful clinical application, it has been reported to undergo long-term corrosion, fatigue fracture and poor response to friction. A number of surface treatments have therefore been carried out in order to improve its biocompatibility. For example, a previous study has reported that Ti surfaces implanted with calcium ions could enhance osseointegration and bone formation *in vivo*[1]. Nevertheless, the lack of consistent and reproducible effects have highlighted the need to understand the basic mechanisms involved in the response of target cells to such surfaces[2]. The present study has therefore measured the effects of ion-implantation of Ti on the adhesion of bone cells *in vitro*, the first phase of the host response to this novel material.

METHODS: Human alveolar bone cells were cultured in Dulbecco's modified Eagle's medium and incubated at 37°C in a humidified atmosphere of 5% CO_2 in air. Commercially pure and polished Ti discs were implanted at 40 keV with Ca ($1x10^{17}cm^{-2}$), K ($1x10^{17}cm^{-2}$) and Ar ($2x10^{17}cm^{-2}$) ions. Control (non-implanted) and test Ti discs were sterilised by ultraviolet light. To measure cell attachment, primary bone cells were pre-labeled for 24 h with ^{3}[H]thymidine, a radioactive precursor of DNA. The radiolabeled cells were harvested, washed and seeded onto the control and implanted Ti discs for 4 h at 37°C. After washing to remove non-adherent cells, the radioactivity remaining associated with the discs was measured to determine the number of attached cells. For scanning electron microscopy (SEM), the adherent cells were fixed, processed, photographed and the average cell area on five representative fields was measured by digital image analysis.

RESULTS: Figure 1 shows that bone cell attachment to Ca-implanted Ti was reduced by 38% compared with control Ti. Moreover, approximately 15 and 20% fewer cells attached to K and Ar-implanted Ti, respectively.

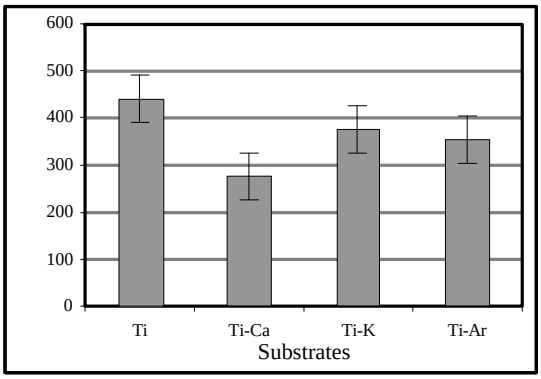

Fig.1: Adhesion of bone cells to Ti surfaces.

Fig. 2: Morphological appearance of bone cell on control–Ti (left) and Ca-implanted Ti (right) discs.

The extent of bone cell spreading was examined to assess the relative biocompatibility of the Ti surfaces. Fig. 2 shows that after 4h of incubation, many rounded cells were still observed on the control Ti disc. In contrast, a substantially increased proportion of highly spread cells with numerous cytoplasmic processes were seen on the Ca- implanted Ti.

Table 1. Bone cell spreading on control and ion-implanted Ti surfaces

Substrate	Cell Area (μm^2)	% Of control
Ti	719	100
Ca - Ti	1532	213
K -Ti	742	103
Ar -Ti	548	76

These morphological observations of cell spreading were consistent with the measurement of average cell area as shown in Table 1. Thus, cells on Ca-Ti were found to have an area which was on average more than twice that of control, whereas bone cells incubated on the K and Ar-implanted discs were spread to the same extent as the control.

DISCUSSION & CONCLUSIONS: The results of the present study show that surface modification of Ti by ion implantation can have a pronounced effect on the adhesion of bone cells. However, while Ca implantation of Ti appeared to decrease the overall level of cell attachment, cells incubated on this substrate nevertheless had a markedly increased average cell area. This observation suggests a high degree of biocompatibility of bone cells on this particular surface. Further studies are now in progress to determine whether different concentrations of implanted Ca ions could enhance the adhesion of the cells without compromising the functional biocompatibility at the gene and protein levels.

REFERENCES: [1] T. Hanawa *et al* (1997) *J.Biomed.Mater.Res*, **36** (1), 131-136. [2] C.R.Howlett (1999), *J.Biomed.Mater.Res,* **44**, 352-353.

European Cells and Materials Vol. 4. Suppl. 2, 2002 (pages 16-17) ISSN 1473-2262

MECHANICAL LOADING OF 3-D MUSCLE CONSTRUCTS

U.Cheema[1], S.Yang[2], V.Mudera[1], G.Goldspink[2] & R.A.Brown[1]

[1]*University College London Tissue Repair & Engineering Centre, Institute of Orthopaedics, UCL, Stanmore, HA7 4LP*

[2]*Department of Surgery, RFUCMS, Royal Free Campus, Rowland Hill Street, NW3 2PF*

INTRODUCTION: Mechanical conditioning of many tissue engineered construct will be critical, particularly mechano-responsive tissues such as skeletal muscle. It has been shown that application of defined uniaxial loads to 3D constructs through the tensioning- culture force monitor (t-CFM), has been shown to regulate protease expression in fibroblasts (Prajapati et al. 2000). Insulin-like growth factor (IGF-1) is an important growth factor in proliferation and differentiation of skeletal myoblasts (Florini et al. 1996), along with it a recently isolated isoform, mechano-growth factor (MGF) is found to be upregulated in skeletal muscle *in vivo* following exercise (Yang et al. 1996).

METHODS: C2c12 mouse myoblasts were seeded into 3D collagen lattices (4 million cells/ml: 75x25 mm) and cultured tethered (static endogenous tension) for 1 day in medium containing 10% Foetal Calf Serum (FCS), this was reduced to 2% FCS from day 2 to day 6, over which period myoblast fusion occurred, to give multinucleated myotubes. At the end of this period 3D constructs were attached in their long axis to the t-CFM for loading. Regimes used (i) cyclic loading (1% strain: 1-10 cycles/hour) (ii) ramp loading (10% strain: 1-10% per hour)

RESULTS: The force generation profile over 24 hours for myotube rich constructs was characterised by a series of rapid contractions(fig.1).

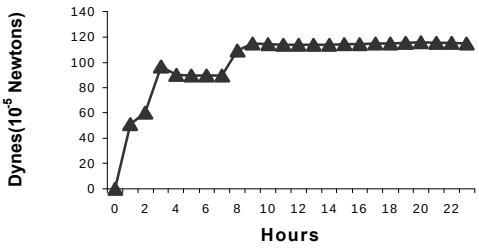

Figure 1. A typical myotube contraction profile. The total force produced, in this case was 115 dynes. Jumps are evident at 0 hours, 2 hours and 7 hours.

Various loading regimes were applied to constructs. It was found that IGF-1 was upregulated in constructs loaded with 10% strain ramp load (fig.3). Interestingly cyclical loading of 1% at 10 cycles per hour (fig.2), lead to a down-regulation in IGF-1.

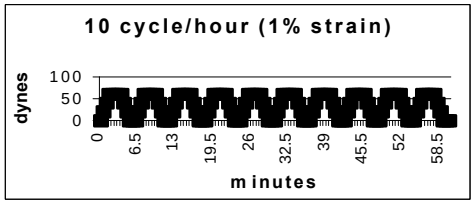

Figure 2. An example of a 10 cycle/hour loading regime applied to a myotube gel

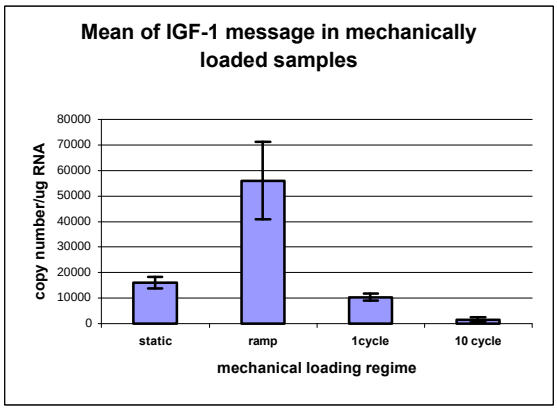

Figure 3. Changes observed in IGF-1 mRNA expression after various loading regimes were applied to skeletal myotube constructs.

DISCUSSION AND CONCLUSIONS: IGF-1 has been shown to be highly mechano-responsive in this simple model muscle. This response is discriminative between types of load, and distinct from responses by MGF (data not shown). These findings confirm the value of this model of skeletal muscle and suggest that it may have utility as the basis for engineered muscle constructs. It also supports the idea that cyto-mechanical cues may be

ideal for controlling tissue development by regulation of growth factor expression.

ACKNOWLEDGEMENTS: This work is funded by the Wellcome trust.

REFERENCES: Florini, J.R., Ewton, D.Z. and Coolican, S.A.(1996) 'Growth hormone and the insulin-like growth factors system in myogenesis'. *Endo. Rev.* 17(5): 481-517. Prajapati, R.T., Eastwood, M., Brown, R.A. (2000) 'Duration and orientation of mechanical loads determine fibroblast cyto-mechanical activation: Monitored by protease release'. *Wound Rep. Reg*. 8:239-247. Yang, S., Alnaqeeb, M., Simpson, H. and Goldspink, G. (1996) 'Cloning and characterisation of an IGF-1 isoform expressed in skeletal muscle subjected to stretch'. *J.Muscle Res. Cell. Motility* 17: 487-495.

European Cells and Materials Vol. 4. Suppl. 2, 2002 (pages 19-20) ISSN 1473-2262

INVESTIGATING THE MECHANICAL BEHAVIOUR AT A CORE-SHEATH INTERFACE IN PERIPHERAL NERVES

R.L.Tillett[1], A. Afoke[2], J.B. Phillips[1] & R.A. Brown[1]

[1] Tissue Repair and Engineering Centre, University College London, London, UK,

[2]Department of Engineering, University of Westminster, 115 New Cavendish St, London W1M 8JS

INTRODUCTION: Knowledge of peripheral nerve anatomy has advanced using histological and microscopic techniques [1], whilst the tensile properties of peripheral nerves have also been investigated [2]. However, the way in which intraneural layers interact and behave mechanically is poorly understood. Movement between intraneural elements is essential during limb movement [3], and is disrupted by trauma. Regeneration of this gliding function will be essential for successful neural tissue engineering and the aim here is to define the important parameters of normal gliding function. Previous work by this group [unpublished] has demonstrated one such mechanically distinct layer, between an inner neural core and outer sheath, in rat sciatic nerve

METHODS: Sciatic nerves were harvested from Wistar rats (200-250g) immediately post mortem and mounted between two clamps, placed 15mm apart. The distal sheath was sutured to the distal clamp and the proximal sheath was cut circumferentially. This secured core to the proximal clamp and sheath to the distal clamp. In a tensile testing machine, traction was applied to the proximal core, pulling core from sheath. Force was measured using a 10N load-cell and core movement monitored using a linear voltage differential transformer. Using an extension rate of 10 mm/minute, a force/extension (pull-out) curve was obtained for each nerve. The movement of core and sheath was videoed for digital image analysis. After nerves had been mechanically tested they were fixed, for scanning electron microscopy. For comparison, strength of core within the sheath was also measured.

RESULTS: As the nerve unit as a whole takes up load, a large amount of force is required to produce a small increase in length (a) *(Figure 1)*. The "maximum pull-out force" occurs when the force applied to the core exceeds the break strength of linking elements between core and sheath. Once linkages break, the core began to glide out of the sheath (b) requiring decreasing amounts of force to maintain a constant increase in length. The mean maximum pull out force was 0.41 ± 0.04N (n=9). Video analysis appeared to demonstrate that sheath stretched by a small amount and then returned to its original length, whilst core underwent a permanent increase in length. The force required to break the core (reinforced by sheath) was 0.63 ± 0.06N (n=6).

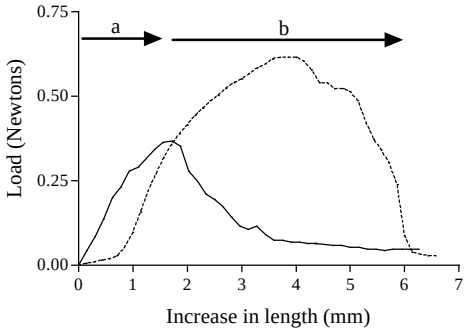

Figure 1. A graph demonstrating representative force-extension curves for core pulling out of sheath (solid line) and core breaking (broken line), for a 15 mm length of rat sciatic nerve

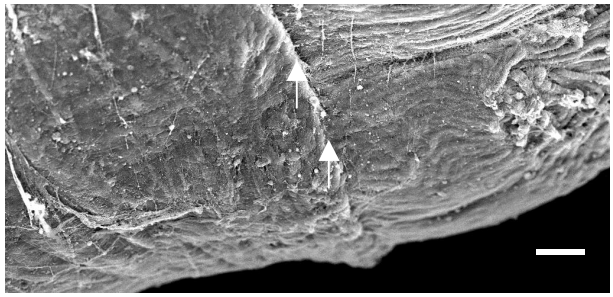

Fig. 2: Scanning electron micrograph of pulled rat sciatic nerve. Arrows indicate the edge of an outer sheath (left), as inner neural core (right) is pulled from it. Scale bar = 100 ìm

DISCUSSION & CONCLUSIONS: A mechanically distinct interface, with consistent mechanical properties, between two layers of peripheral nerve has been identified. A resistance to movement, which can be overcome using a mean force of 0.41 N, exists. This force is smaller than the forces required to break the whole nerve or its components. The resistance to movement could be produced by connecting elements, which break sequentially as the maximum pull-out force is

obtained. Once sufficient numbers have fractured, the core can glide out of the sheath. This mechanism could act to protect the neural core from trauma and its imperfect regeneration would contribute to poor functional recovery.

REFERENCES: [1]P.K.Thomas, C.-H. Berthold and J. Ochoa (1993) Microscopic Anatomy of the Peripheral Nervous System in *Peripheral Neuropathy: Volume 1* (eds P.J. Dyck and P.K. Thomas). [2]R. Grewal, J. Xu, D.G. Sotereanos and S.L.-Y. Woo (1996) *Hand Clinics* **12**:195-204. [3]H. Millesi, G. Zöch and T. Rath (1990). The gliding apparatus of peripheral nerve and its clinical significance. *Ann Hand Surg* **9**: 87-97.

ACKNOWLEDGEMENTS: This work was partly supported by the European Commission grant: QLK3-CT-1999-00625.

HUMAN CHONDROCYTE ADHESION MOLECULES - ROLES IN REGULATION OF CELL FUNCTION AND CARTILAGE REMODELLING

Dr Donald M Salter

Department of Pathology, Edinburgh University Medical School, Scotland, UK.

INTRODUCTION: Cell-matrix interactions are known to be critical in the regulation of a variety of activities including cell proliferation, differentiation and death. In cartilage, where chondrocytes are isolated from neighbouring cells, a specialised pericellular matrix appears to be very important in the regulation of a range of metabolic activities and responses to environmental stimuli such as mechanical loads. These cell-matrix interactions are mediated by a variety of specialised cell surface molecules that can transmit signals from the extracellular space to the cell interior and through activation of intracellular signal cascades regulate gene expression.

The major cell adhesion molecules expressed by chondrocytes are members of the integrin family, CD44 and human melanoma proteoglycan (HMPG/NG2). The function of these molecules, as they relate to chondrocytes are only just beginning to be defined. Integrins such as $\alpha 10\beta 1$, $\alpha 1\beta 1$ and possibly $\alpha 2\beta 1$ appear to be important in chondrocyte adhesion to pericellular type II and type VI collagens whereas $\alpha 5\beta 1$ is involved in adhesion to fibronectin. Evidence is now accumulating for additional, important, roles for these molecules in recognition of mechanical stimuli and regulation of remodeling activities including matrix metalloproteinase production and modulation of apoptotic pathways. $\alpha 5\beta 1$ integrin, in particular, appears to be an important chondrocyte mechanoreceptor stimulation of which results in activation of an interleukin 4 dependent anabolic response. Expression of chondrocyte integrins varies during development and in diseases such as osteoarthrtitis where novel matrix molecules are expressed and active matrix remodelling is taking place. CD44 is a transmembrane molecule which may be expressed as a number of different isoforms as a result of alternative splicing. It has been shown to be the major receptor for hyaluronan and is important for the retention of the gel like proteoglycan rich pericellular matrix around chondrocytes. CD44 may also act as a receptor for collagen and is known to transmit extracellular signals and regulate function of a variety of cell types. Roles in cartilage remodeling are beginning to be defined. HMPG/NG2 is a chondroitin sulphate-rich cell surface proteoglycan which although having collagen and fibronectin binding activities appears to function is cartilage indirectly by regulating integrin interactions with extracellular matrix molecules such as type VI collagen.

The nature of chondrocyte-matrix interactions will depend on the range of integrins and other adhesion molecules expressed by the cells and also the content of the pericellular matrix to which these cells are adherent. The result is a mutual reciprocity influencing cell differentiation and function. Understanding of these interactions, which are modified by a diverse range of factors including cytokines, mechanical stimuli, growth factors and matrix molecules themselves, is important for tissue engineering strategies aimed at production of different forms of cartilage for use in the treatment of human diseases.

REFERENCES: S.J. Millward-Sadler, M.O. Wright, L.W. Davies, G. Nuki and D.M. Salter (2000). Arthritis and Rheumatism 43: 2091-2099. Midwood KS, Salter DM. (2001) J Pathol;195:631-635. Salter DM, Godolphin JL, Gourlay MS. (1995) J Histochem Cytochem ; 43: 447-457.

ACKNOWLEDGMENTS: Work of the Edinburgh Pathology Osteoarticular Laboratory is supported by Action Research, Arthritis Research Campaign and the Chief Scientist Office.

European Cells and Materials Vol. 4. Suppl. 2, 2002 (pages 30-31) ISSN 1473-2262

DIRECTING CELL SHAPE AND MIGRATION BY TOPOGRAPHIC AND ELECTRICAL SIGNALS

A.M. Rajnicek

Department of Biomedical Sciences, Institute of Medical Sciences, University of Aberdeen, Aberdeen AB25 2ZD, Scotland, UK

INTRODUCTION: DC electric fields (EFs) occur naturally within developing tissues and near epithelial wounds. They are required for normal development and wound healing. Application of exogenous EFs stimulates CNS repair and wound healing. Reviewed in ref [1]. The EFs are a consequence of asymmetric ion transport across the tightly sealed epithelium, which produces a transepithelial electrical potential difference of tens of mV. EFs of 400 to 1000 mV/mm exist in the developing amphibian nervous system. *Xenopus* spinal neurites turn toward the cathode of an EF as small as 7 mV/mm *in vitro*, suggesting that EFs guide axons during nervous system development.

The ability of the physical shape of the substratum to direct cell shape and motility during development and wound healing has been largely unappreciated. This is despite evidence that arrays of aligned cells and spaces within embryonic tissues are subsequently used as scaffolds for neuronal growth. Neurons align on parallel substratum grooves ranging from 14 to 1100 nm deep *in vitro*, suggesting that embryonic topography affects axonal guidance [2].

The purse-string like contraction at the edge of an epithelial wound causes cells near the wound to become elongated at a right angle to the wound edge. Collagen fibres within the cornea are arranged parallel to each other within layers. Consequently, cells migrating to fill a corneal wound could encounter radially aligned arrays of cells and parallel arrays of collagen fibers.

We explored directional growth and guidance in primary cultures of *Xenopus* spinal neurons and bovine corneal epithelial cells in response to physiological EFs and parallel substratum grooves. The influence of EFs and grooves were examined separately and in combination. Our aim was to determine the cellular mechanisms for directed EF and contact guidance responses and to establish a hierarchy of these directional guidance cues, which co-exist *in situ*.

METHODS: The procedures for culture of *Xenopus* spinal neurons, corneal epithelial cells, preparation of grooved substrates and electric field application have been described previously [2-4].

In the case of *Xenopus* neurons individual cells were photographed at hourly intervals and the angle of growth was measured with respect to the groove axis and EF direction over 5h. For corneal epithelial cells selected visual fields were photographed at 0h, 1h and 3h. The rate and angle of migration were determined relative to the direction of the grooves or EF. An EF of 150 mV/mm was oriented either parallel or orthogonal to the groove axis. Substratum grooves were 130 nm deep and 1, 2 or 4 μm wide.

RESULTS:

***Xenopus* neurites**: On flat quartz in the absence of an EF *Xenopus* neurite growth was randomly oriented but in an EF neurites turned dramatically toward the cathode (fig1a). When the EF vector and the groove axis were parallel neurite growth was enhanced cathodally. When the EF vector was orthogonal to the groove axis the directional response depended on groove depth (Fig 1b,c). Neurites followed grooves and ignored the EF on 2 μm wide grooves but on 4 μm wide grooves they responded predominantly toward the cathode of the EF rather than following the grooves.

Fig. 1: Xenopus spinal neurons in an EF of 150 mV/mm. (a) on flat quartz (b& c) on quartz with 130 nm deep grooves oriented vertically. Neuronal Cell bodies have been superimposed and neurite

paths traced at the end of 5h of EF exposure. The cathode is to the left. Scale bar is 100 mm.

Bovine corneal epithelial cells: On flat quartz in the absence of an electric field cells migrated randomly in all directions but they migrated faster and more frequently toward the cathode of an EF (fig 2). Cells migrated parallel to the groove direction in the absence of an EF but cathodal migration was enhanced when the EF and groove axis were parallel. Migration parallel to the grooves predominated over that toward the cathode when the grooves and EF were presented orthogonally.

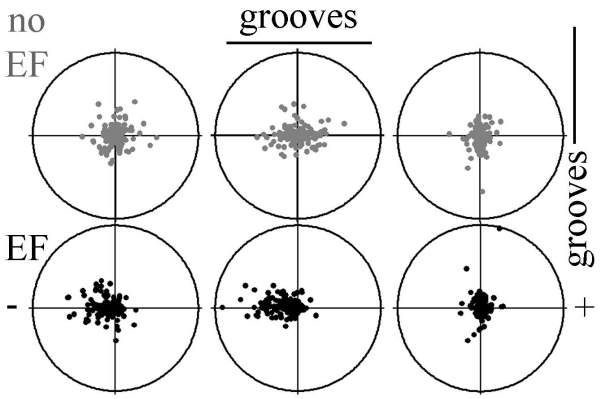

Fig. 2: Bovine corneal epithelial cell migration on flat or grooved quartz. Top row: cells in the absence of an EF. Bottom row: cells in an EF of 150 mV/mm, cathode at left. Left column: flat quartz. Middle column: Grooves and EF vector both horizontal. Right column: vertical grooves and horizontal EF. Each point represents the position of a single cell at the end of a 3h experiment relative to its starting position at the centre of the circle. Radius 70 mm/h.

DISCUSSION & CONCLUSIONS:

We have examined the responses of neuronal and epithelial cells to weak EFs and substratum shape because those guidance cues co-exist in the developing nervous system and near epithelial wounds. In particular we determined whether the cues could enhance directional migration when presented in parallel and determined the hierarchy of guidance cues by presenting them orthogonally.

Neuronal growth cones and corneal epithelial cells migrated toward the cathode of an EF on a planar quartz substratum.

When the EF vector and the groove axis were presented simultaneously and parallel to each other cathodal migration was enhanced.

When the EF vector and substratum grooves were presented simultaneously but at right angles to one another epithelial cells migrated preferentially along grooves, rather than toward the cathode, regardless of the width of the grooves. Therefore, at least at the field strength and groove widths used here (150 mV/mm; 1, 2 or 4 μm), epithelial cells are more sensitive to guidance cues provided by substratum contour than to cues provided by the EF. Neuronal growth cones however, responded in a way that depended on groove width. On grooves 1 or 2 μm wide growth cones migrated along grooves, ignoring an EF presented at a right angle to the grooves. On grooves 4 μm wide however, growth cones ignored the grooves and migrated toward the cathode. Therefore, for Xenopus spinal neurons on narrow grooves substratum contours provide a stronger directional cue than an EF but on wide grooves the EF-induced cathodal migration predominates.

The guidance cues provided by substratum contours and EFs have generally been considered too crude to provide specificity for migrating cells and neuronal growth cones. Our results indicate that this view is too confining. When presented together these cues enhance the directional influence of either cue in isolation. Significantly, the orientation of the cues relative to one another alters the direction of migration. This suggests that even in the case of a uniform EF near a wound or within the nervous system small changes in substratum topography can affect the route along which a cell or growth cone migrates, which consequently affects the efficiency of wound healing or establishment of functional nervous system connections.

REFERENCES: [1] C.D. McCaig, A.M. Rajnicek, B. Song & M.Zhao (2002) *Trends Neurosci.* **25:**354-359. [2] A.M. Rajnicek, S.Britland & C.D. McCaig (1997). *J. Cell Sci.* **110:**2905-2913. [3] A.M. Rajnicek, K.R. Robinson & C.D. McCaig (1998). *Dev. Biol.* **203:** 412-423. [4] M. Zhao, *et al*., (1996). *J. Cell Biol*. **109:** 1405-1414.

ACKNOWLEDGEMENTS: Supported by The Wellcome Trust

Many thanks to my PhD student Louise E. Smith for diligent efforts in the lab and to Colin D. McCaig for continued encouragement.

DEVELOPMENT OF AN INTERFACE MODEL FOR THE GENERATION AND ENGINEERING OF TISSUE INTERFACES IN VITRO.

Marenzana M. and Brown R.A.

Tissue Repair and Engineering Centre, University College London, London, UK

INTRODUCTION: The interface between any newly engineered tissue and pre-existing tissue is absolutely key to tissue engineering, yet this process has so far largely ignored with only a few published reports of the mechanical strength of newly integrated surfaces between connective tissues with other engineered tissues or simply cell-free substrates. Although some correlation between cell migration and matrix deposition has been found, the cellular mechanism of tissue integration is still poorly understood. Work in our laboratory on a tendon - collagen gel interface model[1] has shown measurable adhesion strength increasing with cultivation time dependent on cell migration and surface injury (though not cell proliferation). This model has been evolved to generate a better-defined interface between two collagen lattices, one pre-contracted by resident fibroblasts and the other cell free.

METHODS: A new culture chamber has been designed and fabricated to allow a vertical casting of the cell free gel and then horizontal cultivation immediately after the interface is formed. This can be cultivated for prolonged period of time (> 2 weeks) and can be fitted onto a computer-driven mechanical testing system to perform indentation studies or apply predefined tensile loading.

RESULTS: In this new geometry, stress and strain can be precisely measured, allowing for further modelling of the mechanics of the system by finite element modelling. Baseline (time zero) adhesion force measurements showed good uniformity and reproducibility. Preliminary data also showed that the adhesion force after one week of cultivation was considerably higher.

DISCUSSION & CONCLUSIONS: The current experimental design permits solid interface formation in a controlled manner with a well-defined geometry and the possibility to measure mechanical linkage and/or apply various regimes of mechanical loading. The long-term findings of this research will be beneficial to the development of a new generation of tissue bioreactors.

REFERENCES: [1] C. Cacou, M. Eastwood, D.A. McGrouther, R.A. Brown (1996) *Cell. Eng.*, **1**, 109-114.

ACKNOWLEDGEMENTS: This study has been supported by the Fifth Framework Programme of the European Commission, "Biomechanichal Interactions in Tisssue Engineering and Surgical Repair (BITES)".

European Cells and Materials Vol. 4. Suppl. 2, 2002 (pages 72-73) ISSN 1473-2262

CONFOCAL LASER SCANNING MICROSCOPY (CLSM) STUDY OF HEPATOCYTES CULTURED ON COLLAGEN FILMS AND GELS.

M. Kataropoulou, E. Goldie, G. Connel and M.H. Grant.

Bioengineering Unit, Strathclyde University, Wolfson Centre, Glasgow G4 0NW.

INTRODUCTION: Primary hepatocyte cultures form an integral part of many hybrid artificial liver designs, and the extracellular matrix environment of the cultures is an important factor for optimal expression of hepatocyte-specific phenotype. This study investigates the effect of incorporating 20% chondroitin-6-sulphate ($Ch6SO_4$), a glycosaminoglycan (GAG), into collagen films and gels, and crosslinking the films and the gels with 1,6-diaminohexane (DAH) on the viability of hepatocytes cultured for 48 hours.

METHODS: Hepatocytes were isolated from male Sprague-Dawley rats by collagenase perfusion and seeded at $3x10^6$ viable cells on 60mm Petri dishes in 2ml of Chee's medium containing 5% v/v foetal calf serum. Collagen films were prepared at a concentration of $25\mu g/cm^2$. Collagen gels were prepared as described by Osborne et al. [1]. Viability of the cell cultures was assessed by the fluorescence generated by de-esterification of 25µM carboxyfluorescein diacetate (CFDA) in viable cells measured by CLSM. Cell cultures were first incubated with 0.1% (w/v) ethidium bromide for 6 min in the dark at room temperature to locate dead cell nuclei. They were then washed three times with phosphate-buffered saline (PBS), before incubation with the CFDA solution at 4ºC in the dark for 15 min. After this time, cells were washed a further three times with PBS, and examined by CLSM immediately. CFDA is deacetylated by cytosolic esterases inside the cells to yield carboxyfluorescein, which stains the viable cells green. Ethidium bromide stains the nuclei of the dead cells red.

RESULTS: Cells cultured on plain collagen films were spread out and developed a flat and extended morphology (Fig.1a). This kind of morphology has been shown previously [2]. Hepatocytes on plain collagen gels had an entirely different shape and distribution throughout the surface of the plate; cells maintained a round shape after 48 hours in culture and they were scattered throughout the gel (Fig.1b). Crosslinking the gels with the GAG did not cause any improvement in the substrate (Fig.2b), however, the cells cultured on the films+GAG acquired a different shape compared with those on the plain films (Fig.2a). Cells were stained brighter with CFDA, suggesting an increase in viability, and they had a round shape, similar to that of the cells on the gels. The addition of DAH to the gels caused an increase in the number of cells stained with ethidium bromide, suggesting that there were more dead cells compared with the control (Fig.3b). However, cells on films+DAH remained viable generating green fluorescence from CFDA, and the shape was again more round compared with the plain films (Fig.3a). Finally, cells on gel crosslinked with the combination of the GAG and the DAH were only stained red (Fig.4b), whereas cells on the films+GAG+DAH were still bright green and appeared to be a lot more clustered together compared with the control (Fig.4a).

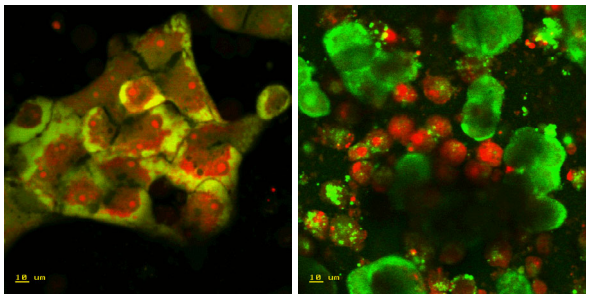

Fig. 1: Primary hepatocytes cultured for 48h on (a) plain collagen film and on (b) plain collagen gel.

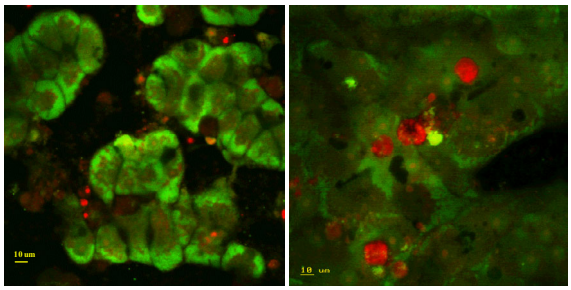

Fig. 2: Primary hepatocytes cultured for 48h on (a) collagen film+GAG and on (b) collagen gel+GAG.

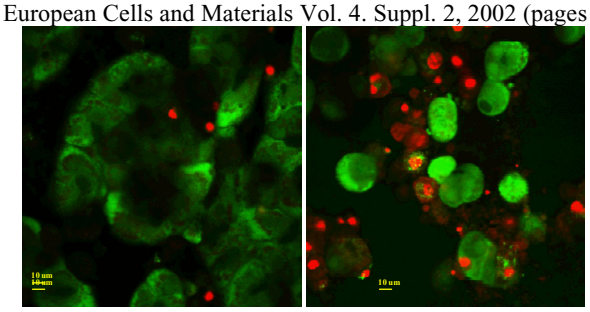

Fig. 3: Primary hepatocytes cultured for 48h on (a) collagen film+DAH and on (b) collagen gel+DAH.

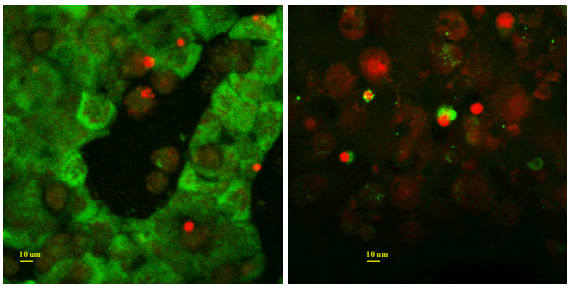

Fig. 4:Primary hepatocytes cultured for 48h on (a) collagen film+GAG+DAH and on (b) collagen gel+GAG+DAH.

DISCUSSION & CONCLUSIONS: When hepatocytes are cultured on a solid substrate, such as collagen-coated polystyrene, they spread out rapidly and develop a characteristic flattened morphology (Fig.1, left). On gel substrates hepatocytes do not flatten, and retain a rounded morphology more similar to the in vivo situation. This has been demonstrated by many previous studies, and the retention of round shape has been correlated with higher expression of in vivo hepatocyte functions [3]. In conclusion, the viability of primary hepatocytes in the crosslinked films appears to be higher compared with the plain film, and the cells retain their round shape. In contrast, crosslinking of collagen gels does not improve cell viability and in fact the presence of DAH in the gels appears to kill hepatocytes.

REFERENCES: [1] C. S. Osborne, W. H. Reid and M. H. Grant (1999) *Biomaterials* 20: 283-290. [2] A. Santhosh and P.R. Sudhakaran (1994) *Mol Cell Biochem* 137: 127-133. [3] W. J. Lindblad, E. G. Schuetz, K. S. Redford and P. S. Guzelian (1991) *Hepatology* 13: 282-288.

European Cells and Materials Vol. 4. Suppl. 2, 2002 (pages 74-75) ISSN 1473-2262

BIOCOMPATIBILTY STUDY USING MICROELECTRONIC MATERIALS TO GROW AND DIRECT TUMOR CELLS

A. Finn, J.Alderman & J. Schweizer

National Microelectronic Research Centre, NMRC, Cork, Ireland,

INTRODUCTION: Over the last 10 years, the ability to grow mammalian cells on microelectronic materials has led to the development of a whole range of biosensors that can measure cellular function. The growth control of cell colonies is important for optimizing cellular recording by forcing the cells to grow on a measuring electrode or gate of a field-effect transistor. The most common materials used for culturing of cells are Silicon Dioxide, Silicon Nitride, Gold, Platinum and Polyimide. Many researchers use Gold or Platinum as a recording electrode for neural electrical studies with silicon nitride as a passivation layer (Borkholder et al, 1998, Wilkinson et al, 1990 and Offenhaeusser et al, 2000). These materials have been shown to be biocompatible with cardiac myocytes. Some researchers (Matsuzawa et al, 1993, Britland et al, 1993) successfully constructed simple neural networks on photo-lithographically patterned substrates. The cells can be confined using a combination of grooves in the substrate and by the selective adsorption of various adhesive proteins such as polylsine and laminin to the substrate.

In this paper, the growth of tumor cells on various microelectronic surfaces will be described as well as efforts to direct the growth of these cells on suitably patterned substrates.

METHODS: Silicon wafers with silicon dioxide, silicon nitride, polyimide, titanium nitride, gold and platinum layers were diced into 8x8mm^2 pieces and cleaned in acetone, IPA and DI water before baking them dry in an oven. They were then placed into 10mm diameter culture plates prior to cell seeding. For the directed growth, a special template was designed containing lines and grids of various sizes and spacings (Figure 1). The line-widths used were 3, 5, 10, 20 and 30 um with spacings of 5, 10, and 50 um. Five of each line-type was drawn and the dimensions of the entire array was 4mm^2. The above patterns were then dry etched into oxide and nitride layers by stopping on an underlying nitride and oxide layer respectively. We then attempted to increase (and decrease) the adhesion properties of these surfaces using a Silanization treatment. Thus, one wafer was coated with Amino-silane (APTES) to make the surface hydrophillic while another was coated with HMDS vapor to make the surface hydrophobic. The substrates were then placed into 10mm^2 culture well plates. Prior to cell culture, all substrates were sterilized by exposure to a UV-light source. Finally the culture medium, containing approximately 10^5 DU-145 adherent prostrate carcinoma cells was put into each well and the cells were kept in an incubator for two days before examination under a standard reflection microscope at x10 magnification.

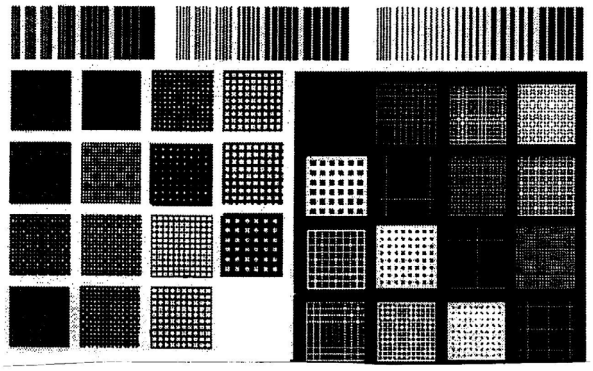

Fig 1: Design template used in selective growth studies.

RESULTS: The results of this study are shown in Figures 1 and 2. Figure 1 shows DU145 tumor cells cultured on a range of microelectronic substrates for 2 days in-vitro. Silicon dioxide, Silicon nitride, Polyimide, Gold and Platinum all resulted in a cell densities and morphologies very similar to the same cells cultured on glass slides. Titanium Nitride, however, produced poor cell densities and morphologies with cell growth being patchy and sparse. This material appears to be unsuitable for culturing of this cell type at least. Figure 3 shows the results obtained after growing these cells on, both treated and untreated, patterned substrates. Confinement varied from poor to moderate and only grooves greater than 10um were able to confine these cells. The silanized surfaces were very different in that the APTES-treated surface produced moderate confinement but the HMDS-treated surface produced very poor cell growth with hardly any confinement either to the surface or to the grooves.

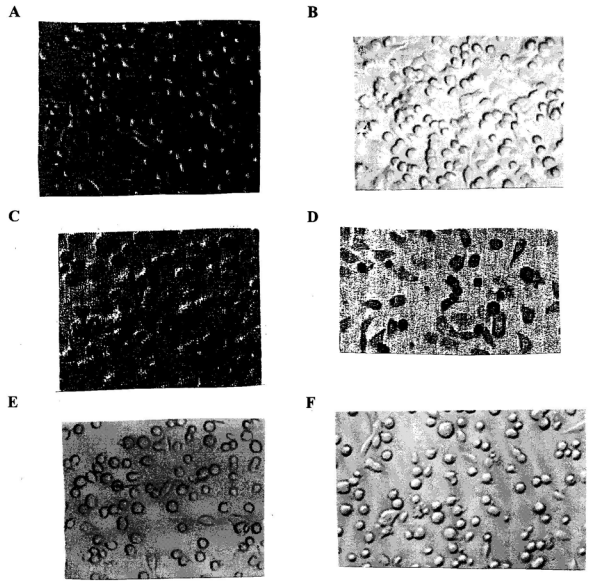

Fig 2: Growth of DU145 tumor cells on various microelectronic materials. (A) silicon dioxide (B) silicon nitride (C) polyimide (D) titanium Nitride (E) platinum and (F) gold at 10^5 cells/ml x10

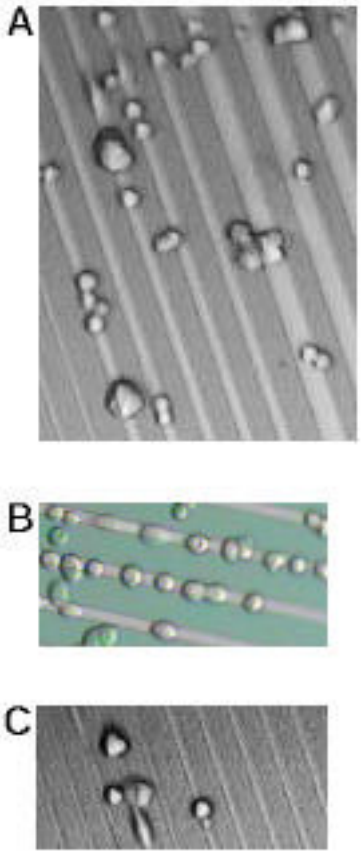

Fig 3: Selective DU145 tumor cell growth on different surfaces. (A) 20um wide untreated silicon dioxide tracks (B) 20um wide silicon dioxide tracks pre-treated with ADTES and (C) 10um wide silicon dioxide tracks pre-treated with HMDS. X20

DISCUSSION & CONCLUSIONS: These results show that tumor cells can be successfully grown on a range of microelectronic surfaces and show no significant differences compared to these cells grown on glass slides. Selective growth of these cells was attempted with some success. The condition of the substrate surface is an important factor in determining selective cell growth. Future work will involve more interesting cell types e.g. neural cells, which have processes that can be guided and directed, using suitably patterned and treated surfaces, and thus the construction of simple neural networks should be possible.

ACKNOWLEDGEMENTS: We would like to thank the staff at NMRC central Fabrication in the design and fabrication of the structures. We are very grateful to Dr T.Cotter for the use of his cell culture facility.

REFERENCES: [1] S.Britland et al, (1993) *Growth cone guidance and neuron morphology on micropatterned laminin surfaces,* J.Cell Science **105**, 203-212 [2] M. Matsuzawa et al, (1993) The *Containment and growth of neuroblastoma cells on chemically modified and patterned substrates,* J.Neuroscience methods **50**, 253-260 [3]M. Matsuzawa et al, (1996) *Chemically modifying glass surfaces to study substratum-guided neurite outgrowth in culture,* J.Neuroscience methods **69**, 189-196.

European Cells and Materials Vol. 4. Suppl. 2, 2002 (pages 21-23) ISSN 1473-2262

TOWARDS AN OPTIMIZATION OF FET-BASED BIO-SENSORS

A. Finn, J.Alderman & J. Schweizer [1]

National Microelectronic Research Centre, NMRC, Cork, Ireland.

INTRODUCTION: In recent years there has been a growing interest in the development of microelectronic biosensors where the electrical activity of neurons and the metabolic activity of tumor cells can be measured in-vitro and non-invasively. Important uses for such devices include pharmaceutical screening systems and further understandings of signal propagation in the brain.

Over the past 10 years, it has become possible to use the ISFET device as a cellular probe. The advantages of the ISFET, as opposed to conventional microelectrodes are (i) the possibility of measuring metabolic activity (via small pH changes in the culture media); (ii) the local amplification of the signal yielding less interference and noise and (iii) the possibility to multiplex transistor arrays. The latter is essential for designing large-scale sensor arrays. Electrical activity in cells has successfully been measured with ISFETS in the past (Fromherz et al, 1991, Offenhäusser et al, 1997) where a neuron sits on top of the non-metalized gate and induces an electrical signal into the ISFET channel. Metabolic activity has also been measured using ISFETS (Baumann et al, 1999) where the H+-sensitive layer of the ISFET, in proximity to a cell population, detects variations in cell metabolism via small (local) pH changes of the weakly buffered culture media.

Due to the high potential of FET-based biosensor arrays, we systematically measured and compared the electrical characteristics of Silicon-On-Insulator (SOI) FET-based devices. This will provide the basis for further performance optimizations, with regard to the recording of neural electrical signals as well as metabolic signals.

METHODS: The ISFET-array design utilizes 16 and 32 gates at different sizes and pitches. P-channel FETS are used for better stability. Each ISFET shares a common source and has individual drain connections for multi-channel read-out. Fabrication of the ISFET array is performed on SOI substrates to eliminate any shorting problems between transistors. Six masks are used in the process: The first mask defines the active-area where the transistors will be formed. A 20nm dry oxide is the grown followed by a V_t-adjust implant. Next the source and drain areas are defined followed by a Boron implant to dope these regions. This is followed by the deposition of 10nm silicon nitride (for the sensing layer) and 0.5um BPSG oxide (for the isolation layer). Next the ISFET gates and contacts are defined simultaneously by wet etching and after the contact regions are etched clear using a fourth mask. Following this etch, 0.6um Aluminium is deposited, patterned and wet-etched. Finally 0.5um of passivation is deposited, patterned and wet-etched to the gate areas and the bond pads. Prior to stripping the resist after the final pattern, 10nm chrome and 50nm Gold is deposited on one of the wafers. A lift-off process is then used to clear the metal everywhere except over the gate areas and bond pads. On another wafer, 10nm of Tantalum is deposited over the entire wafer by CVD technique and oxidized, resulting in Ta205 over the Si3N4, which has been shown to be superior to Si3N4 in terms of pH sensitivity and drift.

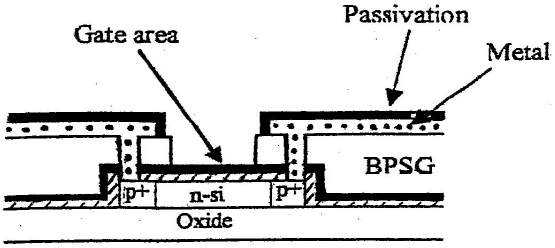

Figure 1:Schematic cross-section of an SOI ISFET

We have fabricated the following device variants:

1. Gate sensing layers: 10nm Si_3N_4 (over the SiO2); 50nm Au./Pt (over the Si_3N_4) and 10nm Ta205 (over the Si3N4).
2. Gate sizes: 30x10, 21x7, 15x5 and 10x1 um^2 at pitches of 100 and 75 um.
3. Passivation layers: 0.5um TEOS oxide and 1.2um Polyimide.

The fabricated chips were mounted in DIL ceramic chip-carriers, wire-bonded and partially encapsulated. A square polystyrene cuvette was attached to the chip carrier to contain 400ul of solution. Electrical measurements with the FETS were carried out using a Ag/AgCl reference electrode (defines gate potential) and a PBS saline solution (pH 7.4).

In order to measure the performance in amplifying neural activity, we applied a test pulse

(amplitude=400uV,width=1ms, frequency=100Hz) to the reference electrode. The FET's drain-source current was then measured and amplified by a one-stage OPA with automatic offset-compensation and low-pass filtering (5kHz cut-off frequency). The drain and gate voltages were adjusted accordingly so that the (small-signal) amplification:noise ratio was maximized. Our main performance indicators have been the peak-to-peak voltage (V_{pp}) and the RMS of noise (V_{NRMS}) (without the test signal) of the filter output. A useful measure for spike detection is the ratio V_{pp} /V_{NRMS}. In order to compare the performance of the FETs with standard microelectrode arrays, we used a 10x10 array of 10x10um^2 platinum electrodes. For pre-amplification, we used a discrete p-channel MOSFET (BS292). The amplifier and filter circuit is the same as that described above.

For the pH sensitivity measurements, we used DU-145 prostrate carcinoma cells, cultured on our SOI ISFETS (gate area 30x10um^2) for 2 days in an incubator. For the measurements, we used weakly-buffered (10mM, pH=7.4) RPMI cell-culture medium and recorded the change in source-drain current over time at driving conditions in which the gate-source voltage was –2.5 V and the drain-source voltage was -0.5 V (approx Ids = -35uA)

RESULTS: Table 1 contains the average measurements of 30x10um^2 FETS, and 10x10um^2 Pt microelectrodes. Table 2 contains averages for Si_3N_4-gate FETs with different gate sizes.

Table1.Average FET/Pt electrode performance.

Device type	*V_{pp} [mV]*	*V_{NRMS} [mV]*	*Ratio*
Si_3N_4-Gate FET	101.8	0.31	340
Au-Gate FET	96.3	0.26	375
Pt-Electrode	5750	15.50	384

Table2.Si_3N_4 gate FETS with different gate sizes.

Device type	*V_{pp} [mV]*	*V_{NRMS} [mV]*	*Ratio*
30x10um^2	101.8	0.31	340
21x7um^2	108.13	0.46	281
15x5um^2	106.25	0.46	230
10x1um^2	335	14	25

The result of the metabolic measurement is shown in Fig.2. The pH-measurements showed a pH sensitivity of approximately 45mV/pH (equivalent to a 3uA change in Ids).

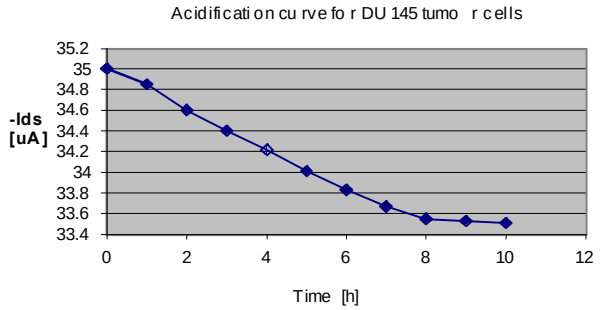

Figure 2: Variation of I_{ds} *with time for DU145 tumor cells.*

DISCUSSION & CONCLUSIONS: There was no major difference between different gate layer-materials, except for the Au-layer which showed slightly better noise performance. However, the metal-layer FETs showed fabrication problems which caused reliability problems. Pitch size and passivation layer have no effect on electrical characteristics but are relevant for cell-studies. The 30x10um^2 FETS showed the best signal-to-noise ratio, which was comparable with that of the micro-electrode. The microelectrodes signals are bi-phasic (in comparison to mono-phasic FET signals) and are more sensitive to interference. We observed higher noise levels for smaller gate areas, in particular for the 10x1um^2. Regarding the pH-measurements, the obtained sensitivity is fairly typical for Si_3N_4-gate ISFETS.

In this initial work, we have systematically characterized various FET transistor types with regard to signal pick-up from neurons, in particular signal-to-noise performance. However, more detailed analyses are necessary to fully exploit the potential of FET-based biosensors.

REFERENCES: [1] W.H Baumann et al, (1999) *A microelectronic sensory system for micro-physiological application on living cells,* Sensors & Actuators B, **55**, 77-89. [2] P. Fromherz et al, (1991) *A neuron-silicon junction: a Retzius cell of the leech on an insulated-gate field-effect transistor,* Science **252**,1290-1293. [3]A. Offenhäusser et al, (1997) *Field-Effect transistor array for monitoring electrical activity from mammalian neurons in culture,* Biosensors & Bioelectronics, **12**, 819-827.

ACKNOWLEDGEMENTS: We are grateful to Prof. A. Offenhäusser (Inst. Thin Films & Interfaces, Research Center Jülich, Germany) for assisting us with the encapsulation of the devices and to Prof. Tom Cotter for the use of his cell culture facility.

EFFECT OF MICROTOPOGRAPHIC CUES ON HUMAN CORNEAL KERATOCYTE ORIENTATION

KY. Then[1,4], Y. Yang[1], A. Curtis[2], W. Monaghan[3], S. Shah[4], P. McDonnell[4] & AJ El_Haj[2]

[1]*Centre for Science & Technology in Medicine, Keele University, England, GB*

[2]*Centre for Cell Engineering, IBLS,* [3]*Dept. Electronics and Electrical Engineering, Glasgow University, Scotland*

[4]*Birmingham and Midlands Eye Centre, England, GB*

INTRODUCTION: It is well known that many cells can orientate in a particular direction in response to a topographical cue. Such property has been explored in bioengineering of tissues which possess specific orientations such as in tendon. Most cells are capable of orientating themselves along narrow fibres as small as 5-50 microns, a phenomenon known as contact guidance first described in 1945 (1). It is known that cells react to topographical cues by changing orientation, adhesion, movement, phagocytosis and cytoskeleton arrangement. The structure of the cornea is also extremely well orientated and interruption to this orientation will result in scarring and loss of optical clarity. In order to bioengineer such a structure, we explore the use of topographical cues for keratocyte orientation and the downstream influences on matrix orientation.

METHODS: Human corneal keratocytes were obtained from discarded corneal-scleral ring after penetrating keratoplasty. Following the removal of epithelium and endothelium, the stroma was chopped in small pieces and put into tissue culture flask in reduced serum media DMEM + 5%FCS + 1% antibiotics and antimycotics + 1% TCH + 1% Ascorbic acid. Cells underwent 2 passages before being used for this experiment. Polycaprolactone (MW 80,000) were used as a scaffold for this experiment. Two membranes were grooved (12.2 X 12.5 X 4 microns) and two were un-grooved. The grooved membrane was embossed using a silica master which is made by photolithography followed by dry-etching. The first pair was stopped after 3 days of culture and the second pair was stopped after 3 weeks. The cellular orientations were viewed under scanning electron microscope, light and reflective microscope.

RESULTS: Human derived corneal keratocytes respond to microtopographical cues by altering their cellular orientation along the direction of the grooves (Fig 1,2). An interesting finding is that the cells orientation changes with time in culture and the effects of multi-layering. Long term culture results in cells forming layers at right angles above the surfaces of the grooved structure. SEM images revealed orientation of the matrix being produced along the axis of the grooves.

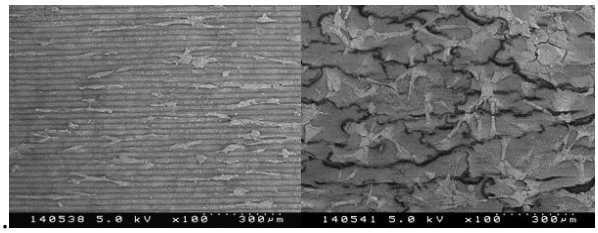

Fig. 1: SEM of human corneal keratocytes grown on grooved and ungrooved polycaprolactone after 3 days in culture. X400

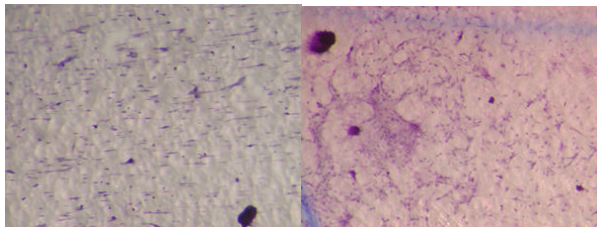

Fig. 2: Reflective microscope of human corneal keratocytes grown on grooved and ungrooved polycaprolactone after 3 days in culture. X50

DISCUSSION: Tissue engineering through contact guidance can be employed for a number of tissues types (2). As with many different cell types, human corneal keratocytes respond to microtopographical cues by altering their cellular orientation along the grooves. The findings have implications not just for bioengineering of a corneal extracellular matrix but also the understanding of corneal wound healing. In particular, the corneal haze effect after excimer refractive surgery might be related to the topographic effect on cellular orientation. A combination of the multi-layering effects observed with a biodegradable matrix could be one way of potentially generating the complex arrangement of corneal matrices and ultimately transparency.

REFERENCES: [1] P. Weiss (1945). *J Exp Zool* **100**;353-86. [2] A. Curtis, M. Riehle (2001). *Phys Med Biol* **46**:R47-R65

ACKNOWLEDGEMENTS: The research was funded through by the Priory of the Order of St.John in Opthamology and the NSMI.

European Cells and Materials Vol. 4. Suppl. 2, 2002 (pages 77-78) ISSN 1473-2262

OPTIMISATION OF BLADDER STROMAL CULTURE ON POLYHIPE

N.O.Umez-Eronini, A.Collins & D.E Neal

Department of Surgery, Medical School University of Newcastle, UK.

INTRODUCTION: Various methods of fabrication of scaffolds for use in tissue engineering of human bladder are currently being utilized. Recent developments include the use of an internal phase polymerization route for the production of highly porous foams (polyHIPE)[1]. The ability to regulate pore and interconnecting hole size independently, and achieve, up to 97% porosity, theoretically make it an ideal scaffold for use in tissue engineering[2]. Using polyHIPE foams we are developing a 3D *in vitro* model for the assessment of the effects of different characteristics of the polymer, on bladder stromal phenotype. We have evaluated the effects of agitated seeding; previously demonstrated to improve seeding density[3], and the addition of hydroxyapertite (HA), to polyHIPE to make it more hydrophilic, on seeding density and infiltration of the urinary tract stromal cells into the polymer.

METHODS: Bladder stromal cultures were derived from tissue obtained from open urological procedures and cultured in DMEM at 37 C and 5% CO_2 cells. Initially cells were seeded statically onto polymer discs (pre-incubated in DMEM for 24 hours) in 100ul aliquots and incubated as above for 24 hours. The experiment was then repeated, and in addition polyHIPE containing hydroxyapertite (HA) was evaluated. The samples were also agitated in an incubator, following seeding for the initial 24hr period. Polymer discs were harvested at day 7 and 22 and fixed in 2% glutaldehyde. The samples where then dehydrated through a series of alcohols, critically point dried and splutter coated with gold. Analysis using a scanning electron microscope was then carried out. Snap fracturing of the polymer discs was used to obtain transverse sections and estimate the depth of colonization of the polymer by the stromal cells.

RESULTS: Static seeding of the polymer discs produced scanty colonies of cells on the surface and no infiltration into polyHIPE foams on evaluation at 7 and 28 days. Agitated seeding of the cells produced a higher density of cells on evaluation at both time points (Fig 1). Infiltration of the polymer by the cells was only seen on the polyHIPE + HA discs despite confluent layers of cells being present on the surface.

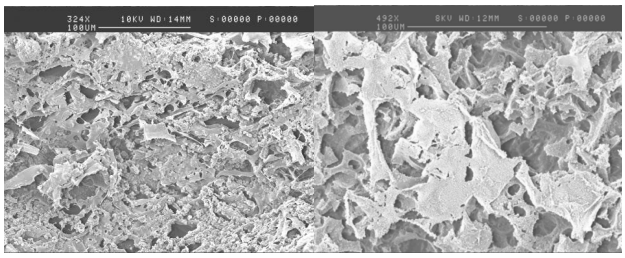

Fig. 1: SEM of Surface of polyHIPE (HA) showing improvement of seeding density with agitated seeding of the cells (left) compared with static seeding (right).

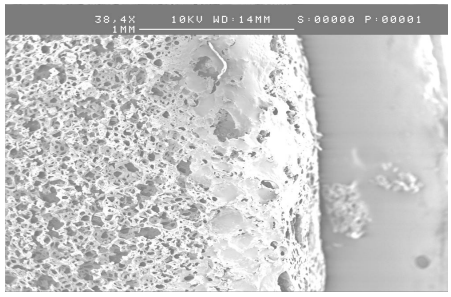

Fig. 2: SEM of transverse section polyHIPE (HA) showing infiltration of cells to 700ìm from the surface on day 22.

DISCUSSION & CONCLUSIONS: PolyHIPE supports the adhesion and growth of bladder stromal cells. The addition of Hydroxyapertite (HA) and the use of agitated seeding methods improved the seeding density and the penetration of cells into the polymer. Although morphologically no differences were seen on SEM, we are currently in the process of phenotypic characterization of the cells to ensure that transformation has not occurred during growth. The phenotypic plasticity of smooth muscle cells is well documented in the literature[4].

REFERENCES: [1] G Akay, V.J Price and S Downes (1998) Microcellular polymers materials as cell growth media and novel polymers. British Patent Application 9825161.4 [2] V.J Price (1999) Preparation, properties and performance of microcellular polymetric material for tissue engineering. PhD Thesis University of Newcastle. [3] B.S Km et al (1998) *Biotechnol Bioeng* 57(1): p46-54. [4] B.S Kim et al (1999) *Exp cell Res* 251(2): 318-28.

ACKNOWLEDGEMENTS: Funding for this project was obtained from the Royal College of

Surgeons England and the Freeman Hospital Trustees. We would also like to acknowledge Maria Bokari at the University of Newcastle for the production of the polymer.

European Cells and Materials Vol. 4. Suppl. 2, 2002 (page 141) ISSN 1473-2262

MODELLING AND SIMULATION OF VASCULAR TISSUE ENGINEERING USING THE FINITE VOLUME METHOD

C.S.Kirk[1], M.Horrocks[2], A.R.Mileham[3] & J.B.Chaudhuri[4]

[1,4]*Depts. of Medical Sciences and Chemical Engineering, University of Bath, UK*

[2] *Dept. of Vascular Surgery, Royal United Hospital, and*

Dept. of Medical Sciences, Univ. of Bath, UK

[3]*Dept. of Mechanical Engineering, Univ. of Bath, UK*

OVERVIEW: It is essential that vascular replacements have a sufficiently robust growth of tissue for a biologically functional material that can withstand the hydrodynamic forces encountered in vivo following transplantation. Growth of these tissue cultures use bioreactors that have been designed and constructed specifically to recreate the chemical and physical environment suitable for tissue growth.

Current research programmes are the subject of computer simulation of the diffusion, adsorption and growth rates which occur in typical cultivation systems with a view to enhancing the design capability and functionality of bioreactors. This will enable improvement in patient care through reduction in time to surgery and an improved *in vitro* cultivation method which more closely resembles that of the *in vivo* condition. It is considered that improvements in the predictive capability of process control, such as the control of oxygen (critical) and nutrient adsorption are vital to maintain progress of advancements in this internationally leading research sector.

This paper discusses the main aims and methodologies involved in using the finite volume method, (FVM) to model and simulate bioreactor and tissue culture performance. As a basis for the current examination, an existing code, (a thermal and atomic diffusion simulator), was translated from that dealing with metallurgical problems in power reactors, (Fig 1) to that dealing with this specialist area of human cell behaviour and tissue engineering.

CONCLUSIONS: The development of an FVM simulation that can rapidly handle computationally intense problems in a 3-dimensional material model has been based on the outputs of previous work[1]. The model provides a basis for the assessment of the finite volume method to simulate problems which include diffusion of nutrients through human cells (vascular and dermal grafts), and provide useful analysis to assess the effectiveness of its use with similar, transport dominant, problems. Assessment of the FVM to handle human cell structures and metabolism has been indicated. This has enabled steps to optimise the bioreactor with a view to providing suitable grafts for transplanting.

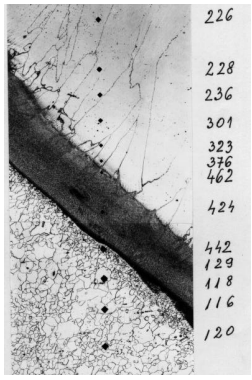

Fig. 1: Micrograph of zones and layering in a typical heterogeneous sample (metallurgical).

REFERENCES: [1] Kirk, C.S., and Mileham, A.R., (2001), Modelling Diffusion in Heterogeneous Transition Welds using the Finite Volume Method, EPSRC Research Report and Assessment, University of Bath, 2001.

MODELLING OXYGEN AVAILABILITY IN BLOOD SERUM, PERFLEUROCARBONS AND AQUEOUS BASED MEDIUM

C.S.Kirk[1] and A.R.Mileham[2]

[1]*Depts. of Medical Sciences and Chemical Engineering, University of Bath, UK*

[2]*Dept. of Mechanical Engineering, Univ. of Bath, UK*

OVERVIEW: The finite volume method has been used in the simulation of atomic diffusion that typically occurs in high-temperature service conditions of post-weld heterogeneous welded joints in power generation plant. This paper reports on the algorithms that supported the investigation and describes their applicability to modelling the moving phase front and the related polymorphic cell used in the simulation of human cell behaviour, particularly applied to the examination of simulations for in vitro experiments using medium containing perfleurocarbons.

A study into the use of the Finite Volume Method to predict diffusion and carbide morphology in elevated temperature applications[1] enabled a better understanding of the complex rate reactions present in heterogeneous welds. This was primarily due to its rapid simulation output and increased grid density when compared with Finite Element Analysis.

The study was directed at welded joints which revealed that a carbon-depleted zone consisting of a ferrite rich, alloy impoverished zone that was susceptible to cracking after welding and which increased in size, with time. This methodology has been applied to the availability of oxygen from oxy-haemoglobin surrounded by blood serum and from oxygen enriched (relative to water) perfleurocarbon medium which can be used in certain types of in vitro experiment. This methodology enables a better understanding of the transfer mechanisms where rates of transfer are diffusion limited and permits simulation of experimental conditions over a range of oxygen or nutrient values including applicability to aqueous based medium.

CONCLUSION: By studying various decomposition models it was possible to derive a similar methodology for the decomposition front considered to be in the form of a moving wave front for oxygen concentrations in oxygen rich medium. It is proposed that the moving surface boundary methodology be adapted and used to model the decomposition of both perfleurocarbons at minimal velocity and to give better understanding of the transfer mechanisms occurring *in vivo* from red blood cells at full flow and restricted flow in or adjacent to capillary beds. This methodology may be extended to provide a basis for considering perfleurocarbons at velocities approaching in vivo conditions and, similarly hypoxic medium.

An equation first applied to modelling metallurgical events was revised to assist practitioners in developing reasoning for the dimension of the moving boundary dimension. This is a modified 'Fick' equation, being :

$$x^2 = \frac{C_c - C_d}{C_b} 2D_i t \qquad (1)$$

where reference is made to the solubility concentrations in various human or laboratory fluids. The chemical composition of the fluid/material determines diffusion before the diffused element reaches any interface. It may be concluded that a reaction coefficient depends on composition (available for diffusion), temperature, solubility and diffusivity but not on any type of dissimilar material combinations. Transport across areas may also be subject to dynamic cell morphology.

REFERENCES: [1] Kirk, C.S., and Mileham, A.R., (2001), Modelling Diffusion in Heterogeneous Transition Welds using e Finite Volume Method, EPSRC Research Report and Assessment, University of Bath, 2001.

LOW CALCIUM IS EXPANDING THE OSTEOPROGENITOR CELL FRACTION IN VITRO: ANOVEL PROCEDURE FOR BONE RERENERATION IN VIVO

H. Bahar[1] , R. Zohar , R. Shoshani , O. Sagi , E. Paschalis , A. Boskey , A. Yaffe[2] , & I. Binderman[1].

[1]*Department of Oral Biology, The Maurice and Gabriela Goldschleger School of Dental Medicine, Tel Aviv University, Tel Aviv, Israel.*

[2]*Department of Prosthodontics, Hebrew University Hadassah School of Dental Medicine, Jerusalem, Israel.*

INTRODUCTION: Tissue engineering of bone requires three essential elements, enrichment of the cellular components, growth and differentiation factors and a scaffolding matrix. The novel aspect of our studies include the use of periosteal cells as opposed to bone marrow, the reproducible and facile expansion of these cells, and the ability to characterize the mineral and matrix that is formed both in vitro and in vivo.

METHODS: We have previously described a two dimensional culture method [1] supporting the growth of osteogenic cells by using low Ca medium (0.25mM). The cells that were grown exhibited proliferateive capacity, responsiveness to mechanical stimulation and to PTH, positive stain for alkaline phosphatase and osteocalcin and matrix mineralization. A 10 fold increase in progenitor, small cell fraction [2] was isolated by flow cytometry (FACS), from subcultures grown in low calcium in comparison to subcultures grown in 1nM calcium. This cell fraction of progenitors were placed in DBM cylinders (demineralized rat femur cortical bone), and implanted in subcutaneous thoracic site of DA young rats [3].

RESULTS: New bone was formed after four weeks in vivo resembling membraneous bone. X-ray microradiography, histology and infrared spectroscopy (FITR) showed bone apposition characteristic to normal bone.

DISCUSSION & CONCLUSION: The results of these experiments propose a novel procedure for expansion of osteoprogenitors that form bone in vivo.

REFERENCES: [1]I. Binderman, E. Berger, N. Fine, Z. Shimshoni, A. Harell, D. Somjen (1989) *Connect Tissue Res* **20**:41-7. [2]R. Zohar, J. Sodek, C. McCulloch (1990) *Blood* **90**:3471-81. [3]EM. Nimni, S. Bernick, D. Ertl, SK. Nishimoto, W. Paule, BS. Strates, J. Villanueva (1988) *Clin Orthop Reia0ted Res* **234**:255-66.

European Cells and Materials Vol. 4. Suppl. 2, 2002 (pages 32-33) ISSN 1473-2262

SHALLOW TOPOGRAPHICAL NANOPATTERNS IN POLYMERS INFLUENCE THE MOTILITY OF MAMMALIAN CELLS

N. B. Larsen[1], N. Gadegaard[1], S. Mosler[1], D. Selmeczi[1], P. Kingshott[1], M. Riehle[2], A. Curtis[2], C. Wilkinson[2] & H. Griesser[3]

[1] *Danish Polymer Centre, Risø National Laboratory, 4000 Roskilde, Denmark*

[2] *Centre for Cell Engineering, IBLS, Glasgow University, Scotland, GB*

[3] *CSIRO Molecular Science, Clayton, Vic 3169, Australia*

INTRODUCTION: The viability of living cells cultured in vitro is known to depend strongly on their chemical environment. The past decade has seen an increasing number of reports describing the additional effect of surface topography on cell viability. Special attention has been given to the contact guidance phenomenon where elongated surface protrusions or depressions cause alignment of the cultured cells. Recently, the induction of more advanced cellular responses by surface nanotopography has been pursued, either targeting attachment or non-attachment of cells. In this work, we have generated square grids of nanometric trenches (30 to 60 nanometers deep) in a thermoplastic polymer and investigated the cellular response to such structural cues.

METHODS: A nanometric master structure possessing 100x100 ìm^2 patches of a square grid of 300 nm wide and 60 nm deep trenches separated by 700 nm in both lateral directions was fabricated by electron beam lithography in 60 nm thick ZEP 520A on silicon with an exposure electron dose of 144 ìC/cm^2.

The master structure was converted into a mould die presenting the inverted surface relief structure by initial coating of the master surface by a 100 nm thick Ni/V evaporated layer, followed by electroplating nickel on this electrically conductive film to a thickness of 300 ìm. The die was mounted in an injection moulding machine and poly(carbonate) (Makrolon DP1-1265) replicas were moulded using a total cycle time of 30s.

The polymer replicas were afterwards coated by an approximately 30 nm thick layer of plasma polymerised heptylamine providing a highly cell compatible surface chemistry. AFM of the e-beam lithography master structure and final coated polymer replicas showed that neither the replication process nor the coating process causes measurable loss of surface feature dimensions in the lateral or vertical directions.

Cells were cultured in CO_2-independent serum-supplemented medium and incubated in a temperature controlled on-stage chamber with a step motor-driven sample translocation device. MDCK (epithelial) or 3T3 (fibroblast) cells in calf-serum supplemented medium were seeded on coated polymer replicas. The processes of cell attachment, spreading and migration were tracked by phase-contrast time-lapse microscopy comparing topographically structured vs. non-structured areas.

RESULTS: The fabrication of plasma polymer coated poly(carbonate) replicas is highly reproducible and fast allowing for the manufacture of larger numbers of identical nanometric pattern often required for cell biological analysis.

A representative AFM micrograph of the resulting polymer replica nanostructure is displayed in Fig. 1.

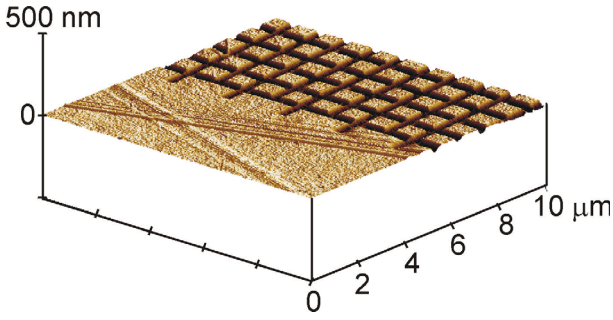

Fig. 1: Atomic Force Microscopy micrograph of a poly(carbonate) replica of the square grid of trenches present on the original.

3T3 cells, an immortal fibroblast line, displaying few extended outgrowths, were shown to rather remain at the edge than to intrude the groove pattern square (see fig. 2).

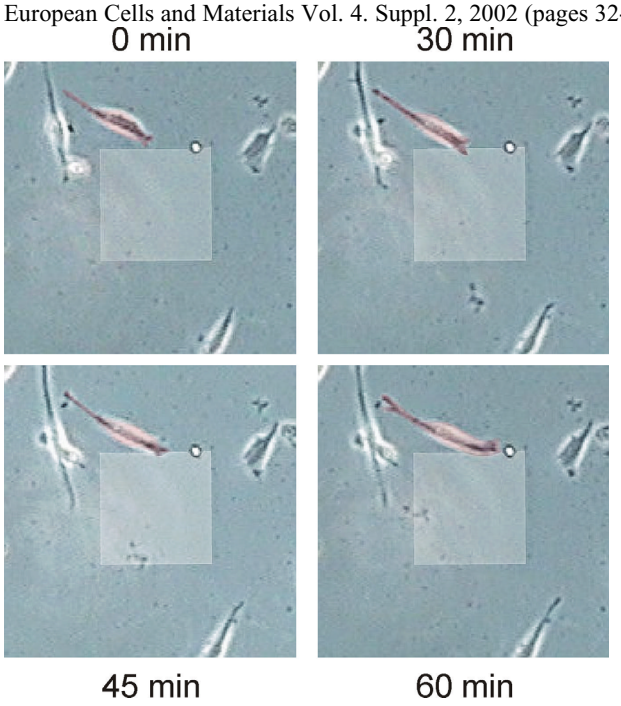

Fig. 2: A fibroblast 3T3 cell (red appearance in top centre of each picture) coming from the non-structured circumference reaches the edge of the nanostructured square (100 x 100 µm^2) in the centre of the image and remains at and aligns to this edge.

The tendency to remain at the edge of structured areas was quantified by averaging the persistence time of cellular outgrowth ends at the edge of structures in comparison to randomly selected control areas on the planar parts of the sample surface. Persistence was defined as an average outgrowth tip speed of less than 16 µm/h. These results are presented in fig. 3.

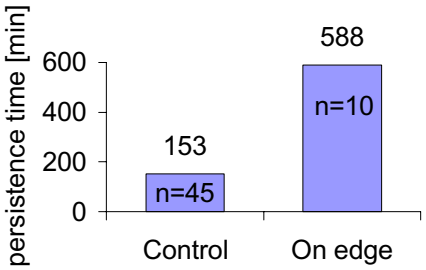

Fig. 3: Persistence time (in minutes) of 3T3 cell outgrowths on planar areas (control) and structure edges.

The adhesion of MDCK cells, an immortal kidney epithelial line, is mainly characterized by less pointed lamellapodi. Analogously to the behaviour of the 3T3 cells, the MDCK cells exhibited alignment of their cell boundary with the outer edge of the structured regions. Occasionally, they partially intruded the grooved square for short periods of time, but barely adhered to the interior areas of the squares.

DISCUSSION & CONCLUSIONS: Both the investigated cell lines clearly respond to the very shallow and narrow trench structures present in the chemically homogeneous polymer surface. However, it is unclear whether the observed effect is due to the presence of a continuous trench surrounding the structured square or due to the two-dimensional surface discontinuities inside the square. Occasionally, cells initially seeded inside the structured areas were observed to either show much delayed attachment or very quickly leave the structured square upon outgrowth contact with the surrounding planar surface regions. Supplementary nanostructure designs presenting a square trench structure exclusively will help to clarify this question. At this point we can conclude that fibroblast and MDCK cells are capable of recognising 60 nm deep and 300 nm wide trenches in a polymer surface resulting in significant changes in their motile behaviour.

REFERENCES: [1] A. Curtis and M. Riehle (2001) *Phys. Med. Bio.* **46**:R47-R65. [2] C.D.W. Wilkinson M. Riehle, M. Wood, et al (2002) *Mater. Sci. Eng. C* **19**:263-268.

ACKNOWLEDGEMENTS: N. B. Larsen gratefully acknowledges the financial support from the Danish Technical Research Council that made this work possible. N. B. Larsen and N. Gadegaard acknowledge additional support from the Danish Graduate School of Biophysics.

European Cells and Materials Vol. 4. Suppl. 2, 2002 (pages 111-112) ISSN 1473-2262

QUANTITATIVE ANALYSIS OF MATRIX REMODELLING IN A 3D COLLAGEN FIBROBLAST CONSTRUCT

N. Wilson Jones, M. Marenza & R. Brown

Tissue Repair and Engineering Centre (TREC), Royal National Orthopaedic Hospital, Stanmore

INTRODUCTION: A major unresolved question in engineering of collagenous tissues is how to control their remodeling to produce larger or smaller structures. We have used an in-vitro model of collagen contraction the culture force monitor (CFM) to study the problem. In this a fibroblast populated collagen lattice (FPCL) is attached to a sensitive strain gauge capable of recording forces generated by the cells in the lattice on a second to second basis. Collagen remodeling occurs as the cells bundle and pull fibrils to "contract" the lattice, but this has so far been a temporary cell dependant change. This can be shown by the complete loss of force with the addition of cytochalasin-D, a potent disruptor of the actin cytoskeleton and cell motor. It is assumed that any force remaining after the addition of cytochalasin-D is a result of permanent material shortening of the collagen fibrillar matrix due to 'remodeling' by the fibroblasts. Understanding of the process is poor and an effective model that can identify and quantify collagen remodeling would be key to further development of new controls for connective tissue engineering generally.

METHODS: Rat tendon fibroblasts were cultured from collagenase digested explant tissue. These were seeded at a density of one million cells per ml into a molded type I collagen lattice. The fibroblast populated collagen lattice (FPCL) floating in media with ascorbic acid, was then attached to the culture force monitor via integrated bars and steel wire 'A' frame connectors, (Fig.1) (1). The force produced within the FPCL was measured at second intervals and processed to give a graphical readout based on ten-minute time points.

The effects of incubation time on collagen remodeling was tested by addition of 20ìM Cytochalasin-D to the FPCL media at 4,12,18,24,48 hr time points and monitoring the force change.

Since a major role is suspected for new collagen synthesis, the effect of TGF-â1 on remodeling was tested by adding to the gel a concentration of 12.5çg/ml. 20ìM Cytochalasin-D was added at 4,12,18,24hrs.

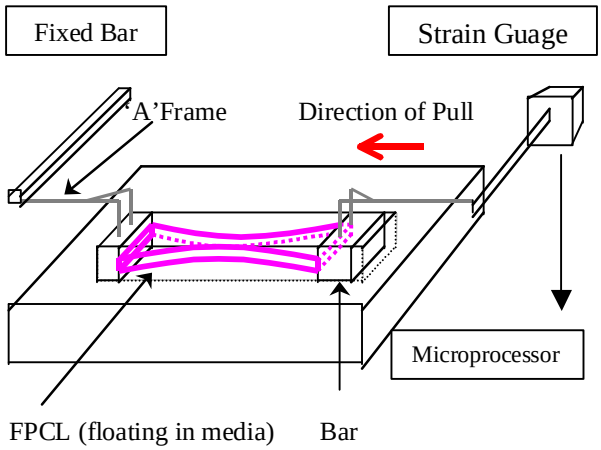

Fig.1: Diagrammatic representation of the culture force monitor (CFM), a fibroblast populated collagen lattice floating in media and attached to a sensitive strain gauge. (Note the waisting of the gel due to forces generated by the fibroblasts)

RESULTS: At four hours there was no evidence of any force being transferred from the cells to the shortened collagen matrix (i.e. total force loss with cytochalasin-D). However as early as 18hrs approximately 40% of the force was retained in the gel after addition of the cytochalasin-D and the 'remodeled force' continued to increase with increasing time to a maximum of 60% of the total at 24hrs.

TGF-ß1 not only increased the force of contraction generated by approxiamety 150%, but also led to a doubling of the total force 'trapped' into a shorter collagen matrix by remodeling (Fig.2).

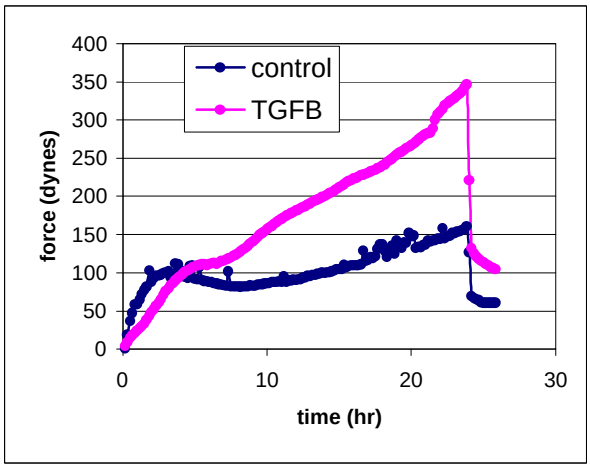

Fig.2: Graphical representation of force generated by cells in FPCl, control is without TGF-ß1. Note force maintained in the gel with TGF-ß1, 100% greater than without TGF-ß1.

DISCUSSION & CONCLUSIONS: We have shown that with this in-vitro model, collagen network 'permanent shortening' (remodeling) can be demonstrated and quantified. This can be demonstrated at time points as early as 18hrs and is enhanced by TGF-ß1. These observations begin to answer a major question in collagen function with broad implications for tissue engineering and tissue repair. This model should enable direct identification of the important control processes.

REFERENCES: (1) Eastwood M, McGrouther DA, Brown RA (1994), A culture force monitor for measurement of contraction generated in human dermal fibroblast cultures: evidence for cell-matrix mechanical signaling, *Biochimica et Biophysica Acta*; 1201 (2): 186-92

ACKNOWLEDGEMENTS:

Research supported by E.U. Framework 5, B.I.T.E.S. funding.

European Cells and Materials Vol. 4. Suppl. 2, 2002 (pages 5-6) ISSN 1473-2262

GENERATION OF HYPERTROPHIC CARTILAGE FOR BONE TISSUE ENGINEERING

BMJ Stringer[1,2], I Phillips[1,2], L Gangemi[1'2], M. Gosal[1], GA Foster[2,3]

[1] Centre for Biomaterials and Tissue Engineering, University of Sheffield, England, GB

[2]CellFactors plc, Cambridge, England, GB

[3]School of Biosciences, University of Cardiff, Wales, GB

INTRODUCTION: Hypertrophic cartilage plays a key role in programming bone formation. Through the process of endochondral ossification hypertrophic cartilage is converted to bone during development from foetus to adult. Moreover, it is the very same process that is recapitulated in fracture repair. Hypertrophic cartilage, therefore, contains the required mix of matrix proteins, cytokines, proteases, and growth factors necessary to orchestrate the formation of vascularised bone in vivo. The potent bone-forming activity of hypertrophic cartilage would likely make it the material of choice for bone tissue engineering, if it were freely available.

In view of the above, this study sought to determine the feasibility of generating human hypertrophic chondrocyte cell lines, capable of inducing osteogenesis, so as to provide a safe and abundant, efficacious alternative to bone allograft.

METHODS: A primary culture of human skeletal cells was prepared from therapeutically aborted foetal tissue of 8-9 weeks gestation. The primary culture was retrovirally-transduced with a temperature sensitive form of the simian virus-40 derived large-T antigen – an immortalising gene[1,2].

Once transduced, cells were cultured in selection medium and replicating colonies of cells isolated to produce homogeneous clones of immortal cells. Reverse transcriptase polymerase chain reaction studies were then performed on RNA isolated from individual colony samples so as to determine their expression of bone/cartilage specific markers. In addition, a bioassay was performed on cell matrix generated from the immortalised, clonal cell lines to determine their osteoinductive ability. The expression of osteocalcin, a late marker for osteoinduction, was also determined by immunoassay.

RESULTS One skeletal cell line in particular was shown to express Type X collagen as well as type I collagen, along with a number of known bone and vascular inductive factors.

In addition, incubation of the foetal cell line-derived matrix with marrow cells induced their formation of colony forming units-fibroblast (cfu-f), and elaboration of a mineralising extracellular matrix. A dose-dependent increase in osteocalcin expression by marrow cell cultures in response to the human cell matrix was also demonstrated.

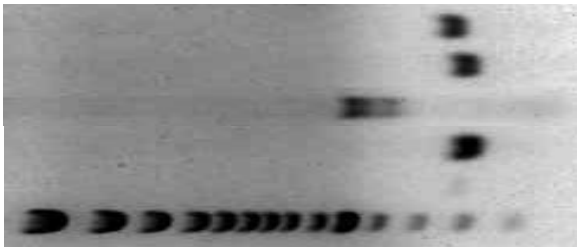

Fig. 1:From the bottom, 100kb DNA ladder (lane 1), water (lane 2), beta actin (lane 3), BMP-2 (lane 4), Type I collagen (lane 5) and type X collagen (lane6) in immortalized human hypertrophic chondrocyte cells.

DISCUSSION & CONCLUSIONS: Hypertrophic chondrocyte cell lines can be generated from human foetal tissue by immortalisation with a temperature sensitive viral oncogene. Furthermore, matrix derived from such human cell lines is capable of inducing marrow-derived osteoprogenitor cells to differentiate into cfu-f's which elaborate and mineralise an extracellular matrix. Therefore, cell matrix generated from human hypertrophic cartilage could potentially provide a safe and abundant, efficacious alternative to bone allograft for skeletal repair and regeneration.

REFERENCES: *[1]*Houghton A Oyajobi BO Foster GA Russell RGG and Stringer BMJ 1998 Immortalization of human marrow stromal cells by retroviral transduction with a temperature sensitive oncogene: identification of bipotential precursor cells capable of directed differentiation to either an osteoblast or adipocyte phenotype after oncogene inactivation *Bone* **22** 7-16. *[2]*Oyajobi BO Houghton A Hatton P Frazer A Graveley R Russell RGG and Stringer BMJ 1998 Expression of type X collagen

and matrix calcification in three-dimensional cultures of immortalized temperature-sensitive chondro-cytes derived from adult human. *J. Bone and Mineral Research* **13** 432-442.

European Cells and Materials Vol. 4. Suppl. 2, 2002 (pages 138-139) ISSN 1473-2262

DEVELOPMENT OF NOVEL SOLUBLE GLASSES FOR TISSUE ENGINEERING OF HARD TISSUE

M Bitar, I Ahmed, JC Knowles, V Salih, M Lewis

Eastman Dental Institute, University College London, UK

INTRODUCTION: Tissue engineering explores cell transplantation[1] using a variety of materials and matrices in order to regenerate fully functioning tissues. This study involves the *in vitro* seeding of bone cells onto a series of soluble phosphate based glasses. The physical properties of the glasses, such as solubility, are determined by their chemical composition, in particular the calcium content. The two main aims of this study are

Phenotypic identification of bone cells.

Identifying the most biocompatible range of glass compositions.

MATERIALS AND METHODS:

Cells: Primary cells were obtained from human alveolar bone explants[2]. MG-63, human osteogenic sarcoma derived[3], cell line was also used.

Glass for cell work: Various glass compositions were produced in the form of 1.5x13 mm discs based on the P_2O_5-CaO-Na_2O System[4]. With the amount of P_2O_5 fixed at 50 mol%, glasses of higher calcium proportion were less soluble when incubated in culture medium. Poly-L-lysine (Sigma) coated glass coverslips were also used as positive controls.

Immunocytochemistry: MG-63 cells were seeded onto the discs. In order to arrest extracellular matrix destined proteins within the cell boundary, cells were incubated in medium containing monensin (Sigma) for 24 h prior to fixing in ice-cold methanol at a 48 h. The primary antibodies used were bone sialoprotein, osteonectin and osteopontin (gift of Prof. L. Fisher). FITC-conjugated IgG were used as secondary antibodies (Stratech Scientific).

Cell adhesion and proliferation assays: Primary cells were seeded on discs placed in 24 opaque well plates, incubated at 37°C in 1 ml of medium per well. Adherent cells were later quantified using the CyQUANT® Cell Proliferation Assay kit at 1, 2, 3 and 7 days post seeding. Similarly, MG-63 cells were quantified after 3 h in culture.

RESULTS: Punctate staining for the glycoproteins osteonectin (Fig 1), osteopontin and bone sialoprotein (data not shown) was evident in the cytoplasm of cells cultured on both soluble glass discs and glass coverslips. Both primary and MG-63 cells adhered to (Fig 2) and survived when plated on phosphate based glasses. Early adhesion data, however, showed that cells have a clear preference to less soluble compositions (Fig 3).

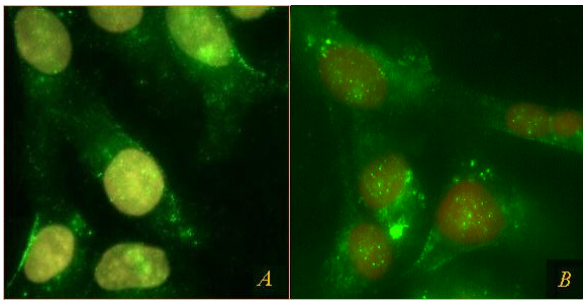

Figure 1. Leica® fluorescent microscope image of MG-63 cells cultured on A. glass coverslips and B. 40 mol% calcium containing glass showing positive staining for osteonectin.

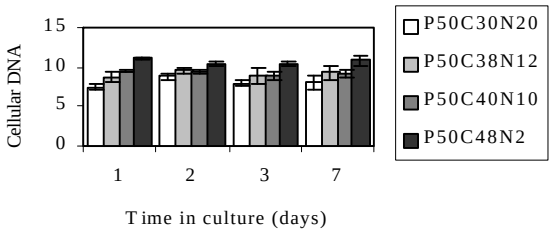

***Figure 2 P**rimary cells proliferation behavior on various compositions at different time points(error bars; ±SD).*

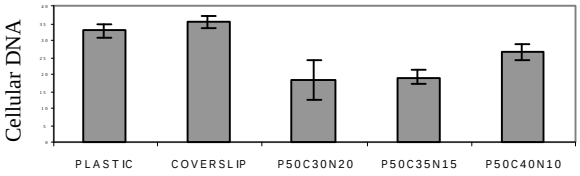

***Figure 3.** Graph showing MG-63 cells adhesion rates on various materials after 3 hours in culture (error bars; ±SD).*

DISCUSSION & CONCLUSIONS: Phosphate based biodegradable glasses support the adhesion and survival of primary and osteoblast-like cells. Whilst proliferation rates have shown no significant increase over time, less soluble glass compositions proved to accommodate higher numbers of

functioning cells. Phenotypic characteristics, of adherent cells, were also preserved on these glasses and observed as positive immunolabeling of several extracellular bone markers.

REFERENCES: [1] E. Alsberg et al (2001) *Crit Rev Oral Biol Med* **12**:64-75. [2] J. Clover, et al (1994) *Bone* **15**:585-591. [3]V.Salih, et al (2000) *J Mater Sci* **11**:615-620.[4]J. E. Gough et al (2002) *J Biomed Mater Res* 5;59(3):481-9.

ACKNOWLEDGEMENT LW Fisher, et al (1995) *Acta Orthop Scand* (Suppl 226) **66**:61-65.

HUMAN CRANIOFACIAL SKELETAL MUSCLE TISSUE ENGINEERING USING A SOLUBLE GLASS FIBRE SUBSTRATE

R. Shah, J.C. Knowles, N.P. Hunt & M.P. Lewis

Eastman Dental Institute, University College London, UK

INTRODUCTION: Craniofacial musculature can be absent or lost due to congenital defects, degenerative diseases, tumours and trauma. Muscle transfers are currently needed to rehabilitate the paralysed mouth, re-animate the eye and restore masticatory function. Autologous replacement of muscle is the prevalent therapy but this is severely limited by the availability of donor tissue (1). Tissue engineering is a realistic alternative and involves seeding cells from a donor source onto a biocompatible, degradable scaffold *in vitro* and either implanting this into the defect site or allowing the support material to degrade and implanting the resulting "organoid". Our work utilizes soluble phosphate based glasses, previously developed and manufactured at the EDI, as scaffolds for primary human craniofacial myoblasts.

METHODS: Soluble glass fibres were pulled using a custom-made fibre-pulling rig. The composition used in these experiments was P_2O_5 (62.9%), Al_2O_3 (21.9%), ZnO (15.2%). The fibres were pulled at 1500 rpm, had a diameter of 6.5 µm and a solubility of 0.16mg/g/day. Primary cells were derived from explants of the human craniofacial masseter muscle. These cultures contained myoblasts that could align and fuse to form multinucleate myotubes (prototypic muscle fibres). Cells were seeded onto glass fibres in standard growth medium (DMEM + 20% FCS) until they reached 100% density when the medium was changed to standard fusion medium (DMEM + 2% FCS). Progress of the cultures was followed by live time-lapse photography using a Leica DMIRB microscope attached to a Cohu CCD camera under software control. The cultures were contained within a controlled environment chamber (37°C, 5% CO2; Solent Scientific) and monitored every 30 minutes over a 24-hour period. Parallel cultures were fixed, fluorescently immunostained with antibodies against the muscle markers desmin and sarcomeric actin and visualized using the Leica microscope set-up.

RESULTS: Optimal adhesion of myoblasts was achieved when (i) fibres were arranged in a mesh where cells gathered at the crossover of fibres, (ii) fibres were pre-incubated in culture medium to allow some leaching of ions and (iii) fibres were coated with basement membrane Matrigel. Under normal conditions, there was little evidence of myotube formation but the addition of Insulin-like Growth Factor 1 (10ng/ml) stimulated myotube formation:

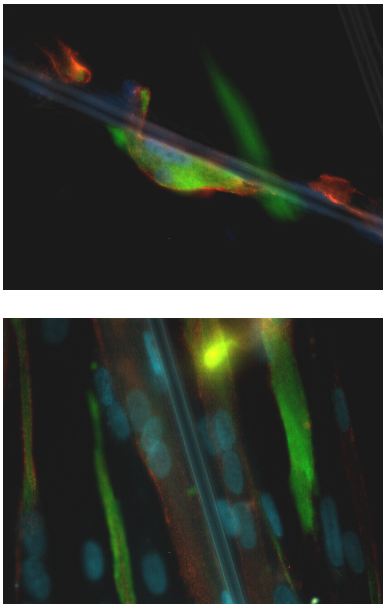

Fig. 1: Formation of myotubes (prototypic myofibres) on soluble glass fibres. Both panels are fluorescence immuncytochemical micrographs showing the muscle speicifc proteins desmin (green) and sarcomeric actin (red). Nuclei are revealed by the dye DAPI that fluoresces blue. The glass fibres will support myotube formation.

DISCUSSION & CONCLUSIONS: Few materials are available for the effective regeneration of skeletal muscle. Soluble glass fibres provide a system in which the solubility is highly controllable and that generates linear fibres of appropriate dimensions. This data showing that normal human craniofacial myoblasts can attach, grow and differentiate on these fibres in tissue culture is a highly encouraging first step in the use of these materials for engineering human skeletal muscle.

REFERENCES: (1) E. Alsberg, et al (2001) *Crit Rev Oral Biol Med* **12**:64-75.

European Cells and Materials Vol. 4. Suppl. 2, 2002 (page 15) ISSN 1473-2262

COMPUTER MODELLING AND EXPERIMENTAL VALIDATION OF SMOOTH MUSCLE CELL GROWTH USING MATRIGEL AS A BASEMENT MEMBRANE MATRIX

C.S.Kirk[1], T. Bodamyali[2], C.R.Stevens[3], & A.R.Mileham[4]

[1]*Depts. of Medical Sciences and Chemical Engineering, University of Bath, UK*

[2, 3]*Dept. of Medical Sciences, University of Bath, UK*

[4]*Dept. of Mechanical Engineering, University of Bath, UK*

OVERVIEW: In the assessment of activities which lead toward functional tissue engineering of arterial replacements, it is evident that a need exists for a support scaffold that is compliant and capable of nominal stretching and recovery. It should have lateral and transverse mechanical properties which would entertain the *in vivo* functionality of an artery under pulsatile flow in a range of internal pressure. Such scaffolds or matrixes are generally limited to polymers or porcine based cross-linked collagen. However, the prior mechanical and developmental history of the collagen and its associated tenacious structure resists ingress of the human smooth muscle cells delaying satisfactory growth and substitution of human collagen. This appears mainly to be due to the dense, aligned, matted structure, slow cell activity, and inadequate digestion of cross-linked porcine collagen.

In parallel work, the mechanical properties of cartilage replacements are being assessed using a gelatinous material (alginate), as a soft matrix support for chondrocyte cells to help them establish growth. In progression from this activity a computer model has been developed[1] and extended, which simulates the growth of human smooth muscle cells in such a gelatinous material but incorporating a surrounding connective tissue of a porcine collagen scaffold. The overall aim has been to simulate growth of an end product that includes a coating of endothelial cells to promote signalling and produce a non-thrombogenic surface. Therefore, another gel form, namely Matrigel, becomes a base for bonding agents or for direct seeding of mature endothelial cells. The computer modelling of the layers in this case was accomplished with a bespoke system using the finite volume method.

This paper reports on both the experimental validation, the methodology of the computational element and output of the simulation.

This has provided the basis for future work and provides basic data for a computer study of the mechanical properties of the Matrigel which may confer improved elasticity and resistance to pressure fluctuations of the type experienced in lower arteries. Overall it is considered that this may provide a suitable growth environment for slow growing smooth muscle cells permitting time for their division and excretion of collagen. In this way, their growth and mobility will be relatively unhindered by the cross-linked porcine collagen.

CONCLUSIONS: This work combines a range of advances in cell culture and computer modeling, providing a rapid growth potential of active cells whilst providing a suitable environment for slow growing smooth muscle cells protected by a clinically acceptable outer sheath of pre-formed collagen or polymer.

Anticipated platforms and focus groups for further research created by this experiment include optimisation of assembly of the gel-based core, development of such matrices for clinical use, procedures and optimisation of pre-preparation of cells, and assessment of functionality prior to transplant.

The model provides a basis for the assessment of the finite volume method and its applicability to computational biology and tissue engineered products.

REFERENCES: [1] Kirk, C.S., and Mileham, A.R., (2001), Modelling Diffusion in Heterogeneous Transition Welds using the Finite Volume Method, EPSRC Research Report and Assessment, University of Bath, 2001.

EFFECTS OF MICRO-AND NANOSCALE SUBSTRATE TOPOGRAPHIES ON THE BEHAVIOR OF HUMAN CORNEAL EPITHELIAL CELLS

A. I. Teixeira[1], G. A. Abrams[2], C. J. Murphy[2] & P. F. Nealey[1]

[1]*Dept of Chemical Engineering, University of Wisconsin-Madison, USA*

[2]*Dept of Surgical Sciences, School of Veterinary Medicine, University of Wisconsin-Madison, USA*

INTRODUCTION: Epithelial cells adhere to specialized extracellular matrices called basement membranes, composed mainly of type IV collagen, laminin and heparan sulfate proteoglycan, that provide physical support and present chemical cues to cells. The human corneal epithelial basement membrane was found to have a felt-like appearance with pores and fibers with lateral dimensions ranging from 22nm to 191nm[1]. We hypothesize that substrate topography of nanoscale dimensions, independently of chemistry, affects the behavior of human corneal epithelial cells. Many cell types align along anisotropic topographic features such as patterns of grooves and ridges, a phenomenon called contact guidance[2]. We analyzed the morphology and orientation of cells cultured on patterns of grooves and ridges with nanoscale dimensions and compared them with the cellular responses to micrometer sized grooves and ridges and to smooth substrates.

METHODS: A layer of UV3 photoresist (Shipley) was coated onto silicon wafers and patterned using electron-beam lithography. The resist patterns were transferred to the underlying silicon by reactive ion etching. The resist remaining after etching was removed and the wafers were coated with a layer of silicon oxide in a Low Pressure Chemical Vapor Deposition reactor. Each substrate consisted of an array of six 4mm^2 patterned fields, separated by smooth areas. The pattern dimensions within each field were uniform. The pitch of the features in the different fields ranged from 400nm to 4000nm in each substrate (pitches equal to 400nm, 800nm, 1200nm, 1600nm, 2000nm and 4000nm).

Human corneal epithelial cells were harvested from corneas donated by the Lions Eye Bank of Wisconsin. After reaching 80% confluence, the cells were suspended in SHEM medium supplemented or not with 10%(v/v) of Fetal Bovine Serum. Cells were plated at a density of 8,500 cells/cm^2 in 24 well plates containing the patterned silicon substrates, previously sterilized with 70% ethanol.

After a 12-hour incubation F-actin and the nuclei were stained with TRITC-phalloidin and DAPI, respectively. Images of the stained cells were obtained from an epifluorescence microscope and were analyzed using Metamorph™ software (Universal Imaging Corporation).

Cells prepared for electron microscopy observation were fixed in glutaraldehyde, post-fixed in osmium tetroxide, dehydrated in graded ethanols, immersed in hexamethyldsilazane and coated with platinum.

RESULTS: A sub-population of the human corneal epithelial cells cultured on substrates patterned with 70nm wide ridges on a 400nm pitch aligned along the direction of the topographic features. Aligned cells were elongated compared with cells cultured on the smooth substrates, which were mostly round. Cells on the patterned substrates that were not aligned were round and were frequently poorly spread. Cell elongation and alignment occurred on all patterns tested. The percentage of aligned cells was constant for pattern pitches ranging from 400nm to 2000nm, and was lower for 4000nm pitch features, on 600nm deep grooves. When the groove depth was decreased to 150nm, the percentage of aligned cells was constant for all pitches tested and was lower than on 600nm deep grooves for pitches from 400nm to 2000nm. Filopodia were able to adhere to both grooves and ridges. The topographic features frequently guided filopodial orientation. Lamellipodia bridged the grooves except at the cell edge along the patterns where lamellipodia often protruded into the grooves.

DISCUSSION & CONCLUSIONS: We have found that human corneal epithelial cells react to topographic features with dimensions similar to those found in the native basement membrane. Our findings may be important in the design of systems for cell culture, tissue engineering and the development of implantable prosthetics.

REFERENCES: [1]G.A. Abrams, S.S. Schaus, S.L. Goodman, P.F. Nealey and C.J. Murphy (2000) *Cornea* **19**:57-64. [2]R.G. Flemming, C.J. Murphy, G.A. Abrams, S.L. Goodman and P.F. Nealey (1999) *Biomaterials* **20**:573-588.

European Cells and Materials Vol. 4. Suppl. 2, 2002 (page 80) ISSN 1473-2262

STUDY OF BOVINE ARTICULAR CHONDROCYTES ON THIN FILM POLYCAPROLACTONE SURFACES

F. Angeli[1], A.C.J. Smith[1], S. Zairi[2], D. Uttamchandani[2] and P. Connolly[1]

[1] *Bioengineering Unit, University of Strathclyde, GB*

[2] *Electronics and Electrical Engineering Department, University of Strathclyde, GB*

INTRODUCTION: In tissue engineering significant progress has been made in the development of biodegradable polymer scaffolds for tissue culture (see [1] for review). Applications for tissue growth and replacement using donor or animal cells are under investigation for a range of tissue types including; cardiac cells, neural tissue, tendon, bone and cartilage. A number of factors are important in achieving successfully engineered tissue such as; polymer type, surface chemistry, oxygenation, nutrient delivery and expression of extracellular proteins. It has also been shown in the field of microchip-cell devices that microstructure is critical to growth and alignment of many cell types (see for example [2]).

The effect of local micro or nanostructure on tissue-engineered cultures has largely been neglected by the field in favour of porous or fibrous scaffold development. Some work on the effects of microstructure exists in this field for fibroblasts, endothelial and epithelial cells and macrophages [3-5]. Cartilage engineering is one aspect of tissue engineering that might benefit from a study of microstructure effects within scaffold materials. To fully study this in a scientific manner it will be necessary to develop micropatterns with controlled 2-D and 3-D structures for use in chondrocyte cultures. This study reports initial results which use an excimer laser system to introduce microstructures on poly-å-caprolactone (PCL), a biodegradable polymer, which has been used as a cartilage scaffold material.

METHODS: Uniform thin films of poly-å-caprolactone (PCL) were generated by spin-casting PCL (Birmingham Polymers, Inc.) in acetone solution onto 76mm*26mm glass slides.

An Excimer Laser (M2000-E, Exitech) was used to treat the PCL films and introduce local microstructures. The system incorporates a 100Hz laser, with a sample positioning accuracy ~1um, sample motions of up to 100mm/sec and maximum fluence levels of ~50J/cm^2.

Bovine cartilage cells were obtained from metatarsophalangeal joint and seeded on the PCL films (pre-sterilised with 70% ethanol) and on 60mm*15mm tissue culture plate (TCP)(Falcon) and tested for a range of cell densities.

RESULTS: Cartilage cells seeded on TCP showed differing behaviours according to cell seeding densities. Cells at lower densities de-differentiated to fibroblasts within several days, as shown in Figure 1. The behaviour of cells on PCL under similar culture conditions will be discussed.

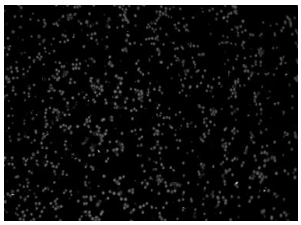

*Fig. 1: Cartilage cells seeded on TCP at a cell density of 5*10^{6}cells/ml. Normal chondrocytes (left) after 24hrs culture and normal and de-differentiated chondrocytes (right) after 7days culture.*

REFERENCES: [1] D.W. Hutmatcher (2000) Biomaterials **21**:2529-2543, [2] P.X. Ma and R. Zhang (2001) J Biomed Mater Res **56**:469-477; [3] P. Clark et al (1991) J Cell Science **99**: 73-77; [4] B. Wojciak- Stothard et al (1996) Exp Cell Res **223**:426-435; [5] A. Curtis and C. Wilkinson (2001) TRENDS in Biotechnology **19(3)**:97-101

European Cells and Materials Vol. 4. Suppl. 2, 2002 (pages 26-27) ISSN 1473-2262

POLYMER TEMPLATES MIMICKING FIBRILAR COLLAGEN

N.Gadegaard[1, 2], S.Mosler[1], N.B.Larsen[1], A. Curtis[2], M.Riehle[2], & C.Wilkinson[2]

[1] *Danish Polymer Centre, Risø National Laboratory, 4000 Roskilde, Denmark*

[2] *Centre for Cell Engineering, IBLS, Glasgow University, Scotland, U.K.*

INTRODUCTION: An important cell biological issue is to understand the relative importance of surface topography and surface chemistry. It has previously been reported that cells may respond to topographies as small as 10 nm [1]. Most of the work presented in literature is based on artificial geometries such as grooves and ridges. Nature makes extensive use of nanometric structural elements. An attempt to mimic the natural environment cells are embedded in was reported by Goodman et al. [2]. They prepared a template from a blood vessel where the cells had been removed only exposing the topography of the extra cellular matrix. From the template it was possible to make a single polymeric replica by casting. The extra cellular matrix consists mainly of fibrillar collagen. Most replicas made for biological testing have been prepared by either casting or embossing. Both methods are relatively time consuming and high numbers are difficult to obtain. Here we present a rapid method of replicating the surface topography of fibrillar collagen networks in polymer substrates. This gives the opportunity to investigate the importance of topography and chemistry independently. Elements of the fibrillar collagen nano topography have been mimicked by use of electron beam lithography.

METHODS: Fibrillar collagen networks were self-assembled from purified bovine dermis extracts. After self-assembly the networks were deposited on silicon substrates and sputter coated with a thin metallic film. This acted as an electrode in the subsequent electroplating process where nickel was electrochemically deposited to a thickness of 300 µm. The resulting nickel die was mounted in an Engel 25 ton injection moulding machine where numerous replicas were fabricated in different commercially available polymers, e.g. poly(carbonate), poly(propylene), poly(methyl methacrylate), poly(L-lactide), and poly(å-caprolactone). A diagram of the process is illustrated in Figure 1. For a more detailed description of the fabrication process see reference [3].

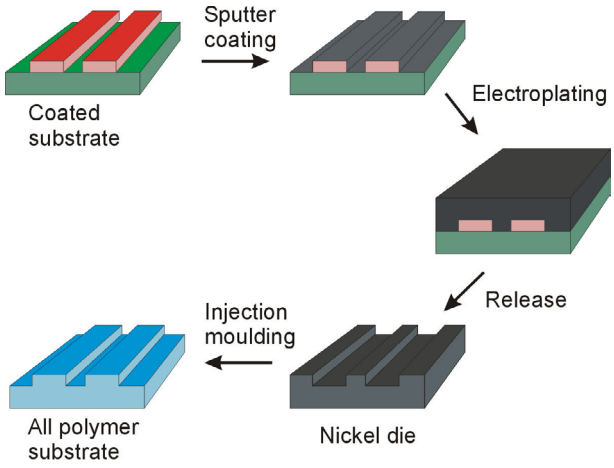

Figure 1. Schematic of the fabrication method from biological template to injection moulded polymeric replica.

RESULTS: Fibrillar collagen possesses a unique nano topography. As the collagen molecules self-assemble in the extra cellular space they are staggered in a way which results in fibrils with a cross-striation. The periodicity of the cross-striation is ca. 68 nm with an amplitude of 3-5 nm. The unique surface topography is readily observed by atomic force microscopy (AFM), Figure 2A. Using injection moulding the surface topography of the fibre networks was successfully transferred to a range of different thermoplastic polymers. An AFM topography image of a replica in poly(carbonate) is illustrated in Figure 2B. Direct comparison of a specific site between the original and the replica was not possible due to the complex structure of the fibrillar networks. The distinct cross-striation is readily transferred. Both periodicity and amplitude are similar to the original structure. Inserts in Figure 2 illustrates supramolecular collagen residues which are also faithfully transferred to the polymeric replica. The residues have a width of ca. 15 nm and a height of mere 2 nm.

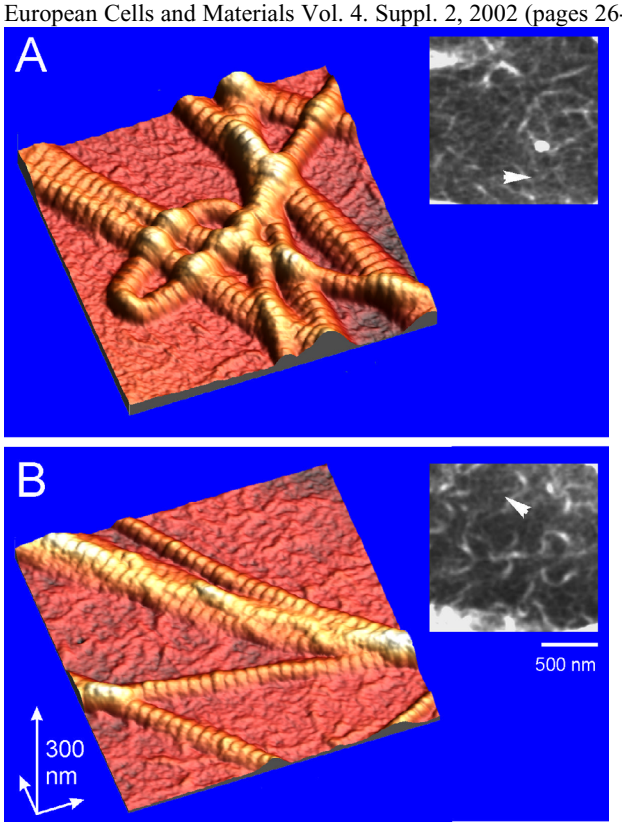

Figure 2. AFM topography images of (A) fibrillar collagen coated silicon substrate and (B) corresponding replica in poly(carbonate). Inserts illustrates supramolecular collagen residues. The colour range from black to white corresponds to 10 nm.

It was attempted to mimic the characteristics of fibrillar collagen by means of electron beam lithography (EBL). Two sub-microscopic features are characteristic of the fibrils. One is the 68 nm cross-striation and the other is the fibre width, which typically is 250-500 nm. The AFM micrograph in Figure 3 illustrates the result of the EBL. The "fibres" having a width of 300 nm were arranged in an orthogonal geometry with a repeat spacing of 1 ìm. The mesh was designed in such a manner that the fibres appeared to be interwoven.

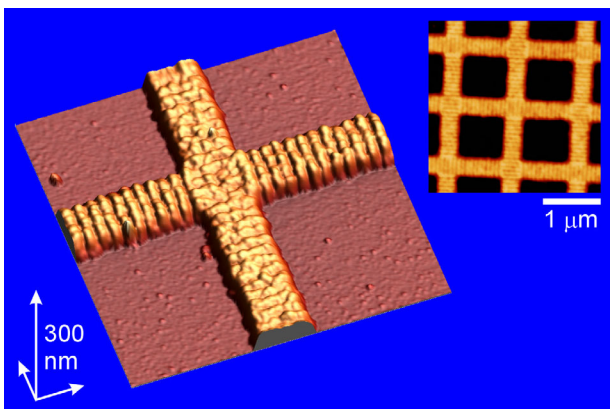

Figure 3. AFM topography image of an electron beam fabricated template mimicking the topography of fibrillar collagen. Insert illustrates orthogonal arrangement of interwoven "fibres".

DISCUSSION & CONCLUSIONS: We have demonstrated that injection moulding can be used to fabricate substrates possessing a high resolution at a high throughput. The resolution of the process is thought to be 10 nm or better in the lateral direction and better than 1 nm in the vertical direction. This is based on the evidence of faithful replication of supramolecular residues and cross-striation characteristics. A range of commercially available thermoplastic polymers have proven to be successful materials, including biodegradable polymers.

We are currently investigating the biological response to the replicas described. It is speculated that the fibrous arrangement of collagen has an effect on cell behaviour. It has been reported that fibroblasts cultured on fibrillar or monomeric collagen coated substrates exhibit different morphology and arrangement of cytoskeletal components [4]. The replicas provide a unique opportunity to investigate the importance of topography.

REFERENCES: [1] A. Curtis and M. Riehle (2001) *Physics in Medicine and Biology* **46**(4): R47-65. [2] S.L. Goodman, P.A. Sims, and R.M. Albrecht (1996) *Biomaterials*, **17**:2087-95. [3] N. Gadegaard (2002) *Injection Moulded Nanostructures and Modified Surface Topographies*, Ph.D. Thesis Danish Polymer Centre. [4] I. Mercier, J.-P. Lechaire, A. Desmouliere, F. Gaill, and M. Aumailley (1996), *Experimental Cell Research*, **225**:245-56.

ACKNOWLEDGEMENTS: N.G. gratefully acknowledges financial support from University of Copenhagen, Risø National Laboratory, and the Danish Research Academy.

European Cells and Materials Vol. 4. Suppl. 2, 2002 (pages 113-114) ISSN 1473-2262

IgG DIFFUSION THROUGH BIOENGINEERED MATERIALS FOR PERIPHERAL NERVE REGENERATION

M. Giacomini[a], S. Bertone[b], F. Caneva Soumetz[a], I. Peragallo[a,b], R. Brown[c] and C. Ruggiero[a]

[a]*Dip. Of Informatics System and Telematics – University of Genova – Via Opera Pia, 13, 16145 Genova Italy (*Mauro.Giacomini@unige.it*)*

[b]*R.I.L.A.B. s.r.l. – Via Guerrazzi 24 – 16146 Genova Italy*

[c]*University College, London*

INTRODUCTION: In successful nerve regeneration, sprouting axons from the proximal nerve stump traverse the injury site, and make new connections with target organs. Axons that fail to reach an appropriate end organ or fail to make a functional synapse will eventually undergo Wallerian degeneration. However, the incidence of recovery is highly variable, and the return of function is never complete. The use of synthetic nerve guidance channels show promises in improving the repair of injured human nerves, and the release of soluble bioactive agents like cytokines, may improve the degree and specificity of neural outgrowth [1]. The fibronectin (FN) guidance material has been already shown to promote axonal growth of sensory and other axons in rat spinal injuries in a way and to an extent not seen with any other non-graft implant to date. Ingrowth of new nerve tissue was dramatic in speed and content [2]. Also hyaluronan (HA) derivative HYAFF-11 (benzyl ester of Hyaluronic Acid) has been tested to be used for the bioartificial nerve guidance first of all because of its well documented biocompatibility and biodegradability and secondly because its particular physical-chemical properties make it processable in various three dimensional forms.

Considering the role of the cytokine TGF-β1 in scar formation and the potentially obtainable improved results in the repair of central and peripheral nervous system injuries with local delivery of neutralising antibody to the pro-fibrotic growth factor TGF-β1, this study focuses mainly on the development of a new mathematical model to predict the diffusion of human antibody anti-TGF-β1 through bioengineered membranes. In order to identify the model parameters, laboratory experiments have been set up, characterising the uptake and release of anti-TGF-β1 to and from FN and HA synthetic nerve guidance channels.

METHODS: Different types of experiments were carried out with a standardised commercial fluorescently labelled human IgG preparation, since anti-TGF-β1 itself is structurally no different from IgG. The tracing of the distribution of labelled IgG through the biomaterial was performed by spectrofluorimetry.

The first kind of experiments were carried out using FN biomaterial as nerve guidance channels of specific dimensions with an empty core space. The FN tubes were filled with a FITC labelled IgG physiologic solution. Different IgG concentrations were used, namely 1 μg/ml in one set of experiments and 10 μg/ml in another set. The two different concentrations were chosen as a compromise between the natural concentration of TGF-β in human tissue and the spectrometer sensitiveness. Sampling was performed at different times, pipetting 100 μl and detecting the IgG concentration by Luminescence Spectrometer.

For the second type of experiments, FN tubes with a FN core were suspended in physiologic solution (PS) in the middle of the diffusion chamber, before having been soaked overnight in a concentrated FITC labelled-IgG solution (50 μg/ml) prepared in PS. FN tube sampling was performed at 48, 72 and 144 h and after sampling the FN tubes were cut in 1 mm thick slices and fixed in paraformaldeid (PFA) in which they were stored until the Luminesence Spectrometer detection.

In the last set of experiments the following dry materials were used: (a) HA sheet, (b) holed (90 to 50 μm diameter) HA sheet, (c) HA tubes + FN, and (d) holed HA tubes + FN cores.

They were previously cut into small pieces and then soaked with the labeled IgG (4 μ/ml) PBS solution, for 90 hours at room temperature. After soaking, they were transferred in PBS to monitor over time (2 weeks) the Ab release.

In all experiments, diffusion was performed at room temperature.

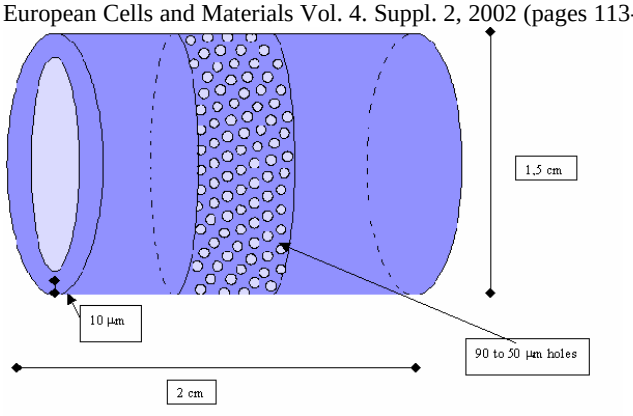

Fig. 1: Scheme of holed HA tube.

RESULTS: In the first set of experiments, results showed that after 3 days, about 15 µg of fluorescent IgG were detectable inside the FN tube, starting from a total of 30 µg, while only 3 µg were detectable outside the tube in the PS surroundings: about 12 µg were missing.
In the second type of experiments the FN tubes reached the maximum of IgG saturation in 72 h. The diffusion rate was very low, reaching in 144 h a maximum of 3.4 % of diffusion.
In the third type of experiments the materials (a) and (b) did not adsorb the Ab, while materials (c), but above all (d) adsorbed the Ab.

DISCUSSION & CONCLUSIONS: The above experimental results, also preliminary, showed that the IgG could be trapped in the FN material for at least the first six days after the implant. According to this, it could be worthwhile to consider the possibility that FN material could be a good Ab depot for long term antibody therapy. In fact, the IgG should stay in the FN material at least 2-4 weeks to get the anti-fibrosis effect during the nerve repair process. The diffusion rate of the first days is critical to the advantage of using therapeutic drugs within the material, in order to retain and release it gradually in vivo.

Based on the promising results obtained, the possible aims for the future could be to improve the detectability of the labelled IgG even at lower concentration in order to mimic as close as possible the natural conditions; and to confirm in longer time experiments, the low diffusion of the human anti-TGF-β1, instead of a general IgG, through FN tubes. The use of the human anti-TGF-β1 itself will be crucial, in order to not have cross-reactions of the antibody with FN or other materials. Moreover, the more quantitative, direct measures within this experimental framework by using the human anti-TGF-β1 antibody will be important to determine its diffusion coefficient (D). This parameter will allow the mathematical model to give a first level estimation of the retention time of the antibody in the interested bioengineered material.

When all parameters are determined, the modelling environment will allow the surgeons who intend to treat regenerating nerves with such type of antibodies to have reliable estimations of treatment times even for in vivo conditions which can be hardly reproduced in an experimental set up.

Finally, the present results seem to be very promising in regards of the possibility to include several therapeutic factors inside the FN guidance channels in the nerve repair process. In fact, other cytokines have specific roles in nerve regeneration: nerve growth factor (NGF) and fibroblast growth factor (β-FGF) control sensory neuronal survival and out-growth, whereas brain-derived growth factor (BDGF) and ciliary neurotrophic factor (CNTF) control motor neuronal survival and out-growth, and interleukin-1 (IL-1) promotes detersion by scavenger macrophages and increased synthesis of neurotrophic factors [3].

REFERENCES: [1] T. Yamamoto, S. Takagawa, I. Katayama, and E. Nishioka (1999) *Clinical Immunology* **92**:6-13. [2] A.S.G. Curtis, C. D. Wilkinson, and B. Wojciak-Stothard (1995) *Journal of Cellular Engineering* **1**:35-38. [3] A. Creange, J.P. Lefaucheur, F.J. Authier, and R.K. Gherardi (1998) *Revue Neurologique* **154**:208-216.

ACKNOWLEDGEMENTS: The present study is supported by the European Union within the project "Tissue engineered nerve repair devices: development of European medical implantable devices and research training focus" (contract number: QLK3-CT-1999-00625).

European Cells and Materials Vol. 4. Suppl. 2, 2002 (pages 115-117) ISSN 1473-2262

THE EFFECT OF DLVO, HYDROPHILIC AND HYDROPHOBIC ENERGIES ON THE AGGREGATION OF CELLS IN SOLUTION

C. Ruggiero[1], M. Mantelli[1] & A.Curtis[2]

[1]*Department of Informatics, Systems and Telematics University of Genoa, 16145 Genova Italy.*

[2]***Centre for Cell Engineering*** *Glasgow University Scotland GB*

INTRODUCTION: Cell adhesion is critical for the assembly of cells into tissues and in the maintenance of tissue integrity. Cell adhesion mechanisms play a key role in cell organization into specific 3-D patterns, forming 3-D structures.
Cell behavior in suspension may be described using the DLVO theory of colloidal stability[1].

Although DLVO theory was originally developed in order to predict the adhesion behavior between non biological lyophobic particles, this theory has been applied to describe adhesion in a wide range of applications, such as biomaterials implants and stability of bacteria in suspension
According to DLVO theory, the interaction energy between two cells is described by the sum of the attractive London-van der Waals energy and of the repulsive electrostatic interaction energy. More recently, the presence of the hydrophilic energy, an extra short range repulsive force, which prevents adhesive contact, has been observed. It was tentatively ascribed to hydration effects at the hydrophilic surface [2]. Specifically, this force has been observed in case of lecithin multi-bilayers, in case of surfactant coated mica surfaces and between mica surfaces in aqueous solution of K+ and Na+. Moreover the presence of another attractive force has been observed[3] in the case of interactions between hydrophobic charged surfaces. This hydrophobic energy is stronger than the van der Waals energy at distances less than 10nm and decays exponentially with the distance.

The work described here focuses on the interaction energy of a system formed by two cells immersed in a medium, taking into account both DLVO energies and hydrophobic energy and hydrophilic energy, and shows how the presence of an energy barrier affects the coagulation rate, which represents the ratio between the dimer concentration and the first derivative of the monomer concentration. This value decreases as a function of the peak value of the curve representing the total energy between two cells.

METHODS: Each cell is represented as a sphere. Although this assumption precludes any evaluation of possible anisotropic effects in the coagulation process, it has been shown that quantitative accuracy of more complex models is retained to a good extent with this assumption, and importantly this allows a significant reduction of the computational complexity.

The electrostatic energy is

$$V_{dl}^{ss} = \frac{ea\,y_0^2}{2}\left[\ln(1+\exp(-kd))\right]$$

where a is the radius of the sphere, ψ_0 is the surface potential of the cell, ε is the dielectric constant of the suspending medium, κ is the reciprocal of the Debye length and d is the shortest distance between the spheres.

The van der Waals energy is

$$V_{vw} = -\frac{A_{121}}{6}\left(\frac{2R^2}{d^2+4Rd} + \frac{2R^2}{d^2+4Rd+4R^2} + \ln\left(\frac{d^2+4Rd}{d^2+4Rd+4R^2}\right)\right)$$

where R is the radius of the spheres, d is the distance between the spheres and A_{121} is the Hamaker constant

The hydrophilic interaction energy between two spheres is

$$V_{hy} = \frac{R}{2}\left(C_1 D_1 e^{-\frac{d}{D_1}} + C_2 D_2 e^{-\frac{d}{D_2}}\right)$$

where R is the radius of the spheres, C_1 and C_2 are the pre-exponential parameter, d is the distance between the spheres and D_1 and D_2 are the decay lengths.

The hydrophobic interaction energy between two spheres is

$$V_{hyp} = -C\frac{R}{2}e^{-\frac{d}{D_0}}$$

where R is the radius of the spheres, C is the pre-exponential parameter, d is the distance between the spheres and D_0 is the decay length.

The coagulation rate in presence of a potential barrier k_s is [4]

$$k_s = \frac{k_r}{W}$$

where k_r is the coagulation rate in absence of a potential barrier and W is a numerical value which can be

approximated as follows

where R is the radius of the cell, k is the Boltzmann constant, T is the temperature, V_{max} is the maximum value of the energy $V = V_{dl} + V_{vw} + V_{hy} + V_{hyp}$ and p is

where k is the Boltzmann constant, T is the temperature, $\partial^2 V / \partial r^2$ is the maximum value of the second derivative of the energy curve with respect to the cell-cell distance.

RESULTS: The interaction energy described above has been calculated considering two cells in a medium. In figure 1 DLVO energies and hydrophilic energy are taken into account for four different set of values of the Hamaker constant (continuous line). These values are taken from the literature and represent a significant range of possible values. Also the second derivative of the energy curves is represented, dotted line, since its maximum is used to calculate the value of p

*Fig 1: total energy between two cells, continuous line, and second derivative, dotted line. Surface potential is –25mV, Hamaker constant is, from bottom to top, 10^{-21}J, $5*10^{-22}$J, $5*10^{-22}$J e $5*10^{-23}$J, C_1=5mJ*m^{-2} C_2=0.132mJ*m^{-2}, D_1=0.5nm D_2=3nm.*

From the plot shown in figure 1, we obtain at 300K the following values for p: 19,03nm^{-1}, 18,05nm^{-1}, 14,74nm^{-1} and 12,53 nm^{-1} which leads to corresponding values for W of 4624.36, 1460.51, 46.09, 14.01.

In figure 2 the case in which DLVO and hydrophobic energies are taken into account is compared to the case in which only DLVO energies are present. It may be observed that the presence of hydrophobic energy decreases the peak value of the energy barrier and increases the coagulation rate. Specifically in this case when only DLVO energies are considered W is about 400, when the hydrophobic energy is also considered W is about 3

*Fig 2: Interaction energy between two cells when only DLVO energies are considered, dotted line, and when DLVO and hydrophobic energy are taken into account, continuous line, with a surface potential of -25mV, Hamaker constant = 10^{-21}J, C=3mJ*m, D_0=1.5nm*

DISCUSSION & CONCLUSION: The influence of the total energy on the dynamic of the aggregation process between two cells has been represented following a quantitative mathematical approach. The tool presented in this work may be uses to represent a wide range of experimental situations, by varying the key parameters taken into account such as Hamaker constant, the Debye length, the surface potential, the temperature, the concentration of the ions in the solution, the pre-exponential parameter and the decay length.

The simulations clearly demonstrates that relationship between the presence and the value of the peak value of the potential barrier in the energy curve and the decrease of the coagulation rate

REFERENCES: [1]B. V. Derjaguin and L. D. Landau, (1941) *Acta Physicochim.*, **14**:633-662. [2]Pashley, R M (1981): *Journal of Colloid Interface Science* **80**:153-162. [3]R. M. Pashley, P. M. McGuiggan, B. W. Ninham and D. F. Evans (1985), *Science* **229**:1088-1089 1985 [4]Evans D.F. and Wennerstrom H. (1994) "*The Colloidal Domain, where Physics, Chemistry, Biology and Technology meet*" VCH publ. Inc., New York.

ACKNOWLEDGMENT: The present paper has been supported by the European Union. Contract numbers: QLK3-CT-1999-00599 and G5RD-CT-2001-00594.

European Cells and Materials Vol. 4. Suppl. 2, 2002 (page 103) ISSN 1473-2262

THE INFLUENCE OF OPSONINS ON CELLULAR REACTION TO POLYETHYLENE WEAR PARTICLES

A. Elfick[1], M.Birch[1], S. Green[2] & A. McCaskie[1]

[1] *Dept. of Trauma & Orthopaedics, University of Newcastle-upon-Tyne, UK*

[2] *Centre for Biomedical Engineering, University of Durham, UK*

INTRODUCTION: Joint replacement has become the most successful of orthopaedic interventions. In the order of 60,000 lower limb joints are replaced each year in the UK. For about 10% of these patients they can expect to experience failure of the joint within 10 years. The principal cause of joint failure is bone resorption; aseptic osteolysis. Osteolysis occurs when the body reacts to the wear debris released from the artificial joint. The process of osteolysis is poorly understood especially with regard to the role of biomolecular mediators of cell response.

The aim of this research is to discern the influence of protein adsorption in the severity of the cellular reaction to a model UHMWPE wear debris.

METHODS: Polyethylene powder (ceridust 3615, median diameter 0.56ìm) was exposed to PBS solutions of proteins; foetal calf serum (FCS), bovine serum albumin (BSA) and bovine immunoglobulin ã (IgG). The development of the adsorbed protein layer was assessed through consideration of the zeta potential (ζ). A Malvern Zetasizer 3000HS was used to measure the electrophoretic mobility with conversion to zeta potential using Smoluchowski's approximation. ζ was recorded immediately on supplementation of a suspension of ceridust in PBS (without divalent cations) with increasing amounts of protein.

Primary rat osteoblasts were challenged with ceridust in a closed system, inverted-culture experiment. Three cell treatments were conducted; ceridust suspended in 25mM HEPES buffered MEM supplemented with either 10%FCS, 2.5%BSA or 1%IgG. Further, four treatment severities were explored; 0, 20, 100 & 200 particles/cell. The cellular reaction was quantified by consideration of cytoskeletal re-organisation using immunofluorescence imaging of actin & vinculin structures.

RESULTS: Figure 1 shows the variation in ζ with varying protein concentration. The FCS sample followed a similar trend to the BSA (not shown). The ζ remained negative for the BSA and FCS samples, whilst IgG become positive at low concentrations.

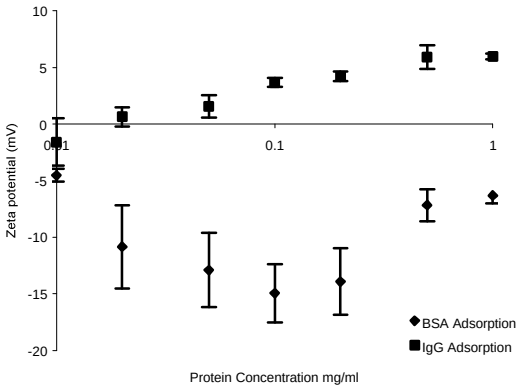

Fig. 1: Variation of ζ with protein concentration.

Preliminary results of the cell culture experiments indicate a normal morphology for these osteoblast-like cells in control samples. Increasing particle loads were seen to compromise cell vitality with this effect being considerably less pronounced in the IgG study.

DISCUSSION & CONCLUSIONS: The kinetics of protein adsorption have been widely studied but the influence of adsorption on the cellular uptake of wear debris has received little attention. The zeta potential studies presented show that particles attain differing adsorbed monolayers. The cytoskeletal studies showed that this, in turn, could modulate the behaviour of the cell. Furthermore, it is noteworthy that the particles possessing a positive surface charge elicit a differing severity of cellular reaction than those with a negative charge. This may suggest that an ionic interaction may be present.

FURTHER WORK The severity of the cellular response will be studied using enzyme linked immunosorbent assay (ELISA). Also, AFM will be using to study the changes in stiffness of the cell in relation to the cytoskeletal modifications.

ACKNOWLEDGEMENTS: This work was funded through an EPSRC Post-doctoral Mobility Award.

European Cells and Materials Vol. 4. Suppl. 2, 2002 (pages 81-82) ISSN 1473-2262

THE ROLE OF PROTEINS IN MODULATING CELL BEHAVIOUR ON MICROPATTERNED SURFACES

R.Barbucci, A.Magnani, S.Lamponi, D.Pasqui

Department of Chemical and Biosystem Science and Technologies and C.R.I.S.M.A., University of Siena, Via A.Moro, 53100 Siena, Italy

Introduction: As certain proteins are able to control specific cell activities such as cell adhesion and proliferation, the pre-adsorption or the binding of specific proteins on to a surface can increase the surface ability to modulate cell behaviour in order to have a pattern of organised cells able to work as a real tissue. The main question that remains is whether such specific proteins can affect cell adhesion and in which way [1].

Methods: In order to verify the influence of physiological protein on modulating cell adhesion on micropatterned surfaces, mouse fibroblasts (3T3 line) were seeded on Hyaluronan (Hyal) micropatterned surfaces with stripes 25μm wide and about 200nm high in the presence or not of Fetal Calf Serum (FCS) in the medium. The cell response as well as the number of adhered cells were evaluated after 2, 4 6, 12 and 24 hours of culture by an optical microscope. In order to determinate the amount of total adsorbed proteins on the tested different domains (silanised glass and Hyal) of the microstructures surfaces, a photoimmobilised Hyal surface, a silanised glass coverslip and a native glass one were immersed in a FCS solution for 24 hours at 37°C and the amount of adsorbed proteins was evaluated by a colorimetric assay. The type of the adsorbed protein on the different substrate were determined by electroforesys.

The influence of specific adhesive proteins such as fibrinogen (Fbg) or fibronectin (Fn) has been studied by binding them to polysaccharide immobilised substrates and analysing the cell behaviour in comparison to that observed on the materials without the protein. On the basis of these results the influence of such specific adhesive proteins in modulating cell behaviour on the micropatterned surfaces is then studied, by adding them to the cell culture. Moreover, in order to understand how these proteins are able to affect cell behaviour, ATR/FT-IR and AFM analysis are performed with particular attention to the protein conformation and distribution on the different domains.

Results: The presence of FCS in the medium plays a key role in modulating cell behaviour. In fact in the presence of FCS, fibroblasts can line up along the microstripes maintaining the alignment for several days [2,3]. On the contrary, without FCS

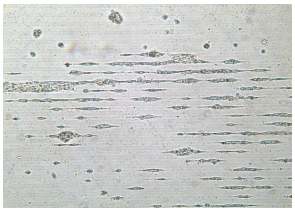

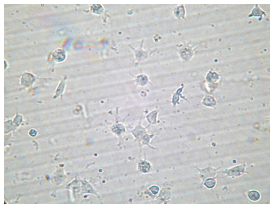

the cell adhere and distribute randomly on the surface and after 6 hours they begin to suffer. The behaviour is showed in Fig 1.

a) b)

Fig1: a) 3T3 alignment along glass-Sil/Hyal microfeatures in the presence of FCS; b) 3T3 random distribution in the absence of FCS.

The amount of the total FCS adsorbed proteins on to the different substrates is reported in the table below.

Table 1: μg adsorbed protein.

Native glass	Silanised glass	Hyal
0.8μg/mm^2	1.1μg/mm^2	0.6μg/mm^2

The binding of Fbg on a Hyal or its sulphated derivative (HyalS) surface has induced an increase of the number of adhered cells, making the polysaccharides a more suitable substrates for cell adhesion.

Discussion & conclusions: These data pointed out that the adhesive proteins such as Fbg or Fn are able to increase cell adhesion on the different substrates and to modulate the behaviour of the cells on the micropatterns. The cell lining up along glass microstripes can be explained in terms of the greater amount of proteins adsorbed on this substrate.

References: [1] M. Balcells, E.R. Edelman (2002) J. of Cellular Physiology, **191**: 155-161; [2] A. Magnani, S.Panfilo, D. Pasqui, A.Priamo, R.Barbucci (2002) submitted to Material Science

and Engineering C; [3] R. Barbucci, S.Lamponi, D.Pasqui, A.Rossi, E.Weber (2002) submitted to Material Science and Engineering C.

Acknowledgements: EU framework V grant QLK3-CT-2000-01500 (Nanomed).

A NOVEL METHOD TO QUANTIFY MECHANICAL TENSION IN CELL MONOLAYERS

J. Trzewik, M. Ates, G.M. Artmann

Cellular Engineering, University of Applied Sciences Aachen, Germany,

Introduction A new technology to analyze mechanical properties of adherent cell monolayers grown on elastic silicon membranes is introduced. Measurements were performed using 3T3 (NIH) fibroblasts under the influence of Cytochalasin D and Thrombin. The stress-strain relation of the cell monolayer-silicon-composite was monitored. The drum-like construct of the culture chamber opens new roads for studying the mechanics of cell monolayers and of ultra flat two dimensional tissue constructs. Steady state as well dynamic mechanical studies can be performed. Defined mechanical boundary conditions together with the known number and orientation of the cells allow precise information on the average tension exerted by a single cell within the monolayer.

European Cells and Materials Vol. 4. Suppl. 2, 2002 (pages 118-119) ISSN 1473-2262

ARTICULAR CARTILAGE INVESTIGATION BY MRI IMAGING

M. La Paglia, J.H. Kuiper, J.B. Richardson, Iain McCall, C. Ruggiero

Department of Informatics Systems and Telematics University of Genoa, Italy

Unit for joint Reconstruction, RL &AH Orthopaedic Hospital

Abstract: Magnetic resonance imaging has become a very powerful tool to investigate articular cartilage in patients with degenerative joint disease. We have set up a system for 3D reconstruction of the knee's structure and have tried to set up software for a completely automated cartilage segmentation based on MRI images, using interpolation algorithms.

Keywords: 3D visualization, segmentation, medical imaging

INTRODUCTION: In the last years magnetic resonance has been established as a valid and completely non-invasive method for mapping the internal structure of the body, joints. After acquisition appropriate software is needed to correctly process and visualize the images. Among the pathologies of the knee the cartilage is one of the most important. It is necessary to segment the cartilage elucidating its boundaries with the surrounding anatomic structures[1]. The more common and easy implemented approach to solve this problem is interactive segmentation, because the morphology of the knee makes it too difficult to use automated algorithms. The present work is a contribution towards a completely automatic procedure, which automatically improves the results obtained, with interpolation algorithms using radial functions to interpolate pixel values.

METHODOLOGY: We used seven datasets of images acquired by MRI scans. Each dataset represents one knee, and consists of 0-60 slices. The images are in DICOM format. The code has been written in C++ language, using the graphics libraries VTK, Visualization Toolkit [2].

The software that has been developed has two modules: 3D reconstruction of the knee structure and cartilage segmentation. In order to visualize, convert and elaborate the image dataset we used the Osiris software from the Digital Imaging Unit (University Hospital of Geneva, 24 Micheli du Crest 1211 Geneva 14 – Switzerland)

3D RECONSTRUCTION: The 3D reconstruction process consists of two steps.

First it is necessary to determine a volume from a set of slices. With the marching cubes algorithm the pixel values between two sequential images are interpolated and the algorithm generates meshes of triangles that lie on the isosurface with established value (this value must be set up by user). In this way a continuous surface, which contains the volume which is being studied, can be constructed.

Second, we need to visualize the volume obtained in the first step of the process. For this purpose several techniques exist. We chose the ray casting rendering technique because it is, generally, the most accurate mapper, and also the fastest on most platforms.

This procedure is implemented by the ray casting algorithm. In this algorithm the rendering window is regarded as a matrix, and its elements represent the pixels (if the dimension is changed, the resolution of the output image also changes). From the observer's position as many rays as the matrix's elements are traced, and hence a prospective view can be constructed.

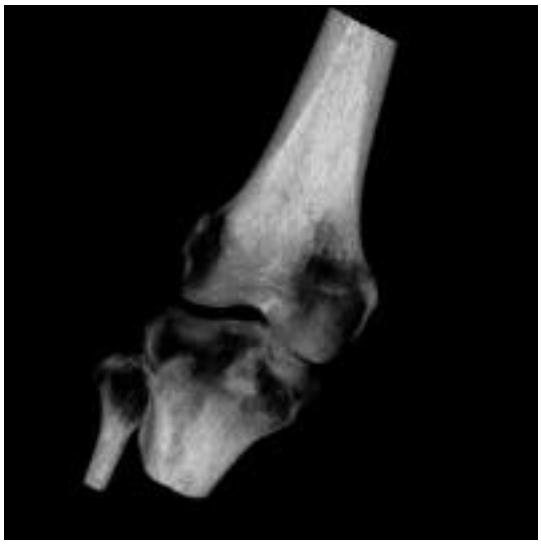

Fig.1.3D reconstruction of the knee

CARTILAGE SEGMENTATION: The cartilage segmentation process is very complex for different reasons. In the first place, magnetic resonance provides insufficient contrast between cartilage and the other tissues, particularly between cartilage and synovial fluid, which are mapped with similar gray level. Secondly, the cartilage morphology is very complex and the voxel value distribution is very irregular. Thirdly, a number of potential artefacts occur in magnetic resonance imaging. These

artefacts affect image quality, and may simulate pathologic conditions and produce interpretation errors [4].

For these reasons, normally cartilage is segmented with an interactive approach. We have tried to set up a completely automated procedure[5][6].

Segmentation techniques, especially those that are automated, may generate islands of misclassified voxels. We solved this problem with a filter based on search for connected pixels. Moreover, to improve the segmentation quality, we have worked on the sequence acquisition choosing the sequence which has the highest image contrast, and subsequently we have filtered the images applying threshold and seed connectivity algorithms. In this way we have obtained a new set of images which we used as input for the 3D segmentation algorithm. After bidimensional processing on all slides the portion of detected cartilage increases.

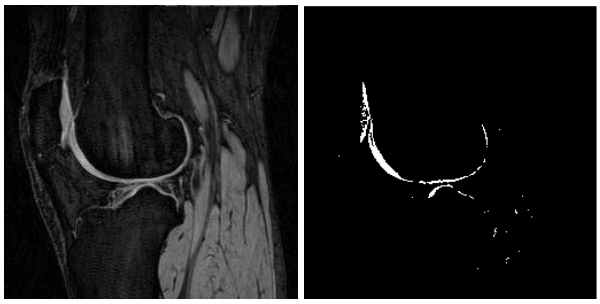

(a) (b)

Fig.2.(a) Image acquired by flash sequence which optimal contrast (b) same image after bidimensional filter.

CONCLUSIONS AND DISCUSSION : The final aim of our work is to obtain a bidimensional projection of the cartilage, from a 3D model obtained after the segmentation process. We can consider this projection like a cartilage map, which surgeons can use to plan surgery (Fig.2).

We have implemented a fully automated algorithm for knee cartilage segmentation in 3D, but some regions of this tissue are not detected. For example, the cartilage at the interface with synovial fluid is not detected because the gray level of these two entities is very similar and this value is superior to the threshold used by the algorithm to discriminate different regions. In order to solve this problem we intend to implement software for automatic labelling of the segmentation quality and a graphic interface to be used when the quality of automatic segmentation is regarded as not acceptable by the user. In order to improve the software, we intend to set up an algorithm for interpolation of the dataset which is obtained after segmentation.

ACKNOWLEDGMENT: The present paper has been supported by the European Union. Contract number: QLK3-CT-1999-00599

REFERENCES [1]K.W. Marshall, D.J. Mikulis and B.M. Guthrie, *Quantitation of cartilage usind magnetic resonance imaging and three-dimensional reconstruction*, Journal of Orthopaedic Research 13:814-823 The journal of bone and joint surgery, Inc 1995 [2]W. Schoroeder, L.S. Avila, K.M. Martin, W.A. Hoffman, C.C.Law, *The vtk user's guide* and vtk on line at website address http://www.kitware.com [3]Imtiyaz S. Talkhani, James E. Richardson *Knee diagram for the documentation of arthroscopic findings of the knee-cadaveric study* The Knee 6(1999) 95-101 [4]Wilfred C.G.Peh, Jimmy H.M. Chan *Artifacts in musculoskeletal magnetic resonance imaging: identification and correction* [5]F. Eckstein, M. Schnier, M. Haubner, J. Priebsc, C. Glaser, K.H. Englmeierand M. Reiser, *Accuracy of cartilage volume and thickness measurements with magnetic resonance imaging*, Clinical orthopaedics and related research Number 352, pp 337-148, 1998 [6]F. Eckstein, H. Graichen, K.H. Englmeier, H. Bonel, M. Reiser *New quantitative approaches with 3D MRI: cartilage morphology, function and degeneration*, The worlwide radiology journal Vol.9 N.6 11-12/1998

European Cells and Materials Vol. 4. Suppl. 2, 2002 (pages 83-85) ISSN 1473-2262

ACELLULAR PORCINE XENODERMIS AS A TEMPORARY WOUND COVER AND SUBSTRATUM FOR CULTURED KERATINOCYTES

E. Matouková[1], P. Stehlíek[2] & P. Vesely[1]

[1]*Institute of Molecular Genetics, AS CR, Prague, Czech Republic*

[2] *BioSkin, s.r.o., Prague, Czech Republic (www.bioskin.cz)*

INTRODUCTION: A correctly chosen cover offers the optimal means for a fast re-epithelization of wounds (burns, donor sites, leg ulcers & other skin defects). There has been a positive experience with primary covering of burn wounds with surviving porcine dermo-epidermal grafts (xenografts) in the Prague Burn Centre of the Charles University Hospital for more than three decades [1,2]. The successful clinical practice led us to develop the dried porcine dermal matrix [3], which was further improved and commercialized as the BIO-SKIN (patent pending) by BioSkin s.r.o., Prague, Czech Republic.

METHODS: The BIO-SKIN is a dried porcine acellular dermal 3D matrix ready for straight covering of wounds or for ex vivo cultivation of primary human keratinocytes (making BIO-SKIN-KERA). It is supplied sterile, spread on the bottom of the culture dish, with long shelf life at room temperature.

RESULTS: Both the BIO-SKIN and BIO-SKIN-KERA proved to fulfill the criteria for an ideal wound cover. They easily attach to the wound bed with automatic adaptation to the wound surface, showing a strong haemostatic effect. Both forms of BIO-SKIN are sufficiently firm to give wound the mechanical protection without limiting movements of limbs. They are not toxic, not sensitizing the surrounding skin or eliciting inflammatory response. They create a barrier against infection from the outside and provide an environment favourable for healing. BIO-SKIN serves as a substitute for xenografts used in treatment of leg ulcers, burns and other wounds. BIO-SKIN-KERA is an advanced form. It combines the properties of biomembranes with the bioactivity of living cells. For application onto the wound, the BIO-SKIN-KERA can be easily peeled off the culture vessel (Fig. 1) and transferred onto the prepared wound in a manner described as upside-down, which means keratinocytes facing the wound and BIO-SKIN serving as the outer cover. Both autologous and allogeneic keratinocytes can be used to produce BIO-SKIN-KERA. The development of a layer of keratinocytes (Fig. 2) on the BIO-SKIN can be

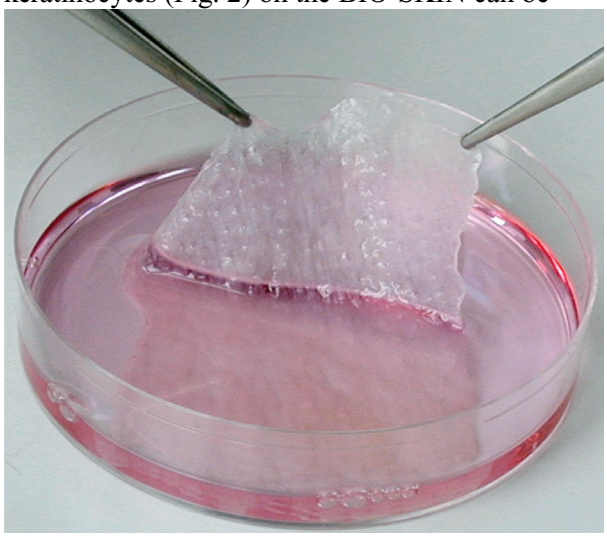

Fig.1:The BIO-SKIN-KERA is easily peeled off from the dish bottom and applied onto the wound after the keratinocyte layer reached confluency.

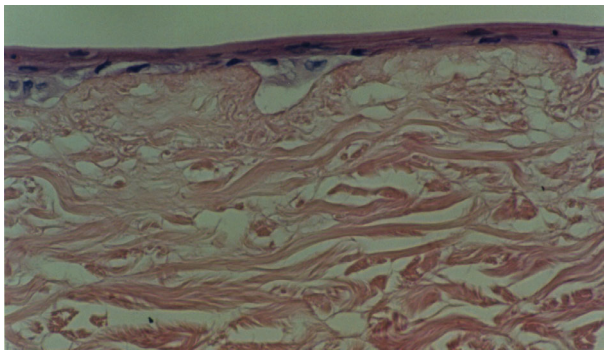

Fig. 2: Histology of BIO-SKIN-KERA: cultured keratinocytes form a layer on the BIO-SKIN.

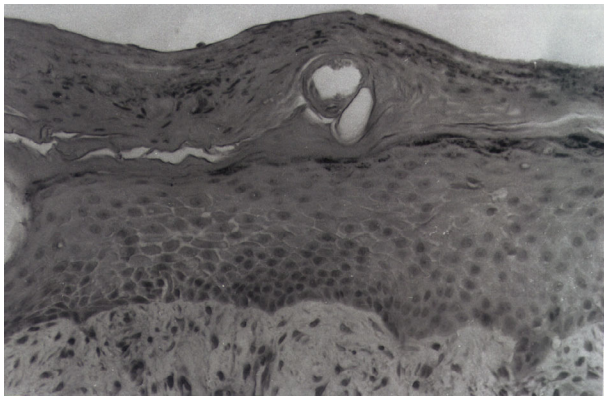

Fig. 3: Biopsy of a healing wound: The newly formed epidermis after 5 days under BIO-SKIN-KERA is fully stratified.

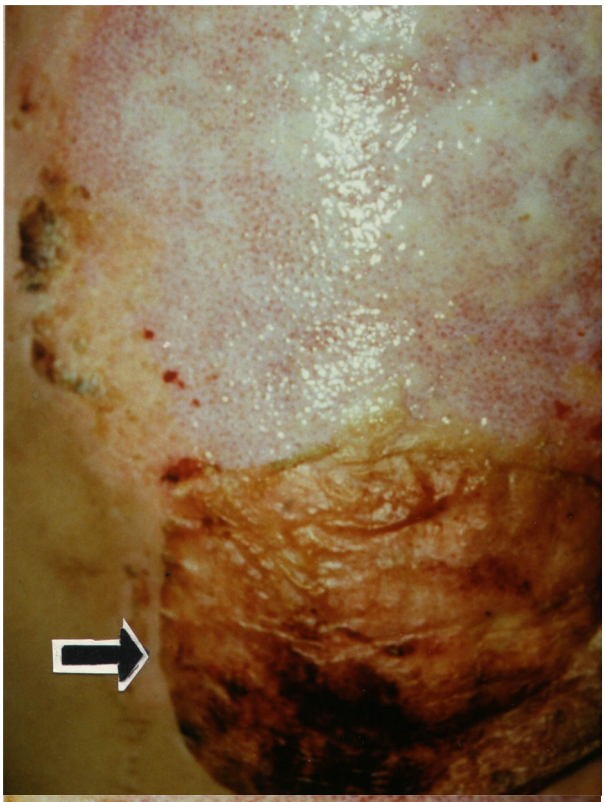

Fig. 4: On day 8 a part of the scalded wound was tangentially excised and covered with BIO-SKIN-KERA. Upper: Two days later BIO-SKIN-KERA turned to a thin brownish membrane (arrow). Bottom: After next three days it was mechanically peeled off, leaving newly formed epithelium underneath (Matoušková et al. 2001a).

monitored on the free surface of the culture dish. Allo-keratinocytes from such a composite skin "take" to the deep dermal wound bed temporarily and they strongly stimulate wound healing (Fig. 3). The forerunner of the BIO-SKIN-KERA has been in practice for more than five years in the Prague Burn Centre with encouraging results (Fig. 4). E.g. donor sites healed within 6-8 days compared to 14-18 days after standard treatment and in immunodeficient patients with prolonged wound healing, it was 7-10 days compared to 32-90 days. [4,5]. Recently, the combination of a proper wound preparation with application of BIO-SKIN-KERA proved to be efficient in preventing conversion of deep dermal burns into full-thickness skin loss [6].

DISCUSSION & CONCLUSIONS: The BIO-SKIN is an equivalent substitute of xenografts with the advantage of long shelf life. It serves as an effective biomembrane cover of donor sites and small or medium skin defects**.** The BIO-SKIN-KERA with allogeneic keratinocytes works out well as bioactive dressing for easy immediate application in emergency. It is based on temporal "take" of keratinocytes, early closure of the wound, and production of cytokines strongly stimulating wound healing. Due to the fast effect and low immunogenicity of dermal matrix and cultured keratinocytes, no rejection appears.

REFERENCES: [1]J. Moserová, E. Bìhounková, R. Vrabec et al. (1974) *Rozhl. Chir*. **53**: 190. [2]J. Moserová, E. Houšková (1989) *The healing and treatment of skin defects.* Basel, S. Karger AG., pp 143-51. [3]E. Matoušková, D. Vogtová and R. Königová (1993) *Burns* **19**:118-123. [4]E. Matoušková, S. Buèek, D. Vogtová et al (1997) *Br J Dermatol* **136**:901-907. [5]E. Matoušková, L. Brož , P. Veselý, R. Königová (2001a) Use of allogeneic human keratinocytes cultured on dried porcine dermis in the treatment of burns. In: *Cultured Human Keratinocytes and tissue engineered skin substitutes* (eds R.E. Horch, A.M. Munster, B.M. Achauer) G. Thieme Verlag, pp. 230-238. [6]E. Matoušková, L. Brož , E. Pokorná, R. Königová (2001b) *Folia Biologica (Praha)* **47**:135-144.

ACKNOWLEDGEMENT The Fig. 4 was reproduced with the permission of Folia Biologica (Praha).

European Cells and Materials Vol. 4. Suppl. 2, 2002 (pages 120-122) ISSN 1473-2262

CELL POSITIONING AND SORTING USING DIELECTROPHORESIS

David Holmes & Hywel Morgan

[1] *Bioelectronics Research Centre, Dept. of Electronics and Electrical Engineering, Glasgow University, Scotland, UK*

INTRODUCTION: In this paper we describe a micro-fabricated cell separation and positioning system based on the AC electrokinetic technique, dielectrophoresis (DEP). The system uses non-uniform electric fields produced by arrays of microelectrodes to manipulate cells held in suspension. Depending upon the mode of operation one can either concentrate a single cell type from a heterogeneous mixture (with all other cell types passing through the device); or alternatively separate different cell types along the length of the device. In the second mode of operation the position at which a cell ends up is based on its size and the dielectric properties of its cellular membrane.

METHODS: DEP has been applied to the separation and manipulation of a vast array of bioparticles since it was first described by Pohl in 1978 [1-3]. The technique has been used to manipulate cells by a number of groups [e.g. 4-9].

The DEP force can be expressed as [2]:

$$\underline{\mathbf{F}}_{dep} = \frac{1}{2}\alpha \upsilon \nabla \left|\underline{\mathbf{E}}\right|^2 \qquad (1)$$

where α is the effective polarisability, ν is the volume of the particle and $\underline{\mathbf{E}}$ is the electric field. Figure 1 shows how $\nabla\left|\underline{\mathbf{E}}\right|^2$ varies with position above an array of interdigitated electrodes [10].

Fig. 1: Plot showing how the gradient of the magnitude of the electric field squared varies above an interdigitated electrode array. Different lines represent different heights above the array.

A schematic diagram of the DEP-separator is shown in figure 2. The system consists of two separate arrays of interdigitated bar electrodes integrated into the one device. When particles enter the device they are carried in a fluid stream and are distributed randomly throughout the chamber volume. Using negative DEP forces, the initial electrode array concentrates the wide distribution of particles entering the device into a well-defined sheet positioned midway between the upper and lower channel walls. Particles then enter the second or 'separation' electrode array, which is energised such that a positive DEP force acts upon either all the particles or a desired sub-population of particles, pulling them out of solution onto the electrode surface. In this paper we will concentrate on the situation where all the cells are undergoing positive DEP and are being attracted to the separation electrode.

Fig. 2: Schematic diagram of the DEP particle separator. A binary mixture of two cell types are first focused into the central plane of the channel and then follow distinct trajectories banding at different positions along the channel length.

Particles held at the electrodes can be imaged on the device. All the captured cells can subsequently be eluted for further processing by turning off the electric field (or applying negative DEP) whilst continuing to flow fluid through the device.

RESULTS: Separation devices were fabricated on standard glass microscope slides. The electrode arrays were patterned using standard photolithography and wet etching techniques. A 100µm deep flow channel was defined in SU8 photoepoxy, with the channel lid aligned and glued in place using UV curable glue. Inlet and outlet holes were drilled prior to gluing the lid.

Experiments were carried out using mixtures of cultured human monocytes (THP-1 cell line) and human peripheral blood mononuclear cells (PBMCs). PBMCs were collected from the buffy coat after density gradient centrifugation of whole blood over a Histopaque-1077 gradient. Cells were labeled prior to mixing with CellTracker™ dyes (Molecular Probes). The THP-1 monocyte cell line was labeled green and PBMCs were labeled red.

The magnitude and direction of the DEP force depends upon the relative polarisabilities of the cells and the suspending media. Cells were therefore resuspended at known concentrations in a low ionic strength media (dH_2O containing Ficoll400 (3.5% w/v), sucrose (9% w/v), glucose (0.1% w/v) with the addition of small amounts of phosphate buffer) of pH 7.4, osmolality ~290mOs/m and conductivity ~10mS/m.

Cell suspensions were fed into the device using a syringe pump. A typical set of experimental conditions being: flow rate of 1ml/hr, $5V_{p\text{-}p}$ @

20MHz applied to the focusing electrodes, and $8V_{p-p}$ @ 200kHz applied to the separation electrodes. Figure 3 shows a fluorescence image captured after 0.5ml of cell suspension has flowed through the device under the above conditions.

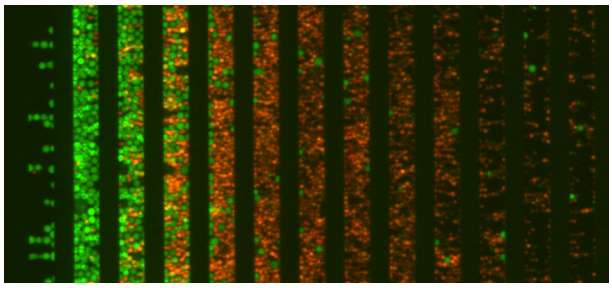

Fig. 3: Fluorescence image of THP-1 cells (green) and PBMCs (red) banding on the separation electrode array. The vertical black stripes are the 40µm wide electrodes of the separation array.

From figure 3 it is clear that the mean positions of the two cell types differ. Figure 4 shows a plot of cell numbers versus distance along the length of the separation electrode array for a similar experiment.

DISCUSSION & CONCLUSIONS: Figures 3 and 4 show a nice tight band of THP-1 cells and a more smeared out band of PBMCs. This difference in distribution profiles is due to the THP-1 cell population being relatively homogeneous; while the PBMC population is composed of a number of cell sub-types. The PBMC sub-populations are; Monocytes, T-lymphocytes and B-lymphocytes (most Granulocytes are removed in the centrifugation step). Each of these sub-populations has different size and dielectric properties [4].

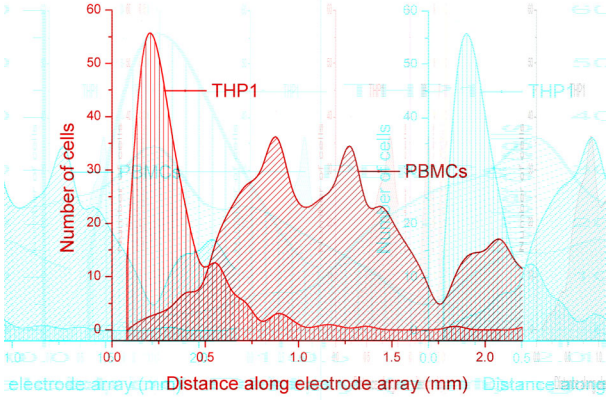

Fig. 4: Position of the different cell types along the separation electrode array for a mixture of PBMCs and cultured THP-1 cells.

If the experimental conditions are kept the same the cell types will band reproducibly in the same position on the separation array. Varying the applied experimental conditions, such as changing the flow rate or the magnitude or frequency of the signal applied to separation electrodes results in the position of the cell band changing. Cell types other than those described will band at different positions determined by their size and dielectric properties.

In this paper we have presented a novel DEP electrode configuration, which relies upon initially focusing all the cells in the flow stream to the central plane of the flow channel. Cells then enter a second region where they undergo positive DEP and are attracted the separation electrode array where they are held.

REFERENCES: [1]HA Pohl (1978) *Dielectrophoresis.* Cambridge University Press. [2]R. Pethig (1996) Crit Rev Biotech **16**(4):331-348. [3]TB Jones (1995) *Electromechanics of Particles*. Cambridge University Press. [4]J Yang, *et al.* (1999). Biophys J **76**(6): 3307-3314. [5]J Yang, *et al.* (2000). Biophys J **78**(5): 2680-2689. [6]GH Markx, *et al.* (1994) J Biotech **32**(1): p. 29-37. [7]FF Becker, *et al.* (1994) J Phys-D **27**(12):2659-2662. [8]FF Becker, *et al.* (1995) PNAS **92**(3): p. 860-864. [9]M Stephens, *et al.* (1996) Bone Marrow Transplan **18**(4):777-782. [10]H Morgan *et al.* (2001) (vol 34, pg 1553, 2001) J Phys D **34**(17): 2708-2708.

ACKNOWLEDGEMENTS: This work was funded in part by an EPSRC studentship awarded to DH. THP-1 cells were a gift from Dr S Robertson at Glasgow Royal Infirmary. Thanks to Ms ME Sandison and Dr C Mills for blood samples.

European Cells and Materials Vol. 4. Suppl. 2, 2002 (pages 86-87) ISSN 1473-2262

CELL-SURFACE PROTEOGLYCANS ARE DIFFERENTIALLY REGULATED BY CHONDROCYTES DURING ADAPTATION TO CELL CULTURE

A.D. Murdoch, R.A. Oldershaw and T.E. Hardingham

UK Centre for Tissue Engineering, University of Manchester, Manchester, UK

INTRODUCTION: Articular cartilage chondrocytes are characterised by their relatively sparse distribution and low rate of division in the tissue, and their ability to elaborate an extensive extracellular matrix containing characteristic collagens and proteoglycans. Tissue engineering applications using chondrocytes as the cell source usually require monolayer culture to expand cell numbers from a limited initial source. This results in well-documented changes in extracellular matrix molecule expression as the cells adapt to the culture conditions [1]. The response of cells to both pericellular matrix molecules and other soluble stimuli such as growth factors and cytokines can be modulated by cell-surface molecules such as the proteoglycans betaglycan (TGFβ type III receptor), CD44 (hyaluronan receptor) and the syndecan (transmembrane heparan sulphate proteoglycan) [2] and glypican (GPI-anchored HSPG) [3] families. However, relatively little is known about the expression of these molecules by chondrocytes or how this expression might be modulated by growth in culture [4]. In this study we have determined the expression levels of 11 cell-surface proteoglycans in intact cartilage, and followed how their expression levels change in different patterns during enzymatic release from the tissue and on subsequent monolayer culture.

METHODS: Human articular cartilage from the tibial plateau was obtained with informed consent and following local research and ethical committee approval from patients undergoing total knee replacement for osteoarthritis. Cartilage samples from grossly normal areas were dissected from the underlying bone. Portions of the cartilage were powdered in a Braun Mikrodismembrator and dissolved in TriReagent. RNA was isolated from the aqueous phase of the TriReagent extract using the GenElute spin column system (Sigma). Chondrocytes were released from the remaining cartilage by digestion for 1h in trypsin and 18h in collagenase and designated passage 0 (P0). Cells were plated on tissue culture plastic at 50000 cells/cm^2 in DMEM +10% FBS and antibiotics and maintained at 37^{0}C in 5% CO_2. At confluence, cultures were designated as P1. Subsequent passages were obtained by trypsinisation and division of cells at a 1:2 ratio. RNA was extracted from P0, P1 and P2 cells using the standard TriReagent protocol. RNAs were converted to cDNA with M-MLV reverse transcriptase and random hexamers (Promega) and quantitative PCR was performed on 1 µl of cDNA in a 25µl reaction volume. Signals were detected using a SYBR green detection kit (Eurogentec) in an ABI 7700 Sequence Detector with gene-specific primers designed on PrimerExpress software. Average Ct values were normalised with the $2^{-\Delta Ct}$ method to the level of glyceraldehyde-3-phosphate dehydrogenase expression.

RESULTS: We examined the relative transcript levels of the cell-surface proteoglycan genes in RNA extracted directly from cartilage (Figure 1. white bars).

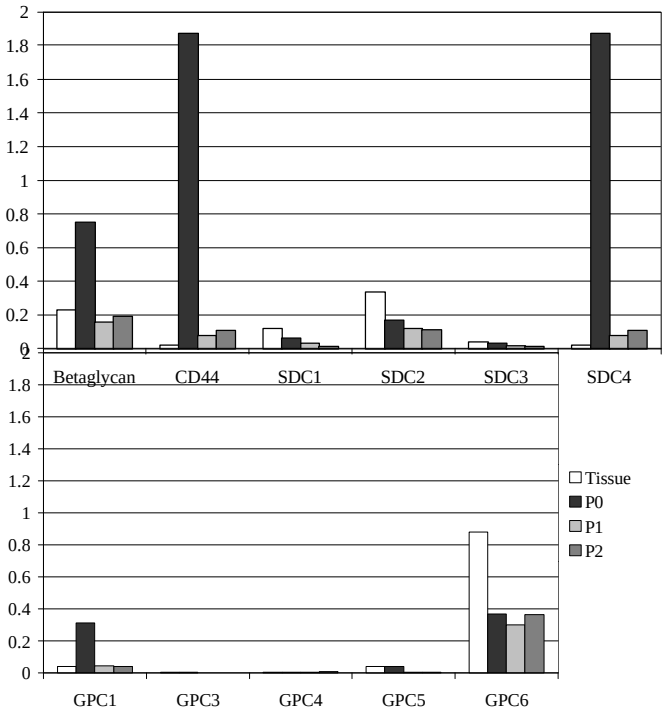

Fig.1: Expression levels of the 11 proteoglycans studied relative to the expression of glyceraldehyde-3-phosphate dehydrogenase mRNA in the intact tissue and at passage 0,1 and 2. SDC – syndecan; GPC – glypican.

Modest levels of expression were found for betaglycan and syndecans -1 and -2. The highest level of expression was for the recently discovered glypican-6. Very low levels of expression of CD44, syndecan-3 and glypicans -1 and -5 were also found. The changes in expression of the proteoglycans during the proteolytic digestion of the cartilage and during subsequent culture could be divided into two groups. In the first group, syndecan-1 and -2 and glypican-6 expression levels decreased when the cells were released from the cartilage and continued to fall in monolayer culture. In contrast, in the second group containing betaglycan, CD44, syndecan-4 and glypican-1, there was a large increase in expression during the overnight digest to form a cell suspension, but these levels had returned to those found in the tissue by the time the cells had first reached confluence in monolayer.

DISCUSSION & CONCLUSIONS: In this study we have measured the relative expression levels of 11 cell-surface proteoglycans in human articular cartilage and cultured chondrocytes and have identified glypican-6 as a major transcript of chondrocytes. During isolation and adaptation to monolayer culture, the expression levels of syndecan-1 and -2 and glypican-6 exhibited a steady decrease. In contrast there were dramatic increases of betaglycan, CD44 and syndecan-4 expression during digestion of the cartilage to a cell suspension. In view of the activity of CD44 as a receptor for hyaluronan and the close association of syndecan-4 with focal adhesions in other cell types, these changes may reflect a response of the chondrocytes to the removal of their immediate pericellular matrix. Freshly isolated cells (equivalent to our P0) have sometimes been used as a reference source to examine changes in chondrocyte gene expression and have been assumed to be similar in expression to cells in tissue [4]. The dramatic changes we have found in the expression of some of the genes studied in the cell suspension at P0 indicate that caution should be exercised in making this assumption. The results demonstrate the sensitivity of chondrocyte cell surface proteoglycan expression to cell-matrix interactions, and the changes we have found in expression may help modulate the response of cultured chondrocytes to growth factors and chemokines.

REFERENCES: [1] P.D. Benya, S.R. Padilla & M.E. Nimni (1978) *Cell* **15**: 1313-1321. [2] A. Woods (2001) *J.Clin.Invest.* **107**: 935-941. [3] J. Filmus & S.B. Selleck (2001) *J.Clin.Invest.* **108**: 497-501. [4] J. Grover & P.J. Roughley (1995) *Biochem.J.* **309**: 963-968.

ACKNOWLEDGEMENTS: This work was supported by joint IRCol funding from BBSRC, MRC and EPSRC.

THE RE-EXPRESSION OF CHONDROCYTIC PHENOTYPE BY PASSAGED HUMAN ARTICULAR CHONDROCYTES IS IMPROVED BY VIRAL TRANSDUCTION OF SOX9

SR Tew*, Y Li**, AM Russell**, JM Prince*, RE Hawkins** and TE Hardingham*

UK Centre for Tissue Engineering, **Stopford Building, University of Manchester, Manchester, UK; ***Patterson Institute for Cancer Research, Christie Hospital, Manchester, UK*

INTRODUCTION: The expansion of articular chondrocytes for tissue engineering purposes leads to loss of chondrocytic function which can be difficult to regain. We have transduced SOX9, a transcription factor crucial for the induction and regulation of the chondrocyte phenotype[1], into monolayer expanded human articular chondrocytes using a retroviral vector. The cells were grown in pellet or alginate cultures and the expression of marker genes and the extent of their extracellular matrix (ECM) production was compared with that of untransduced cells.

METHODS: Human articular chondrocytes (HAC), from tissue obtained following total knee arthroplasties, were grown as monolayers in Dulbecco's Modified Eagles Medium (DMEM) supplemented with 10% foetal calf serum (FCS) (Invitrogen). Between passages 2-5 cell growth was accelerated by stimulation with growth factors and the cells were transduced with a retrovirus or adenovirus containing human SOX9 cDNA. After transduction, the cells were >90% positive. They were grown as monolayers, pellet cultures or encapsulated in alginate beads.

Total RNA was prepared from monolayer and pellet cultures using Tri Reagent (Sigma) or from alginate beads using a GenElute mammalian RNA purification kit (Sigma). cDNA was reverse transcribed and then amplified by PCR on an ABI 7700 Sequence Detector using a SYBR Green Core Kit (Eurogentec) with Collagen I, II and SOX9 specific primers. Relative expression levels normalised using GAPDH.

Pellet cultures were also fixed in 4% formaldehyde and embedded in paraffin wax for histological analysis. 5µm sections were cut and stained with 0.1% safranin-O. Sections were then labelled with antibodies to collagen I, collagen II (both Calbiochem), chondroitin-4-sulphate or chondroitin-6-sulphate (antibodies 2B6 and 3B3- a kind gift from Prof. Bruce Caterson, Cardiff, UK).

RESULTS: SOX9 increased collagen II gene expression in monolayer chondrocytes at late passages (5-10). In addition retroviral SOX9 overexpression improved the re-expression of chondrocyte phenotype in alginate culture.

Collagen II was not stimulated in pellet cultures but pellets formed from retorvirus SOX9 transduced cells weighed more, produced more safranin-O staining extracellular matrix (figure 1) and contained larger quantities of chondroitin-6 sulphate than control pellets.

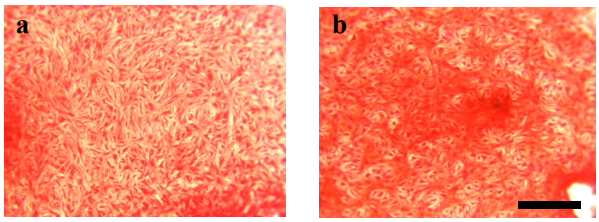

Fig. 1: Matrix accumulation in pellets formed from (a) control HAC or (b) retroviral SOX9 transduced HAC. Safranin-O staining, scale bar = 200mm.

DISCUSSION & CONCLUSIONS: Passaged HAC show major loss of expression of matrix genes. We have shown that continuous expression of SOX9 via a retrovirus improves collagen II expression in monolayer culture of late passage HAC and also enhances their ability to respond to 3-dimensional cultures. Alginate cultures successfully potentiated type II collagen expression in transduced cultures but pellet cultures did not. However, pellets containing transduced cells accumulated more ECM. Overexpression of SOX9 also seemed to modulate the sulphation pattern of chondroitin sulphate, stimulating an increase in 6-sulphation. It has been shown that SOX9 regulates the re-expression of the chondrocyte phenotype but that the effect is restricted to early passages[2]. This study indicates that introducing elevated levels of SOX9 expression enables the cells to be more receptive to chondrogenic cues and also has major effects on the nature and extent of their ECM formation. This strategy offers potential for studying cartilage matrix formation by passaged human chondrocytes.

REFERENCES: [1] de Crombrugghe et al (2000) *Matrix Biol* **19**:389-94 [2] Stokes et al (2001) *Biochem J* **360**:461-70

European Cells and Materials Vol. 4. Suppl. 2, 2002 (page 140) ISSN 1473-2262

PROTEIN ADSORPTION ONTO N-CONTAINING HEMA COPOLYMERS

R. Sariri[1]& A. Ghanadzadeh[2]

[1]*Department of Biology, Gilan University, Rasht, Iran*

[2]*Department of Chemistry, Gilan University, Rasht, Iran*

INTRODUCTION: The use of hydroxyethyl methacrylate (HEMA) as a biomaterial is associated with a number of particular problems, the most important of which is its biocompatibility. A biomaterial with low biocompatibility will be rejected by the biological site. This will be manifested in many ways depending on the environment in which the biomaterial is used. In this research attempt was made to improve HEMA biocompatibility by use varying quantity of a charged co-monomer. Adsorption of protein onto biomaterial is the most important biological response to it. Once adsorbed, the protein is very difficult to be removed and the first protein layer serves as a favorable medium for consequent adsorption of other protein layers, lipids and different inorganic ions such as calcium.

METHODS: HEMA was copolymerized with different amounts of N-vinyl imidazole (NVI) and N-(30sulfopropyl)-N-methacryloxyethyl-N,N dimethyl ammonium betaine (SPE) in order to study the effect of these co-monomers on protein adsorption onto HEMA. 1% ethylene glycol dimethacrylate (EGDM) was used as cross-linking agent. The equilibrium water content (EWC) of the co-polymers was between 35 to 70%. The co-polymers were shaped into 1-cm disks of 0.1 cm depth. The transparent disks were spoiled in 0.5 mg/ml lysozyme solution at room temperature for 24 hours and the protein adsorbed was measured by UV spectrophotometer at 280 nm. The disks were rinsed with distilled water once and mounted directly into the UV cell and their absorption was measured against a blank of the same polymer type and size.

RESULTS: The chemical structures of N-containing co-monomers used for polymerization with HEMA show the presence of a quaternary nitrogen (positively charged). The results of lysozyme adsorption onto both copolymers are compared with pure hema in Table I.

Table 1. The quantity of lysozyme adsorbed onto HEMA copolymers.

Monomer Wt (%)	Comparative surface charge	Lysozyme (mg/cm^2)
ITC (0.0)	-	0.066
NVI (1.0)	+	0.038
NVI (3.0)	++	0.022
NVI (5.0)	++	0.023
SPE (1.0)	++	0.018
SPE (3.0)	+++	0.010
SPE (5.0)	+++	0.012

DISCUSSION & CONCLUSIONS: Lysozyme is a positively charged protein with a small size which is easily adsorbed to HEMA with methacrylic acid (MAA) impurities. Incorporation of NVI and SPE with positive charges reduces the negative charge on HEMA surface and introduces some positive charge. Aa a result, adsorption of positively charged protein, lysozyme, is reduced. It is also shown that the higher percentages of these co-monomers have a higher positive effect on enhancing the HEMA biocompatibility. It can be suggested from these results that the biocompatibility of HEMA in terms of protein adsorption can be increased by choosing an appropriate monomer in a known amount to be co-polymerized with HEMA. Choosing the co-monomer is important in order to control the effect of MAA which is always present as impurity in HEMA.

REFERENCES: [1] J. Fitton (1993) *Cells, Surfaces and Adhesion*, Ph.D. thesis, Aston University. [2] W. Norde, J. Lyklema (1990) *J Colloid Interface Sci.* **2**:3, 183-188. [3] R. Sariri (1995), Acidic and Basic Impurities in HEMA, 19th. Annual Clinical Conference, British Contact Lens Association.

ACKNOWLEDGEMENTS: This research was financially supported by Deputy of Research, Gilan University.

STUDIES ON PROTEIN RELEASE FROM A NOVEL PVA HYDROGEL

A.C. Egan, A.Tudor Evans, A.G.Smith, N.J.Crowther, D. Eagland, S.Britland.

School of Pharmacy, University of Bradford, Bradford BD7 1DP, England.

INTRODUCTION: Synthetic polymeric hydrogels are materials used in the production of various types of wound dressings. Most often these dressings are intended to maintain wound hydration and to act as a barrier to reduce the likelihood of opportunistic or intercurrent infection. Hydrogel materials could also be useful as drug delivery devices, capable of releasing bioactive species such as growth factors directly into the wound. However, the 'dose' of the released materials will have to be accurately controlled to achieve optimal effects on processes such as cell recruitment, migration, division and differentiation [1]. Delivery of growth factors is a complex task not least because of the variation in their molecular weight (MW) from smallest, epidermal growth factor at 6 kDa, to one of the largest, platelet-derived growth factor at 35 kDa. To attain this level of control will require careful manipulation of the microstructure and chemical composition of the hydrogel material. The present abstract describes studies on the release kinetics of proteins of known molecular weight and isoelectric point from a PVA hydrogel stabilised using a novel and patented crosslinker [2]. We have also conducted AFM and SEM investigations into the micro- and ultrastructure of the hydrogel in both hydrated and dehydrated forms.

METHODS: The hydrogel used was a copolymer; poly(vinyl alcohol) (PVA) and poly(vinyl acetate) (PVAc), with a novel crosslinker, PD2000®, in aqueous solution and was studied using different formulations; (A) PVA:PD2000 ratio 20:1, (B) PVA:PD2000 = 10:1 (C) PVA copolymer (differing ratio of PVAc to PVA):PD2000 ratio = 20:1. Release of cytochrome C (MW 12 kDa) was measured by absorbance (550nm) over a 48 hour period. All formulations were studied in fully polymerised and partially polymerised state. Release of pre-stained mixed molecular weight markers (31, 36, 55, 61.5, 84, 116 and 185 kDa) was measured over a 96-hour period, using western blotting. All formulations were studied in fully polymerised state only.

RESULTS: Manipulation of hydrogel composition allows variation in the release kinetics of cytochrome C over a time-scale of 48 hours to 2 weeks.

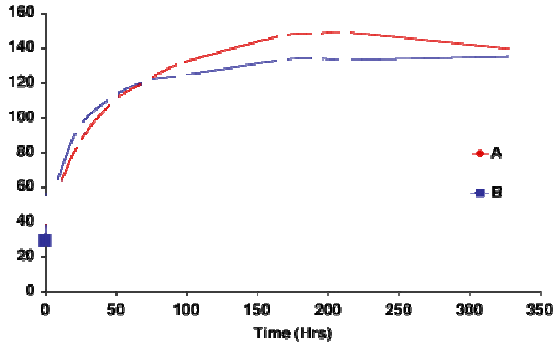

Fig. 1: Release of 12kDa protein Cytochrome C from partially polymerised novel hydrogel.

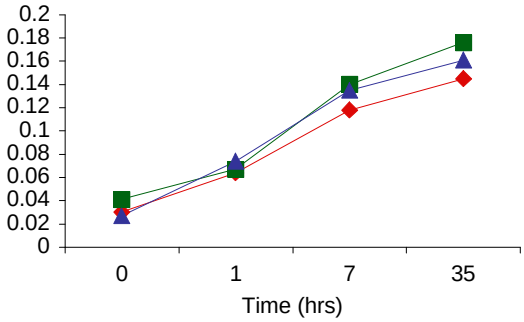

Fig. 2: Release of 12kDa protein Cytochrome C from fully polymerised novel hydrogel.

Using the same hydrogel formulation as before western blotting indicated no release of mixed weight molecular markers of 31kDa and higher over a 96-hour period.

DISCUSSION & CONCLUSIONS: The present formulation of this novel hydrogel allows controlled release of low molecular weight proteins, similar in size to growth factors. Larger molecules were not released after 96 hours suggesting that they had become trapped physically or electrochemically within the gel. Modification of the gel properties should make it possible to fine-tune the release kinetics of proteins known to involved in pathophysiological processes such as wound repair.

REFERENCES: [1]A. Albini et al (1985) Fibroblast Chemotaxis. *Collagen Rel. Res.* 5. pp. 283-296. [2]D. Eagland and N. Crowther, Bradford University, Bradford, UK, Patent number GB2317895 (1998).

European Cells and Materials Vol. 4. Suppl. 2, 2002 (pages 89-90) ISSN 1473-2262

CELL MIGRATION AND DIVISION AT THE EDGES OF MODEL WOUNDS IN KERATINOCYTE SHEETS ARE ORIENTED BY SUBSTRATUM MICROTOPOGRAPHY

A.G.Smith, A.T. Evans and S.T.Britland

School of Pharmacy, University of Bradford, Bradford BD7 1DP, England.

INTRODUCTION: Primary keratinocyte cultures have been extensively used as models of skin wound healing. The HaCat human immortalised keratinocyte cell line displays a migration index similar to that of primary human keratinocytes[1]. Substratum topography has long been known to influence cell movement in culture. We have investigated whether substratum topography influences the axis of cell division and the orientation of cell migration from the edges of a model wound using confluent HaCaT monolayers as models of intact epidermis.

METHODS: HaCaT human immortalised keratinocytes[2] were grown to confluence on tissue culture plastic substrates in RPMI 1640 media gassed with 5% CO_2 in air. The HaCaT monolayers were dissociated intact from the surface by incubation for 3 h with dispase II (2.4 U/ml in RPMI 1640 media) and transferred onto planar or microtopographic fused-silica substrata pretreated with human fibronectin at 10 ug/ml in the same culture media as before. Viability of the cells comprising the HaCaT explants was demonstrated by MTT assay[3]. A small 'wound' was introduced into the monolayer and subsequent cellular activity monitored by phase-contrast and video microscopy.

RESULTS: The monolayers remained intact and became adherent to the culture substrata after 12h. Outgrowth of proliferating cells from the edges of the explants was conspicuous after 24h. On planar surfaces the proliferation and migration of cells showed a radial pattern of outgrowth from the explant edge [Fig.A]. On microtopographic gratings the orientation of cell outgrowth from the explant edge was parallel to the orientation of the grooves of the grating. The cells formed string-like assemblies that were themselves aligned within the grooves [Fig.B]. The underlying substratum microtopography facilitated the emergence of migratory cells from the border of monolayers. Positive MTT staining verified the continuing viability of the cells in the HaCaT explants.

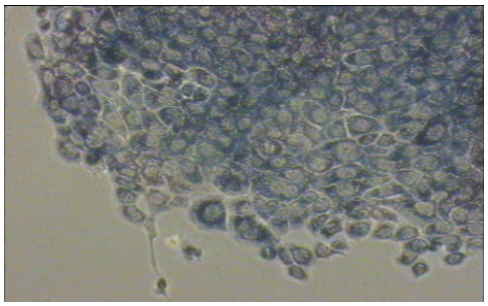

Fig. A: Outgrowth from HaCaT explant on planar fused silica 24hrs after plating (MTT stain)

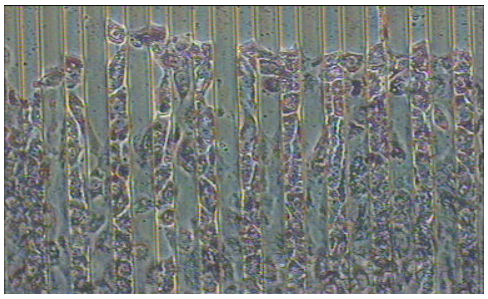

Fig.B:Outgrowth from HaCaT explant on topographic grating 24hrs after plating (MTT stain)

DISCUSSION & CONCLUSIONS: This abstract reports that HaCaT monolayers can be dissociated intact from culture surfaces and subsequently grown on alternative substrates as viable entities. In contrast with the random cell outgrowth from control explants, outgrowth of HaCaTs from the monolayer explant on the grating exhibited topographic guidance. This novel approach has provided an *in vitro* equivalent to epidermis as a model for studying the effect of morphogenetic influences on keratinocyte proliferation and migration. These studies provide the basis for further investigation of the role of topographic and other microenvironmental guidance cues on migration, division and differentiation of cells in organized structures with defined physiological roles.

REFERENCES: [1] S.Charvat, C. Le Griel, M.C. Chignolet (1999) *Clin. Exp. Metastasis.* **17**:677-685. [2] P. Boukamp, R.T. Petrussevsska, et al (1988) *J Cell Biol.* **106**:761-771. [3]J.Carmichael et al. (1987) *Cancer Res*. **47**:936.

ACKNOWLEDGEMENTS: Microfabrication; Prof. Wilkinson, Bill Monaghan and Mary Robertson, Dept. Electronics, Univ. Glasgow.

European Cells and Materials Vol. 4. Suppl. 2, 2002 (pages 91-92) ISSN 1473-2262

SUCCESSFUL SUB-CULTURE OF HUMAN DERMAL FIBROBLASTS AND INTACT HACAT MONOLAYERS FROM HYDROGEL CARRIERS

A.G.Smith, S.T.Britland, N. J. Crowther, D.Eagland.

School of Pharmacy, University of Bradford, Bradford BD7 1DP, England.

INTRODUCTION: Hydrogel polymers have been used as wound dressings and possess several characteristics which facilitate wound healing, such as the maintainance of tissue hydration. In some clinical situations, after burn injuries for example, it may be advantageous to have a method for vitro amplification of the patient's own cells followed by autografting to repopulate the affected area. A method has been developed for multifunctional derivatisation of PVA hydrogels with ECM molecules to enable cell adhesion and amplification but which also allows these cells to be subsequently detached enzymatically. We have succeeded in growing primary Human fibroblasts and monolayers of HaCaT keratinocyte cells on fibronectin-derivatised PVA hydrogel carriers (FNHG) and later transplanted them onto tissue culture plastic surfaces. We report our findings.

METHODS: Primary human dermal fibroblasts (ethics approval granted) and HaCaT human immortalised keratinocyte cells[1] were seeded at approx $1x10^4ml^{-1}$ onto a hydrogel substratum comprising a poly(vinyl alcohol) (PVA) and poly(vinyl acetate) (PVAc) with novel crosslinker, PD2000® surface derivatised with human fibronectin (10ug/ml)[2]. The FNHG+fibroblast culture was inverted and transferred into a second tissue culture plastic (TCP) petri dish and maintained in Hams F10 media for 6 more weeks. HaCaT monolayer cultures were enzymatically removed intact from the derivatised hydrogel surface by incubation for 3h with dispase II (2.4 units/ml) in RPMI 1640 media. Intact monolayers were also transferred to TCP substrates and maintained in gassed (5% CO_2) RPMI 1640 media for several days. Viability of the HaCaT explant was demonstrated by MTT assay[3]

RESULTS: Dermal fibroblasts [Fig.A]and HaCaT cells [Fig.B] adhered to FNHG and reached confluence 5-7 days after seeding. 24 hours after inversion a small population of fibroblasts had begun to migrate from the hydrogel carrier onto the TCP [Fig.C]. After enzymatic removal of the HaCaT monolayer from the FNHG carrier the monolayer had firmly attached to TCP 12 hours after transplantation. Evidence of cell proliferation and migration at the edges of the transplanted monolayer was seen after 24h. [Fig.D]. MTT staining revealed a high density of viable HaCaT cells within the transplanted monolayer. Within 5 days of transfer, the HaCaT explant reestablished confluence.

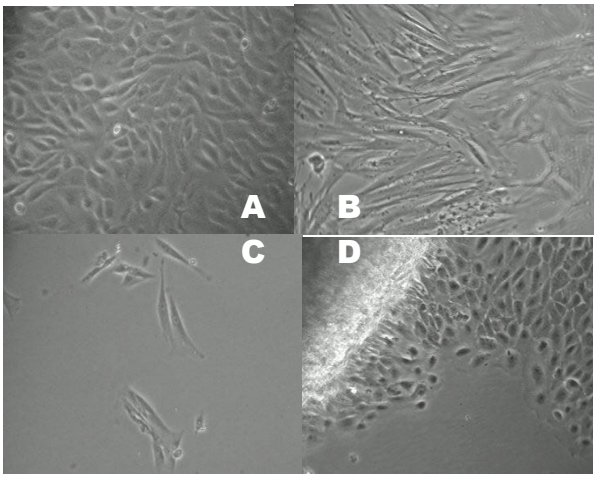

Figure 1: Cell cultures on FNHG day5[Fig.A] Fibroblasts [Fig.B] HaCaTs Explants from FNHG to TCP 24h after transfer [Fig.C]Fibroblasts [Fig.D] HaCaTs

DISCUSSION & CONCLUSIONS: These experiments have shown that FNHG substrates support the attachment, proliferation and migration of human dermal fibroblasts and intact HaCaT cell monolayers. Successfully culturing Human fibroblasts in the presence of FNHG suggests good biocompatibility and illustrates it's potential as a substrate for growth and expansion of cells in vitro. Cells transferred from FNHG onto TCP were viable and capable of subsequent proliferation and migration. This study has demonstrated that FNHG can serve as a vector for transfer of viable cell cultures from one substratum to another.

REFERENCES: [1]P. Boukamp, R. Petrussevsska, et al. (1988) *J. Cell Biol.* **106**:761-771. [2]D. Eagland, N. Crowther, University of Bradford; UK Pat. No. GB2317895. [3]C. R. Nuttelman et al. (2001) *J. Biomed. Mater. Res.* **57**:217-223. [4]J. Carmichael et al. (1987) *Cancer Res.* **47**:936.

European Cells and Materials Vol. 4. Suppl. 2, 2002 (pages 91-92) ISSN 1473-2262

European Cells and Materials Vol. 4. Suppl. 2, 2002 (pages 39-40) ISSN 1473-2262

ARTICULAR CHONDROPROGENITOR CELLS EXHIBIT PLASTICITY IN THEIR DIFFERENTIATION PATHWAY

Archer, CW*, Bishop JC*, Redman SN*, Thomson B# and Dowthwaite GP*.

+Cardiff School of Biosciences, Cardiff University, Museum Avenue, PO Box 911, Cardiff CF10 3US, Wales +44(0)29 20875206.

#Smith and Nephew GRC, York Science Park, Heslington, York, YO1 5DF, UK

INTRODUCTION: There are two major problems afflicting current cartilage repair strategies. One problem is tissue integration between host and reparative tissue. The second problem is the generation of a repair tissue with the structural characteristics of articular cartilage. Previous studies have shown that articular cartilage grows by apposition from the articular surface towards the subchondral bone and that this growth is driven by the proliferation of surface zone cells (1, 2). Additionally, a population of cells with an increased cell cycle time was identified within the surface zone, a property typical of many stem cell populations (2). Here, we describe the isolation and partial characterisation of a cell population from the articular surface that has many properties common to known stem cells of other tissues.

METHODS: Tissue culture and differential adhesion assay: Cartilage slices were isolated from the surface (SZ), middle (MZ) and deep (DZ) zones of 7 day old bovine metacarpal-phalangeal joints by fine dissection and incubated in pronase (0.1% in DMEM/5%FCS) for 3 hours at 37oC followed by collagenase (0.04% in DMEM/5%FCS) for 16 hours at 37oC. Chondrocytes were counted and seeded onto fibronectin (10mg ml-1)-coated or PBS/1% BSA-coated 35 mm dishes at 4,000 cells ml-1 in serum free DMEM (DMEM-) for 20 minutes. After 20 minutes, media and non-adherent cells were removed and placed in similarly treated dishes for a further 40 minutes before this media and nonadherent cells were placed in a third dish. After removal of media at 20 and 40 minutes, fresh DMEM- was added to the remaining cells, which were cultured for up to 10 days. In all experiments 6 fibronectin and 6 uncoated dishes were used for each zone of cartilage. Fibronectin was used as a ligand in the experiments since it is known to be differentially expressed in cartilage during mammalian development (3). Within three hours of plating, chondrocyte adhesion was assayed by counting the total number of cells per dish using phase contrast microscopy and expressed as a percentage of the initial seeding density. Additionally, colonies of chondrocytes consisting of more than 32 cells were counted at 0, 3, 6 and 10 days after differential adhesion (n = 6 experiments). Colony forming efficiency (CFE) was calculated by dividing the number of colonies by the initial number of adherent cells. In some experiments (n = 3) the number of cells per colony were counted to determine the average number of cells per colony. Results were analysed using the Students t test.

Chondroprogenitor plasticity: Colony forming cells were isolated as described above. Twenty four hours after differential adhesion, chondrocytes were transfected with pseudotyped retrovirus encoding lac z for 24 hours. Transfected cells were incubated for up to 5 days before being lifted from the dishes, resuspended at 1 x 105 cells 10ml-1 in additive free DMEM- and injected into limb buds of stage 23 chick embryos. Embryos were incubated for up to 7 days, sacrificed and the limbs reacted histochemically for b-galactosidase activity prior to wax embedding and serial sectioning Controls comprised transfected deep zone cells isolated in tandem with the surface zone cells and injected into embryos on the same day.

RESULTS: *Colony forming efficiency:* At days 0 and 3, no colonies containing more than 32 cells were present in any sample. At 6 and 10 days, the CFE of surface zone chondrocytes initially cultured on fibronectin for 20 minutes was greater than that of the other samples ($p < 0.01$ at 6 days, $p < 0.001$ at 10 days). In addition, the CFE of surface zone cells initially cultured for 20 minutes on fibronectin was greater at 10 days compared with that at 6 days ($p < 0.05$). No change in CFE was evident between 6 and 10 days for any other sample ($p > 0.05$ in all cases). Additionally, the average number of cells per colony was greater in surface zone cells initially grown on fibronectin for 20 minutes at both 6 ($p < 0.05$) and 10 ($p < 0.01$) days compared with all other samples.

Chondroprogenitor plasticity: Examination of serial sections of stage 36 chick embryos reacted for β-galactosidase activity revealed labelled surface zone cells in a variety of tissues including:

cartilage, muscle, tendon and bone. Sections from embryos injected with deep zone cells revealed either no labelled cells or very few cells incorporated into loose connective tissue.

DISCUSSION & CONCLUSIONS: The ability of a population of cells to form large numbers of chondrocyte colonies from a low seeding density taken together with previous results demonstrating the prolonged cell cycle time at the articular surface (2) strongly suggest that a subpopulation of progenitor chondrocytes resides in the articular surface. This conclusion is strengthened by the fact that bovine surface zone cells subjected to differential adhesion exhibit plasticity in their differentiation pathway and can engraft into various avian tissues

REFERENCES: 1)Archer, CW (1994), Ann Rheum Dis 53, 624-630; 2)Hayes et al (2001) Anat Embryol 203,469-79. 3)Salter et al (1995); J Histochem. Cytochem. 43, 447-457.

AFFILIATIONS: This work was funded by The Arthritis and Rheumatism Campaign, UK and Smith + Nephew plc

European Cells and Materials Vol. 4. Suppl. 2, 2002 (pages 24-25) ISSN 1473-2262

INFLUENCE OF SOFT MICROMETRIC TOPOGRAPHY ON BONE CELLS

Mathis Riehle[1], Iva Tolic-Norrelykke[2], Lucia Csaderova-Sokolikova[1], Mary Roberston[1], Anne MacIntosh[1]

[1] *Centre for Cell Engineering, IBLS, University of Glasgow, Glasgow, UK*

[2] *Niels Bohr Institute, Biophysics Group, Copenhagen, DK*

Introduction: In this paper we describe the reaction of rat calvaria bone cells to fabricated micrometric grooves in the surface of a collagen-coated hydrogel. Soft biomaterials such as hydrogels have a wide range of current and possible future medical applications like drug delivery, wound cover or as scaffold materials for tissue engineering. Because of this the fundamental interaction of cells with such soft materials was investigated. The interaction of cells with the surface of a material is governed not only by the chemical qualities and the topographic shape of the surface but also by its mechanical properties. If the cell can actively deform the surface then this mechanical testing can result in a change of the sensory feedback through the cytoskeleton or other putative mechanosensors, which in turn can lead to changes cell behaviour and probably gene expression. To visualise how the cells interact mechanically with the surface the deformation of the surface has to be determined. Recently a new technology has been developed to do this by imaging surface embedded fluorescent beads, and measuring the displacement with an automated image analysis based on FFT [3].

Materials and Methods: Microfabricated grooved surfaces were created by photolithography and reactive ion etching in fused silica according to [1]. The surface of glass coverslips was aminosilanised and activated with glutaraldehyde. The grooved soft substrates were created by casting polyacrylamide gels in between the grooved quartz and the activated coverglass. Spacers were used to control the thickness of the gels. After setting the grooved quartz substrate was removed and the acrylamide surface activated by UV illumination following the methods established in [2] using a heterobifunctional crosslinker (sulfoSANPAH, Pierce, UK) with a UV activated and a succinimide functionality. After UV activating sulfoSANPAH on the substrates the succinimide functionality was used to immobilise either collagen or fibronectin. The remaining active groups were masked with Glycine, after removing excess protein with buffers of low ionic strength. The gels were imaged on a DI Nanoscope IIIa AFM and the mechanical properties measured using the bead method developed by Lo [4], based on these measurements the change in mechanical properties were modelled to estimate the influence of a changed layer thickness. Primary bone cells were isolated from 4 calvariae of neonatal Rats using serial digestion with Collagenase I. The cells were maintained in DMEM and used after reaching confluence.

Results: The structures were good replicas of the original and were flat within 5nm as measured by AFM.

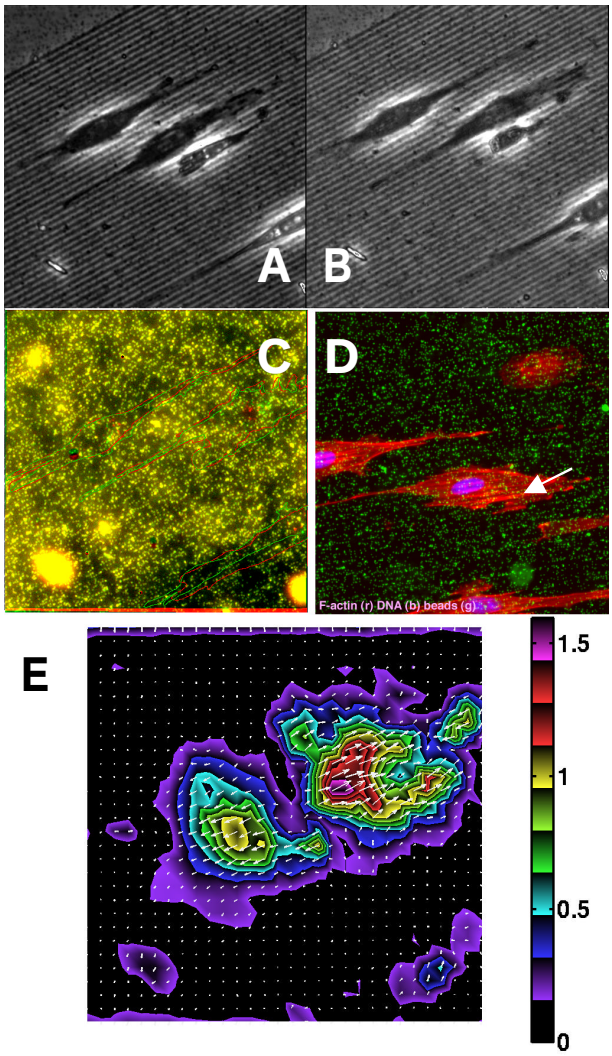

Fig) Exemplary distplacement experiment: A and B the cells in Phase contrast at 0 and 15min, C the bead displacement as seen by overlaying the two images used to calculate the displacement map E.

The same cells after staining F-actin (red), DNA (purple), and the beads (green).

The mechanical properties as modeled by ABACUS showed that these depended very strongly on the thickness of the gel layer, with an increased Youngs modulus even at 170µm thickness. This showed that the cells would not "see" the soft biomaterial but that the underlying hard material would dominate if the layer thickness was below 40-50µm. These differences were reflected in the cytoskeleton of the cells – thin gels resulted in a cytoskeleton similar to those in cells on a hard substrate. The adhesion of cells to the substrates was markedly reduced compared to glass. When attached and spread the behaviour was not different from cells on rigid groove ridge structures of the same dimensions: cell movement would predominantly be up and down along grooves. The F-actin cytoskeleton was not as well established as on a hard substrate but differed not between the soft substrates used. If the cells happened to lie between ridges they pulled these together and developed a peculiar mushroom shape with the pedestal in the groove and a cap on top of the two ridges. If the cells were close to each other (e.g. Fig 1) then the displacement generated by them would be coordinated, thus indicating that the cells were mechanically interacting. The same figure shows that the groove ridges seem to be the main area of F-actin formation. These structures are probably involved in generating the displacement.

Discussion: The results show that the mechanical and topographical properties of the surface have to be considered if the integration of artificial materials with living cells is to be successful. Future research will show how these factors are integrated in the cell by changing surface mechanics, topography and chemistry.

References: [1] Clark, P et al. Development 108, 635-644 (1990). [2] Wang, Y. L. & Pelham, R. J. Methods In Enzymology 298, 489-496 (1998). [3] Butler, J. P., et al. Am J Physiol 282, C595-605 (2002). [4] Lo, C. M., et al. Biophys. J. 79, 144-152 (2000).

Affiliations: I would like to thank the EPSRC for the grant GR/R51009 and the IBLS for the startup dowry.

Acknowledgements: I would like to thank Chris Wilkinson and Adam Curtis for continuous support and Bill Monaghan for technical help with the fabrication.

European Cells and Materials Vol. 4. Suppl. 2, 2002 (pages 107-108) ISSN 1473-2262

SCULPTURED THIN FILMS AND GLANCING ANGLE DEPOSITION

K. Robbie, K. Kaminska, T. Brown, G. Beydaghyan

Department of Physics, Queen's University, Kingston, Ontario, Canada

INTRODUCTION: Recent progress in the ability to manufacture chemical and physical form on small scales has enabled the study of biological systems in new ways. Single cell or single molecule studies have replaced analysis of ensembles, with progress toward a consistent chemistry/biology/physics description of cellular behavior. Single molecule bonding studies with atomic force microscopes, self- and directed-assembly systems, and hybrid organic/inorganic systems are some examples of current work. At the nanometer scale, quantum mechanical effects blur the distinction between biological, chemical, and geometric effects. Understanding how biological systems interact with diverse physical form and chemistry is of prime research interest. Here we present a vacuum deposition technique for producing nanostructured surfaces with controlled three-dimensional form, and encourage discussion on suitable investigations of chemical, biological, and cellular interactions.

METHODS: When a material is heated in vacuum, it evaporates. The vapour traverses the vacuum and condenses as a thin film on any line-of-sight surfaces. Mirrors, eyeglasses, and cutting tools are coated this way with aluminum, magnesium fluoride, and titanium nitride layers, respectively. The films are usually dense, similar to the vapour material in bulk. Many simple organics can be vacuum coated, enabling the growing organic light emitting diode industry. Our technique, called Glancing Angle Deposition [l,2], tilts the vapour receiving substrate at a large angle relative to the vapour flux. Roughening during film growth, combined with atomic shadowing, promotes a porous structure with topological features typically near 100nm. Dynamically varying the geometry (tilting and rotating the substrate) controls the time-evolution of the growth, resulting in materials with designable nanostructured forms.

RESULTS: Although the range of structures that can be produced is limited, many geometries can be produced with this technique, including controlled chirality, porosity, chemistry, and anisotropy [2,3]. The two figures show tilted and plan view images of example sculptured thin films, obtained with field-emission scanning-electron microscopes,. In one experiment the thin film shown in *Figure 1* was saturated with simple nematic liquid crystal molecules. Influenced by the helical columns, the liquid crystal texture exhibited a chiral nematic phase.

Fig. 1: Chiral MgF_2 thin film on glass substrate. Helical pitch is approximately 300nm.

Fig.2: Plan view of an array of titanium (Ti) pillars 10-40nm in diameter.

DISCUSSION & CONCLUSIONS: Biological response to micro and nano structure is significant, and glancing angle deposition is a powerful technique to engineer myriad nanostructured forms.

REFERENCES: [1] K. Robbie and M.J. Brett, "Method of depositing shadow sculpted thin films", U.S. Patent No. 5,866,204. [2] K. Robbie, M.J. Brett, and D.J. Broer, "Chiral thin film/liquid crystal hybrid materials", Nature 399, 764-766, (1999). [3] I.J. Hodgkinson, Q.H. Wu, B. Knight, A. Lakhtakia, and K. Robbie, "Vacuum deposition of chiral sculptured thin films with high optical activity", Applied Optics 39 (4), 642-649, (2000).

ACKNOWLEDGEMENTS: A letter from Adam Curtis prompted my interest in this topic. His patient encouragement is appreciated.

European Cells and Materials Vol. 4. Suppl. 2, 2002 (pages 104-105) ISSN 1473-2262

CELLULAR ATTACHMENT TO UV OZONE TREATED PATTERNED SURFACES

A.H.C. Poulsson[1], S.A. Mitchell[1], M.M. Browne[1], N.Emmison[1], A.J.Johnstone[2], R.H.Bradley[1]

[1]Advanced Materials Surfaces & Interfaces Research Group, Robert Gordon University, Scotland, UK, [2]Department of Orthopaedic Surgery, Aberdeen University Medical School, Scotland, UK

INTRODUCTION: The controlled attachment of cells to a variety of materials surfaces is currently of interest for the development of a range of devices for biomedical applications[1,2]. Surface chemical treatments to control initial cellular attachment rates and patterning on polymer surfaces have been focused on by this group[3,4]. This study has investigated the effect of ultraviolet – ozone (UVO) oxidation technique coupled with physical masking to produce micro-patterned chemistry to control attachment of TE85 human osteoblast sarcoma cells (HOS) to polystyrene (PS) dishes. This work has also been supplemented by work done on Chinese hamster ovarian (CHO) cells in this group.

METHODS: Untreated 20cm^2 PS tissue culture dishes (Nunc, Denmark) were irradiated in a UVO treater for various times, figure 1. Using 250 mesh TEM grids (pitch 100μm, bar width 30μm, hole width 70μm) and 1 cm^2 square masks to produce oxidised and non-oxidised patterning. The oxidised dishes were prepared for cell culture by washing in 3ml of distilled water for 10 min on a rocking platform, to remove loosely bound low molecular weight oxidation material known to be produced by this treatment[4]. Surface chemical composition of treated and untreated dishes was characterised by x-ray photoelectron spectroscopy (XPS) Kratos Axis HSi 5 channel using monochromated Alk$_\alpha$ radiation (1486.6 eV). Surface topography was examined using atomic force microscopy (AFM) Digital Instruments Nanoscope IIIa under ambient conditions. TE85 HOS cells were cultured in Dulbecco's minimal essential medium (DMEM) supplemented with 10% foetal calf serum (FCS) non-essential amino acids (0.01 ml^{-1}), penicillin (25 units ml^{-1}) and streptomycin (0.025mg ml^{-1}) and L-Glutamine (2mM) (supplied by Labtech, UK) under normal cell culture conditions with 5% CO_2 at 37°C. Cells were grown to 80% confluence, and had a real passage number of 60, before being trypsinised for seeding at a density of 10,000 cells/cm^2. After plating the dishes were placed in the incubator and monitored at time points up to 72hrs. Images were obtained with a digital camera, Leica DC (Switzerland), mounted on an optical microscope, Leica DMIL (Germany).

RESULTS & DISCUSSION: Analysis of the untreated PS dishes showed no surface oxygen and were hydrophobic in character. XPS analysis of the unwashed UVO treated PS surfaces shows that the surface oxygen concentration increased with increasing treatment time up to 34% (600 seconds treatment) as shown in figure 1.

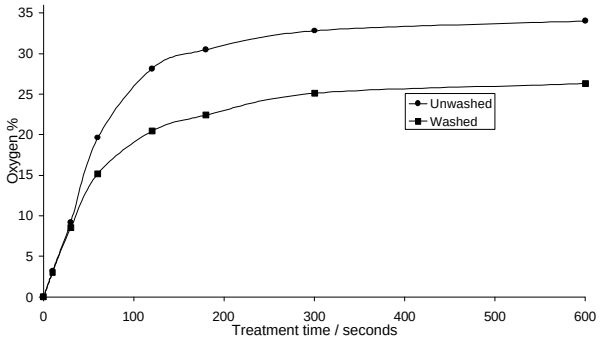

Fig 1: Oxygen concentration of washed and unwashed UVO treated PS surfaces

Following the washing procedure the surface oxygen concentrations decreased as a result of the removal of low molecular weight oxidised material, as has been previously reported, along with the corresponding surface functional group chemistry and XPS chemical shift data[4]. Analysis of the high resolution C 1s spectra from all treated samples was consistent with the presence of C-O and O-C=O type groups. Topographical analysis using AFM showed an increase in surface roughness with increasing treatment time. The detailed effects of masking on the topography are currently being investigated, and surface roughness may therefore have an effect on cellular attachment.

A proliferation rate of 1.99 relative to untreated PS was calculated for growth between 24 and 72 hours incubation for 30 second treatment. This shows that cells not only attached more readily in the treated areas but also that oxidation appears to influence the proliferation rate.

To study the effects of chemical heterogeneity, the cells were imaged at specific time points up to 72hrs after plating in treated, non-treated and tissue culture PS dishes. For all the treatment times, after

24hrs, the cells were observed to have preferentially attached to the oxidised areas of the surface and showed little attachment to the non-oxidised, hydrophobic, regions.

This patterning was shown most clearly in the 30 second treated dishes, which had 8.52% surface oxygen concentration , figure 2.

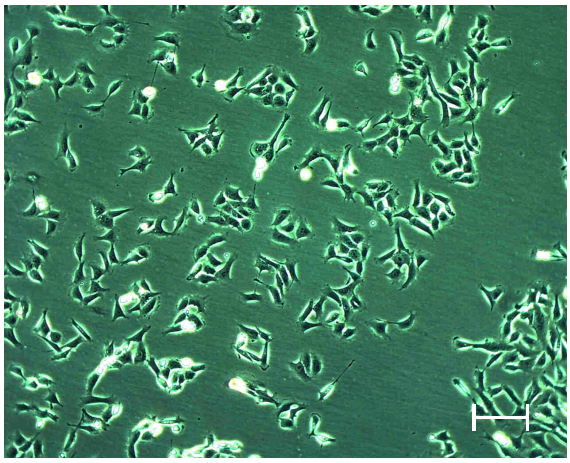

Fig. 2: HOS cell attachment after 24hrs to patterned PS dish following 30sec UV/O irradiation treatment, using a 250 mesh TEM grid scale bar is 100mm.

It is therefore clear that initial attachment of HOS cells occur in the hydrophilic regions produced by this masking technique. This behaviour has also been observed with CHO cells. Beyond 48hrs the defined grid pattern becomes obscured due to cell proliferation.

CONCLUSIONS: This study shows that surface oxidation can be used to control the proliferation and area of attachment for two different cell types on PS surfaces. Cells were shown to preferentially attach to hydrophilic regions of the PS surface, which may be due to cell migration. This behaviour persists for the first 48hrs for both cell lines under the conditions described. Thereafter cell modifications to the non-oxidised, hydrophilic regions of the PS surfaces allow the cells to proliferate and attach in these areas. Further investigation is therefore needed to identify whether the surface properties are being altered after the initial 48hrs. Overall the oxidation has a positive effect on the proliferation rate of both the cell types we have investigated. Using this technique we have also demonstrated that it is possible to spatially control cellular adhesion.

REFERENCES: [1]D.G.Castner and B.D.Ratner. (2002) *Surface Science*:**500**:pp28-60. [2]A.Welle and E.Gottwald.(2002) *Biomedical Microdevices*: **4**:1:pp33-41. [3]S.A.Mitchell, N.Emmison and A.G.Shard. *Surface and Interface Analysis*. (In Press). [4]D.O.H.Teare, N.Emmison, C.Ton-That and R.H.Bradley. (2000) *Langmuir*: **16**: pp2818-2824.

ACKNOWLEDGEMENTS: Financial aid is acknowledged from the SHEFC RDG 1008 by A.H.C.Poulsson and M.M.Browne, and the EPSRC by S.A.Mitchell grant number GR/M86996. Cells were kindly provided by the Orthopaedics Department, Aberdeen University Medical School, Forresterhill, Aberdeen.

European Cells and Materials Vol. 4. Suppl. 2, 2002 (page 13) ISSN 1473-2262

PROTEIN AND CELL DELIVERY SYSTEMS

Kevin Shakesheff[1] and Steve Howdle[2]

[1]*Tissue Engineering Group, School of Pharmaceutical Sciences, University of Nottingham, NG7 2RD*

[2]*School of ChemistryUniversity of Nottingham, NG7 2RD*

Tissue engineering and the pharmaceutical sciences share a common goal of using therapeutics to reverse disease conditions. Pharmaceutical therapeutics have traditionally been simple synthetic molecules or plant-derived products that are easy to administer to patients. Within the pharmaceutical community there is a trend towards the use of more complex therapeutic agents, e.g. proteins and cells, that regenerate tissue structures. Hence, there is considerable convergence between the scientific developments within these fields.

A number of major challenges are encountered in the use of proteins and cells as therapeutics:

- They are fragile species that lose activity during conventional manufacturing processes.
- Their functionality is intrinsically linked to their environment within the body.
- Their therapeutic effect is location dependent.
- They may be eliminated rapidly by the body.

As a consequence of these challenges it is essential to design delivery systems that optimize the adminstration of proteins and cells, alongside the development of the therapeutics themselves.

This talk will review the challenges of protein and cell therapy, the potential clinical benefits of successful use, and a number of delivery systems under development.

The key features of any delivery system for proteins are:

- It should be manufactured within conditions that do not denature the protein.
- The system should release the protein at the desired rate after administration.
- Adminstration methods should be clinically acceptable.

The challenge is even greater in designing cell delivery systems because the behaviour of the therapeutic cell must be controlled after administration.

At Nottingham, we are developing methods that use the supercritical carbon dioxide to process polymer materials, proteins and cells. In addition, we are interested in the role of self-assembly in the formation of cell aggregates and scaffolds within the body.

European Cells and Materials Vol. 4. Suppl. 2, 2002 (pages 94-95) ISSN 1473-2262

FIBROBLAST AND KERATINOCYTE BEHAVIOUR ON SUBSTRATES PLASMA-PATTERNED WITH FOULING AND NON FOULING DOMAINS

R. Gristina[1], E. Sardella[2], L. Detomaso[2], G. Senesi[1], P. Favia[1] & R. d'Agostino[1]

[1] *Instutute of Inorganic Methodologhies and Plasmas (IMIP), CNR Bari, Italy*

[2]*Department of Chemistry, University of Bari, via Orabona 4, 70126, Bari, Italy*

INTRODUCTION: Radiofrequency (RF, 13.56 MHz) driven low pressure plasmas can modify the surface of materials by means of: **a)** deposition of thin films (PE-CVD); **b)** treatments (grafting of functional groups, cross-linking); and **c)** dry etching (surface ablation) [1]. These processes are very popular in the field of biomedical polymers and devices due to their ability to change in a controlled, sterile and original way, surface chemistry and properties of solids with no change of the bulk. Since their use in microelectronics in the 70s', plasma processes have penetrated many other industrial arenas, including that of biomaterials. Plasma processes have been optimised to improve the biocompatibility of medical devices, for sterilization and, recently, to transfer geometric micro-patterns at the surface of biomedical polymers [2, 3], with the aim of driving adhesion, spreading and growth of cells along definite directions on biomaterials. This approach is of evident utility in cell and tissue engineering.

This contribution describes how cells react to polymer substrates surface-modified with plasma processes developed in our lab. These processes have been combined, with the use of *physical masks*, to develop surfaces micro-patterned with cell-adhesive and cell-repulsive domains, which become thus able to drive cell adhesion, spreading and growth along defined directions.

METHODS: Non fouling polyethyleneoxide (PEO)-like coatings plasma-deposited in continuous conditions from diethyl-glycol-dimethyl-ether (DEGDME)/Ar feeds have been utilized for cell-repulsive domains. Coatings deposited from Acrylic Acid vapors /Ar feeds (pdAA) in continuous and modulated plasmas have been utilized as cell-adhesive domains. TEM copper grids (TAAB) with different patterns have been utilized as *physical masks* for the deposition of the cell-repulsive layer onto pdAA-coated substrates. Optically flat polystyrene (PS, Goodfellow) substrates have been utilized. Cell-adhesive tracks large tens of μms spaced with wider cell-repulsive non fouling domains have been seeded with keratinocyte and fibroblast cell lines. Cell shape and alignment have been carefully evaluated during the first two days of culture.

RESULTS: When low fragmentation conditions (low RF power, in our case) are utilized for the deposition, hydrophilic PEO-like coatings with very good cell-repulsive properties are obtained. This behavior is correlated with the fraction of intact EO (ethylene oxide, -CH_2CH_2O-) units respect to all oxygen-containing groups[2] (hydroxyl, carbonyl, carboxyl,…). This parameter, defined as *PEO character*, can be checked by means of X-ray Photoelectron Spectroscopy (XPS). Good cell-repulsive properties characterize the coatings with PEO character of 75% or higher. The morphology of cells adhering to coatings with a lower PEO character is a function of this parameter. Figure 1 shows the response of cells tested in our lab on coatings with different PEO-character.

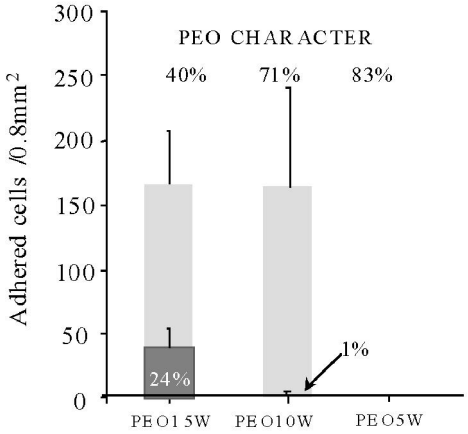

Fig. 1: Adhesion/spreading results (NCTC 2544 keratinocytes, 24 h of culture) for coatings of different PEO character. Plasma conditions: DEGDME 0.4 sscm; Ar 5 sscm; pressure 400 mtorr; RF power 5-15 W. The histogram show the percent of spread (dark grey) respect to the number of adhered cells (light grey). PEO5W (i.e., deposited at 5 W of power) coatings are cell-repulsive.

PdAA coatings can be obtained with different surface density of COOH groups, which tune their cell-adhesive and spreading properties. The surface density of COOH respect to all other oxygen-containing groups (C3%) can be measured by means of XPS.

Both adhesion and spreading of cells have been found increased, albeit to a different extent, by the increased density of COOH surface groups, as shown in Table 1.

Table 1: Adhesion/spreading results (NCTC 2544 keratinocytes, 24 h of culture) for pdAA coatings with different –COOH density (C3%). Plasma conditions: AA 3 sscm; Ar 20 sscm; pressure 230 mtorr; RF power 20W. DC = Duty Cycle (modulated plasmas).

C3%	Adhered cells on 0,8 mm^2	Spread cells %
DC 3% C3= 26±3%	43.0±5.5	60±2.2
DC 20% C3= 18±3%	33.0±7.5	39±5.7
continuous plasma C3= 13±3%	32.0±5.8	9.6±0.8

Thin (5-20 nm) PEO-like and pdAA coatings have been deposited in sequence, in order to develop on the substrates cell-adhesive (pdAA) tracks long hundreds of μms and large tens of μms, spaced by large cell-repulsive (PEO-like) areas. Cell culture experiments on the patterned substrates revealed that keratinocytes and fibroblasts adhere aligned along the inside border of the cell-adhesive tracks, while adhere randomly spread inside the same domains. Cell adhesion has been inhibited on the PEO-like areas spacing the cell-adhesive tracks. An example of cell-cultured fouling/ non fouling patterned PS substrates is shown in Figure 2.

DISCUSSION & CONCLUSIONS: As evident from our results, cell-adhesive and -spreading properties of polymeric biomaterials can be tailored by means of PE-CVD coatings of proper chemical composition. The control of the plasma process revealed to be crucial to secure the reproducibility of the deposition. The adhesion between the substrates and the coating is an other key issue, and can be guaranteed also in wet (cell culture) conditions, when substrates are properly plasma pre-treated (*e.g.*, in a NH_3 discharge), to provide hydrophilicity to their surface. The pre-treatment is extremely important when hydrophobic substrates are to be coated with hydrophilic coatings (like PEO-like and pdAA).

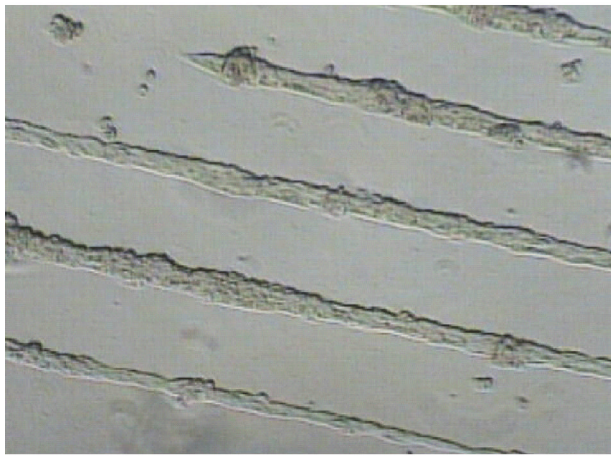

Fig. 2: Alignment of 3T3 fibroblasts on micro-structured (cell-adhesive pdAA tracks about 30 mm wide, cell-repulsive PEO5W spaces) PS samples.

In the case of patterned samples, a satisfactory replica of the pattern of the grids has been achieved, with good space resolution in the micron scale. A very good mask/substrate contact is important to achieve this. Effects of both surface chemistry (PEO-like, pdAA) and topography (edge of the tracks) have been recorded on cell adhesion, confirming that cells can "feel" both surface features in culture conditions.

Combining plasma chemistry with modification techniques able to shape the topography of substrates of biomedical interest in the micron and in the nanometer scale is certainly a field worth to be explored more in detail, and prolific of applications for cell and tissue engineering, as well as for biosensors and diagnostics.

REFERENCES: [1]*Plasma processing of polymers* (eds R. d'Agostino, P. Favia, and F. Fracassi) Kluwer Acad Publ NATO ASI Series E: Appl Sci **346**, (1997); [2]A. Ohl, K. Schröder, et al (1999) *Surf Coat Tech* **116-119:** 802-808; [3]*Plasmas & Polymers* **6(3)** and **7(2)**.

ACKNOWLEDGEMENTS: The EC project Nanobiotechnology and Medicine "NANOMED" (QLK3-CT-2000-01500, EC 5thFP Quality of Life) is acknowledged for funding this research.

European Cells and Materials Vol. 4. Suppl. 2, 2002 (pages 123-124) ISSN 1473-2262

ADVANCES IN THE STUDY OF BONE DEVELOPMENT IN SIMULATED MICROGRAVITY

O.S. Fleming[†], S. Reddy[‡], and A. Mantalaris[†]

[†]Department of Chemical Engineering and [‡]Faculty of Medicine, Imperial College, London, SW7 2BY, UK

INTRODUCTION: Mechanical loading is essential for skeletal integrity. Both microgravity and reduction of mechanical load lead to rapid bone loss resulting from an uncoupling between bone resorption and formation [1]. Earth bound conditions such as osteoporosis and extended bed rest show the same results as microgravity exposure. The mechanisms behind bone loss still remain elusive.

Overcoming the problem associated with spaceflight calls for counter measures not only to prevent bone loss, but also to maintain the functional-mechanical integrity of the tissue during prolonged spaceflight. The use of bioceramic materials as a deterrent for bone loss has proved successful not only in terms of prevention but also at the molecular level [2].

Previous research using the *in-vitro* mouse long bone model has been used to study the effects of microgravity on bone development [3]. The results from these experiments were obtained by taking a section through the bone and determining the area of mineralisation. However, bone is not a 2-D object and therefore conducting analysis in this way could lead to misleading results.

In this work, we investigated the effects of bone mineralisation in simulated microgravity using the NASA Bioreactor (HARV) and the Random Positioning Machine (RPM). The effects of two bioactive materials will also be investigated: Bioglass® 45S5 and 58S. Analysis was performed using AnalySIS® 3-D reconstruction software to obtain quantitative data.

METHODS: Murine feotal femurs of gestation age E16 were used in the study. The culture medium consisted of 88% α-MEM, 10% rat serum, 1% sodium-β-glycerophosphate, 1% penicillin streptomycin. The femurs were cultured using the RPM, NASA Bioreactor and 1G control environments for 4 days.

Bone samples were sectioned by thin cryo-genic sectioning followed by application of the Von Kossa stain (to highlight mineralisation within the sections). Image analysis software, analySIS®, was used to create composite 2-D planes of the bone sections using multiple image alignment followed by 3-D reconstruction of the planes (using 6 thin sections of know thickness and distance from each other) to generate a 3-D image of the bone.

Figure 1. NASA Bioreactor (left) and the RPM (right)

RESULTS: Following harvest at day 4 of culture, the bones were fixed and cryo-sectioned to generate consecutive thin sections spanning the whole bone. Van Kossa staining of the thin sections revealed the extent of mineralisation of the bones at the different conditions. Composite images of the bone thin sections under 10x magnification allowed us to evaluate to obtain quantitative data with regards to the area of mineralisation. Figure 1 shows the composite images generated using multiple image alignment. It was obvious, that the bones under normal gravity conditions showed a greater amount of mineralisation. When extent of mineralisation (area of mineralisation over the area of the bone section) was analysed from the midsections of the bones using the image analysis software, it showed that the mineralisation had decreased in both the NASA and RPM bioreactors, with the RPM condition showing a 10% decrease in mineralisation (Table 1).

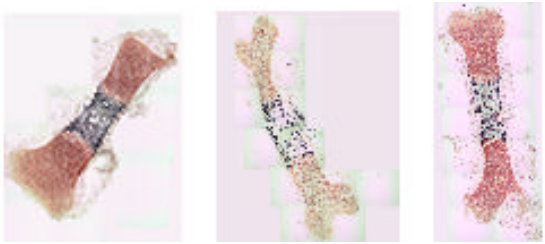

Figure 3. Composite images of the murine foetal bones obtained through multiple image alignment (10x magnification). The section in the left is that

of the bone at 1G gravity conditions, the one in the middle is from the NASA bioreactor, and the one in the right is from the RPM.

However, when a 3-D reconstruction was performed, as shown in Figure 2) and the extent of mineralisation (the ratio of the volume of mineralisation over the total bone volume), it was found that there was no difference between the NASA reactor and the 1G groups. Interestingly, the RPM showed an increase in mineralisation.

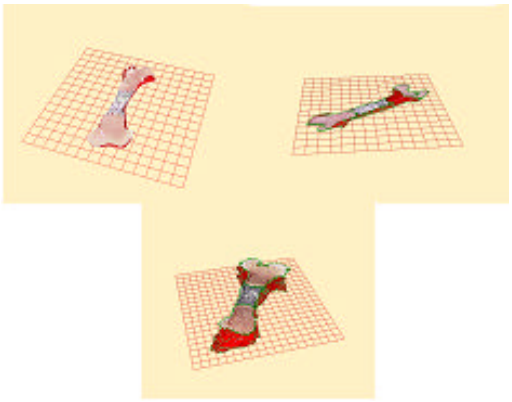

Figure 2. 3-D reconstruction of the murine foetal bone sections. The extent of mineralisation was then calculated as the ratio of the volume of mineralisation over the volume of the bone.

Table 1. Quantitative data of the extent of mineralisation obtained using the midsections of the bones and using a 3-D reconstructed bone.

% Mineralisation	1G	NASA	RPM
Midsection	22.19	20.93	19.9
3-D Reconstruction	17.85	17.2	22.4

DISCUSSION & CONCLUSIONS: Our qualitative results showed that there was a clear decrease in mineralisation under the simulated microgravity conditions using both the NASA and RPM bioreactors. Specifically, the density of mineralisation was observed to be the greatest in the 1G cultured bones, whereas it was the lowest in the RPM cultured bones. In addition, bone collar in the 1G group was intact in contrast to the bones grown in microgravity, which were discontinuous.

However, a quantitative analysis of the results proved more difficult to interpret and demonstrated the care with which any statistical analysis of the results needs to be done. Specifically, whereas the quantitative analysis of the extent of minerilisation using the midsections showed that there was a statistically significant decrease in both the NASA and RPM cultured bones, the results obtained using the 3-D reconstructed bones did not show the same trend. This could be explained by the arbitrary nature of selecting the midsections of the bone for analysis, which would result in variations between samples. We feel that the proper methodology would be to 3-D reconstruct the bones and use these for analysis. Such analysis may show that the extent of mineralisation, meaning the mineralised zone does not decrease in microgravity. Therefore, although the density of mineralisation decreased, the process by which the growth plate of the mineralised zone is extended was not affected. That could potentially mean that osteoclast activity is up-regulated, hence the decrease in mineralisation. However, this is just a potential observation and further analysis is required.

In this report we present our strategy for elucidating the effects of microgravity on bone development using simulated microgravity culture conditions and quantitative image analysis tools.

REFERENCES: [1]P.J.Marie, D.Jones, L.Vico, A.Zallone, M.Hinsenkamp, and R.Cancedda, (2000), Osteobiology, Strain, and Microgravity: Part1. Studies at the Cellular Level. [2]L.L. Hench, J.M. Polak, I.D. Xynos, L.D.K. Buttery, (2000), Bioactive materials to control cell cycle, Materials Research Innovations, 3:313-323. [3]J.J.W.A. Vanloon, D.J. Bervoets, E.H. Burger, S.C. Dieudonne, J.W. Hagen, C.M. Semeins, B.Z. Doulabi, J.P. Veldhuijzen, (1995), Decreased mineralization and increased calcium-release in isolated fetal mouse long bones under near weightlessness, Journal of Bone and Mineral Research, 10:550-557.

European Cells and Materials Vol. 4. Suppl. 2, 2002 (pages 136-137) ISSN 1473-2262

ENGINEERING A HUMAN BONE MARROW LYMPHOPOIESIS MODEL

A. Mantalaris[1] and J.H.D. Wu[2]

[1] *Department of Chemical Engineering, Imperial College, London SW7 2BY, UK*

[2]*Department of Chemical Engineering, University of Rochester, Rochester, NY 14627, USA*

INTRODUCTION: Bone marrow is the haematopoietic tissue as well as a primary immune organ. Its intricate, three-dimensional architecture facilitates cell-cell and cell-matrix interactions and provides a microenvironment that supports self-renewal and multilineal differentiation. Traditional *in vitro* culture systems (flask cultures) are suffering from the absence of normal marrow spatial organization and cellular interactions with the extracellular matrix. Furthermore, there exists a lack of consistent, single-stage human lymphopoiesis models or methods that allow for the study of the intricate cell-cell interactions in lymphopoiesis and are not limited in the production of only B-cells but also include the other cell types present in the bone marrow [2]. We have developed a novel human *ex vivo* bone marrow model that mimics bone marrow both structurally (through the use of a scaffold) and functionally [3]. Specifically, the 3-D culture system supported the development of lymphocytes (B- and T-cells) at different maturation stages, including lymphocyte stem cells (TdT^+).

METHODS: The 3-D cultures were inoculated with human mononuclear cells (3 x 10^6 cells/ml) isolated from a bone marrow aspiration from normal consenting adults. The medium (changed daily), consisted of 70% (v/v) McCoy's 5A medium, 1 x 10^{-6} M hydrocortisone, 50 u/ml penicillin, 50 mg/ml streptomycin, 0.2 mM L-glutamine, 0.045% sodium bicarbonate, 1x MEM sodium pyruvate, 1x MEM vitamin solution, 0.4x MEM amino acid solution, 12.5% (v/v) heat inactivated horse serum, and 12.5% heat inactivated FBS. The cultures were depopulated weekly by gently stirring and mixing the bed of porous microspheres to release the non–adherent cells. For the T-lymphopoiesis experiments, the medium was supplemented with 50 ng/ml rh SCF, 1000 U/ml rh IL-2, and 2 ng/ml rh IL-7. For the hydrocortisone experiments, the cultures were fed with complete medium for 10 days at which time hydrocortisone was removed. The cultures were analysed by differential cell analysis, paraffin-thin sections, immunohistochemistry (cytoplasmic-μ and TdT), flow cytometry (CD3, CD4, CD8, CD10, CD19, CD20, CD21, CD45RA, CD45RO, TCRαβ, TCRγδ). In addition, mRNA was isolated from the cultures and differential gene expression analysis was performed using the RNA arbitrarily primed PCR (RAP-PCR) technique.

RESULTS: Immunohistochemistry confirmed the presence of lymphoid stem cells (nuclear TdT stain) and pre-B cells (cytoplasmic-μ), as shown in Figure 1.

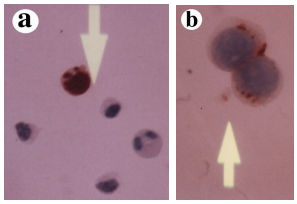

*Fig. 1: Evidence for early B-cell lymphopoiesis in the 3-D cultures. Panel (**a**) shows a TdT^+ (arrow) lymphoid progenitor cell from the 3-D reactor culture at week 2. The nuclear TdT is stained red. Panel (**b**) shows a pre-B lymphocyte (arrow) which is stained red for cytoplasmic μ chains (the heavy chain of antibody; week 5.5).*

Flow cytometric analysis of the cell-output from the 3-D human bone marrow cultures confirmed the presence of pro-B ($CD10^+$), as shown characteristically in Figure 2, immature B ($CD19^+$), and mature B-cells ($CD20^+$, $CD21^+$) in the absence of exogenous growth factors.

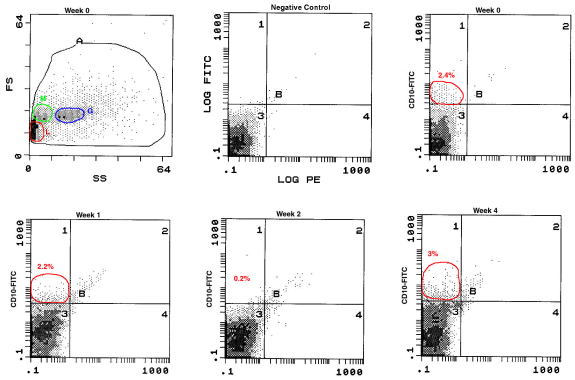

Fig. 2: Flow cytometric analysis of the CD10 antigen expression in the three-dimensional mimicry.

Flow cytometric analysis, further showed the presence of T-cells, both T-helper ($CD4^+$) and T-cytolytic ($CD8^+$). These T-cells expressed the normal T-cell receptors TCR$\alpha\beta$ and TCR$\gamma\delta$. Addition of T-cell specific lymphokines resulted in expansion of the T-cells, mainly of T-helper cells.

Hydrocortisone removal resulted in the increase in the cell- output by week 2. The increase in the cell-output was maintained throughout the culture, with week 3 being the most dramatic. Towards the later stages of the cultures, the difference in the cell-output between the hydrocortisone-free and hydrocortisone-supplemented cultures decreased, as shown in Figure 3.

Fig. 3: Cell output kinetics from the human 3-D culture system. Hydrocortisone was removed at day 10.

The differential display technique (RAP-PCR), which was used to examine any differences in the gene expression pattern between hydrocortisone-supplemented and hydrocortisone-free cultures, showed that that withdrawal of hydrocortisone resulted in a different gene expression pattern. Among the genes identified, thus far, is the heme-regulated initiation factor 2 alpha kinase gene [4].

DISCUSSION & CONCLUSIONS: Our results indicate that the 3-D human bone marrow culture system supports the development of human *ex vivo* lymphopoiesis in a more physiologically relevant manner than current existing models. It meets several key criteria of an optimal *in vitro* human B-lineage developmental model, since it supports the growth of B-lineage progenitor populations with cell surface phenotypes consistent with most of the major B-lineage developmental subpopulations present in normal human bone marrow, including pro-B cells, cycling pre-B cells, and immature and naï ve B cells. Further, this model appears to support both the commitment of multipotent stem cells to B-lineage development and the progression of these committed progenitors into functionally mature B cells.

Our data also confirm the presence of T-cells in the cell-output. Both T-lymphocyte subtypes, helper and cytotoxic, were present (in the absence of exogenous growth factors) at a ratio that was similar to the bone marrow *in vivo*. Moreover, most T-cells expressed, as expected, the $\alpha\beta$ TCR. Furthermore, the T cells in the bioreactor were stimulated in a manner consistent with their subtype when exogenous lymphokine-specific growth factors were added, suggesting that these cells are functional.

The stimulation of the cell-output in the three-dimensional mimicry is in sharp contrast with the traditional flask cultures where the cell-output drops, although this could be due to the presence of 2-mecraptoethanol in the culture medium. Cell viability, after the removal of hydrocortisone, remained high and comparable to the hydrocortisone-containing cultures, although in the hydrocortisone-free cultures it was always lower. Eventually, cell viability in the hydrocortisone-free cultures decreased to lower levels than the hydrocortisone-supplemented cultures with prolonged culture time. Finally, RAP-PCR confirmed that withdrawal of hydrocortisone resulted in a different gene expression pattern. Among the genes identified, thus far, is the heme-regulated initiation factor 2 alpha kinase gene, which plays a role in reticulocyte maturation.

REFERENCES: [1]Gartner, S. and Kaplan, H.S. (1980) Log-term culture of human bone marrow cells. Proceedings of the National Academy of Sciences USA 77, 4756-4759. [2]Fluckinger, A.-C., Sanz, E., Garcia-Lloret, M., Su, T., Hao, Q.-L., Kato, R., Quan, S., Hera, A.d.l., crooks, G.M., Witte, O.N. and Rawlings, D.J. (1998) *In Vitro* Reconstitution of Human B-Cell Ontogeny: From $CD34^+$ Multipotent Progenitors to Ig-Secreting Cells. Blood 92, 4509-4520. [3]Mantalaris, A., P. Keng, P. Bourne, A.Y.C. Chang, and J.H.D. Wu (1998). Engineering a human bone marrow model: a case study on *ex vivo* erythropoiesis. Biotechnology Progress 14:126-133. [4]Omasa, T, Y-G. Chen, A. Mantalaris, and J.H.D. Wu. (2002). Molecular cloning and sequencing of the human heme-regulated eukaryotic initiation factor-2 alpha (eIF-2alpha) kinase from bone marrow culture, DNA Sequence 13(3):133-137.

ACKNOWLEDGEMENTS: The authors would like to thank the NSF, NASA, and the Onassis Foundation for their support.

European Cells and Materials Vol. 4. Suppl. 2, 2002 (page 93) ISSN 1473-2262

SHALLOW TOPOGRAPHICAL NANOPATTERNS IN POLYMERS INFLUENCE THE MOTILITY OF MAMMALIAN CELLS

D. Selmeczi, S. Mosler, S. Nyrup, N. Gadegaard, & N. B. Larsen

Danish Polymer Centre, Risø National Laboratory, 4000 Roskilde, Denmark

Ph: +45 4677 4713, Fax: +45 4677 4791, e-mail: david.selmeczi@risoe.dk

INTRODUCTION: The time course of cell-substratum adhesion events markedly reflects the cytocompatibility of a solid surface. Direct comparison of differing surface samples under equal culture conditions and quantitation of the observed cellular responses are highly desirable for the evaluation of surface engineering approaches.

Accordingly, we constructed a phase contrast microscope-based setup which is capable of imaging several samples in parallel. The microscope is equipped with a digital camera, motorized focussing and a temperature-controlled, humidified chamber, which is mounted to a computer-controlled translation stage.

METHODS: Prior to an experiment, samples are immobilized in a culture dish and covered with cells suspended in CO2-independent medium. After placement in the chamber, sites of interest and a suitable time interval are programmed for automatic image acquisition in autofocus mode. Images are saved in site-specific files. Subsequent image processing yields quantitative data, preferably the time course of cell spreading, average cell area and proliferation.

RESULTS: As an example, the comparison of four different commercial culture surfaces is presented in our poster, a bacteriological and two tissue culture grade polystyrenes as well as a collagen-coated glass, seeded with MDCK epithelials. The results from two of the culture dishes are shown in Fig. 1 and 2. The revealed difference of all samples proves this set-up to be a powerful tool for the evaluation of cell adhesiveness of engineered surfaces at small material consumption.

ACKNOWLEDGEMENTS: N. B. Larsen gratefully acknowledges the financial support from the Danish Technical Research Council that made this work possible. D. Selmeczi and S. Mosler acknowledges support from the Danish Graduate School of Biophysics.

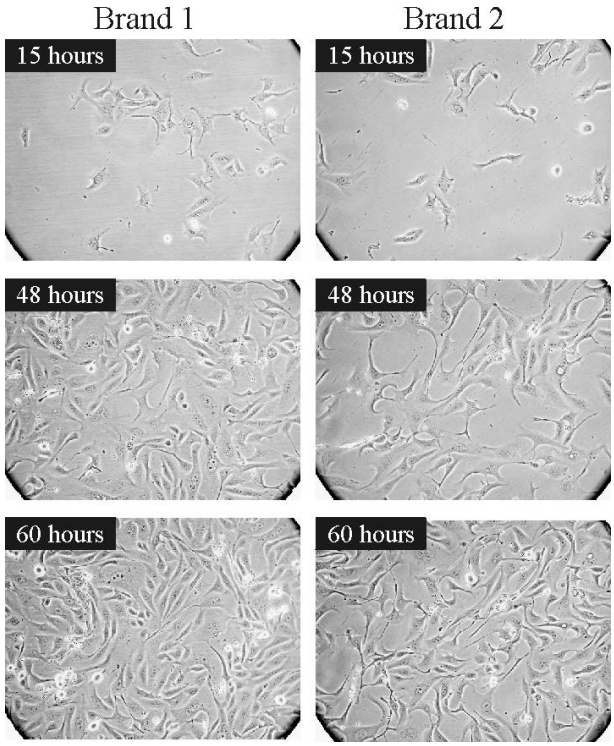

Fig. 1: Time lapse snapshots of MDCK cells cultured on two different brands of culture dishes. The number of cells after 60 hours is notably larger on the Brand 1 culture dish.

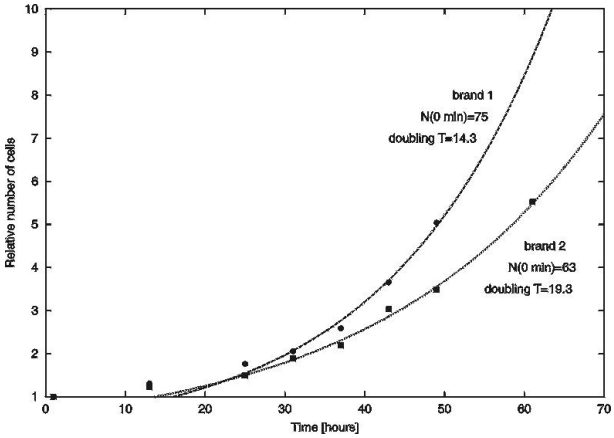

Fig. 2: Quantitative measure of the number of cells based on time lapse video sequences of MDCK cells cultured on two different brands of culture dishes. The doubling time on Brand 1 dishes is 14.3h compared to 19.3h on Brand 2 dishes.